NATURAL IgG IS INNATE IMMUNE RESPONSIVE

– elucidation of mechanisms of action

SASWATI PANDA

(*M.Sc. Biotechnology, Indian Institute of Technology, Bombay*)

A THESIS SUBMITTED

FOR THE DEGREE OF DOCTOR OF PHILOSOPHY

DEPARTMENT OF BIOLOGICAL SCIENCES

NATIONAL UNIVERSITY OF SINGAPORE

2013

"The universe is full of magical things, patiently waiting

for our wits to grow sharper." Eden Phillpotts

DEDICATED WITH LOVE TO MY FAMILY

DECLARATION

I hereby declare that the thesis is my original work and it has been written by me in its entirety. I have duly acknowledged all the sources of information which have been used in the thesis.

This thesis has also not been submitted for any degree in any university previously.

S Panda. 24/1/2013

Saswati Panda

24 January 2013

ACKNOWLEDGEMENTS

This work would not have been possible without the exceptional support of many people who selflessly provided me with their valuable time, help and care. I would like to take this opportunity to express my most sincere respect and acknowledgement to all those who helped me in completing this thesis.

I would like to extend my deepest gratitude to my supervisor, Prof. Ding, for giving me an opportunity to work in her lab. I truly appreciate her guidance, patience, understanding and encouragement that immensely helped me throughout my candidature. I have learnt a lot from her. I sincerely thank her for the meticulous effort and commitment in inculcating the attributes of a good researcher in me. Her enthusiasm towards science and eagerness to explore the unknown has truly been inspiring.

I would also like to thank Prof. Ho Bow and Prof. Andrew Tan for their time, guidance and valuable suggestions. I also thank Prof. Jayaraman Sivaraman, Prof. Liou Yih Cherg and Prof. Low Boon Chuan, who are my thesis advisory members, for their guidance.

I would like to express my gratitude to Dr. Zhang Jing, for the innumerable hours I spent with her discussing scientific problems. Her guidance and experience helped me in my initial phase of candidature. I also thank Dr. Yang Lifeng for her help in computational studies. I specially thank Dr. Enoka Bandularatne (Comparative Medicine) for her expert veterinary advice during the *in vivo* siRNA knockdown work in mice.

I am grateful to Dr. Garnett Kelsoe (Duke University, USA) for the $AID^{-/-}$ mice, obtained with kind permission from Dr. Tasuku Honjo (Kyoto University, Japan) and Dr. Sivasankar Baalasubramanian (Singapore Institute for Clinical Sciences) for providing $C3^{-/-}$ mice (Jackson Laboratories) and serum. I thank Dr. Ming Teh (Department of Pathology, National University Hospital, Singapore) for his advice on assessing the germinal centers per white pulp area in spleens of mice. I also thank Prof. Ganesh Anand for his advice

on hydrogen deuterium exchange experiments. I would like to thank NUS for the graduate research scholarship.

I would like to express my sincere thanks to all my former and current lab mates Ruijuan, Prem, Bin, Sae Kyung, Pradeep, Susan, Zhu Yong, Jun, Yuan Quan, Imelda, Rebecca, Neha, Shania, Porkodi, Karthik, Zhiwei, Shalini and Glenn, for their continuous support, friendship and suggestions and for making the lab a pleasant place to work in. I also thank Michelle for help in mass spectrometry, Tong Yan for help in confocal microscopy, CeLS vivarium staff for taking care of the mice and Subha for the administrative assistance.

I express special heartfelt thanks and appreciation to my grandfather, Dr. N.C. Panda, who has always inspired me to be curious and explore the mysteries of science. I am truly grateful to my parents, Dr. S.K. Panda and Aruna Panda and my brother, Aditya Panda, for their continuous love, encouragement and the confidence they showed in me, which gave me the strength to persevere and work hard to achieve my goal.

Last, but not the least, I thank Almighty God for his boundless love and blessings.

TABLE OF CONTENTS

SUMMARY

Natural antibodies are defined as the pool of antibodies present in newborns and individuals without any prior infection. Natural antibodies consist of IgM, IgG and IgA isotypes. Although decades of research has focused on elucidating the function and detailed mechanism of action of natural IgM which is poly-reactive by virtue of its high avidity, there is a lack of knowledge as far as natural IgG and IgA antibodies are concerned. Natural IgG, which constitute the majority of natural antibodies in the serum, have been deemed non-reactive as they do not recognize any antigen. Here, we demonstrate that natural IgG is not non-reactive but in fact, it plays a crucial role in innate immunity, in collaboration with PRRs like ficolins. In particular, we have shown through *in vitro* FACS studies that natural IgG recognizes a wide variety of microbes through the help of ficolins in both humans and mice. By *ex vivo* analyses, we further showed the formation of IgG**:**ficolin complexes in the serum and spleen during infection in mice. To gain more credence on the importance of natural IgG in immune defense, we demonstrated, through *in vivo IgG* siRNA knockdown mice (partial IgG) and *AID*$^{-/-}$ mice (no IgG) studies, that natural IgG is crucial in protecting the mice from infection. The innate defensive role of natural IgG was further supported by IgG reconstitution studies in *AID*$^{-/-}$ mice which promoted survival, especially in the early phase of infection. We found that the IgG**:**ficolin mediated pathogen recognition occurs independently of complement C3. To understand the mechanism of action of IgG with the aid of ficolin, we characterized the binding using various techniques including flow cytometry, ELISA, surface plasmon resonance (SPR) and *in situ* proximity ligation assay

(PLA) studies under normal physiological condition and infection-inflammation conditions. We found that the infection-inflammation condition where low pH and low calcium levels prevail, led to a 100-fold increase in affinity between the proteins and subsequently more number of complexes were formed on the monocytes. Consistently, significantly higher degree of phagocytosis of the opsonized pathogen was observed under the infection-inflammation condition. We performed hydrogen-deuterium exchange mass spectrometry (HDMS) and site-directed mutant SPR binding studies, which gave us a comprehensive idea of the binding interface and the residues involved in interaction between IgG and ficolins. Arginine and Lysine residues of IgG and ficolins were found to be crucial for interaction under normal condition, while Histidine was the critical residue involved in enhancing the binding under infection-inflammation condition. Taken together, this thesis has illustrated that natural IgG is not non-reactive but interacts with microbe-associated lectins like ficolins. These findings will alter our perception of the fundamental role of natural antibodies in the recognition of pathogens and provocation of innate immune defense. Knowledge gained in this study would be essential in our continuing effort to develop new and efficient molecular therapies for infectious diseases (474 words).

LIST OF TABLES

CHAPTER 1

CHAPTER 3

LIST OF FIGURES

CHAPTER 1

CHAPTER 2

CHAPTER 3

CHAPTER 4

LIST OF ABBREVIATIONS

ABTS	2,2'-azino-bis[3-ethylbenzthiazoline-6-sulfonic acid]
AD	Activation Domain
Ade	Adenine
Ala	Alanine
Amp	Ampicillin
Arg	Arginine
Asp	Aspartic acid
BD	Binding Domain
BSA	Bovine serum albumin fraction V
CFU	Colony-forming unit
C3	Complement 3
CRD	Carbohydrate-recognition domain
CRP	C-reactive protein
˚C	Degree Celsius
dNTP	Deoxynucleoside triphosphate
DAPI	4',6-diamidino-2-phenylindole
DMEM	Dulbecco's Modified Eagle's Medium
E. coli	*Escherichia coli*
EDTA	ethylenediaminetetraacetic acid
ELISA	Enzyme-linked immunosorbent assay
FBG	Fibrinogen beta gamma
FBS	Fetal Bovine Serum
g	Relative centrifugal force
GC	Germinal center
GlcNAc	N-acetyl-D-glucosamine
h	Hours
HEK 293	Human Embryonic Kidney 293 cells
His	Histidine
hpi	Hours post-infection
IL6	Interleukin 6
IL8	Interleukin 8
ITAM	Immunoreceptor tyrosine-based activation motif
ITIM	Immunoreceptor tyrosine-based inhibitory motif
kDa	Kilo Dalton
K_D	Dissociation constant
kg	Kilogram
LA	Lipid A

LB	Luria-Bertani
LiAc	Lithium Acetate
Leu	Leucine
LPS	Lipopolysaccharide
LTA	Lipoteichoic acid
Lys	Lysine
min	minutes
m/z	Mass/charge
ml	milli liter
MALDI-TOF	Matrix-assisted laser desorption ionization-Time of flight
MASP	Mannose Binding Lectin (MBL)-associated serine protease
MBL	Mannose-binding lectin
MBS	MES-buffered saline
MBST	MES-buffered saline with Tween-20
MES	2-(*N*-morpholino)ethanesulfonic acid
Met	Methionine
MHC	Major histocompatibility complex
mol. wt.	Molecular weight
OD	Optical density
P. aeruginosa	*Pseudomonas aeruginosa*
PAMP	Pathogen-associated molecular pattern
PBS	Phosphate-buffered saline
PC	Phosphocholine
PCR	Polymerase chain reaction
PEG	Polyethylene Glycol
PLA	Proximity ligation assay
PRR	Pattern recognition receptors
PC	Phosphatidylcholine
QDO	Quadruple DropOut
rpm	Revolutions per minute
RPMI	Roswell Park Memorial Institute
s	seconds
S. aureus	*Staphylococcus aureus*
S. epidermidis	*Staphylococcus epidermidis*
SDS	Sodium Dodecyl Sulfate
siRNA	Small interfering RNA
SP-A	Surfactant protein A
SP-D	Surfactant protein D
SR	Scavenger receptor
Trp	Tryptophan

TBS	Tris-buffered saline
TBST	Tris-buffered saline with Tween-20
TCR	T-cell receptor
TE	TRIS-EDTA
TLR	Toll-like receptor
TMB	3,3',5,5'-Tetramethylbenzidine
TNF-α	Tumor necrosis factor-alpha
Tris	tris(hydroxymethyl)aminomethane
Trp	Tryptophan
v/v	Volume/volume
w/v	Weight/volume

Chapter 1

INTRODUCTION

CHAPTER 1: INTRODUCTION

1.1 Infection and pathogen

Infectious diseases are caused by pathogenic microorganisms, such as bacteria, viruses, parasites or fungi. These diseases have the ability to spread either directly or indirectly, from person to person or from animals to humans, hence they are termed as transmissible or communicable (Ryan and Ray, 2004). These diseases have plagued mankind throughout history and continue to pose a threat as they are fatal in many cases. According to WHO reports, the most prevalent diseases in humans include pneumonia, tuberculosis, diarrhoea, malaria, measles and HIV/AIDS, which account for half of all the premature deaths, inflicting mostly children and young adults worldwide every year, causing 300 million illnesses and more than 5 million deaths each year (The World Health Report 2004).

Infection is defined as the invasion and multiplication of harmful foreign organisms in the host. There are various factors involved in the progression of an infectious disease: (i) an entry site for the organism to gain access to the interior of the host, (ii) size of the inoculum and virulence of the invading organism, (iii) access to favorable host sites where the organisms can usurp nutrients and multiply to give rise to higher numbers and (iv) susceptibility or ability of the host to fight and clear the organism by virtue of its immune defense system (Morse 1995).

As mentioned earlier, pathogens range from bacteria to viruses to fungi. Pathogenic bacteria comprise of various species like gram negative *Pseudomonas*, *Escherichia*, *Salmonella* or *Shigella* and gram positive

Strepcoccus, *Staphylococcus* or *Clostridium* species. These bacteria cause a range of deadly diseases like pneumonia, typhoid, tetanus, diphtheria and tuberculosis. Pathogenic viruses fall into a big group including *Polyomavirus, Adenoviridae*, *Herpesviridae*, *Retroviridae*, amongst others. Some notable viral infections include polio, smallpox, measles and chickenpox. Fungi such as *Candida*, *Aspergillus*, *Pneumocystis* and *Cryptococcus* species are known to cause notorious opportunistic diseases and secondary infections (The World Health Report 1996).

These pathogens can be transmitted to the host through a variety of routes including airborne, direct or indirect contact, sexual contact and respiratory, oral or rectal route or through various body fluids like blood (**Figure 1.1**) (Benenson 1990; Isada et al., 2003).

In this study, *Pseudomonas aeruginosa* (*P. aeruginosa*) was used as a model pathogenic microorganism for *in vitro* and *in vivo* studies. *P. aeruginosa* is a versatile opportunistic pathogen that infects individuals with compromised natural defenses. The immunologically challenged individuals become more susceptible to *P. aeruginosa* infection due to several reasons, including disruption in the epithelial barrier (as found in a patient with a burn wound), a depletion in neutrophil count (for example, in cancer patients), the presence of a foreign body and abruption in mucociliary clearance (in an individual with cystic fibrosis) (Lyczak et al., 2000). *P. aeruginosa* infections also occur after patients have been hospitalized. In addition, numerous factors account for the success of *P. aeruginosa* (Bleves et al., 2010) as a nosocomial pathogen. It can utilize a broad spectrum of nutrients and can thus grow in

hospital drains, sinks and even disinfectant solutions. It is intrinsically resistant to a large number of antibiotics and can acquire resistance to many others, making treatment difficult. The propensity of *P. aeruginosa* to form biofilms further protects it from antibiotics and from the host immune system (Harmsen et al., 2010). In addition, it employs a large arsenal of pathogenicity factors to interfere with host defenses. Thus, *P. aeruginosa* has remained a biomedical healthcare challenge. Hence, we were interested to study how the host immune system factors counter this pathogen and help to clear it off the system.

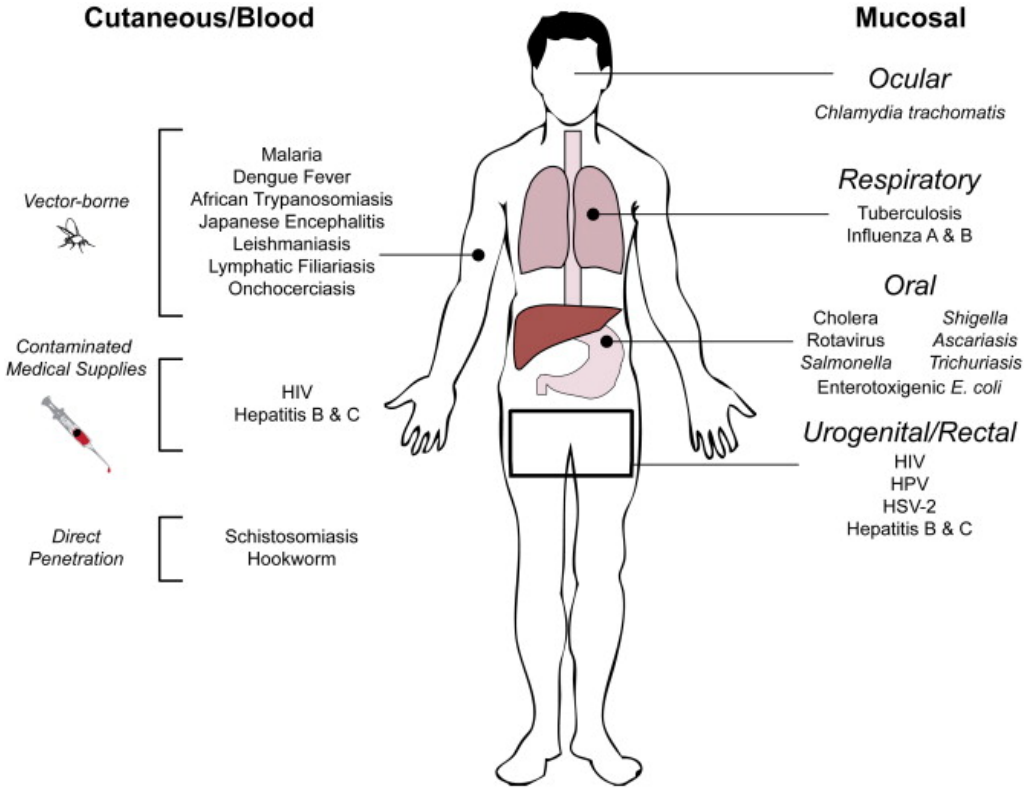

Figure 1.1: Entry routes for the infectious pathogens into the humans. Pathogens enter the body through a variety of routes. They could enter via vector delivery (such as mosquitoes, sandflies, and fly bites), direct penetration through epidermis or be injected directly into the blood stream through use of contaminated medical supplies. Another mode of transmission can occur through mucosal surfaces, which could be either respiratory, oral (gastrointestinal), urogenital (reproductive) or ocular. Some pathogens, such as HIV and hepatitis B and C, can enter the body through multiple routes. Adapted from Look et al., (2010).

1.1.1. Pathogen-associated molecular patterns

Once inside the host, the pathogens are recognized as "non-self", as they express an assortment of conserved molecular motifs termed as "pathogen-associated molecular patterns" (PAMPs), that is foreign to the host. The well-known bacterial PAMPs comprise of lipopolysaccharide (LPS) on outer membrane of gram negative bacteria, lipoteichoic acid (LTA) on cell wall of gram positive bacteria, bacterial flagellin and peptidoglycan (PGN) (Beutler 2004). Viral PAMPs include nucleic acid variants such as double-stranded ribonucleic acid (ds RNA), single stranded RNA (ss RNA) or unmethylated CpG motifs. Fungi exhibit conserved β-1, 3-glucans on their surface that alerts the host to recognize them as intruders. By virtue of these conserved PAMPs on the microbes, they are effectively recognized by sensor proteins in the host, which then mount an immune response against the pathogen.

LPS

Lipopolysaccharide (LPS) is a complex molecule consisting of a lipid backbone and a polysaccharide tail that are joined together by a covalent bond. It is a major component of the outer membrane of Gram-negative bacteria (**Figure 1.2A**). It plays a crucial role in maintaining survival of the bacteria as LPS increases the negative charge of the cell membrane, thus stabilizing the overall membrane architecture and integrity. It is one of the most potent biological endotoxin that is able to bring about a strong immune response in the host (Raetz and Whitfield 2002). LPS is composed of three integral parts

(**Figure 1.2B**):

(i) Lipid A is the inner most hydrophobic moiety that anchors LPS to the outer membrane of the bacteria. It consists of two phosphorylated glucosamine carbohydrate units with multiple fatty acid chains attached. It is considered a potent immune activator with 6 acyl chains, which give rise to optimal endotoxicity. It is released into the host upon bacterial lysis and causes pyrogenic action and severe inflammatory symptoms which may lead to fatal septic shock (Raetz et al., 2009).

(ii) O-antigen comprises part of the polysaccharide component of LPS and is a repetitive polymer consisting of monosaccharides linked with O-glycosidic linkages. It forms the outermost domain of LPS molecule and is connected to the core oligosaccharide. Its structure is variable across various species and strains of bacteria (Raetz and Whitfield, 2002).

(iii) Core polysaccharide contains an oligosaccharide that attaches it to the lipid A moiety. It comprises of sugar residues like 3-deoxy-D-mannooctulosonic acid (also known as KDO, keto-deoxyoctulosonate) and heptose (Hershberger and Binkley, 1968), along with other non-carbohydrate components that make it diverse among bacterial species and strains.

Despite variations in the structure of LPS across bacterial species, in terms of the number of repeating units in O-antigen, the lipid A moiety is fairly conserved and plays an important role in acting as a potent endotoxin component of LPS. It can be recognized in picomolar levels by the host innate immune sensors like Toll-like receptors (TLR4), present on macrophages and endothelial cells (Poltorak et al., 1998).

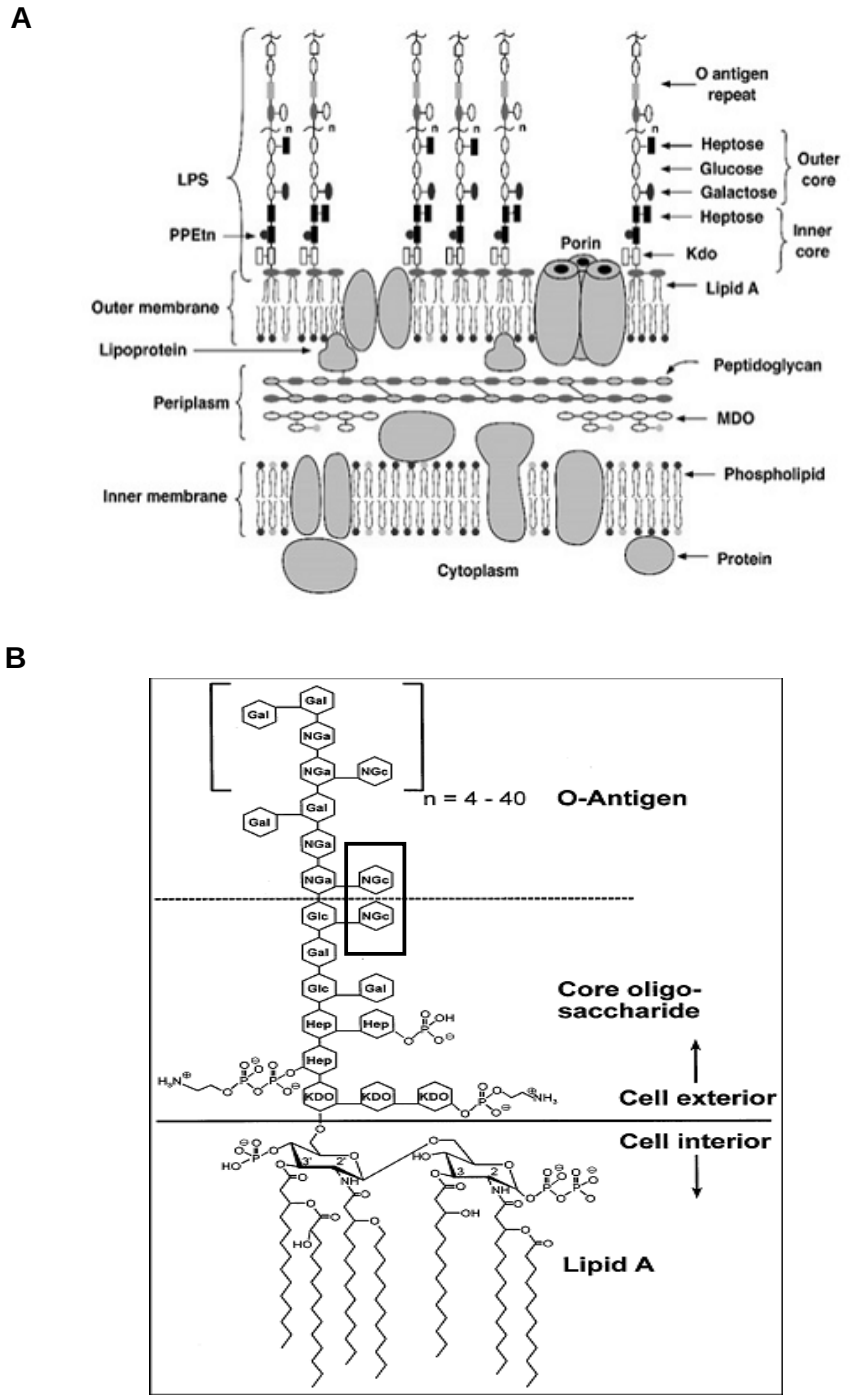

Figure 1.2: Schematic diagram of the cell membrane of gram negative bacteria and the chemical structure of LPS. (**A**) The cell membrane of gram-negative bacteria comprises of two lipid bilayer membranes separated by a periplasmic space. LPS is located on the outer membrane of the cell membrane. (**B**) LPS is composed of Lipid A embedded in the outer cell membrane and core polysaccharide and O-antigen exposed to the exterior of the cell. The N-acetyl glucosamine (GlcNAc/NGc) residues in LPS structure are boxed. Adapted from Raetz et al., 1991 and Ohno and Morrison, (1989), with modification.

Upon recognition, lipid A triggers the host immune system to produce an array of pro-inflammatory cytokines, such as IL6, IL8, TNFα and IL1β and other co-stimulatory molecules that prime the adaptive immune system. It also stimulates the production of various mediators in endothelial cells that help in clearing the infection (Beutler and Poltorak, 2000). However, this immune response has to be carefully modulated. Systemic immune dysfunction and uncontrolled inflammation may lead to overproduction of inflammatory mediators leading to severe sepsis and eventually, death (Russell 2011).

GlcNAc

N-acetylglucosamine (GlcNAc) is a monosaccharide derivative that forms the basic structural unit of PAMPs such as LPS (Figure 1.2B, inset), PGN and chitin (**Figure 1.3**). GlcNAc is present on the surface of the invading pathogens and serves as a crucial recognition molecule that is identified as "non-self" by the host. It is also present in the host as a moiety of blood group glycoproteins, but is shielded off from the host scavengers by terminal sialic acid residues on these proteins. GlcNAc is primarily recognized by the host innate immune soluble lectin receptors like the ficolins and mannose-binding lectin (MBL). As it lacks a basic orientation, it is recognized by lectin receptors only at high concentrations (Garlatti et al., 2007; Zhang et al., 2009), which then activate the downstream complement cascade to bring about the lysis of the microbe along with evoking a pro-inflammatory immune response. Figure 1.3 shows a representation of the GlcNAc moiety within LPS molecule.

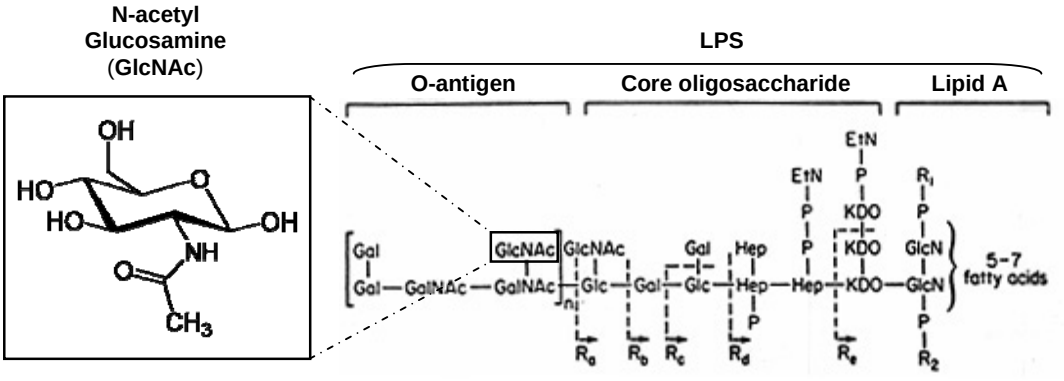

Figure 1.3: Structure of N-acetyl glucosamine (GlcNAc), a crucial component of LPS molecule on gram negative bacterial cell membrane. Adapted from http://en.wikipedia.org/wiki/File:N-Acetylglucosamine.svg and http://textbookofbacteriology.net/endotoxin.html, with modification.

Apart from being present on microbial surfaces, GlcNAc is also found in the host, shielded from the immune system in normal healthy individuals. It is present within the membrane bilayer of the host cells facing inwards towards the cytoplasm under normal conditions, wherein it plays a part in several physiological events. However, tissue injury and apoptosis may expose GlcNAc on the infected or dying host cells to the immune cells, which leads to phagocytosis and clearance of these cells from the host by macrophages. Besides acting as a central recognition moiety in PAMPs and dysfunctional host cells, GlcNAc has also been proposed to be effective in the treatment of various autoimmune diseases such as multiple sclerosis and osteoarthritis (Reginster et al., 2001; Felson and McAlindon, 2000). This is possibly due to its suppressive action on antibodies that limits their activity and on unprimed T cell response that interferes with functions of antigen presenting cells. Furthermore, recent studies have shown that children with treatment-resistant autoimmune inflammatory bowel disease display significant improvement upon GlcNAc administration (Salvatore et al., 2000). However, more research

needs to be done to explore the potential benefits and risks associated with this treatment regime.

1.1.2. Antigens

Recognition of PAMPs by innate immune sensors helps to defend the host by controlling bacterial proliferation and secreting nonspecific anti-microbial molecules during the first line of defense. However, this does not guarantee protection to the host against any subsequent infection as the immune receptors encoded in the host genome do not retain any memory of the PAMP recognition and the pathogen. To solve this problem and prepare the host for subsequent challenges, the adaptive immunity comes into action to provide long term memory and protection, by virtue of its ability to recognize specific patterns on the pathogen called antigens.

Antigens are generally peptides, proteins and polysaccharides forming components of cell wall, capsules, flagella, fimbrae and toxins of bacteria, viruses and other microorganisms (Janeway et al., 2005). They are normally categorized into following subtypes:

(i) Exogenous antigens enter the host from outside the body. Once they are in the system, they are normally phagocytosed by antigen-presenting cells (APCs). APCs process and present these antigens on class II major histocompatibility (MHC) to T helper cells ($CD4^+$). Activated $CD4^+$ T cells secrete cytokines to activate other immune cells, in order to control humoral and inflammatory responses (Watts 1997).

(ii) Endogenous antigens are produced within a host cell as a result of

normal cell metabolism or due to a bacterial or viral infection. They are presented to cytotoxic T cells (CTLs; $CD8^+$) through class I MHC molecules. Activated CTLs produce toxins to cause lysis or apoptosis of the infected host cell. Negative selection occurs to induce tolerance to self-antigens and recognize them from "non-self" antigens of the invading pathogen (Sant 1994).

(iii) Auto antigens are host antigens that are normally not recognized by the immune system but provoke an immune response in autoimmune diseases (Marshak-Rothstein and Rifkin, 2007).

The structural part of an antigen recognized by the antibody is called an epitope. Epitopes could be subdivided into: (i) conformational or discontinuous epitopes comprising of amino acids or segments from various parts of polypeptide antigen that are brought together in three-dimensional structure to give rise to the epitope and (ii) linear or continuous epitopes that are specific peptides of a protein antigen (Goldsby et al., 2003).

1.2. The host immune system

In order to combat the pathogens, the host has an elaborate immune system that includes a wide range of biomolecules and processes that act in a synchronized fashion to provide protection against the deadly invaders. To achieve this endeavour, the immune system first employs a group of molecules called "pattern-recognition receptors" that have the ability to detect a wide variety of infectious microbes such as bacteria, viruses and fungi and more importantly differentiate them as "non-self" as opposed to host's own "self" factors (Medzhitov et al., 1997). Upon specific recognition, the host employs

multiple defense mechanisms to neutralize and eventually clear the microbe from the system. These pathways mainly include phagocytosis, antimicrobial peptides, inflammatory cytokines and the complement system (Janeway et al., 2005). In addition to these general non-specific first line defenses, higher organisms such as jawed vertebrates have developed even more sophisticated defense mechanisms, wherein they specifically recognize the pathogen with high affinity antibodies, tune the immune system to adapt to the pathogen over time in developing an immunological memory, and recognizing and mounting an even stronger response in the event of a later infection by the same pathogen (Pancer and Cooper, 2006).

The immune response is classified into different stages when the host encounters a pathogen for the first time. The first line of defense comes from innate mechanisms that act instantly and are broader in terms of pathogen recognition. This is followed by activation of effector cells that secrete inflammatory mediators which aids in pathogen removal, but does not generate any immunologic memory. In case the pathogen evades this early phase of defense, acquired or adaptive immune response ensues wherein antigen-specific effector cells target the pathogen and generate memory cells that can prevent any future attack by the pathogen. **Figure 1.4** depicts the typical immune response as it seemingly occurs in two well-defined phases.

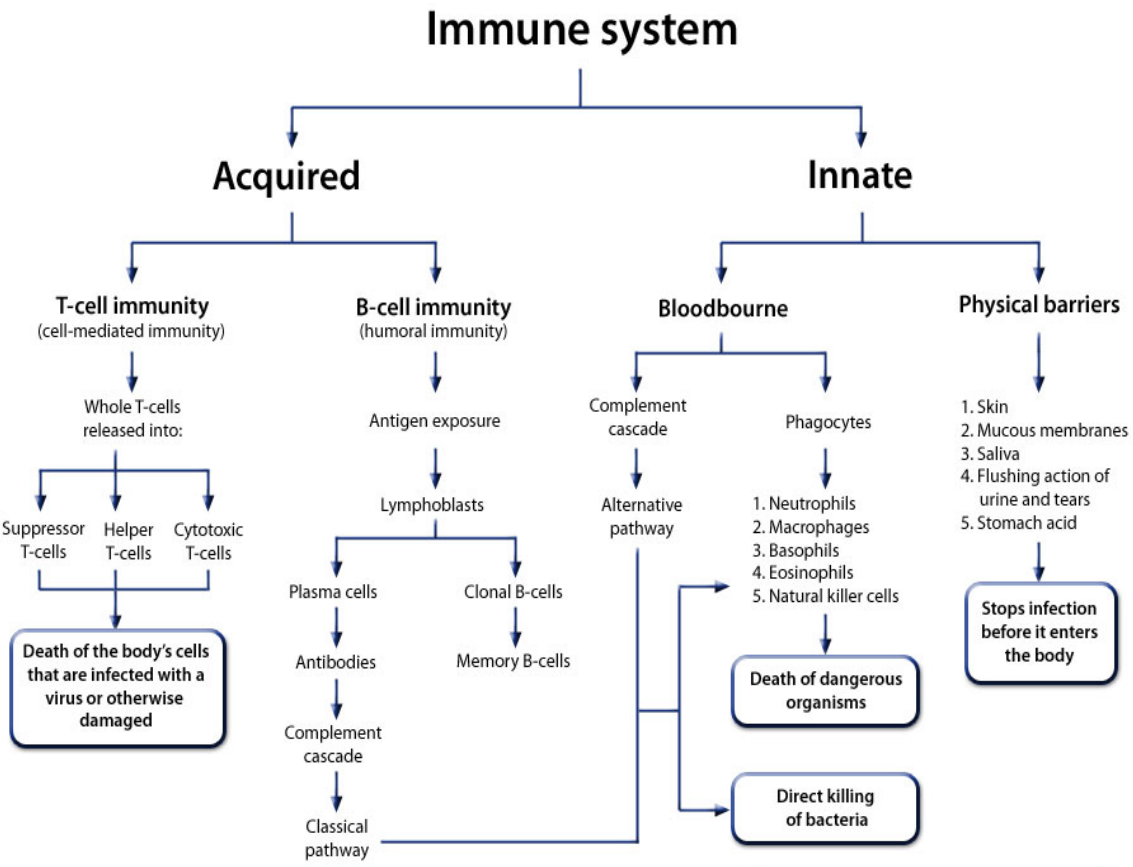

Figure 1.4: The response to an infection occurs in two phases. The innate immunity displays immediate response, broad spectrum specificity and depends on germline encoded receptors to recognize the pathogens. Adaptive or acquired immunity occurs at a later stage and uses antigen-specific receptors that are formed by gene segment rearrangements in B and T cells, which undergo clonal expansion before differentiating into effector cells that clear the infection. Adapted from http://www.virtualmedicalcentre.com/anatomy/immune-system/20.

1.2.1. Innate immunity

The innate immune system is the first line of defense against a foreign attack. It is non-specific in nature and comprises of a variety of cells and mechanisms that defend the host in immediate response to an infection (Janeway and Medzhitov, 2002). Innate immunity is considered to be an evolutionarily older defense strategy (Hoffmann et al., 1999). It carries out various effector

functions such as acting as physical barrier to the pathogen, recruiting immune cells to sites of infection by producing chemical factors called cytokines, activating the complement cascade to promote lysis and clearance of the pathogen, identification and removal of foreign substances from tissues by specialized white blood cells like macrophages and neutrophils (Janeway and Medzhitov, 2002). However, the innate immune system lacks memory and hence is deemed unable to launch a more effective response in the event of subsequent similar attacks. In this context, the innate immune system is construed to help in activating and shaping the second level of more specialized defense system called the adaptive immune system.

Pattern recognition receptors

Pattern recognition receptors (PRRs) are germline-encoded proteins, which sense the presence of microorganisms during the innate immune response. They do this by recognizing structures conserved among microbial species, which are called pathogen-associated molecular patterns (PAMPs). PRRs are also responsible for recognizing endogenous molecules released from damaged host cells, termed danger-associated molecular patterns (DAMPs) (Medzhitov and Janeway, 1997). The PRRs are broadly classified into different groups based on their location: transmembrane proteins such as Toll-like receptors (TLRs) (Medzhitov et al., 1997) and C-type lectin receptors (CLRs) (Epstein et al., 1996; Holmskov 2000), as well as cytoplasmic proteins such as Retinoic acid-inducible gene (RIG)-I-like receptors (RLRs) and NOD-like receptors (NLRs) (Inohara et al., 1999; Bertin et al., 1999). These PRRs

are expressed by not only by macrophages or dendritic cells as well as other non-professional immune cells. Upon sensing PAMPs or DAMPs by the PRRs, a cascade of pathways are activated leading to upregulation of transcription of pro-inflammatory cytokines such as tumor necrosis factor (TNF), interleukin (IL)-1, and IL6 (Adachi et al., 1998), chemokines and antimicrobial proteins and proteins involved in the modulation of PRR signaling (Kopp and Medzhitov, 1999). The expression patterns of the inducible genes differ based on PRR activation. The cytokines produced carry out a wide variety of effector functions like regulation of cell death of infected tissues, modification of vascular endothelial permeability, and recruitment of red blood cells to the infected tissue and induction of production of the acute-phase proteins (Dinarello 2007). A list of common PRRs is given below in **Table 1.1**.

Collectins and ficolins are well-known PRRs which belong to the family of soluble CLRs. They are present in serum and on the mucosal surfaces. The human collectins comprise of mannose-binding lectin (MBL) (Takahashi et al., 2006) and surfactant protein A and D (SP-A, SP-D) (Pikaar et al., 1995), which are composed of carbohydrate-recognition domains (CRDs) attached to collagenous regions. They are structurally similar to ficolins, which are composed of the fibrinogen-like domain (FBG) and collagen-like domain. The FBG domain, alternatively known as fibrinogen-like domain, is similar to the C-terminal region of the beta and gamma chains of fibrinogen, hence it is also referred to as Fibrinogen Beta Gamma (**Figure 1.5**).

Table 1.1: Examples of major pattern recognition receptors and their ligands.

Receptor	Ligand	Reference
Toll-Like:		
TLR1	triacylated lipoproteins	(Alexopoulou et al., 2002; Takeuchi et al., 2002)
TLR2	peptidoglycan, lipoproteins, zymosan	(Takeuchi et al., 1999; Underhill et al., 1999)
TLR3	double-stranded RNA, poly I:C	(Alexopoulou et al., 2001)
TLR4	LPS, RSV F protein	(Poltorak et al., 1998; Kurt-Jones et al., 2000)
TLR5	flagellin	(Hayashi et al., 2001)
TLR6	diacylated lipoproteins	(Hajjar et al., 2001)
TLR7	imidazoquinolines	(Hemmi et al., 2002)
TLR8	imidazoquinolines	(Gorden et al., 2006)
TLR9	bacterial DNA, unmethylated CpG motifs	(Hemmi et al., 2000)
Soluble:		
CD14	lipopolysaccharide	(Haziot et al., 1996)
LBP	lipopolysaccharide	(Schumann et al., 1990)
MBL	terminal mannose residues	(Jack et al., 2001)
CRP	phosphocholine	(Yother et al., 1982)
PTX3	fungal motifs	(Garlanda et al., 2002)
SP-A&D	fungi	(Holmskov et al., 2003)
Ficolins	GlcNAc	(Holmskov et al., 2003)
Scavenger:		
MSR1	lipid A, lipoteichoic acid	(Thomas et al., 2000)
MARCO	Gram-positive, gram-negative bacteria	(Kraal et al., 2000)
Mannose Receptor	α-mannan	(Ezekowitz et al., 1990)
Dectin-1	β-glucan	(Brown and Gordon, 2001)
Complement:		
FcγR	IgG-opsinized particles	(Daeron 1997)
CR1	C1q, C4b, C3b, MBL	(Wong et al., 1985)
CR2	iC3b, C3d, C3dg	(Dempsey et al., 1996)
CR3	iC3b	(Ehlers 2000)
CR4	iC3b	(Ross et al., 1992)
Intracellular:		
Nod2	muranyl dipeptide, lipoproteins	(Girardin et al., 2003; Inohara et al., 2003)
PKR	double-stranded RNA	(Meurs et al., 1990)
OAS	double-stranded RNA	(Rebouillat et al., 2000)

* Adapted and modified from Dempsey et al., 2003 (with modifications).

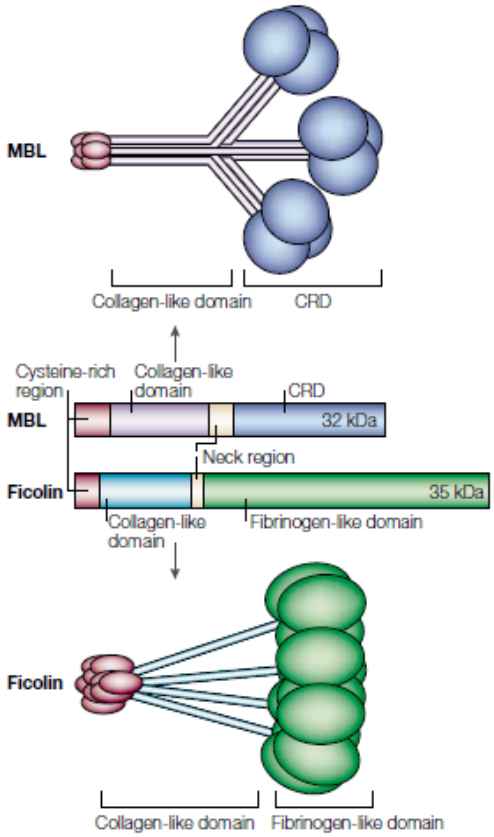

Figure 1.5: The schematic diagram of the structures of MBL and ficolins. Both of the PRRs contain the collagen-like domain, a neck region and the PAMP recognition domains: carbohydrate-recognition domain (CRD) for MBL and fibrinogen beta gamma/fibrinogen-like domain (FBG) for ficolins. Adapted from Fujita (2002).

These PRRs exhibit specific and selective binding to PAMPS like mannose, glucose, L-fucose, N-acetyl-mannosamine (ManNAc), and N-acetyl-glucosamine (GlcNAc) (Holmskov et al., 2003). These PAMPs must be present at a terminal non-reducing position and clustered on the microbe to form a "pattern", for high-avidity recognition to take place.

Ability to recognize these factors helps the PRRs to distinguish microbes from host cells (Garlatti et al., 2007). Carbohydrate structures on host cells terminate in sugars such as, galactose or sialic acid, which are not recognized by PRRs (Hansen et al., 2000). However, exception might occur in

host cancer cells and apoptotic cells which get aberrantly glycosylated, and hence are recognized and cleared by PRRs (Ma et al., 1999; Muto et al., 1999).

Ficolins

Ficolins were first described as transforming growth factor *β*-binding proteins present in porcine uterus (Ichijo et al., 1991). Porcine ficolins consist of two homologous molecules, designated ficolin-α and -β (Ichijo et al., 1993). Ficolin-α is found in the liver and blood. Ficolin-β, which is about 80% identical to ficolin-α, is expressed mainly in neutrophils. In mice, there are also two isoforms of ficolin present. Ficolin A is present in liver and blood, while ficolin B (60% identical to ficolin A) is expressed in the bone marrow and spleen and is present on macrophages (Liu et al., 2005). In humans, there are three isoforms of ficolins present, M-ficolin (ficolin-1); L-ficolin (ficolin-2); and H-ficolin (ficolin-3). All three isoforms exist as homotrimers and polymers (Holmskov et al., 2003) (**Figure 1.6**).

M-ficolin, predominantly found in monocytes and granulocytes (Teh et al., 2000; Rorvig et al., 2009), is the homologue of murine ficolin-B (Endo et al., 2004) and porcine ficolin-β. It has been found to recognize common microbial PAMPs like GlcNAc. L-ficolin is the homologue of murine ficolin-A (Endo et al., 2004) and porcine ficolin-α. It is an oligomeric protein assembled from 35-kDa subunits (Matsushita et al., 1996) and exhibits lectin-like activity after recognizing PAMPs such as 1, 3-β-D glucan on yeast and fungal cell walls (Ma et al., 2004) and GlcNAc on LPS of bacteria (Krarup et

al., 2004). In particular, L-ficolin binds to GlcNAc next to galactose at the non-reducing terminal of the oligosaccharide. H-ficolin, the third ficolin, was originally identified and defined by auto-antibodies present in a small minority of auto-immune lupus patients (Andersen et al., 2009). It is synthesized in the liver and secreted into the bile, blood, lung and bronchi (Akaiwa et al., 1999). H-ficolin is the most abundant plasma ficolin and it exhibits highest potency at activating complement *in vitro*. H-ficolin binds to GlcNAc and GalNAc but not mannose or lactose. M- and L-ficolin share 80% identity in amino acid sequence, whereas H-ficolin shares about 50% identity with the other two isoforms (Zhang et al., 2009). However, all three ficolins share around 80% similarity in their FBG domain which recognizes PAMPs, suggesting that their ability to recognize pathogens and carry out effector functions may be conserved.

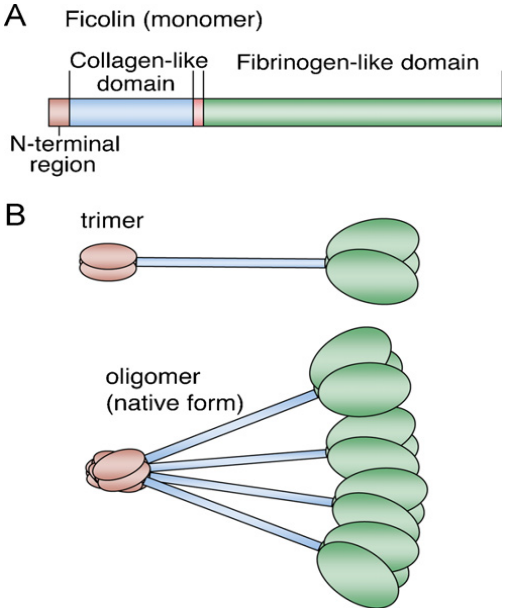

Figure 1.6: Domains and oligomeric structure of ficolins. (**A**) The ficolin monomer consists of a collagen-like domain, a neck region and a fibrinogen beta gamma/fibrinogen-like domain (FBG). (**B**) Trimers and oligomers (four to eight trimers) are formed by disulphide bond formation between the collagen-like domains of individual monomers. Multimers form a bouquet-like structure where FBG functions as the PAMP recognition domain. Adapted from Endo et al., (2011).

Overall, the characterization of the ficolins present in human, mouse and pig serum/plasma and in the body fluids of ascidians revealed that they all share a common specificity for GlcNAc (Matsushita et al., 1996; Matsushita et al., 2001). The ficolin genes in other species such as hedgehog, xenopus, worms and fruitfly are yet to be fully characterized. Upon recognizing the pathogens, the ficolins activate the lectin complement pathway (Teh et al., 2000; Matsushita et al., 2001; Kuraya et al., 2005). A comparison of the tissue distribution, ligand specificity and function of human and mouse ficolins is summarized in **Table 1.2**.

Table 1.2: The tissue distribution, ligand spectrum and functions of ficolin isoforms in humans and mice.

Characteristics of human and mouse ficolins.

Species	Ficolins	mRNA expression	Protein identified	Binding substance	Function
Human	L-ficolin	Liver	Serum	Acetylated compounds, (1→3)-β-D-glucan, LPS, capsular polysaccharides of *Streptococcus agalactiae*, lipoteicoic acid, CRP, PTX3, fibrinogen, fibrin, DNA, elastin, corticosteroid	Association with MASP and complement activation, opsonin
	H-ficolin	Liver, lung	Serum, bile duct, bronchus, alveolus	Acetylated compounds, PSA from *Aerococcus viridens*, LPS from *Hafnia alvei*	Serum H-ficolin is associated with MASP and activates complement
	M-ficolin	Monocyte, lung, spleen	Serum, monocyte, granulocyte, alveolar epithelial cell	Acetylated compounds (GlcNAc, GalNAc, sialic acid)	rM-ficolin is able to associate with MASP and activate complement
Mouse	Ficolin A	Liver, spleen	Serum	GlcNAc, GalNAc, elastin	Association with MASP and complement activation
	Ficolin B	Bone marrow, spleen (myeloid cell lineage)	Bone marrow	GlcNAc, GalNAc, sialic acid	Association with MASP and complement activation, opsonin

*Adapted from Matsushita (2012)**.**

Pathophysiological significance of ficolins

Ficolins have been implicated to play an important role in preventing various infectious diseases. L-ficolin binds to the GlcNAc in the capsular polysaccharide of type III group B streptococci and leads to activation of the lectin pathway (Aoyagi et al., 2005). L-ficolin also binds to lipoteichoic acid (LTA) of gram-positive bacteria (*Staphylococcus aureus*, *Streptococcus*

agalactiae, *Bifidobacterium animalis*, *Streptococcus pyogenes*, and *Bacillus subtilis*) (Lynch et al., 2004; Aoyagi et al., 2005). In addition, L-ficolin has been found to bind exclusively to some strains of capsulated *S. pneumoniae* serotypes (11A, 11D, and 11F). Recently, the porcine counterpart of L-ficolin has been shown to curb the infection of porcine reproductive and respiratory syndrome virus *in vitro* (Keirstead et al., 2008). H-ficolin has shown to be a more powerful direct opsonin than L-ficolin (Jensen et al., 2007). It was firstly identified as a serum antigen target for an auto-antibody present in the sera of some patients with systemic lupus erythromatosus (SLE), suggesting that it may be an important player during the auto-immune response. Concentration of anti-H-ficolin antibodies was found to correlate positively with disease activity (Yoshizawa et al., 1997). Recent studies have highlighted the role of H-ficolin in preventing bacterial sepsis and necrotising enterocolitis in newborns, wherein it was shown to bind to pathogens and activate complement which clears them (Schlapbach et al., 2010; Schlapbach et al., 2011).

Ficolins have also been reported to bind to late apoptotic cells and mediate phagocytosis possibly through the calreticulin-CD91 receptor complex present on the surface of macrophages (Ogden et al., 2001). Ficolins possibly bind to DNA on permeable dying cells (Jensen et al., 2007). It has been found that H-ficolin results in uptake of late apoptotic cells by macrophages (Honoré et al., 2007). These studies show that ficolins may be involved in the maintenance of tissue homeostasis and dysfunction in the activity of ficolins might adversely affect the removal of dying host cells and

lead to the development of autoimmune diseases.

1.2.2. Adaptive immunity

The adaptive immune system is the second line of defense, which is highly specific in its ability to recognize and remember specific pathogens and to mount stronger, faster and long-lasting responses when the host re-encounters the same pathogen in future (Janeway et al., 2005). Adaptive immune responses are carried out by white blood cells called lymphocytes. There are two broad classes of such responses - *humoral* and *cell-mediated*. These effector functions are carried out by different classes of lymphocytes, called B cells and T cells, respectively (Janeway et al., 2005). In humoral immune responses, B cells are activated by professional APCs like macrophages and dendritic cells, and differentiate into plasma cells, with the help of T-helper cells. The plasma B cells are short lived cells (2–3 days) which secrete antigen-specific antibodies. Some of the plasma B cells become long-lived memory B cells, which respond quickly to any future attack by the same pathogen. Antibodies secreted by the B cells circulate in the bloodstream and permeate the other body fluids, where they bind specifically to the foreign antigen that stimulated their production. Upon binding to the antigen, antibodies inactivate the invading microbes and limit the spread of infection by directing the immune complexes to the spleen (Janeway et al., 2005).

In cell-mediated immune responses, naïve T cells encounter the antigen presented by dendritic cells or B cells and are activated to react directly against a foreign antigen. The activated T cells secrete cytokines

leading to the expansion of the T cell population. Some T cells may become helper cells and secrete cytokines that attract other immune cells like macrophages, neutrophils and other lymphocytes to the site of infection to phagocytose and kill the pathogen. Another subset of T cells may become cytotoxic in nature and track down and kill the infected host cells displaying virus antigens on their surface, so as to limit the infection and its spread to other normal cells and tissues (Delves and Roitt, 2000).

Antibodies (antigen specific)

Antibodies are glycoproteins belonging to the immunoglobulin superfamily that are secreted into the bloodstream by the plasma B cells. They are typically made of basic structural units consisting of four polypeptide chains: two identical heavy chains and two identical light chains, joined together by disulphide bonds (Burton and Woof, 1992). There are five isotypes of mammalian antibodies: IgM, IgG, IgA, IgD and IgE, depending on the specific heavy chain present (Janeway et al., 2005; Stavnezer and Amemiya, 2004). A typical structural representation of various antibody isotypes is shown below in **Figure 1.7**.

IgM is a pentamer having the highest avidity amongst all isotypes. It is the first antibody isotype to be present before class-switching occurs and helps in eliminating pathogens in the early stages of humoral immunity. IgG is the major isotype present in the serum and consists of four subtypes (IgG1, IgG2, IgG3 and IgG4). IgG is the only isotype that can cross the placental barrier to provide immunity to the fetus and newborns. IgA is present at the mucosal

surfaces like the gut, respiratory tract and the urogenital tract, where it plays an essential role in mucosal immunity. It is also found in secretions like saliva, tears and milk. Besides these immunoglobulins, IgD helps in activating basophils and mast cells, whereas IgE is an important factor in allergy and parasitic infections. Besides these functions, antibodies also enhance other defense mechanisms like activation of the complement system, enhancement of phagocytosis and stimulation of other immune cells (Alberts et al., 2002; Harlow and Lane, 1988). **Figure 1.8** shows a representation of the different biological activities carried out by antibodies.

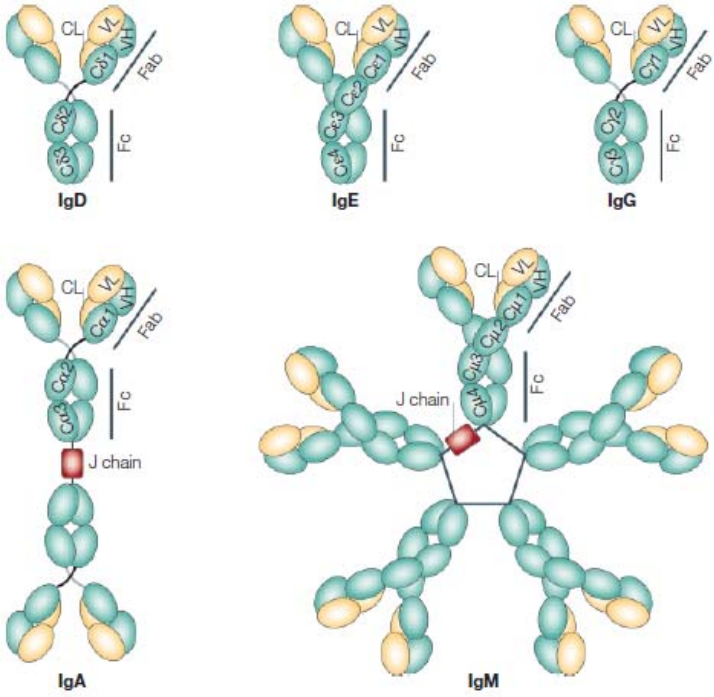

Figure 1.7: Structural representation of mammalian antibody isotypes. Antibodies are composed of two identical heavy chains and two identical light chains, linked by disulphide bridges. The isotype of antibody is determined by its heavy chain, with all isotypes sharing the same light chains. Light chains fold into a variable domain (V_L) and a constant domain (C_L), whereas heavy chains are composed of one variable domain (V_H) and either three (in IgG, IgA and IgD) or four (in IgM and IgE) constant domains. The antigen-binding sites at the tip of the Fab regions are formed from the variable domains of both the heavy and light chains. The Fc region mediates interaction with effector molecules, such as complement and Fc receptors. Adapted from Rojas and Apodaca, (2002).

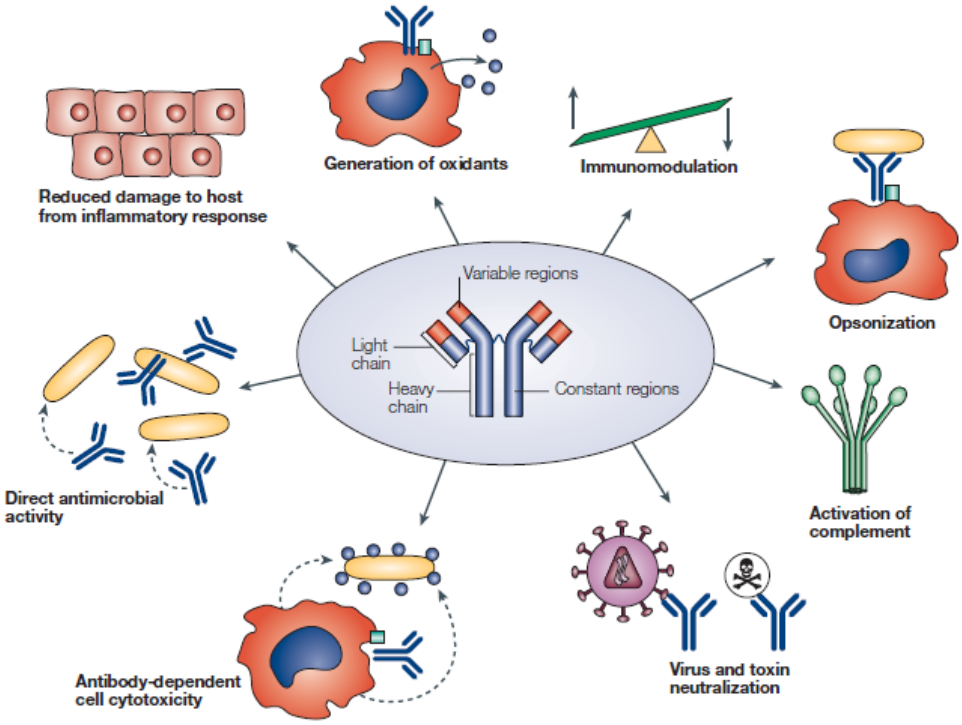

Figure 1.8: The biological activities of antibodies. Antibodies may directly bind and neutralize toxin and viruses, as well as collaborate with other serum factors to carry out opsonization, complement activation and generation of oxidants, upon antigen exposure. They also help to reduce the extent of damage to the host by reducing the inflammation once the infection has been cleared. Other functions include antibody-dependent cell cytotoxicity and immuno-modulation. Adapted from Casadevall et al., (2004).

Mechanisms leading to production of different antibody isotypes

Several genetic mechanisms have evolved that allow B cells to generate a diverse pool of antibodies upon antigenic stimulation. The primary event occurring in naïve B cells is the *V(D)J recombination* (Jung and Alt, 2004), which occurs in the bone marrow and is catalyzed by enzymes called VDJ recombinases (Oettinger et al., 1990). Naïve B cells produce only IgM, which is the first heavy chain segment in the immunoglobulin locus. When a naïve B

cell encounters a pathogen displaying the particular antigen, it enters the dark zone of the germinal center in the spleen where it undergoes affinity maturation, producing antibodies with increased affinity for the antigen (Kelsoe 1996; Tarlinton 1998; MacLennan 1994). Upon entering the germinal centers, the B cells undergo proliferation which is accompanied by a high rate of mutation in the immunoglobulin heavy and light chain genes (somatic hypermutation), carried out by an enzyme called Activation-induced cytidine deaminase (AID) that mutates cytosine to uracil. This process generates antibodies with several fold higher affinity for the same antigen. Next, the B cells that have undergone somatic hypermutation undergo clonal selection so that only the B cell progeny producing antibodies with the highest affinity for the antigen are able to survive. The remaining B cells undergo apoptosis (Tarlinton and Smith, 2000). Once the B cells have undergone SHM and clonal selection, class-switch recombination occurs in the light zone of the germinal center to generate the different isotypes (IgG, IgA, IgD or IgE) of the antibody with the same variable domains but distinct constant domains in their heavy chains (Stavnezer et al., 2008). This process is catalyzed by a variety of enzymes including AID (Muramatsu et al., 2000; Revy et al., 2000). The B cells finally differentiate into memory B cells and plasma B cells producing high affinity antigen-specific antibodies. **Figure 1.9** gives an overview of all the B cell selection processes taking place in the germinal centers.

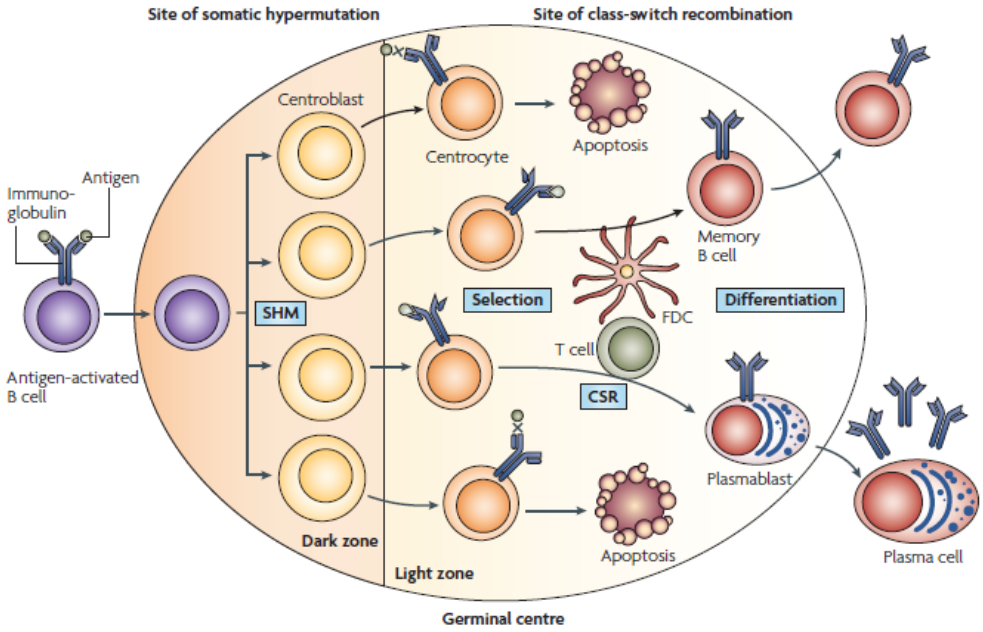

Figure 1.9: B cell selection process in the germinal center during an immune response. Antigen-activated naïve B cells differentiate and undergo proliferation in the dark zone of the germinal center. During proliferation, the process of somatic hypermutation (SHM) introduces base-pair changes into the V(D)J region of the rearranged genes encoding the immunoglobulin variable region (IgV) of the heavy chain and light chain. The differentiated B cells then move to the light zone, where the modified antigen receptor, with help from T helper cells and follicular dendritic cells (FDCs), is selected for improved binding to the immunizing antigen (clonal selection). Newly generated B cells that produce lower affinity antibodies undergo apoptosis and are removed. B cells then undergo immunoglobulin class-switch recombination (CSR). Antigen-selected mature B cells eventually differentiate into memory B cells or plasma B cells. Adapted from Klein and Dalla-Favera, (2008).

Natural antibodies (non-antigen specific)

Apart from the antigen-specific antibodies produced upon immune response, a pool of spontaneously occurring immunoglobulins is also present in human cord blood, in "antigen-free" mice, and in normal individuals in the absence of prior foreign antigen stimulation. These antibodies are referred to as "natural antibodies" (Avrameas 1991; Coutinho et al., 1995). They are produced by the B1 cell lineage. B1 cells differ from the conventional B2 cells (producing

antigen-specific antibodies in immune response) in that they are generated predominantly during fetal and neonatal development (Kantor and Herzenberg, 1993; Hardy and Hayakawa, 1994). They are mainly found in the peritoneal and pleural cavities. Their precursors develop in the fetal liver and omentum. In adults, the B1 B cell population is maintained at a constant size owing to the self-renewing capacity of these cells, due to which the serum levels of natural antibodies are maintained (Boyden 1966; Michael 1969). These B1 B cells recognize altered-self components (DAMPs) such as asialylated glycoproteins with exposed terminal galactose residues, and secrete low affinity antibodies. The natural antibodies are usually of IgM, IgG3 and IgA subclass (Boyden 1966; Manz et al., 2005; Kantor and Herzenberg, 1993). Anti-α gal antibody is one of the most abundant *bona fide* natural antibodies in the human serum. The repertoire of natural antibodies is very restricted compared to the conventional antibodies, due to preferential usage of J_H-proximal V_H gene segments and the lack of terminal deoxynucleotidyl transferase activity in precursor B cells during early ontogeny (Yancopoulos et al., 1984; Feeney 1990).

Pathophysiological significance of natural IgM

Amongst the natural antibody isotypes, natural IgM is a pentamer and possesses potentially 10 antigenic binding sites. The high valency enables IgM to have a polyreactive character and identify multiple phylogenetically conserved structures like nucleic acids, phospholipids and carbohydrates (Briles et al., 1981). The repertoire of natural IgM remains unaffected by

external antigens (Haury et al., 1997). Many studies have identified a protective role of natural IgM in numerous viral, bacterial, fungal and parasitic infections (Zhou et al., 2007). Viruses, including the vesicular stomatitis virus (VSV), lymphocytic choriomeningitis virus and influenza virus, are bound and neutralized by natural IgM (Ochsenbein et al., 1999; Baumgarth et al., 2005). Mice deficient in natural IgM are increasingly susceptible to infection owing to decreased neutrophil recruitment, increased bacterial load and elevated levels of LPS and pro-inflammatory cytokines in the serum due to lack of bacterial clearance. Reconstitution with IgM purified from uninfected mouse serum provided immediate defense against bacterial peritonitis to mice (Boes et al., 1998). Natural IgM has also been shown to play a role in clearing *S. pneumoniae* and *Cryptococcus neoformans* infections (Brown et al., 2002; Subramaniam et al., 2010).

Natural antibodies have also been shown to link between innate and adaptive immune systems. During the innate immune response, natural IgM limits the spread of infection by employing various strategies like neutralization, forming immune complexes with the help of complement factors leading to complement activation and elimination of the pathogen by lysis. In addition, natural IgM is also involved in priming the subsequent adaptive immune response by contributing to antigen recruitment in secondary lymphoid organs (**Figure 1.10**).

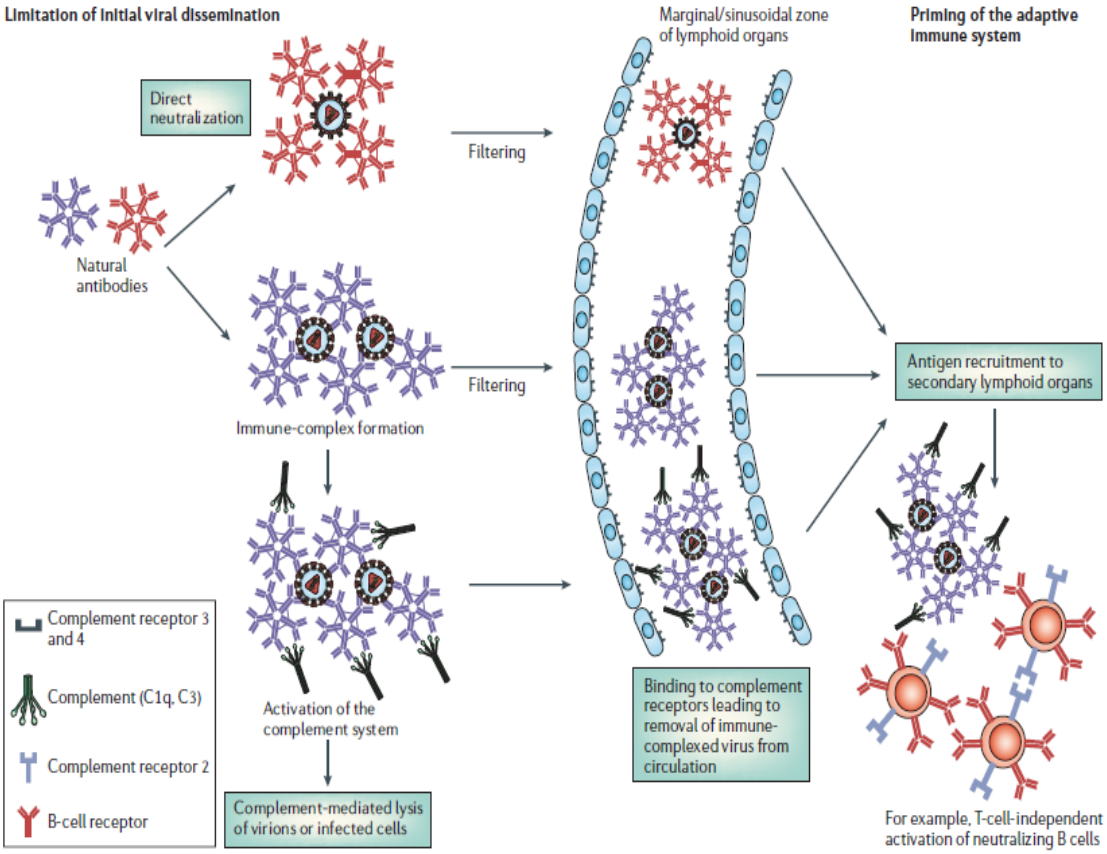

Figure 1.10: Natural antibodies serve as a link between innate and adaptive immune systems. The natural antibodies restrict the pathogen invasion by direct neutralization, complement activation and elimination in the marginal/sinusoidal zone of secondary lymphoid organs. They also prime the adaptive immune system by contributing substantially to antigen recruitment in secondary lymphoid organs. Adapted from Hangartner et al., (2006).

Natural IgM has been further shown to participate in several patho-physiologic activities like apoptosis, B cell homeostasis, inflammation, artherosclerosis and auto-immunity. Due to its pentameric structure, natural IgM is known to bind to complement factor C1q with high affinity (Czajkowsky and Shao, 2009) and carry out effector functions like the activation of complement cascade and clearance of apoptotic cells (Quartier et al., 2005; Ogden et al., 2005). Natural IgM could also bind to MBL bound to

apoptotic cells and vice versa (Nauta et al., 2003) (**Figure 1.11**). It is also implicated that natural IgM influences other effector functions like antigen uptake by phagocytes and enhancement of B cell responses, by binding to its putative receptor, Fcα/μR (Shibuya et al., 2000).

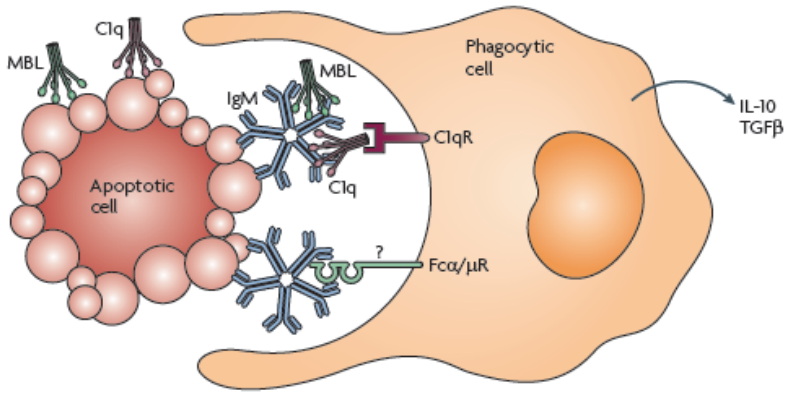

Figure 1.11: Natural IgM directs apoptotic cells to macrophages through recruitment of C1q and MBL. Complement factor C1q binds to the Fc region of pentameric natural IgM and functions together with MBL to promote the phagocytosis of apoptotic cells. Ingestion of apoptotic cells by phagocytes promotes an immunoregulatory milieu including the secretion of anti-inflammatory cytokines IL-10 and TGFβ and clearance of potential auto-immune epitopes from the body tissues. Adapted from Ehrenstein and Notley (2010).

Despite a vast amount of information available on natural IgM and its role in immunity, the physiologic existence and function of natural IgG and IgA antibodies, which comprise a majority of natural antibodies in serum and mucosa, has been an enigma and a subject of interest since their discovery ((Boyden 1966; Michael 1969). Because of their low affinity, non-specific character and low valency when tested in isolation, they have been deemed incapable of launching an attack on invading pathogens.

1.2.3. Does the innate immune system shape the adaptive immune system?

Although the immune system acts in apparently two separate phases, there are

several reports where the innate and adaptive immune systems are shown to cooperate to effectively fight the infection. Adaptive immunity is controlled by innate immune PRR induced signals at multiple checkpoints dictating the initiation of the adaptive response depending on the origin of the antigen, the type of response, the magnitude and duration of the response depending on the dose of the antigen, and the production of long-term memory (**Figure 1.12**). This instruction is largely dissipated through triggering the maturation of dendritic cells from highly phagocytic, weakly immunogenic, tissue-resident cells into weakly phagocytic, highly immunogenic, lymph node-homing cells that are competent to induce tailored T-cell responses to non-self antigens acquired in the periphery (Iwasaki and Medzhitov, 2004; Banchereau and Steinman, 1998).

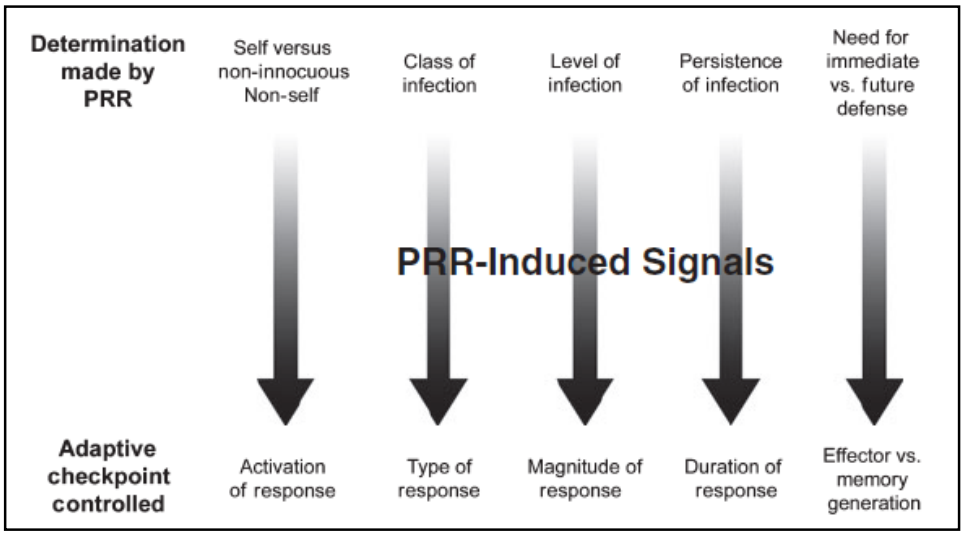

Figure 1.12: PRR-mediated control of checkpoints of adaptive immunity. PRRs detect the features of the antigen during an infection and induce signals that control adaptive immunity at various checkpoints. This ensures controlled activation of the adaptive immune response. A failure to properly regulate the immune response results in various immune pathologies like auto-immunity, allergy and failure to protect from infection. Adapted from Palm and Medzhitov, (2009).

PRRs differ in their ability to trigger the adaptive immune response. For example, TLRs are sufficient to induce both T- and B-cell responses by themselves, whereas others like the mannose receptor and scavenger receptors require other components to induce adaptive immune responses. This depends on the ability of the PRR to detect the presence, extent, duration of infection, origin of microbial antigens, as well as its ability to relay this information to the adaptive immune system (Iwasaki and Medzhitov, 2004). Thus, it is evident that both the arms do not act individually but the innate system indeed influences its adaptive counterpart to optimize the immune response.

1.3. Host-pathogen interaction and immune response

In order to tackle a wide variety of pathogens, different components of the immune system have evolved to protect the host in an efficient manner. The innate immune defense which is the first line of protection against the invading microorganisms has evolved into two different arms: the cellular and humoral components (Basset et al., 2003). These defense components perform effector functions in their own specialized manner. The humoral components like the collectins, ficolins, LPS-binding protein, pentraxins and complement, help to recognize the PAMPs associated with the pathogen. Upon recognition, they function to directly or indirectly (PRR**:**PRR interactome formation) to eliminate the pathogen through various defense mechanisms, like activation of the complement. Alternatively, the PAMPs may be recognized by cellular PRRs present on immune cells with the help of soluble PRRs, and become phagocytosed, leading to the production of pro- and anti-inflammatory

cytokines that control the spread of infection to neighboring healthy cells. Subsequently, these mechanisms lead to activation of the adaptive immune response which launches a more specific attack in the event of any future infection (**Figure 1.13**).

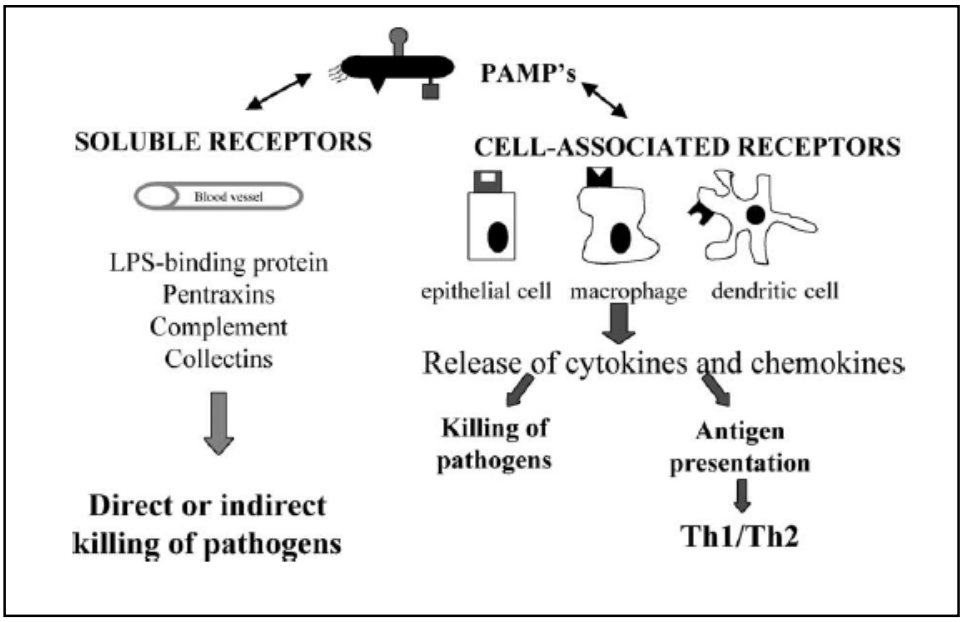

Figure 1.13: Receptors involved in detection and elimination of the pathogen in innate immune response. Pathogens are detected by soluble and cell-associated PRRs, which lead to direct or indirect killing of the pathogen, release of cytokines and chemokines which boost the innate immune response and alert the adaptive immune response. Figure adapted from Basset et al., (2003).

1.3.1. Formation of PRR:PRR interactome – immune complexes

To cater to the wide variety of microbes and damaged host cells, the PRRs of the innate immune system collaborate with each other to mount a stronger more effective immune response. This is an important defense strategy as PRRs are limited in number compared to the wide variety of antigen-specific antibodies that are later produced by the adaptive immune system. An important example of PRR:PRR interactome formation is the collaboration of

CRP and ficolin during infection. CRP is an activator of the classical complement pathway, whereas ficolins initiate the lectin complement pathway. Human L- and M-ficolins were found to interact with CRP via their FBG domain (Zhang et al., 2009). This leads to two autonomous complement amplification pathways (**Figure 1.14**), giving a boost to the bactericidal activity. Infection-inflammation condition induces local acidosis (pH 6.5) and hypocalcaemia (2.0 mM calcium), which plays an important role in strengthening the interaction and hence boosting the immune response (Zhang et al., 2009).

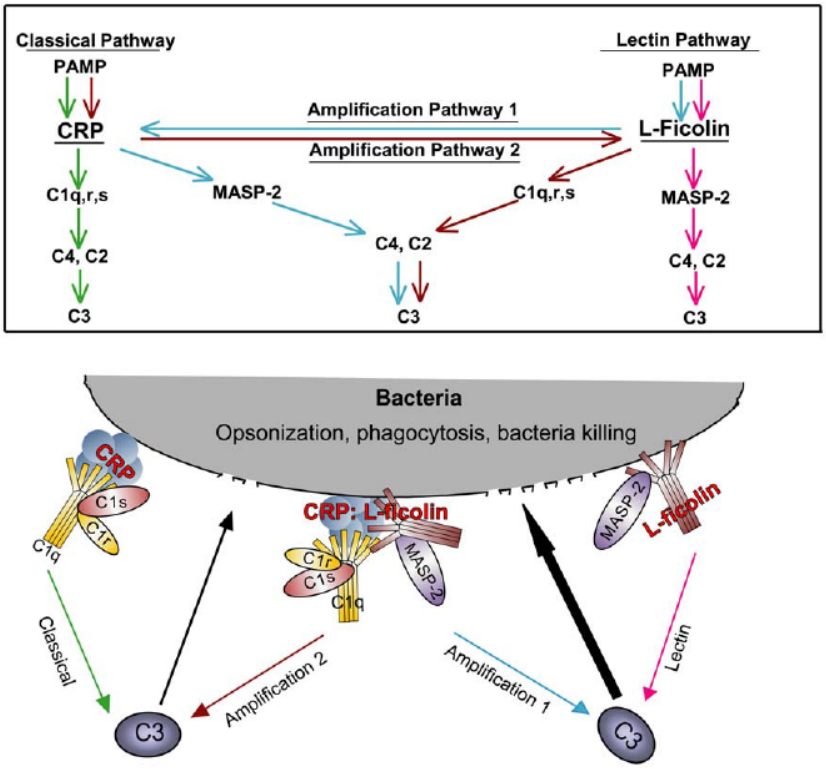

Figure 1.14: L-ficolin and CRP interact to form an interactome having enhanced anti-microbial activity. The infection-inflammation condition triggers the formation of CRP**:**ficolin interactome on the bacterial surface, resulting in amplified activation of the complement pathway. By this collaboration, two autonomous pathways function simultaneously to boost the classical and lectin complement pathways. Adapted from Zhang et al., (2009).

Furthermore, the importance of PRR**:**PRR interactome was also shown in other studies wherein M-ficolin present on the surface of monocytes collaborates with CRP in the serum and GPCR43 (receptor on monocytes) to form a triple complex, that carried out a range of functions which transduced the immune signals into the host cell and regulated the immune response to restore homeostasis (Zhang et al*.,* 2010). Therefore, the formation of PRR**:**PRR interactomes during an immune response is an important defense strategy for effective microbial clearance.

1.3.2. Infection induces local acidosis and hypocalcaemia

The human immune system makes use of the ensuing inflammatory response during infection to combat the pathogen (Bistrian 2007). During the acute phase response, there is a spike in the concentrations of several proteins like CRP (Gewurz et al., 1982; Marnell et al., 2005) and inflammatory cytokines (Gallin 1999). During this process, local acidosis prevails which leads to infiltration of neutrophils and macrophages to the site of injury (Issekutz and Bhimji, 1982). This activates a respiratory burst (van Zwieten et al., 1981; Wright et al., 1986), which leads to local drop in pH levels. Local acidosis is associated with a number of inflammatory diseases such as trauma-induced infection (Baranov and Neligan, 2007), acute renal failure (Zar et al., 2007) and intra-abdominal infection (Simmen and Blaser, 1993). These pathological conditions are associated with a drop in pH resulting in lower serum pH, ranging from 5.5-7.0 (Martinez et al., 2006). Simultaneously, mild hypocalcaemia also occurs, which is a characteristic of bacterial infections

(Beers 2000). The possible explanation for this drop in calcium level in the serum is due to the intracellular NF-κB activation which requires calcium influx into the immune cells (Feske 2007), which is further strengthened under acidic condition (Cairns et al., 1993; Trevani et al., 1999). This event causes a transitory drop in the extracellular calcium levels at the site of infection where the immune cells are present. These transient changes, which cause a drop in local pH and calcium levels result from pathogenic metabolic disorder (Morris and Low, 2008).

Local acidosis and hypocalcaemia have been shown to play a crucial role in host defense. It induces stronger interaction between CRP and ficolin, which leads to the amplification of complement pathways (Zhang et al., 2009). TLRs 3, 7, 8 and 9 all require acidic environment for their activation of the endosomes (Iwasaki and Medzhitov, 2004). Extracellular acidosis also has implications in boosting the adaptive immune response where it activates dendritic cells (Vermeulen et al., 2004) and CD8+ T cells in the peripheral tissues to improve MHC class I-restricted antigen presentation by the neutrophils (Ackerman and Cresswell, 2004). These studies suggest that pH and calcium conditions resulting from inflammation during an infection may play a crucial role in favor of the host to eliminate the pathogen. In this thesis, we used the simulated infection-inflammation condition referring to pH 6.5 and 2.0 mM calcium levels while the normal/uninfected physiological condition referring to pH 7.4 and 2.5 mM calcium levels, for our *in vitro* studies concerning interaction between the proteins involved during pathogen recognition and subsequent clearance.

1.3.3. Complement activation

The extracellular responses to an infection are triggered and carried out by soluble components of the immune system. One of the important components of the humoral immune system is the complement. The complement system consists of a tightly regulated network of proteins that play an important role in host defense and inflammation. Complement activation results in opsonization of pathogens, lysis and their removal by phagocytes through the process of phagocytosis. Complement also plays an important role in adaptive immunity involving T and B cells that help in the elimination of pathogens (Dunkelberger and Song 2010; Molina et al., 1996) and in maintaining immunologic memory, preventing pathogenic re-invasion.

Complement activation is known to occur through three different pathways: classical, lectin and alternate involving proteins that mostly exist as inactive zymogens, which are sequentially cleaved and activated. Antigen-specific antibodies and ficolins bind to the pathogen and initiate classical and lectin pathways, respectively. All the pathways converge at the canonical complement C3, which is the most abundant complement protein found in the blood. This results in the activation of C3a, C3b, C5a and the formation of the membrane attack complex (C5b-9) on the microbial surface leading to lysis (**Figure 1.15**). The complement C3 is known to bind covalently with heavy chain of immunoglobulins when in the presence of immune complexes (Sahu et al., 1994). Hence, during the course of our study, we will be interested to study whether C3 plays a role in helping natural IgG in recognizing the pathogen and is involved in subsequent immune response.

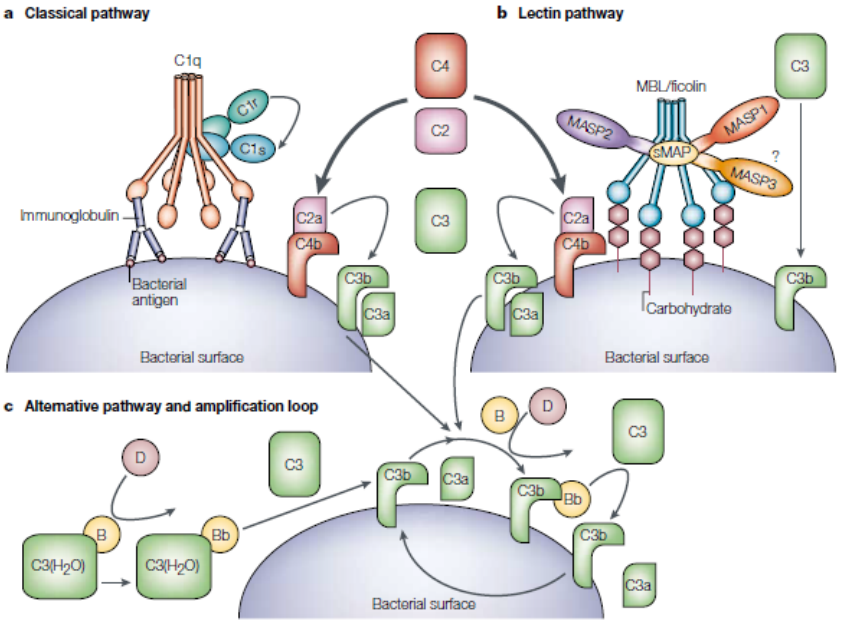

Figure 1.15: Activation of the classical, lectin and alternative complement pathways. All the pathways are initiated by different mechanisms, but converge at the activation of complement C3. Adapted from Fujita (2002).

1.3.4. Phagocytosis

Phagocytosis is an important process in innate immune defense which results in the uptake and removal of the opsonized pathogens by phagocytes. This process is accompanied by intracellular signals that trigger diverse cellular processes (**Figure 1.16**), such as cytoskeletal rearrangement, alterations in membrane trafficking, activation of microbial killing mechanisms, production of pro- and anti-inflammatory cytokines and chemokines, activation of apoptosis, and production of molecules required for efficient antigen presentation to the adaptive immune system (Aderem and Underhill, 1999; Greenberg 1999).

Phagocytes express a broad spectrum of receptors that participate in

particle recognition and internalization. Some of these receptors are capable of transmitting intracellular signals that trigger phagocytosis, while other receptors appear to participate in binding or to increase the efficiency of internalization. One of the prominent phagocytic receptors is the group of Fc receptors (FcRs). IgG-opsonized particles are recognized by several surface receptors that bind to the Fc region of IgG (FcγRs) (Ravetch and Bolland, 2001; Daeron 1997). Phagocytes such as macrophages or neutrophils express different combinations of FcγRs. FcγRs fall into two classes: (a) receptors that contain immunoreceptor tyrosine-based activation motifs (ITAM) in their intracellular domains that recruit kinases and activate phosphorylation cascades, and (b) receptors that contain immunoreceptor tyrosine-based inhibition motifs (ITIM), which recruit phosphatases that inhibit signaling (Ravetch and Bolland, 2001; Daeron 1997). Activating receptor with high affinity (FcγR1) binds IgG opsonized particles and triggers internalization through actin polymerization beneath the particle, membrane recruitment to the site of particle contact, membrane extension outward to surround the particle, finally leading to particle engulfment (Aderem and Underhill, 1999). The efficiency of the process is regulated by co-ligation of the inhibitory FcγR (FcγRIIB) (Ravetch and Bolland, 2001). Microbe internalization by FcγR1 on phagocytes is usually accompanied by the production of pro-inflammatory cytokines like IL8 and activation of antimicrobial mechanisms (Daeron 1997; Ravetch and Clynes, 1998).

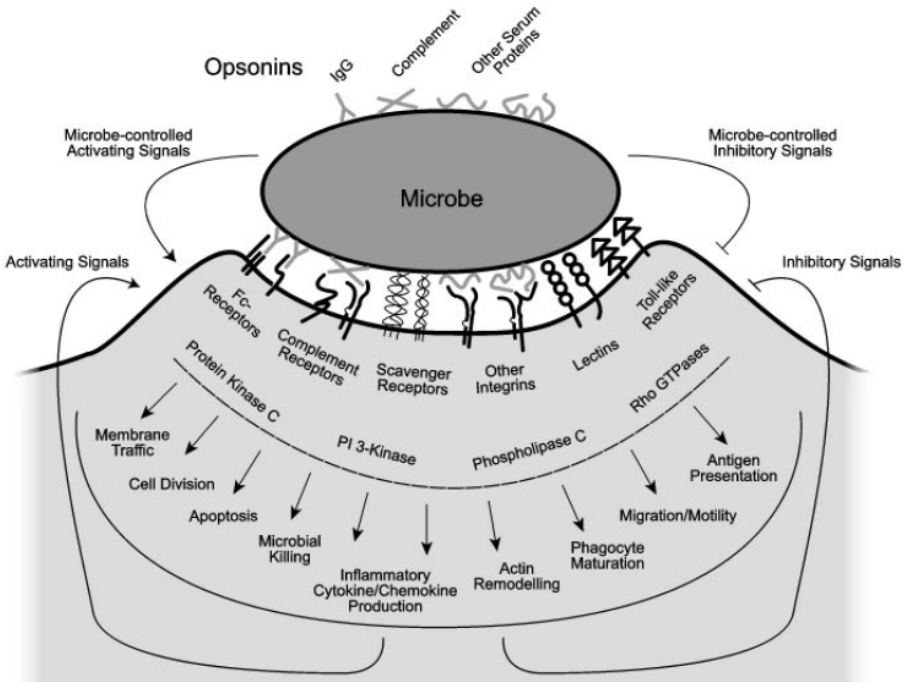

Figure 1.16: Receptor and signaling interactions during phagocytosis of microbes. Multiple receptors simultaneously recognize microbes both through direct binding and by binding to opsonins on the microbial surface. Receptor engagement induces many intracellular signals, resulting in many pathways. Signaling during phagocytosis may subsequently serve to activate or inhibit further phagocytosis and microbe-induced responses. Many pathogenic microbes actively regulate phagocyte responses. Adapted from Underhill and Ozinsky (2002).

1.3.5. Inflammatory response – pro- and anti- inflammatory cytokines

Inflammation is an ensuing process during infection that involves the coordinated delivery of soluble factors and cells in the blood to the site of infection or injury. In the case of microbial infection, inflammation could be triggered by phagocytes which recognize the pathogen through receptors such as TLRs and FcγR1 receptors (Barton 2008). The initial recognition is mediated by the tissue resident macrophages and mast cells, leading to the production of a variety of inflammatory mediators like cytokines, such as IL8 and TNF, chemokines, vasoactive amines, eicosanoids and products of

proteolytic cascades. These effectors elicit the exudate of plasma proteins and leukocytes (mainly neutrophils) to the site of infection (Pober and Sessa, 2007). The activated neutrophils attempt to kill the invading agents by releasing the toxic contents of their granules, which include reactive oxygen species (ROS) and reactive nitrogen species, proteinase 3, cathepsin G and elastase (Nathan 2006). These highly potent effectors do not discriminate between microbial and host targets, so collateral damage to host tissues is unavoidable (Serhan and Savill, 2005). Therefore, upon arresting the infection, host immune cells release anti-inflammatory cytokines like IL10 in order to resolve and repair the inflamed host tissues post elimination of the pathogen. Failure to resolve the inflammation may result in severe consequences for the host, culminating in auto-immunity, inflammatory tissue damage and sepsis and eventually death.

1.4. Hypothesis, rationale and specific aims of this thesis

Based on published reports and findings from our lab, the following **observations** have been made, which provoked the hypothesis for this thesis:

1. PRR**:**PRR interactome formation is a crucial event in innate immune defense. For example, CRP and ficolin interact with each other during infection to boost anti-microbial response. This phenomenon is evolutionary conserved from horseshoe crab (Ng et al., 2007) to humans (Zhang et al., 2009).
2. Infection-inflammation condition result in local acidosis (Issekutz and Bhimji, 1982) and hypocalcaemia (Beers 2000), which strengthen PRR**:**PRR interactome formation (Zhang et al., 2009; Zhang et al., 2010), leading to efficient elimination of the pathogen.
3. Amongst the natural antibody isotypes, only natural IgM has been shown to be effective against the pathogens, by virtue of its polyreactivity (Boes et al., 1998; Ochsenbein et al., 1999). Natural IgG and IgA have been deemed non-reactive, due to their low affinity.
4. M- and H-ficolins were shown to interact with IgA (Zhang et al., 2010; Panda et al., unpublished data).

Based on the above observations, we **hypothesize** that:

Natural IgG and IgA antibodies interact with ficolins, forming a formidable PRR:PRR immune complex, to mount a strong immune response against pathogens, and this is regulated by the ensuing infection-inflammation condition.

The following **specific aims** are structured to study and validate the potential collaboration of natural antibodies with ficolins and the anti-microbial action resulting from this interaction. Experiments are designed to characterize the IgG**:**ficolin interaction, study the biological significance of this interactome formation at the outset of infection, and show the clearance of the pathogen from the host (**Figure 1.17**).

1. To determine the potential role of natural IgG, with the aid of ficolins, in pathogen recognition and removal.
2. To characterize the interaction and binding interface between natural IgG and ficolin under normal physiological and infection-inflammation conditions.
3. To decipher the mechanism of natural IgG**:**ficolin-mediated innate immune defense.
4. To examine the patho-physiological significance of natural IgG during *in vivo* primary infection in IgG deficient mice.

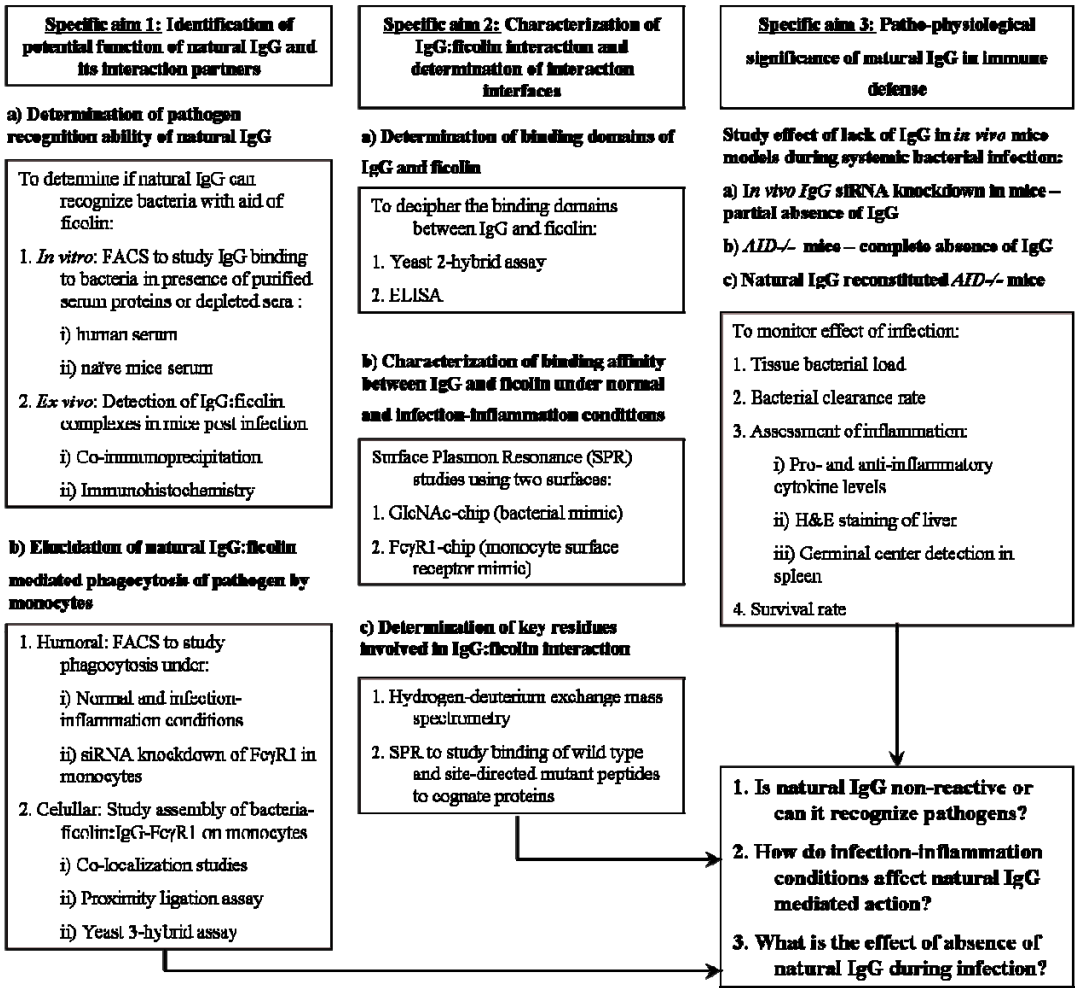

Figure 1.17: Overview flowchart of the three specific aims designed to test the hypothesis.

Chapter 2

MATERIALS AND METHODS

CHAPTER 2: MATERIALS AND METHODS

All *in vitro* experiments in this thesis were performed according to national and institutional guidelines on ethics and biosafety (Institutional Review Board, Reference Codes: NUS-IRB 08-296). Mice breeding and *in vivo* experiments were carried out in compliance with institutional guidelines and approved by the Institutional Animal Care and Use Committee, NUS (Protocol no.: 108/08, 049/11 and BR14/11).

2.1 Materials

2.1.1. Bacterial strains

Pseudomonas aeruginosa strain PAO1 has been previously used in multi-drug resistance trials (Kwon and Lu, 2006; Wu et al., 2008), experimental simulation of *P. aeruginosa* infection (Taylor et al., 2007) and biofilm formation studies (Richards et al., 2008). The lab-adapted PAO1 (Filiatrault et al., 2006; Prince et al., 2008) used in this study was kindly provided by Professor B. H. Iglewski (University of Rochester, Rochester, USA). The pDSK-GFP plasmid which was subsequently transformed into PAO1 to form the green fluorescent PAO1 strain, was kindly provided by Professor Zhang Lian-Hui (Institute of Molecular and Cell Biology, Singapore). This pDSK-GFP plasmid contains GFP functional fragment cloned into the *Hind* III and *Sma* I sites in the pDSK 519 vector. The fluorescent *P. aeruginosa* containing pDSK-GFP plasmid is henceforth referred to as PAO1-GFP. The *Staphylococcus aureus* (ATCC 25923)*, Staphylococcus epidermidis* (ATCC 12228) and *Escherichia coli* Top 10 strains were from ATCC.

2.1.2. Mice

6-8 week old Balb/c and C57BL/6 mice were inbred in "specific pathogen-free" conditions at the NUS CARE facility. They were transferred to Center for Life Sciences, animal bio-safety level 2 (ABSL2) facility for the infection experiments carried out under approved protocol no. 108/08. The *C3*$^{-/-}$ mice (Jackson Laboratories) breeding pairs were kindly provided by Dr Sivasankar Baalasubramanian (Singapore Institute for Clinical Sciences). The *AID*$^{-/-}$ mice were a generous contribution from Dr Garnett Kelsoe (Duke University, USA), obtained with kind permission from Dr Tasuku Honjo (Kyoto University, Japan). These knockout mice (both B6 background) were also bred under specific pathogen-free conditions under approved breeding protocol no. BR14/11. Both males and females were used for the infection study without any bias (protocol no. 049/11).

2.1.3. Serum

Human serum samples were obtained from healthy uninfected adult donors with informed consent, under institutional guidelines (IRB Ref. Code: 08-296). The concentration of the pooled sera was measured using NanoDrop™ ND-1000 Scientific, Wilmington spectrophotometer (Thermo Fisher Scientific) to ensure that equal amounts of proteins were used in each experiment. Depletion of ficolin, IgG or C3 was achieved by incubating the serum overnight at 4˚C with anti-ficolin, Protein G or anti-C3 coupled beads, respectively. 10% (v/v) simulated "normal" and "infection-inflammation" sera were prepared by diluting the normal healthy sera in TBS buffer (25 mM Tris, 145 mM NaCl,

pH 7.4, 2.5 mM $CaCl_2$) and MBS buffer (25 mM MES, 145 mM NaCl, pH 6.5, 2 mM $CaCl_2$), respectively (Zhang et al., 2009). The selection of these buffers was based on the criteria of Good's buffers, the components of which do not affect the studies in a biological system, and hence are deemed suitable for use in biochemical and biological research (Good et al., 1966).

For collection of mice serum, blood was obtained by cardiac puncture and allowed to clot at 37˚C for 1 h. The samples were then spun down at 1500 g for 20 min at 4˚C. Serum was collected by gently aspirating into a clean tube and stored at -20˚C.

2.1.4. Biochemicals, antibodies and proteins

GlcNAc was purchased from Sigma-Aldrich (St. Louis, MO). Deoxynucleotide triphosphates (dNTPs) were from Promega. All restriction enzymes were from New England Biolabs or Fermentas, unless otherwise stated. The horseradish peroxidase substrate, ABTS (2,2'-azino-bis[3-ethylbenzthiazoline-6-sulfonic acid]) was from Roche Diagnostics (Mannheim, Germany). GlcNAc-BSA was from Dextra Laboratories (Reading, UK). GlcNAc-Sepharose beads was from Pierce (Rockford). Protein G spin columns were from Sartorius and Protein G beads were from GE Healthcare. Other common chemicals of molecular biology grade were from Sigma-Aldrich or Merck, unless otherwise stated. Plasmids containing full functional cDNA fragments of L-, H- and M- ficolins, kindly provided by Professor T. Fujita (Fukushima Medical College, Fukushima, Japan) were used in the subsequent cloning process and functional studies. The full length, FBG and

collagen-like domains of L-, H- and M-ficolins were recombinantly expressed and purified using Ni-NTA affinity chromatography. Recombinant human FcγRI (1257-FC), anti-human FcγRI (MAB1257), anti-H-ficolin (AF2367) and anti-goat secondary NL557-conjugated (NL001) antibodies were from R&D Systems (Minneapolis). Anti-L-ficolin (HM2091) and anti-M-ficolin (HP9039) antibodies were from Hycult. Anti-human IgG (I-1011), anti-mouse IgM (μ-chain specific, M8644), anti-mouse IgA (α-chain specific, M8769), anti-mouse IgG (g-chain specific, M2650) and anti-actin (A2066) antibodies were from Sigma. Human IgG isotypes 1, 2 and 3 specific antibodies, detecting the corresponding heavy chain, were from Invitrogen (A10630, 05-3500 and 05-3600). Anti-mouse ficolin (648102), anti-mouse GL7 (14-5902) & Alexa-488 anti-mouse B220 (clone: RA3-6B2, 53-0452) antibodies were from BioLegend and eBioscience, respectively. Secondary anti-goat, anti-rabbit and anti-mouse with HRP-conjugation were from Dako A/S (Denmark). Monoclonal anti-*Staphylococcus epidermidis* (MA1-35789) and polyclonal anti-human/mouse C3 (PA1-29715) antibodies were from Thermo Scientific. Polyclonal antibodies against *Pseudomonas aeruginosa* (ab68538), *Staphylococcus aureus* (ab20920) and *Escherichia coli* (ab25823) were from Abcam. Secondary anti-rabbit, anti-mouse, anti-goat and anti-rat antibodies conjugated with Alexa-488, Alexa-594 or Alexa-647, were purchased from Invitrogen (Carlsbad).

2.1.5. Medium and agar

Luria Bertani (LB) broth was prepared by mixing 0.5 % (w/v) yeast extract

(Difco), 1 % (w/v) tryptone (Difco) and 0.5 % sodium chloride in deionised water, and adjusting the pH to 7.0. Synthetic Defined Medium (SD medium) was prepared by dissolving 0.67 % (w/v) yeast nitrogen base without amino acid (Difco), 2 % (w/v) glucose and appropriate amino acid supplements in deionised water, and adjusting the pH to 5.8. Depending on the nutrient selection required, one of the following supplements was added to the SD medium: 0.074 % (w/v) Trp Dropout (DO) supplement, 0.069 % (w/v) Leu DO supplement, 0.064 % (w/v) Trp/Leu DO supplement, or 0.06 % (w/v) Trp/Leu/His/Ade DO supplement. For the yeast-three hybrid assay, the ready-to-use medium of SD-Leu-Trp-His-Met was purchased from Clontech (Palo Alto, CA). For preparing the medium where adenine was required, additional 0.003 % (w/v) adenine hemisulfate was added. LB agar was prepared by adding 1.5 % (w/v) agar (Difco) to LB media. For preparing SD agar, 2 % (w/v) agar was added to the liquid media. For antibiotic containing media, ampicillin or kanamycin was added at final concentration of 100 μg/ml or 50 μg/ml respectively, to the medium or agar unless otherwise stated.

2.2. Purification of native H-ficolin from human serum

Native H-ficolin was purified from uninfected human serum from healthy adult donors. The proteins in uninfected human serum were precipitated using 4-8% PEG 6000 and dissolved in TBST (TBS containing 0.05% Tween-20). The proteins were chromatographed through an 8-ml human serum albumin (HSA)-conjugated Sepharose 4B column (Tachikawa et al., 1991). The eluate was then passed through an 8-ml column containing acetylated-HSA-

Sepharose 4B beads (Tachikawa et al., 1991). The column was sequentially washed with TBST followed by TBST containing 200 mM GlcNAc. H-ficolin bound to the column was eluted in two steps: (1) using 1 M Na-acetate, 0.05% Tween 20, 10 mM $CaCl_2$, pH 7.5, (2) 10 mM diethylamine, 0.05% Tween 20, 10 mM $CaCl_2$, pH 11.5. Eluate from the second step was neutralized with 10 mM Tris-HCl, pH 7.4. The eluted proteins were then concentrated through a 1 ml MonoQ column (GE healthcare). The bound proteins were further eluted with a second buffer containing 1 M NaCl. The eluate buffer was exchanged to TBS using centrifugal filter devices with a 3 kDa mol. wt. cut off pore size (Amicon Ultra, Millipore).

2.3. Purification of native IgG from human and mice serum

Native IgG was purified from uninfected human serum or pooled mice serum using Vivaspin pre-packed Protein G spin column (Sartorius), according to the manufacturer's instructions. SDS-PAGE (12% resolving gel) under reducing conditions and mass spectrometry were used to check the purity and confirm the identity of IgG.

2.4. Expression and purification of recombinant ficolins (full-length, FBG and collagen-like domain)

The functional fragments of full length or domains (FBG and collagen-like domain) of L-, H- and M-ficolins were cloned into mammalian expression vector, pSecTag2B (Invitrogen) in frame with the vector sequence as a Histidine-fusion clone, recombinantly expressed and purified.

For protein expression, HEK 293T cells were used as the mammalian

host system. HEK293T are derived from HEK 293 cells that stably express the simian virus 40 (SV40) large T antigens. Hence, vectors containing the SV40 promoter and origin can replicate to produce high copy numbers, ranging from 400-1000 plasmids per cell, within HEK 293T (Ho et al., 2009). Transfection into HEK293T was carried out using lipofectamine 2000 (Invitrogen) according to the product instructions. The culture supernatant was collected at 48 h post-transfection. The supernatant was clarified to remove cell debris by centrifuging at 1500g for 10 min and passed through a 0.2 μm filter. 300 μl Ni-NTA beads (Qiagen, Valencia, CA) was added to 30 ml clarified supernatant and incubated overnight at 4˚C. The beads were then packed into the 10 ml poly-prepTM chromatography column (Biorad, Hercules, CA). The beads were washed with 50 ml wash buffer containing 20 mM Tris, 500 mM NaCl, pH = 8.0 with 20 mM imidazole (Sigma-Aldrich) to remove non-specifically bound proteins. The bound recombinant His-tagged proteins were eluted out using elution buffer (20 mM Tris, 500 mM NaCl and 250 mM imidazole, pH 8.0), into 6 fractions of 120 μl each.

2.5. Analysis of purified proteins

2.5.1. Bradford protein assay

The concentration of the protein in solution was assayed using Bradford protocol (Bradford 1976). The reagent contains 0.01 % (w/v) Coomassie Brilliant Blue G-250, 8.5 % (v/v) orthophosphoric acid and 4.7 % ethanol. For protein estimation, 1 ml of the Bradford reagent was mixed with 50 μl of diluted protein sample by vortexing. Absorbance was read at $OD_{595\ nm}$ after 2

min. The protein content in each sample was calculated from a standard curve plotted from the absorbance readings of known concentration range of BSA (Fraction V, Sigma-Aldrich), ranging from 1 μg to 20 μg. The protein samples were measured in duplicates.

2.5.2. SDS-PAGE and Western blot immunodetection

Equal amounts of serum proteins, purified proteins (IgG, ficolin or IgG**:**ficolin complex) or eluted samples from GlcNAc- or Protein G- bead pulldown assays were boiled at 95 ^{o}C for 5 min and electrophoresed on 12% SDS-PAGE under reducing conditions, and transferred to PVDF (BioRad) membrane for 1 h at 70 V. The membrane was blocked for 2 h with 5% (w/v) skimmed milk in 50 mM Tris, pH 7.4, 145 mM NaCl, 0.05% (v/v) Tween-20 (TBST). After blocking, the membrane was washed four times with TBST for 15 min each and then first probed with the primary antibody (overnight at 4˚C). After washing four times with TBST, the membrane was probed with the corresponding secondary antibody in the recommended titer for 1 h, and washed four times in TBST. The immunosignals were detected using Supersignal West Pico Chemiluminescent Substrate (Pierce) and exposed to X-ray film (Fujifilm, Japan).

2.5.3. Mass spectrometry

The proteins were separated on the 12% reducing SDS-PAGE and stained with Coomassie blue. The protein band of interest was excised and in-gel digested with trypsin (Promega) as previously described (Ng et al., 2007). The

trypsinized peptide samples were analysed by matrix-assisted laser desorption ionization time-of-flight (MALDI-TOF) using Voyager-DE STR Biospectrometry Workstation (Applied Systems) in the Proteins and Proteomics Centre, National University of Singapore. The peptide mass and sequences were analysed using Matrix Sciences Mascot search (http://www.matrixscience.com).

2.6. Simulation of "normal" and "infection-inflammation" conditions in uninfected human serum

Infection-inflammation condition is characterized by mild acidosis and hypocalcaemia. Local acidosis is a hallmark of infection that occurs due to infiltration of inflammatory cells to the site of injury; leading to a respiratory burst that result in a drop in local pH to values ranging from 5.5-7.0 (Martinez et al., 2006). Simultaneously, serum samples of infected patients have also been shown to have lower calcium levels i.e. <2.12 mM calcium (Aderka et al., 1987), as compared to healthy serum (2.2 to 2.6 mM) (Beers 2000). Therefore, we have adopted pH levels of 7.4 and 6.5 and calcium concentrations of 2.5 and 2 mM to represent "normal" and "infection-inflammation" conditions, respectively.

Henceforth, the two conditions used in the study are defined as: (i) normal condition (pH 7.4, 2.5 mM calcium) and (ii) the infection-inflammation condition (pH 6.5, 2 mM calcium). The buffers used to dilute the serum to simulate these conditions for the *in vitro* studies are according to previous reports from Miyazawa and Inoue, 1990 and Aubert et al., 2006:

(i) normal condition - TBS buffer containing 25 mM Tris, 145 mM

NaCl, pH 7.4 and 2.5 mM $CaCl_2$

(ii) infection-inflammation condition - MBS buffer containing 25 mM MES, 145 mM NaCl, pH 6.5 and 2 mM $CaCl_2$

2.7. Bacterial opsonization and phagocytosis assays

2.7.1. IgG binding assay on bacteria by flow cytometry

Cultures of *P. aeruginosa* PAO1, *E. coli* Top 10, *S. aureus* or *S. epidermidis* were prepared for flow cytometry. Briefly, a single colony was inoculated in 10 ml LB broth overnight (37˚C, 220 rpm) and a secondary culture was prepared the following day by diluting the overnight culture with fresh LB broth (1:100) and incubating at 37˚C, 220 rpm for 3-5 h till O.D. reached 0.7-1.0 (bacterial log phase). The bacteria were then fixed with 5% acetic acid for 5 min at room temperature, and washed thrice with TBS. Next, the bacterial surface was blocked to avoid non-specific binding, with 3% (w/v) HSA in TBST (blocking buffer) at room temperature for 1 h with shaking. To assess the binding of the purified IgG to the bacteria, the bacteria were incubated with (i) purified human IgG with or without ficolin and (ii) purified mouse IgG with or without IgG-depleted or IgG- and ficolin-depleted serum, for 2 h at room temperature. Depleted serum was used to specifically study the role of ficolin in enabling IgG deposition on the bacteria. Bacteria were then washed to remove the unbound proteins and stained with primary anti-human IgG (1:500) or anti-mouse IgG (1:500) (Sigma), followed by staining with Alexa 488-conjugated secondary anti-goat (1:500). Bacteria incubated with specific primary antibody and stained with corresponding Alexa 488-conjugated

secondary antibody (1:500) served as a positive control. The bacteria were washed thrice with TBST and fixed with 4% paraformaldehyde for 15 min. After three washes, the bacteria were diluted in PBS (140 mM NaCl, 10 mM phosphate, 2.7 mM KCl, pH of 7.4) which was also the running buffer for the flow cytometry. Flow cytometry was performed using the Dako Cyan Cytomation LX (Becton Dickinson). The counts were analyzed by WinMDI version 2.8.

2.7.2. Phagocytosis assay

To assess the degree of bacterial phagocytosis by primary human monocytes, GFP tagged *P. aeruginosa* (PAO1-GFP) were cultured in LB broth containing 25 μg/ml kanamycin selection medium for GFP plasmid containing bacteria, in a similar manner as previously described (Section 2.7.1). For the phagocytosis assay, the GFP-bacteria were incubated with IgG, ficolin or both the proteins at room temperature for 2 h in 500 μl of "normal" or "infection-inflammation" buffers to opsonized the GFP-bacteria (1:10 diluted uninfected serum served as a positive control and IgG with HSA served as a negative control). The opsonized GFP-bacteria (10^7 cfu) were incubated with 10^6 human monocytes in a ratio of 10:1 at 37˚C for up to 60 min. Phagocytosis was stopped by adding 1 ml ice-cold PBS. Following incubation, the monocytes were collected, washed thrice with TBS or MBS buffers and fixed with 4% paraformaldehyde (PFA). The extent of phagocytosis was assayed by counting the percentage of monocytes with GFP fluorescence (a measure of the degree of phagocytosis), by flow cytometry using the Dako Cyan

Cytomation LX (Becton Dickinson).

2.8. *In vitro* protein:protein interaction assays

2.8.1. Yeast 2-hybrid assay

In yeast 2-hybrid assay, full-length or specific domains of L-, H- or M-ficolins and IgG or IgA cDNAs (without their signal sequences) were cloned to generate fused products with the DNA-binding domain of Gal4 in the bait plasmid pGBKT7 (BD Biosciences), or the activation domain of Gal4 in the prey plasmid pGADT7-Rec (BD Biosciences) (**Figure 2.1**), and then co-transformed into *S. cerevisiae*, strain AH109. The co-transformants were cultured on the SD-Trp$^-$Leu$^-$ plates to check for the presence of both plasmids, and onto SD-Trp-Leu-His-Ade (QDO) plates for up to 5 days to check for protein:protein interaction. Selection was carried out according to the manufacturer's instructions. Reciprocal cloning of the cDNA was also performed into prey and bait plasmids and the interaction were confirmed in a similar manner as described above.

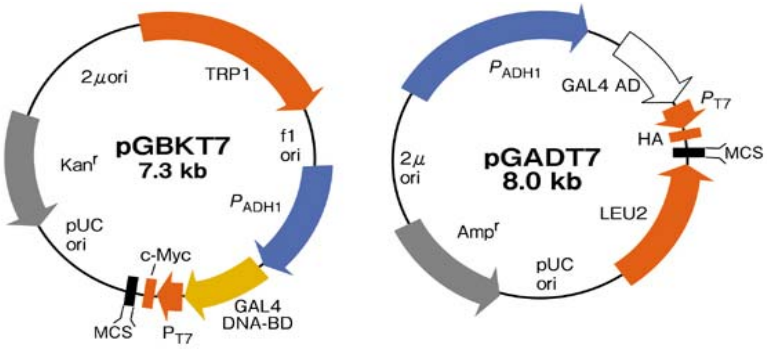

Figure 2.1: BD Matchmaker™ Two-hybrid system vector map of bait vector (pGBKT7) and prey vector (pGADT7). pGBKT7 is a bait vector that encodes the GAL4 DNA-binding domain (BD) and the Trp selection marker. pGADT7 is a prey vector that encodes GAL4 activation domain (AD) and the Leu selection marker. Picture adapted from http://catalog.takara-bio.co.jp/clontech/product/basic_info.

2.8.2. Yeast 3-hybrid assay

Yeast 3-hybrid system was performed to test the potential protein**:**protein interactions amongst H-ficolin, IgG and FcγR1. The cDNA cloned into MCS I site in the bait vector codes for a protein that can participate in the interaction as a bridge or a stabilizer or an inhibitor, in this system (**Figure 2.2**). H-ficolin in pGADT7 vector was used as prey. IgG and FcγR1 were cloned into MCS I and MCS II sites, respectively, of the pBridge bait vector. FcγR1 cDNA cloned into MCSII site was constitutively expressed. Expression of IgG (in MCS I site) was controlled by a conditional methionine promoter, which means that IgG was expressed only in the presence of methionine. This allows expression to be switched on or off by culturing in media with or without methionine. The bait and prey vectors were co-transformed into the yeast, which were then plated onto SD-Trp$^-$Leu$^-$ and cultured for 3 days. The transformants were then re-streaked onto the SD-Trp$^-$Leu$^-$, QDO, and QDO-Met plates for 5 days. The growth of the yeast in the QDO-Met plates would indicate a complex between H-ficolin, IgG and FcγR1. All cloning vectors and culture media used in yeast 2- and 3-hybrid assays were from Clontech (Palo Alto, CA).

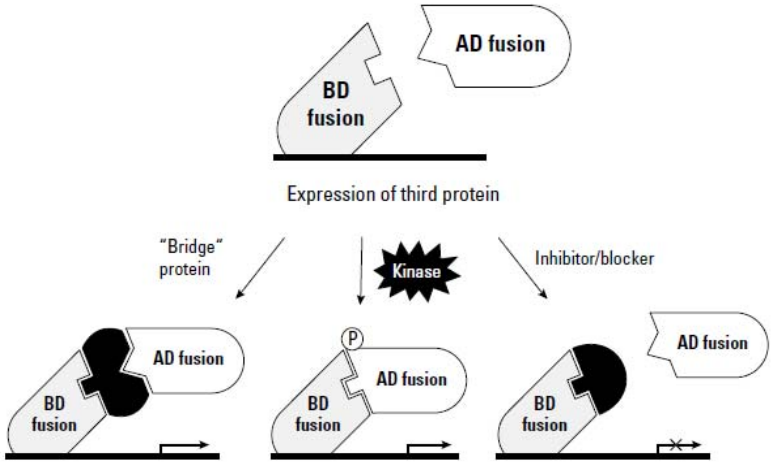

Figure 2.2: Schematic diagram of yeast three-hybrid system. pBridge expresses both the DNA-BD fusion and the third protein acting as a bridge between the proteins. The activation domain fusion is expressed from a separate two-hybrid system vector. The conditionally expressed third protein can play a structural bridging, modifying or inhibitory role in the interaction that restores reporter gene expression. Adapted from http://www.clontech.com/images/pt/PT3212-5.pdf.

2.8.3. ELISA for measurement of protein:protein binding

ELISA was performed to test the interaction between specific IgG isotypes (IgG1, IgG2, IgG3) to ficolin (pre-bound to GlcNAc) or the binding of IgG to full-length or specific domains (FBG or collagen-like domain) of ficolin. Briefly, 1 µg of GlcNAc-BSA was immobilized onto Maxisorp™ plate (NUNC, Denmark) by incubating overnight at 4˚C. The wells were washed three times with TBST, followed by blocking with 1% (w/v) HSA in TBST (blocking buffer) at 37˚C for 2 h. After three washes, 0.8 µg of either L-, H- or M-ficolin (full-length, FBG or collagen like domains) was added and incubated at 37˚C for 2 h. Then, increasing doses of purified IgG or uninfected human serum were added and incubated at 37°C for 2 h. After washing the wells thrice with TBST to remove unbound proteins, the bound IgG was

detected with primary anti-human IgG antibody (1:3000) followed by HRP-conjugated secondary antibody (1:3000). After adding ABTS substrate (Roche Diagnostics, Germany) and incubating for 15 min, the absorbance was read at 405 nm. Wells incubated with HSA on ficolin pre-bound to GlcNAc served as a negative control. Previously, it has been reported that MBS was used to adjust the serum condition to achieve acidosis (Miyazawa and Inoue, 1990). Thus MBS containing 25 mM MES, 145 mM NaCl and 2 mM calcium adjusted to pH 6.5 (infection-inflammation condition), and TBS containing 25 mM Tris-HCl, 145 mM NaCl and 2.5 mM calcium, adjusted to pH 7.4 (normal condition) were used as the binding buffers to study the effect of ensuing change in pH and calcium levels on protein**:**protein interaction under infection-induced local acidosis and hypocalcaemia as compared to normal physiological condition.

2.8.4. Surface Plasmon Resonance (SPR)

BIAcore 2000 instrument (BIAcore AB) was used to demonstrate real-time biointeraction between the proteins. For generating a bacterial surface mimic, GlcNAc-immobilized chip was prepared by diluting GlcNAc-BSA (Dextra Labs, UK) to 10 μg/ml with 10 mM sodium acetate, pH 4.0 and immobilizing on CM5 chip (BIAcore AB) using amine-coupling chemistry, according to the manufacturer's specifications. Ficolin FBG at 200 nM was allowed to bind to the GlcNAc-immobilized chip. To characterize binding of IgG or its peptides to ficolin, separate injections of increasing concentrations of IgG or its peptides under normal or infection-inflammation condition were performed at

a flow rate of 30 µl/min. Dissociation was at the same flow rate. Regeneration was effected by injecting 15 µl of 0.1 M NaOH at 30 µl/min.

To study the interaction between ficolin FBG or its peptides and IgG bound to FcγR1, first CM5 chip was immobilized with FcγR1 using amine-coupling chemistry, to generate a monocyte surface mimic. Then 50 nM IgG in running buffer was injected over FcγR1-immobilized chip followed by separate injections of increasing concentrations of ficolin FBG or its peptides under normal or infection-inflammation condition. Injection of HSA instead of ficolin FBG served as the negative control. BIAevaluation 3.2 software was used to calculate the binding affinity (K_D) using 1:1 Langmuir binding model. $K_D = k_{off}/k_{on}$; where k_{off} = dissociation rate constant ($M^{-1}s^{-1}$) and k_{on} = association rate constant (s^{-1}). All the surface plasmon resonance curves used in K_D calculation were normalized against buffer alone controls. The resonance unit difference before and after injection represents the protein-protein interaction. The binding curves (black) are overlaid with the fit of 1:1 interaction model (red). The plots shown are representative of three independent experiments.

2.9. Cell culture and transfection

2.9.1. Isolation of primary human monocytes from buffy coat

Buffy coat was obtained from the NUHS Blood Bank (IRB Approval No: 08-296). Peripheral Blood Mononuclear Cells (PBMCs) were purified from the buffy coat by ficoll-hypaque (Sigma-Aldrich) gradient centrifugation according to a standard protocol (Cao et al., 2005). Primary human monocytes

were further purified by magnetic cell sorting using the EasySep Monocyte Isolation Kit (Stem Cell Technologies) according to the manufacturer's instruction.

2.9.2. Cell culture

The primary monocytes and U937 cells were cultured at 37°C in RPMI 1640 (Invitrogen) supplemented with 10% (v/v) FBS (Invitrogen), 100 IU/ml penicillin and 100 μg/ml streptomycin (Invitrogen). HEK293T cells were cultured in DMEM (Invitrogen) supplemented with 10% FBS, 100 IU/ml penicillin and 100 μg/ml streptomycin.

2.9.3. Transfection by Lipofectamine 2000

HEK 293T cells were transfected with the cloned expression plasmids using Lipofectamine^{TM} 2000 (Invitrogen) according to the manufacturer's instructions. Briefly, 24 h prior to transfection, the cells were plated in a 75 cm^2 culture flask (Iwaki, Japan) at a density of 1x 10^6 cells/ml with 20 ml of supplemented DMEM containing 1% penicillin-streptomycin and 10% FBS to achieve 90-95% confluency at the time of transfection. The medium was replaced with 18.75 ml of pre-warmed (37˚C) un-supplemented DMEM just before transfection. An aliquot of 30 μg DNA (pSecTag2B containing ficolin full-length, FBG or collagen-like domain genes) and 75 μl of Lipofectamine^{TM} 2000 were individually diluted in 1.875 ml of un-supplemented DMEM and pre-incubated for 5 min at room temperature. The diluted DNA was added to the diluted LipofectamineTM 2000 followed by incubation for 20 min at room

temperature. The complexes constituting DNA to Lipofectamine™ 2000 at a ratio of 1:25 (w/v) was then added to the cells and incubated at 37˚C, 5% CO_2 for 6 h before replacing the medium with supplemented DMEM.

2.10. Characterization of binding sites between ficolin and IgG

2.10.1. Hydrogen deuterium exchange mass spectrometry (HDMS)

To determine the interaction interface between IgG and H-ficolin, hydrogen–deuterium exchange mass spectrometry (HDMS) (Schuster et al., 2008) was performed under normal and infection-inflammation conditions. The experiment was performed by first combining 2 µl each of the protein solutions at concentrations of ~2.5 mg/ml with 18 µl of a deuterated buffer, which changed the composition of the aqueous buffer to 90% deuterium oxide. After incubating for 0, 1, 2, 5, or 10 min, the hydrogen–deuterium exchange reactions were quenched by the addition of 180 µl of ice-cold, 0.1% (v/v) trifluoroacetic acid (Sigma-Aldrich) to lower the pH of the reaction to 2.5. An aliquot of 100 µl of the quenched reaction was then mixed with 50 µl pepsin bead slurry (Pierce), previously activated by washing three times in 500 µl 0.1% trifluoroacetic acid, pH 2.5, at 4˚C. After mixing with pepsin, the mixture was vortexed for 30 s followed by incubation on ice for 30 s. This alternating cycle was repeated for 5 min. The exchanged mixture was then centrifuged for 1 min at 7000g at 4°C, divided into three aliquots, flash-frozen in liquid N_2, and stored at -80°C until analyzed. The pepsin-digested protein was analyzed by mass spectrometry with MALDI using the 4800 Plus MALDI TOF/TOF Analyzer (Applied Biosystems, Foster City, CA). Deuterium back-

exchange that might have occurred during the analysis was determined by carrying out control experiments where the IgG and H-ficolin were individually deuterated for 24 h at 25°C. **Figure 2.3** demonstrates an overview of the process involved in HDMS.

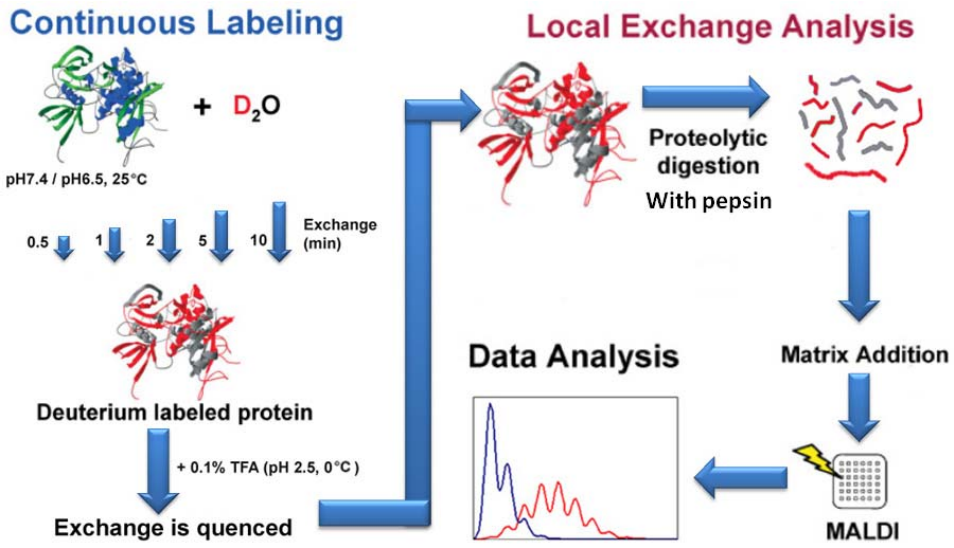

Figure 2.3: The concept and experimental procedure of hydrogen-deuterium exchange mass spectrometry (HDMS). The hydrogen-deuterium exchange is done by continuous labeling. Briefly, D_2O buffer is added to a protein solution such that the final deuterium incorporation is >90%. After a set period of time, the labeled protein is mixed with ice cold 0.1% Trifluoroacetic acid (TFA) at pH 2.5 to quench the exchange reaction. Quenched samples are digested with pepsin to generate peptides that are subsequently analyzed by online MALDI-MS. The resulting data analysis provides information on deuterium-exchange in short fragments of the peptide backbone, and thus is termed the local exchange analysis. Adapted from Thomas et al., 2005, with modifications.

The HDMS spectra obtained from mass spectrometry were analyzed using Data Explorer version 4.9 based on the theoretical mass of two prominent peptides (theoretical m/z = 932.42 and 1452.73). The average mass of a peptide was calculated by determining the centroid of its isotopic envelope using Decapp software (University of California San Diego, La Jolla, CA). Differences between the centroid value of the deuterated and non-

deuterated peptides indicates the average number of deuterions incorporated. Exchange at side chains was determined to be 4.5% of fast-exchanging side-chain hydrogen atoms based on dilution factors. Data analysis corrected for the side-chain deuteration was carried out prior to back-exchange correction. Finally, a correction factor was applied to account for the amount of back exchange. Kinetic plots of deuteration best fit were made to a single exponential model accounting for deuterions that were exchanging at a rapid rate (mainly solvent-accessible amides). The best fit was implemented in GraphPad Prism version 5 (GraphPad Software, San Diego, CA). Changes in deuterium incorporation of > ±10% were considered significant.

2.10.2. Computational prediction of binding sites of IgG:ficolin

In collaboration with Dr. Yang Lifeng (Postdoctoral fellow, SMA-CSB), we performed parallel *in silico* prediction of the binding sites between H-ficolin FBG and human IgG.

Molecular Dynamics simulation

The crystal structures of the monomers of H-ficolin FBG (ligand-free; PDB entry code: 2J64) and human IgG Fc (PDB entry code: 1H3Y) were used for molecular dynamics simulations at constant pH. The structure simulations were conducted with a 30 Å cut-off and a 2 fs time step based on the Generalized Born implicit solvation model (Mongan et al., 2004). A constant value for the dielectric constant was used during the simulations in water. A 2 ns simulation was conducted at a constant temperature of 300 K. AMBER

simulations were conducted with the sander module in the AMBER 9.0 MD package with all simulation parameters. The simulated structure was used for Zdocking.

Zdock and Rdock

The models were subjected to energy minimization in Discovery Studio 2.5 (Accelrys Inc.) and used as the template in the following simulations. Docking of H-ficolin FBG and IgG Fc is based on the ZDOCK and RDOCK programs developed at Boston University. ZDOCK is a rigid-body protein-protein docking algorithm, followed by RDOCK, an interface refinement minimization algorithm. It was used to explore the rotational and translational space of a protein-protein system. The averaged structure was extracted at equal intervals from the last 1 ns MD simulation and used as the starting structures for ZDOCK simulations. An angular step of 6 deg was used, which results in 54000 poses. In the refinement stage of RDOCK, the 2000 best poses of near native structures obtained in the initial stage were refined and re-ranked using a more detailed energy function that took into account conformational changes as well as a solvation term.

The top 100 poses were then categorized into different clusters, and the top poses which fitted with our experimental data were selected for further analysis.

2.10.3. Site-directed mutant peptides

Based on *in silico* predictions and HDMS studies, we designed wild type and mutant peptides (Arg to Ala, Lys to Ala or His to Ala mutations) of H-ficolin

or IgG to study their binding motifs to the cognate proteins. The peptides were synthesized by Genemed Synthesis Inc., California, USA, and purified to >95% under pyrogen-free condition. Peptides were dissolved in water to make a 2 mM stock solution, aliquoted and stored at -20˚C. The binding of these peptides to the proteins was tested by SPR under normal and infection-inflammation conditions, as described in Section 2.6.

2.11. *In vitro* functional study of the impact of IgG:ficolin recognition of PAMP/bacteria

2.11.1. PAMP stimulation

Primary monocytes were plated at a cell density of 0.5 x 10^6 cells/ml/well into 24-well plates for 12 h prior to the experiment. GlcNAc-Sepharose beads (used as a bacterial mimic) were incubated with either IgG, ficolin or both for 30 min. The opsonized bacterial mimic was added to the replicate wells to stimulate the monocytes. The medium and cells were collected after 24 h, separated by centrifugation and processed further.

2.11.2. Measurement of cytokine production

For IL8 measurement, the primary human monocytes were plated at a density of 0.5 X 10^6 cells/ml/well into 24-well plates. The cell culture medium, advanced RPMI, was renewed before addition of opsonized GlcNAc beads (Section 2.11.1). To test the functional significance of FcγR1 in IgG**:**ficolin mediated PAMP recognition and signaling, the monocytes knocked down of *FcγR1* were treated under similar conditions. Cell supernatant was collected

24 h after stimulation, clarified by centrifugation at 1000g for 5 min at 4^{o}C and diluted 100 times before ELISA. Secreted IL8 was quantified with OptEIA human IL8 ELISA (BD Biosciences) immunoassay kit according to the manufacturer's instructions. The absorbance was read at 405 nm.

2.12. Cellular protein:protein interaction assays

2.12.1. *In situ* proximity ligation assay (PLA)

To determine cellular protein:protein interaction, *in situ* proximity ligation assay (PLA) was performed using the Duolink detection 563 kit (Olink Biosciences, Uppsala, Sweden) following the manufacturer's instructions. The technique of *in situ* proximity ligation assay was developed by Soderberg and colleagues to study protein**:**protein interactions in cells (Soderberg et al*.,* 2007). Target protein is recognized by binding a "probe" consisting of a pair of proteins attached to DNA onto the target protein. It can readily detect and localize protein interactions without the need for tedious genetic engineering to tag and over-express proteins, thus providing us a convenient way to study membrane protein interactions. Therefore, endogenous protein interactions *in situ* in cells and tissue can be visualized using regular immuno-staining antibodies combined with the generic Duolink™ kit. Each pair of protein**:**protein interaction is visualized as a red fluorescent dot. The principle of PLA is summarized in **Figure 2.4**.

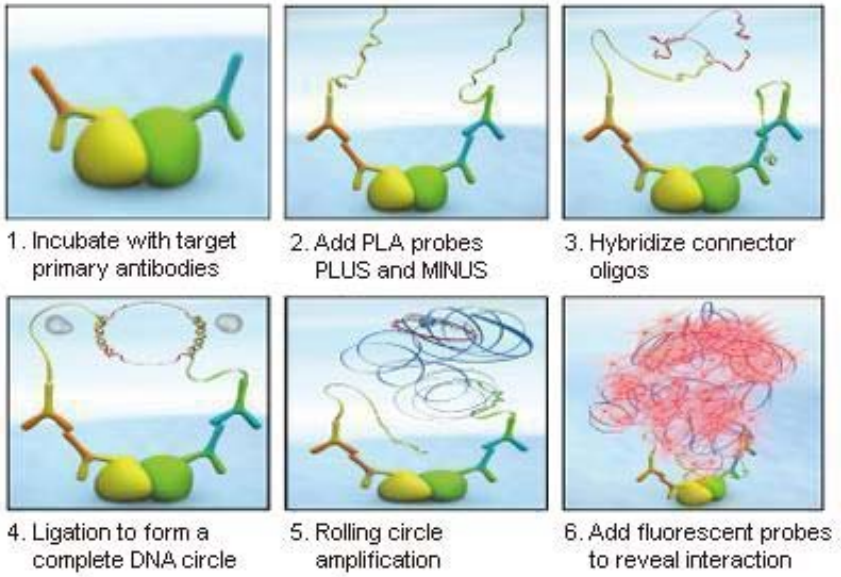

Figure 2.4: An overview of proximity ligation assay. The cells were first incubated with the proteins, then incubated with the compatible primary antibodies, followed by Duolink plus and minus secondary antibodies, conjugated with oligonucleotides. Subsequently, two connector oligonucleotides were added to hybridize with the complementary oligonucleotides conjugated to antibodies, followed by ligation to a closed circle. Rolling-circle amplification (RCA) using the ligated circle as a template generated concatemeric (repeated sequence) products. Fluorescently labeled oligonucleotides that were hybridized to the RCA product generated a distinct fluorescent dot when visualized by fluorescence microscopy. Adapted from http://www.immunoportal.com/modules.php.

Primary monocytes or U937 or HEK293T were plated at a density of 0.5 X 10^6 cells/ml/well onto 12-well plates with cover slips (Sterilin, London, UK) for 24 h before the assay. The cells were incubated with GlcNAc-beads pre-opsonized with IgG, ficolin or both for 20 min at 37˚C. Cells were washed once with PBS (137 mM NaCl, 10 mM phosphate, 2.7 mM KCl; pH is 7.4) and fixed with 4% (w/v) paraformaldehyde (Sigma-Aldrich) in PBS. The interactions between IgG**:**ficolin, IgG**:**FcγR1 and ficolin**:**FcγR1 were detected using compatible primary goat anti-ficolin:rabbit anti-IgG, rabbit anti-IgG:mouse anti-FcγR1 and goat anti-ficolin:mouse anti-FcγR1, respectively.

The secondary anti-rabbit PLUS, anti-mouse MINUS, anti-goat MINUS and anti-goat PLUS probes were from Olink Biosciences. Samples without primary antibodies served as experimental negative controls. Samples incubated with GlcNAc-beads pre-incubated with IgG and HSA were the biological negative control for protein**:**protein interaction. The two oligonucleotides present in the two PLA probes will hybridize if they are in close proximity (as in protein-protein interaction) during the hybridization step. Following that, the two hybridized oligonucleotides were ligated by Duolink ligase, amplified by Duolink Polymerase and detected by red fluorescently labeled oligonucleotides, which are visible under microscopy. The procedures for detection were according to the manufacturer's instructions. PLA signals (each red dot signifying an interaction) were visualized using LSM 510 Meta Confocal Laser Scanning system (Carl Zeiss). All images were taken through a 100x oil immersion lens.

2.12.2. Co-localization assays by immuno-florescence

For co-localization analysis of IgG**:**ficolin, IgG**:**FcγR1 or ficolin**:**FcγR1 (with or without IgG), cells were plated onto 12-well plates with coverslips (Sterilin, UK) at a density of 0.5 X 10^6 cells/ml. The cells (human primary monocytes or U937 cell line) were then incubated with the GlcNAc-beads pre-opsonized with the proteins for 20 min at 37^{o}C, after which they were washed thrice with PBS and fixed in 4% paraformaldehyde for 15 min. Non-specific staining between the primary antibodies and the cells was blocked by incubating in blocking buffer (3% BSA in PBS) for 30 min at room temperature. Then, the

cells were incubated with the respective primary and secondary antibodies diluted in incubation buffer (3% BSA in PBS containing 0.05% Tween 20) for 60 min at room temperature and washed thrice with PBS containing 0.05% Tween 20. To stain the nucleus, a drop of Prolong Gold antifade reagent with DAPI (Invitrogen) was added. Imaging was performed using an LSM META 510 confocal microscope (Carl Zeiss) under a 63x/100x oil objective.

2.13. siRNA knockdown studies

2.13.1. *In vitro* knockdown of *FcγR1* in human monocytes

FcγR1 was silenced by transfecting 10^6 primary monocytes with 0.8 μg siRNA pool (Dharmacon ON-Target*plus* siRNA pool) using Amaxa Human Monocyte Nucleofector kit, Nucleofector program Y-001 (Amaxa, MD) according to the manufacturer's instructions. Transfections were performed within 2 h of cell plating. Control siRNA pool (Dharmacon ON-Target*plus* non-targeting pool) was used for comparison. The knockdown effect of siRNA was checked by Western blotting at 72 h post-transfection. Whole cell lysates of control and target siRNA-treated cells were probed with FcγR1 and actin antibodies to check the efficiency of FcγR1 depletion.

2.13.2. *In vivo* knockdown of *IgG* in mice

We generated *IgG*-knockdown mice to study the loss of function of natural IgG in uninfected mice during infection. The ficolin level was maintained, as it is known that the general function of ficolin may be compensated by other plasma proteins.

Implantation of osmotic pump for continuous release of IgG-siRNA

Alzet pumps are miniature infusion pumps that are routinely used for systemic administration of drugs or siRNA into mice, when implanted subcutaneously. Owing to the unique mechanism by which these pumps operate, compounds of any molecular conformation can be delivered predictably at controlled rates, independent of their physical and chemical properties (Alzet.com).

IgG-expression knockdown in 8-week old Balb/c mice was generated using validated *IgG* siRNA, a method which is used for *in vivo* gene knockdown (http://www.alzet.com/research_applications/siRNA.html). The siRNAs were from Ambion (sense: 5'→3' GGAUGGUGAAACUAAAUAUtt; antisense: 5'→3' AUAUUUAGUUUCACCAUCCtc). HPLC-purified and endotoxin-tested non-targeting siRNA (Ambion) was used as a negative control. The siRNA were dissolved in pyrogen-free PBS before use. 15 or 30 nmol/kg/day siRNA, viz, 0.2 or 0.4 mg/kg/day, respectively) or PBS was infused for 14 days into the mice through subcutaneously implanted osmotic minipumps (1002, Alzet) according to manufacturer's instructions (**Figure 2.5**).

For the subcutaneous implantation of the pump, the site chosen was on the dorsum, slightly caudal to the scapulae such that the pump does not put pressure on vital organs or impede respiration. Briefly, the mouse was anaesthetized with 1:1 mixture of ketamine (0.2 ml/kg) + xylazine (0.2 ml/kg). An incision was made 1.5 times the diameter of the pump perpendicular to the pump's longitudinal axis. The subcutaneous tissue was spread to create a pocket for the pump. The pocket should be large enough to allow some free

movement of the pump but not so large that it will slip. The pump should not rest immediately beneath the incision. Then, the filled osmotic pump was inserted, delivery portal first. The wound was closed with suture. The mouse was injected subcutaneously with analgesic buprenorphine (2.5 mg/kg; 0.1 ml/kg) and saline (0.2 ml/kg) and the wound was treated with topical antibiotic, banocin, for two consecutive days post-surgery to expedite recovery. This procedure was performed under the training of a professional veterinarian (Dr. Enoka Bandularatne, Comparative Medicine, NUS).

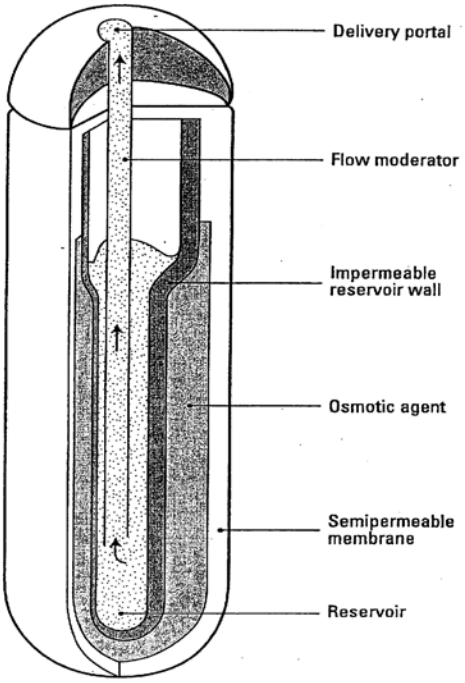

Figure 2.5: Cross-section of the osmotic pump used for sub-cutaneous administration of PBS, control or *IgG* siRNA into mice. The figure shows the design, components and mechanism of action of the action which pumps the siRNA solution at a constant rate or 14 days. Adapted from http://www.alzet.com/downloads/book_chpt.pdf.

Measurement of IgG levels in serum

IgG concentration was determined in the pooled mice serum by using a commercial ELISA kit (Roche) according to manufacturer's instructions. Briefly, wells were incubated with 50 µl capture antibody overnight at 4˚C, followed by three washes with the wash buffer (0.9% w/v NaCl containing 0.1% v/v Tween-20). Then, they were incubated with blocking buffer (TBS containing BSA, 1% w/v) for 2h at room temperature. Following three washes, 50 µl standard and serum samples (diluted in blocking buffer) were added and incubated for 2h at room temperature. The wells were then washed thrice followed by incubation with 50 µl conjugate antibody for 1 h. Finally, the wells were washed to remove any unbound antibody and incubated with 50 µl ABTS substrate solution for 1h prior to reading at $OD_{405\ nm}$.

2.14. In vivo infection of mice with *P. aeruginosa*

Culture of *P. aeruginosa* PAO1 was prepared as described previously (Section 2.7.1) and 10^6 or 10^7 cfu were injected into mice intravenously through the tail vein. Briefly, the mice were weighed prior to the injection and the injection volume determined by the weight of the animal, i.e. 10% of the body weight. The mice in the cage were placed near a heat lamp to increase the blood flow to the tail. Then, they were transferred to restrainer to restrain their mobility while allowing access to the tail vein. The tail was next sanitized by wiping with alcohol swab. The needle was inserted just far enough to get the bevel inside the vein and kept as flat and parallel as possible to the tail. After removing the needle, the site was held with gauze to stop bleeding.

2.15. *Ex vivo* protein:protein interaction assays

2.15.1. IgG:ficolin complex detection in mice serum by Co-IP

IgG**:**ficolin complexes were pulled down by adding 20 µl Protein G Sepharose to equal amounts of serum and incubating for 1 h at 4˚C with shaking. Serum incubated with only Sepharose beads acted as a negative control. The beads were washed thrice with PBS and boiled in reducing loading buffer (containing β-mercaptoethanol) and electrophoresed on 12% SDS-PAGE under reducing conditions. Ficolin that was previously pulled down by the beads (through its interaction with IgG) was detected by Western blot using anti-ficolin antibody.

2.15.2. Tissue co-localization assays by immuno-florescence

Mice were euthanized, and spleen and liver tissues were removed, washed in PBS and immediately frozen in Jung tissue freezing medium (Leica Microsystems) using liquid nitrogen. Tissues were sectioned at a thickness of 5 µm using Leica Cryostat 1850 and mounted onto Superfrost* Plus slides (Fisher Scientific). For co-localization analysis of IgG**:**ficolin, the slides were first fixed in 4% paraformaldehyde for 15 min. After three washes with PBS, non-specific staining between the primary antibodies and the tissue was blocked by incubating in blocking buffer (3% BSA in PBS) for 30 min at room temperature. Then, the tissue section was incubated with the respective primary and secondary antibodies diluted in incubation buffer (3% BSA in PBS containing 0.05% Tween 20) for 60 min at room temperature and washed thrice with PBS. To stain the nucleus, a drop of Prolong Gold antifade reagent

with DAPI (Invitrogen) was added. Imaging was performed using an LSM META 510 confocal microscope (Carl Zeiss) under a 100x oil objective.

2.16. Assessment of extent of infection and damage in tissues of mice

2.16.1. Bacterial load determination

Mice were infected intravenously through tail vein injection with 10^6 or 10^7 cfu *P. aeruginosa* for the indicated time. For bacterial counts in the spleen, liver, lung and serum were collected and resuspended in PBS, excised into small pieces, mixed with 5 mg/ml saponin, and incubated for 10 min at 37˚C to release the internalized bacteria. The samples were centrifuged at 1200g for 10 min, resuspended in PBS, serially diluted, and plated on LB agar plates, and viable bacterial counts were scored after overnight incubation at 37^{o}C.

2.16.2. Measurement of cytokine levels in pooled serum

Blood was collected from infected or uninfected mice by cardiac puncture, allowed to clot, spun down at 1000g for 5 min and serum was collected. IL6, TNFα and IL10 concentrations were determined in the pooled serum by using commercial ELISA kits (BD Biosciences) according to manufacturer's instructions. Briefly, the capture antibody in recommended dilution was immobilized onto Maxisorp™ plate (NUNC, Denmark) by incubating overnight at 4˚C. The wells were washed three times with PBST, followed by blocking with PBS containing 10% FBS (assay diluent) at room temperature at 1 h. After two washes, standards and serum diluted in assay diluent were added and incubated at room temperature for 2 h. After washing the wells 5

times with PBST, the bound mouse IL6, TNFα and IL10 were detected with respective working detector solution (detection antibody + SAv-HRP reagent). Following 7 washes to remove any unbound antibody, substrate solution (TMB and hydrogen peroxide) (BD OptEIA^{TM}) was added and the $OD_{450\ nm}$ was read within 30 min.

2.16.3. Hematoxylin and eosin staining of liver

Tissues were isolated from mice, embedded in tissue freezing medium (Leica Microsystems) and flash frozen in liquid nitrogen. The frozen moulds were stored in -30˚C until further use. 5 µm thick sections were cut using the Leica cryo-sectioning machine at -27˚C. The sections were carefully mounted onto Superfrost* Plus slides to avoid air bubbles. After air drying for 15 min, the sections were fixed with 4% paraformaldehyde for 15 min and washed 3 times with PBS.

Hematoxylin and eosin staining is a widely used technique to observe tissue morphological changes. The method involves application of hemalum, which is a complex formed from aluminum ions and oxidized haematoxylin, that colors nuclei of cells blue. The nuclear staining is followed by counterstaining with an aqueous or alcoholic solution of eosin Y, which colors cytoplasmic structures in various shades of red, pink and orange based on constitution.

The method included staining the sections with hematoxylin for 5 min followed by a quick wash with 0.1% hydrochloric acid for 2 s. The slides were left under gentle and indirect running water until the solution was clear. Then,

the slides were counter-stained with eosin for 30 s, followed by a quick wash to remove any unbound dye. The slides were then dehydrated in a series of dehydration steps for 2 min each in: 75% ethanol, 90% ethanol, absolute ethanol and xylene. The slides were pat dried and a drop of mounting agent (DPX moutant, BDH Chemicals Ltd) was added on the tissue slide prior to adding the cover slip (0.13-0.16 mm thick, Menzel Glaser). Images were taken using Mirax Midi microscope (Carl Zeiss) using 2x and 20x lens magnification and offline analysis was done using Mirax viewer software (Carl Zeiss).

2.16.4. Germinal center detection by immunostaining of spleen

The germinal centers (GCs) are sites of B cell activation during an immune response (MacLennan 1994; Victora and Nussenzweig, 2012). Hence, the extent of infection was assessed by studying development of germinal centers. Spleen tissue was frozen, sectioned and fixed using a similar protocol as mentioned above for making liver sections. The slides were rehydrated in PBS for 10 min and blocked for 1 h at room temperature using blocking buffer (3% BSA in PBST). Next, the samples were incubated overnight with anti-B220 (B-cell specific), anti-GL7 (germinal center specific) and anti-*P. aeruginosa* antibodies at 4˚C to detect GC B cells and *P. aeruginosa* in spleen sections. The slides were washed 3 times for 15 min each in PBS. Then, they were incubated with Alexa 594 anti-rat secondary antibody (1:500) for 1 h at room temperature. Following 3 washes with PBS, the slides were mounted with DAPI containing mounting media and visualized at 100X magnification, using

an LSM META 510 confocal microscope (Carl Zeiss, Germany).

2.16.5. Calculation of germinal centers per mm^2 of white pulp area of spleen

The germinal centers (GCs) per mm^2 of white pulp area were calculated as previously described (Weinstein et al., 2008). Briefly, the frozen sections were cut at 5 μm thickness, mounted onto Superfrost* Plus slides, fixed with 4% PFA and stained with hematoxylin and eosin. The total white pulp area and spleen area (in mm^2) was measured using Image J software for each spleen section. The total number of GCs was manually counted using bright field microscopy. The number of GCs per mm^2 of white pulp area was calculated by dividing the counted number of GCs by the total white pulp area. The percentage of white pulp for each spleen section was calculated by dividing the total white pulp area by total area of each spleen-section. Three consecutive sections per spleen were studied to acquire an average value of GCs per white pulp area and the percentage of white pulp area per spleen. Six mice per group per time point were studied.

2.17. Reconstitution of mice with natural IgG

In order to prove the biological significance of natural IgG, the *AID*$^{-/-}$ mice (lacking IgG) were reconstituted with IgG (purified from uninfected WT mice) upto the levels found in WT mice, prior to the infection. Natural IgG reconstituted into the mice was purified as previously described (Section 2.3) and checked by flow cytometry to be non-binding and non-antigen specific to *P. aeruginosa* PAO1 strain.

For reconstitution, 6h prior to infection, *AID*$^{-/-}$ mice were injected intravenously with 2 mg IgG (2 mg/ml IgG in PBS; 0.1ml/10g body weight) to restore the levels to normal serum levels of IgG found in wild type mice. Infection and further experiments were carried out in a similar manner as described above.

2.18. Statistical analysis

Data represent means ± SEM of three independent experiments with triplicates each. *p* values of less than 0.05 are considered significant by two-tailed Student's t test. Differences in survival of mice post infection were calculated using the log-rank test. *: $p<0.05$, **: $p<0.01$ and n.s.: $p>0.05$.

Chapter 3

RESULTS

CHAPTER 3: RESULTS

3.1. Ficolins interact with both IgG and IgA

IgA was recently identified to be an interaction partner of ficolin isoforms, M-ficolin and H-ficolin. Since the FBG domain of all the three ficolins share ~80% homology, and this is the domain which interacts with other PRRs (Zhang et al., 2009), we tested the ability of the recombinant FBG domains of L-, H- and M-ficolins to recognize IgA and IgG. As a preliminary test for potential single chain domain-specific interactions between the immunoglobulins and the ficolins, we performed yeast 2-hybrid assays and showed that indeed all three ficolin FBG domains interact with IgA (**Figure 3.1A**) and IgG (**Figure 3.1B**). The H-ficolin isoform showed the strongest interaction (red boxes). Yeast was used for this preliminary study as it is known to be a robust organism for studying protein-protein interaction, with ability to form disulphide bonds and maintain reduced state glutathione (Young 1998).

3.2. Purification of native IgG and ficolin (from uninfected human serum) and recombinant ficolin FBG

To understand the interaction between ficolins and IgG and their subsequent role in anti-microbial defense, we first purified native H-ficolin and IgG from uninfected human serum. We also purified recombinant FBG domains of ficolins from transfected cell culture supernatants, to be used for further experiments.

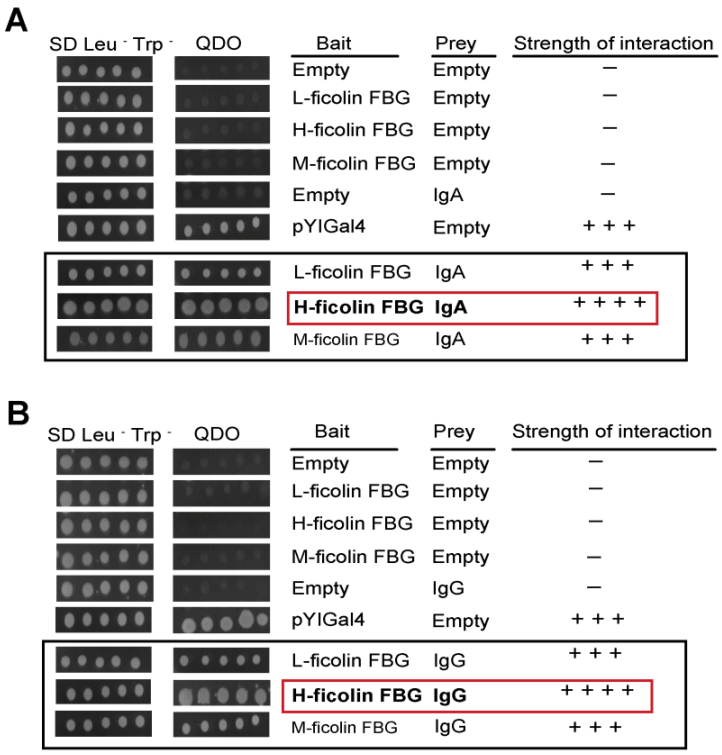

Figure 3.1: Identification of interaction between ficolins and immunoglobulins. Yeast two-hybrid screening shows that the FBG domain of L-, H- and M-ficolin interacts with the heavy chains of (**A**) IgA or (**B**) IgG, with H-ficolin FBG showing strongest interaction (red boxes).Colonies growing on the SD-Trp$^-$Leu$^-$ plates indicate the successful co-transformation of both bait and prey plasmids. Growth on the QDO plates indicates interaction between ficolin FBG and IgA or IgG. Transformation of the empty vector plasmid with the protein of interest excludes the possibility of autoactivation. pYIGal4 plasmid was used as a positive control. Data are representative of three independent experiments.

3.2.1. Purity of native H-ficolin purified from uninfected human serum

H-ficolin is a ficolin isoform that is secreted by lung and liver into the serum (Matsushita et al., 1996; Andersen et al., 2009). Thus, native H-ficolin was purified from the serum as described (Section 2.2).

To determine the purity and the size of the purified native H-ficolin from uninfected human serum, the purified fraction of H-ficolin were electrophoresed on 12% SDS-PAGE under reducing conditions. Coomassie blue staining of the SDS-PAGE gel showed a clear single band at 37 kDa for

H-ficolin (**Figure 3.2A**). Other proteins that non-specifically co-purified in the purified H-ficolin pool were less than 5% of the total purified protein (Figure 3.2A).

The purity of H-ficolin fraction was also verified by mass spectrometry. The peak profile in mass spectrometry indicates that the purified H-ficolin is of high integrity and is qualified to be used in the subsequent experiments (**Figure 3.2B**).

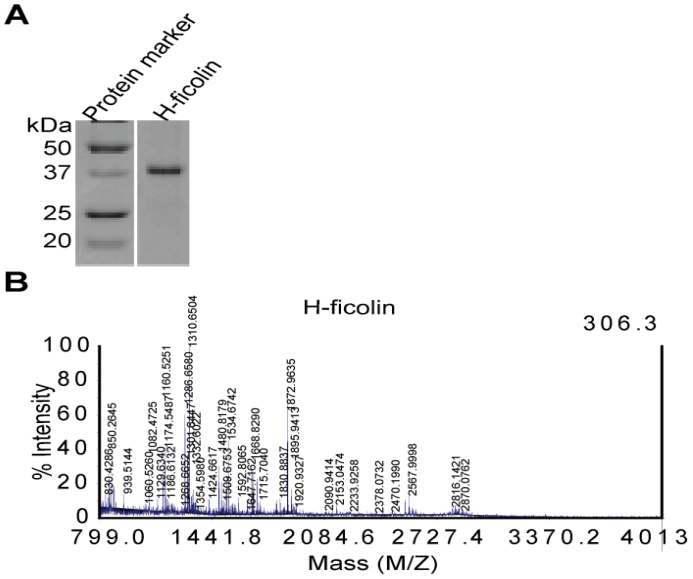

Figure 3.2: Purity of human native H-ficolin. (**A**) One µg of purified native H-ficolin was resolved on 12% reducing SDS PAGE and stained with Coomassie-blue. (**B**) Mass spectrometry of the purified H-ficolin. One µg of H-ficolin was trypsin-digested and analyzed by MALDI-TOF-TOF to check for purity of the sample. H-ficolin was found to be >95% pure. Peptides with molecular weight indicated show the fragments that are consistent with H-ficolin finger prints in the database.

3.2.2. Purity of native IgG purified from uninfected human serum

"Natural IgG" has been defined as the whole repertoire of IgG in the serum of uninfected animals and individuals previously not exposed to foreign antigens (Ochsenbein et al., 1999). Hence, we have studied uninfected serum that would presumably contain natural IgG. We purified the pool of native IgG

from uninfected human serum as described (Section 2.3).

The purity of native IgG was verified by Coomassie blue staining (**Figure 3.3A**) and mass spectrometry (**Figure 3.3B**). The single band on the Coomassie blue stained SDS-PAGE gel and the profile of the peaks in mass spectrometry indicate that the purified IgG is of high integrity and hence qualified to be used in further experiments.

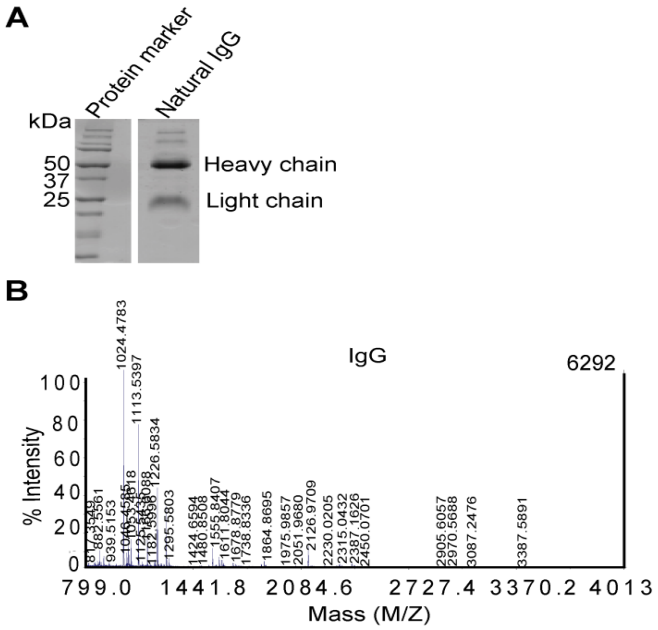

Figure 3.3: Purity of human native IgG. (**A**) One µg of IgG was resolved on 12% reducing SDS PAGE and stained with Commassie blue. (**B**) Mass spectrometry of the purified IgG. One µg of IgG was trypsin-digested and analyzed by MALDI-TOF-TOF to check for purity of the sample. IgG was found be >95% pure. Peptides with molecular weight indicated show the fragments that are consistent with IgG finger prints in the database.

3.2.3. Purity of recombinant FBG domains of L-, H- and M-ficolins

Functional fragments of FBG domains of all three ficolins were cloned individually into the pSecTag 2C plasmid (without signal sequence) in frame with the His tag. Mammalian expression vectors containing FBG domains of ficolins were transfected into the HEK 293T cells individually using

lipofectamine 2000. Cell culture supernatant was collected 48 h after transfection. The recombinant proteins, each with a His tag were purified using Ni-NTA affinity resin. Six elution fractions of 120 µl each for each protein were collected. Coomassie blue staining of SDS PAGE gel showed a single band indicating that the protein is of high purity (**Figure 3.4**). Hence, these purified proteins were qualified to be used in subsequent experiments.

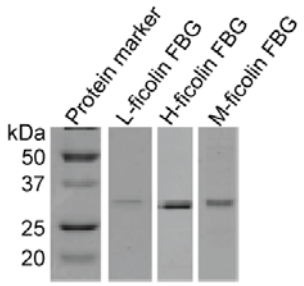

Figure 3.4: Purification of recombinant FBG domains of ficolins. Recombinant FBG domains of the three ficolins were expressed in HEK293T separately, purified from culture supernatant and eluted out from Ni-NTA beads using elution buffer. The eluted fractions were electrophoretically resolved on 12% SDS PAGE under reducing conditions. The purity and integrity of proteins were checked by Coomassie blue staining.

3.3. Functional significance of natural IgG:ficolin interaction

3.3.1. Ficolins recruit natural IgG onto the bacteria

To understand the mechanism of IgG**:**ficolin-dependent innate immune defense, we purified ficolins and IgG from uninfected healthy human serum and tested their interactions with representative Gram negative bacteria (*P. aeruginosa* and *E. coli*) and Gram positive bacteria (*S. aureus* and *S. epidermidis*). Since the mean steady-state concentrations of L- and H-ficolins in the serum are 7 and 15 µg/ml, respectively, and the ficolin concentrations are not known to increase in an infection, we employed these concentrations in our experiments under both normal (pH 7.4, 2.5 mM Ca^{2+}) and infection-

inflammation (pH 6.5, 2.0 mM Ca^{2+}) conditions. Flow cytometry showed that IgG was deposited on the bacteria, dose-dependently of all three forms of ficolin (**Figure 3.5**; cyan and dark blue), with H-ficolin recruiting the highest deposition of IgG. In the absence of ficolin, IgG did not bind bacteria (Figure 3.5; red), suggesting that it requires ficolin to recognize the pathogens, except for *S. aureus*. This deviation may be due to Protein A, a known ligand of IgG, which is present on the surface of *S. aureus* (Graille et al., 2000), hence causing a small binding shift. These results suggest that a systemic infection could trigger the formation of IgG**:**ficolin complexes, which opsonize the bacteria.

3.3.2. Natural IgG, aided by ficolin drives phagocytosis of *P. aeruginosa*

To investigate the fate of the bacteria opsonized with IgG**:**ficolin complex, we incubated GFP-labeled *P. aeruginosa* with human monocytes in the presence of the proteins, and examined the dynamics of phagocytosis. FACS analysis showed that IgG**:**ficolin-opsonized bacteria were phagocytosed more significantly than the bacteria incubated with either ficolin or IgG alone (**Figure 3.6**). Antigen-specific immunoglobulins are known to bind their corresponding antigens displayed on the invading microbe to enable phagocytosis (Anderson et al., 1990). However, our results showed that although natural IgG alone was unable to bind directly to the bacteria (Figure 3.6, +IgG alone), it was able to induce phagocytosis of the bacteria when in the presence of ficolin. This suggests that the 'dormant' pool of natural IgG was recruited by ficolin pre-bound to the bacteria, which was subsequently

phagocytosed by the monocytes. A similar effect was seen with 1:10 diluted serum, which served as a positive control, although the function of natural antibodies in the serum was reduced because of dilution, as was earlier reported (Ochsenbein et al., 1999). Infection, which induces local acidosis and hypocalcaemia (Aderka et al., 1987) enhanced phagocytosis (Figure 3.6, red), most robustly with IgG**:**H-ficolin opsonized bacteria. Thus henceforth, we focused on IgG**:**H-ficolin mediated response unless otherwise stated.

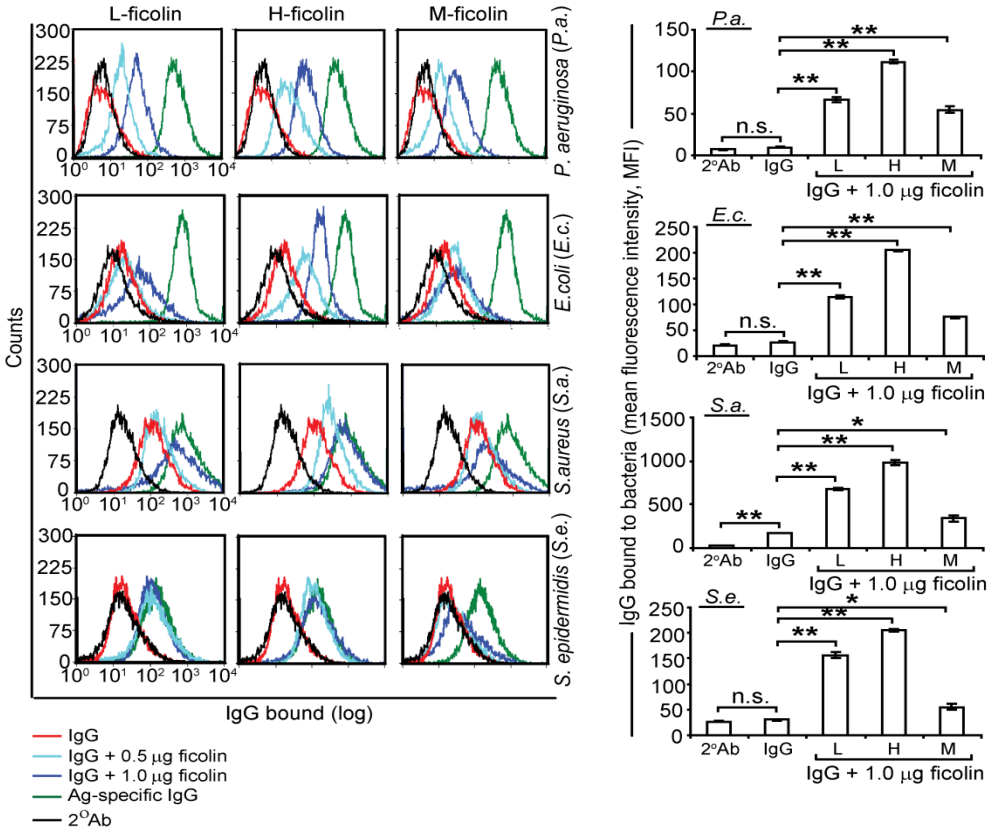

Figure 3.5: Ficolins recruit natural IgG onto the bacteria. FACS analysis quantifies binding of IgG (purified from uninfected human serum) to 10^6 cfu bacteria. The bacteria were opsonized either with IgG alone (red) or IgG in complex with 0.5 µg ficolin (cyan) or 1 µg ficolin (dark blue), and incubated with primary anti-human IgG antibody followed by staining with Alexa 488-conjugated secondary antibody. Positive control (green) included bacteria opsonized with antigen-specific IgG prior to staining with Alexa 488-conjugated secondary antibody. Bacteria stained with secondary antibody alone (black) served as the negative control (see key below the figure). The right panel compares the mean fluorescence intensity (MFI) of IgG bound to the bacteria when incubated with IgG alone [IgG] or IgG in the presence of 1.0 µg ficolin (L-, H- or M- ficolin). Three replicates per sample were tested.

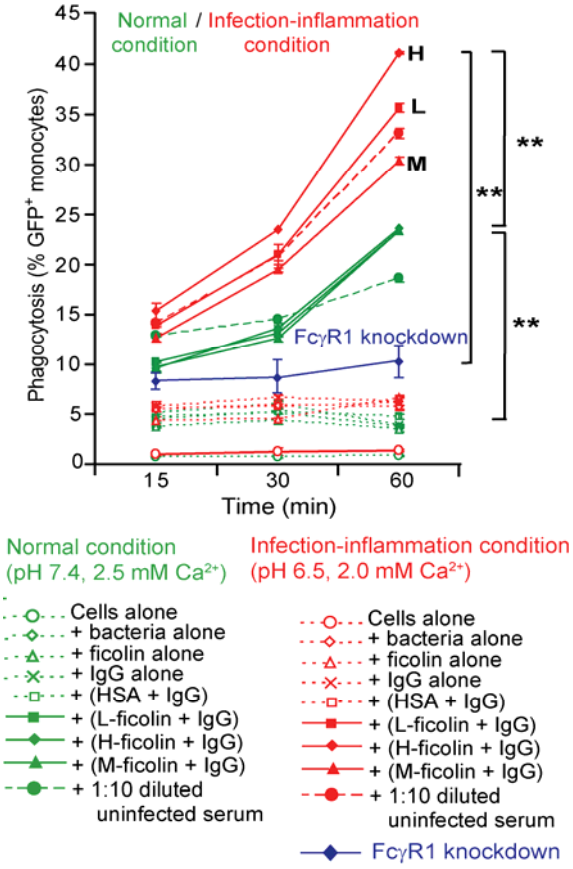

Figure 3.6: Natural IgG, aided by ficolin, drives phagocytosis of bacteria. Quantification of phagocytosis of 10^7 cfu of GFP-expressing *P. aeruginosa* (opsonized with the proteins, individually or in complex – see key below the figure) by 10^6 human primary monocytes. FACS analysis of phagocytosis (% GFP-positive monocytes) was performed under normal (pH 7.4, 2.5 mM Ca^{2+}, green) and infection-inflammation condition (pH 6.5, 2.0 mM Ca^{2+}, red). Knockdown of human monocyte FcγR1 significantly reduced phagocytosis (blue), indicating that IgG**:**ficolin-opsonized bacteria is phagocytosed via FcγR1 on the monocytes. Three replicates per condition per time point were tested. Data are representative of three independent experiments.

3.3.3. Infection-inflammation condition increases recruitment of natural IgG to PAMP-associated ficolin

To investigate the basis of increased IgG**:**ficolin complex, which increased phagocytic efficiency under infection-inflammation condition, we checked for natural IgG deposition on GlcNAc-beads (bacterial mimic) under both normal

and infection-inflammation conditions, in the absence or presence of ficolin. Notably, the amount of H-ficolin engaged on GlcNAc-Sepharose beads (+GlcNAc; henceforth referred to as GlcNAc-beads) remained the same under both conditions, but infection-inflammation condition induced a 3.5-fold more natural IgG recruited (**Figure 3.7**). With Sepharose beads alone (-GlcNAc), or in the absence of ficolin (Ficolin$^-$ serum), no IgG was pulled down, indicating the specificity of: (i) ficolin for GlcNAc and (ii) IgG for ficolin bound to the bacterial mimic (GlcNAc).

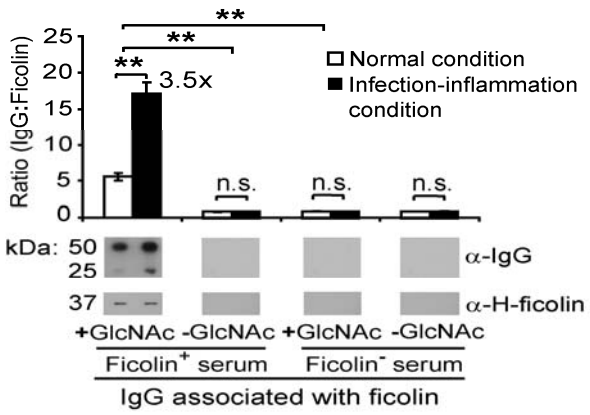

Figure 3.7: Ficolin recruits more natural IgG on the bacterial mimic under infection-inflammation condition. Co-IP to determine the specific interaction between IgG and ficolin in human serum. GlcNAc-Sepharose beads (+GlcNAc) were used as bacterial mimic and incubated with serum under normal (white bar) and infection-inflammation (black bar) conditions, in the presence (Ficolin$^+$ serum) and absence (Ficolin$^-$ serum) of ficolin. Sepharose beads alone (-GlcNAc) were used as a negative control. Under infection-inflammation condition, IgG (50 kDa heavy chain and 25 kDa light chain) was recruited more intensely (3.5x more than normal condition) onto the GlcNAc-beads in the presence of ficolin. Data are presented as ratio of density of IgG to ficolin deposited on beads, and representative Western blots are shown. Three replicates per condition were tested. Samples were derived from the same experiment, resolved under 12% reducing SDS-PAGE and the gels and blots were processed in parallel.

3.3.4. *FcγR1* knockdown in human primary monocytes reduces IgG:ficolin mediated phagocytosis

FcγR1 is a known high-affinity receptor for IgG-opsonized bacterial

complexes (Indik et al., 1995), which induces phagocytosis (Burton et al., 1988). By knocking down FcγR1 in human monocytes (**Figure 3.8**), phagocytosis of IgG**:**ficolin-opsonized bacteria was significantly reduced (Figure 3.6, blue line), indicating specific interaction between natural IgG and FcγR1.

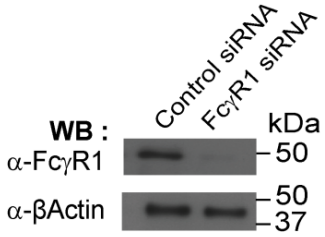

Figure 3.8: Knockdown of FcγR1 in human primary monocytes. Immunoblot analysis of FcγR1 levels in control or *FcγR1* siRNA treated monocytes. For FcγR1 knockdown, 10^6 monocytes were nucleofected with either control or *FcγR1*-specific siRNA. Whole-cell lysates of siRNA-nucleofected cells were prepared after 72 h and immunoblotted for FcγR1 or β-actin (loading control) to show the efficiency of FcγR1 knockdown.

3.3.5. IL8 secretion by monocytes is upregulated accompanying phagocytosis

We next considered host factors associated with phagocytosis of IgG**:**ficolin-opsonized bacteria. IL8, a pro-inflammatory chemokine produced by monocytes, is prominently induced by FcγR1-mediated phagocytosis (Marsh et al., 1996; Foreback et al., 1998; Laterveer et al., 1995) of *P. aeruginosa* (Kube et al., 2001). Here, GlcNAc-beads were used as the bacterial mimic instead of whole bacteria since ficolin specifically recognizes GlcNAc moieties of PAMPs, hence allowing us to directly query the recognition leading from interactions amongst ficolin, IgG and FcγR1, rather than through TLRs (since TLRs respond to multiple PAMPs on the bacteria).

We found that phagocytosis of GlcNAc-beads opsonized with IgG:H-

ficolin markedly induced IL8, whereas in the absence of GlcNAc-beads, neither individual proteins nor IgG**:**H-ficolin complex induced IL8 production, indicating that no random immune activation occurred in the absence of a PAMP/pathogen (**Figure 3.9**). Moreover, IL8 production was significantly higher under infection-inflammation condition, suggesting that local acidosis and hypocalcaemia also trigger the monocytes to recognize the opsonized bacterial mimic in a specific manner and mount a stronger attack by producing more pro-inflammatory cytokines during an infection. Knockdown of FcγR1 led to a decrease in cytokine production showing that IgG**:**ficolin mediated bacterial recognition takes place likely through the FcγR1 receptor. Collectively, we have shown the role of natural IgG in bridging the ficolin-bound bacteria to FcγR1 on the monocytes, leading to phagocytosis and pro-inflammatory response.

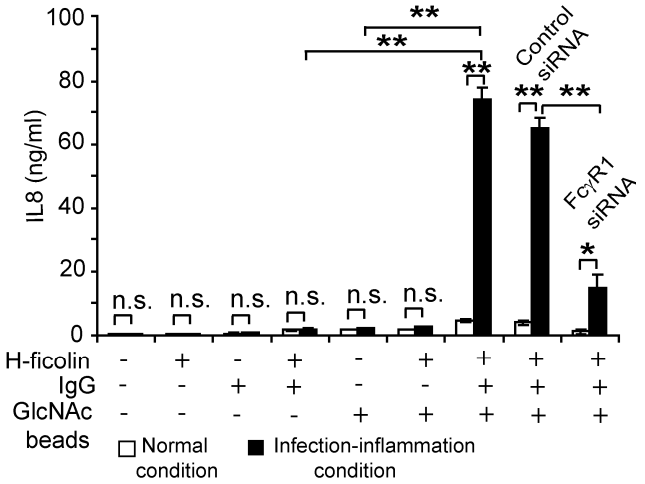

Figure 3.9: Natural IgG, aided by ficolin, drives phagocytosis of bacteria and upregulates IL8 secretion by human primary monocytes. ELISA quantifies IL8 secreted by 10^6 monocytes under infection-inflammation condition (black) compared to normal condition (white). The monocytes were incubated for 24 h with GlcNAc-beads opsonized with individual proteins or the complex. Monocytes incubated without GlcNAc-beads or proteins alone were used as negative controls. *FcγR1* knockdown significantly reduced IL8 production. Three replicates were performed per condition. *p<0.05; **p<0.01; n.s., not significant. Data are representative of three independent experiments.

3.4. Characterization of IgG:ficolin interaction

3.4.1. IgG interacts with FBG domain of ficolin through its Fc region

IgG**:**ficolin interaction was consistently stronger under infection-inflammation condition (Figure 3.7), prompting us to characterize their biophysical interactions under mild acidosis and hypocalcaemia. As a preliminary analysis of the potential interaction of single chain domains between ficolin and IgG, we used yeast 2-hybrid assay to characterize the domain specific interaction between ficolin and IgG. Full length, FBG or collagen-like domain of H-ficolin and full-length or Fc region of heavy chain IgG were separately cloned into both bait and prey vectors. The co-transformants were plated onto the SD-$Trp^{-}Leu^{-}$ plates to check for the presence of both plasmids, and cultured on QDO plates to check for protein**:**protein interaction, which showed that ficolin FBG interacts with the Fc region of IgG (**Figure 3.10**, red boxes).

3.4.2. Infection-inflammation condition increases IgG:ficolin interaction

We further studied the effect of pH and calcium on IgG**:**ficolin interaction by studying interaction under normal and infection-inflammation conditions. ELISA results showed that (i) Ficolin bound to immobilized GlcNAc-BSA, and dose-dependently recruited IgG (purified from uninfected serum) through its FBG domain, (ii) amount of IgG bound to ficolin increases under infection-inflammation condition and (iii) H-ficolin bound to GlcNAc recruits maximum IgG amongst all three ficolins tested (**Figure 3.11**).

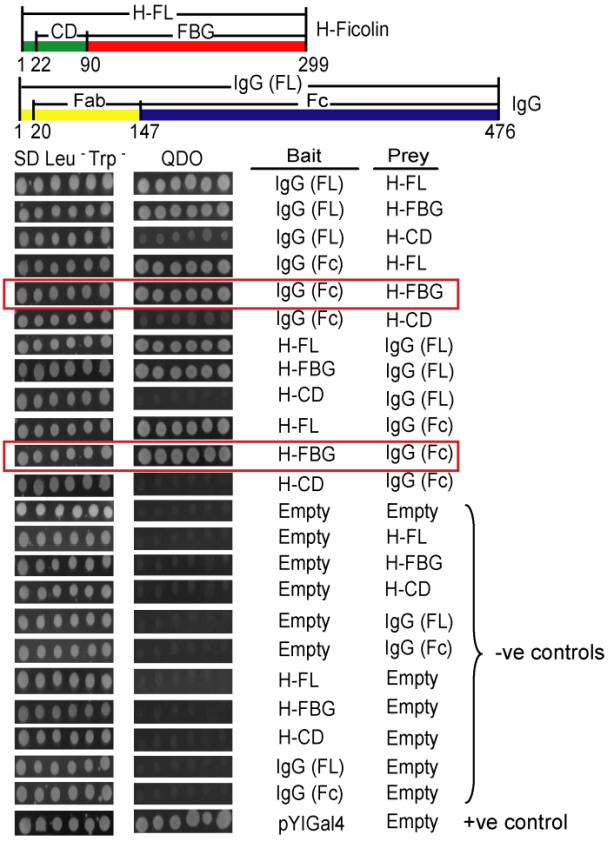

Figure 3.10: Ficolin FBG interacts with IgG Fc. Delineation of the single chain interaction domains of H-ficolin and IgG heavy chain by yeast two-hybrid. The FBG and collagen-like domain of H-ficolin and full-length and Fc region of IgG were individually subcloned. To compare the strength of interaction, yeast colonies were serially diluted and plated on QDO plates. Either in bait or prey vectors, the H-ficolin FBG showed strongest interaction with IgG Fc (red boxes). FL:full-length, Fc: constant region of IgG heavy chain, FBG: fibrinogen-like domain, CD: collagen-like domain. Data are representative of three independent experiments.

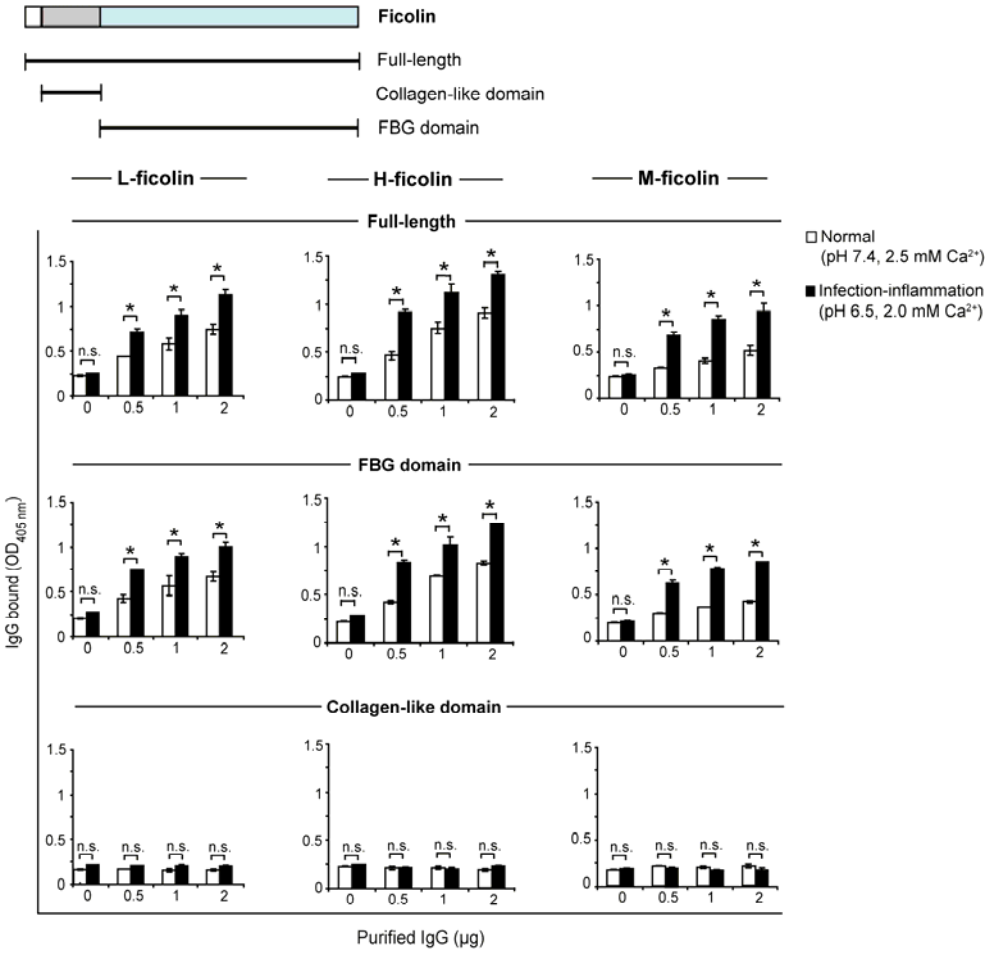

Figure 3.11: Infection-inflammation condition increases the recruitment of IgG to FBG domain of ficolin. ELISA shows binding of IgG (purified from uninfected human serum) to recombinant full-length ficolin and ficolin domains (FBG domain and collagen-like domain), which were pre-immobilized on GlcNAc-BSA in 96-well plates, under normal (white bar) and infection-inflammation (black bar) conditions. 1 µg ficolin (full-length, FBG or collagen-like domain) was bound to 0.8 µg GlcNAc-BSA, immobilized onto each well of the maxisorp plate and increasing doses of IgG were added to test the interaction. The full length ficolin, FBG and CD domains are represented diagrammatically above the graphical plots. Three replicates per condition were tested. Data are representative of three independent experiments.

3.4.3. IgG3, the natural IgG isotype, specifically interacts with ficolin

We tested the binding of three predominant serum IgG isotypes to ficolin, of which IgG3 is known to be the natural IgG isotype (Michael et al., 1969, Sidman et al., 1986). IgG1 and IgG3 isotypes are known to bind to FcγR1 with

highest affinity whereas IgG2 binds with very low affinity (Burton et al., 1988). First, we showed all three isotypes to be present in both the uninfected human serum and the whole purified IgG used in our study (**Figure 3.12**). Then, we showed that IgG3 exhibits the highest dose-dependent binding to ficolin, particularly under the infection-inflammation condition (**Figure 3.13**). In contrast, both IgG1 and IgG2 showed little to no binding to ficolin under either normal or infection-inflammation condition. This suggests that natural IgG3 binds specifically to ficolin, and the immune complex is recognized by FcγR1, for subsequent phagocytosis.

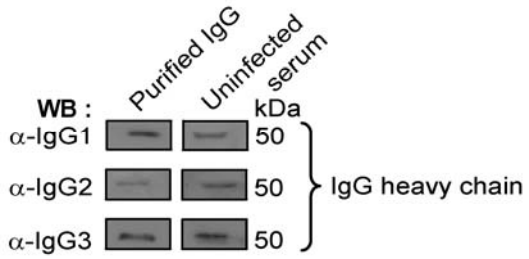

Figure 3.12: Immunoblot detection of IgG isotypes: IgG1, IgG2 and IgG3 in uninfected human serum and in purified whole IgG. The samples were resolved on 12% reducing SDS-PAGE and the gels and blots were processed in parallel. The immunoblots were probed with the respective antibodies against the IgG isotype-specific heavy chain (50 kDa) of IgG1, IgG2 and IgG3.

3.4.4. IgG:ficolin interaction affinity on bacterial mimic increases 100-fold under infection-inflammation condition

To understand the mechanism underlying how infection-inflammation condition triggered stronger interaction between IgG and ficolin FBG, we used surface plasmon resonance (SPR) to characterize real-time molecular interactions between FBG & GlcNAc and between FBG & IgG under normal and infection-inflammation conditions. To achieve this, we immobilized GlcNAc-BSA on a CM5 chip to mimic the bacterial surface; henceforth

referred to as GlcNAc-immobilized chip. We found that all three ficolin FBGs bind GlcNAc within the same range of affinity under both conditions (**Figure 3.14**).

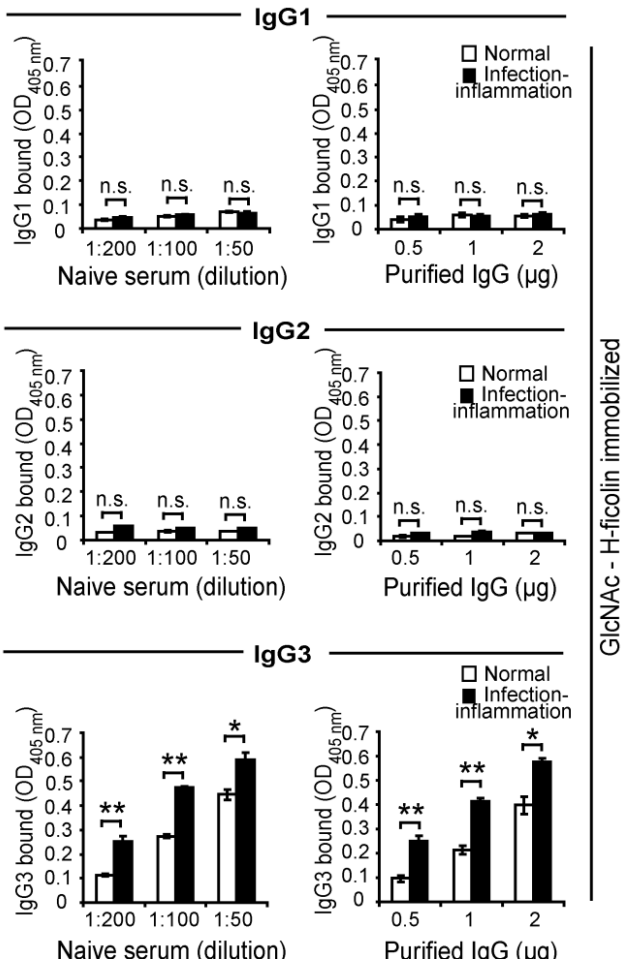

Figure 3.13: IgG3, the natural IgG isotype, specifically binds to ficolin. ELISA of IgG isotypes (present in uninfected human serum and in purified IgG) binding to H-ficolin which was pre-immobilized on GlcNAc-BSA in 96-well plates. Binding studies were performed under normal (pH 7.4, 2 mM Ca^{2+}; white bar) and infection-inflammation (pH 6.5, 2.0 mM Ca^{2+}; black bar) conditions. IgG3 exhibits the highest dose-dependent binding to ficolin, which significantly increased under the infection-inflammation condition. Antibodies against the IgG isotype-specific heavy chain (50 kDa) of IgG1, IgG2 and IgG3 were used to detect binding to H-ficolin. Three replicates per condition were tested.

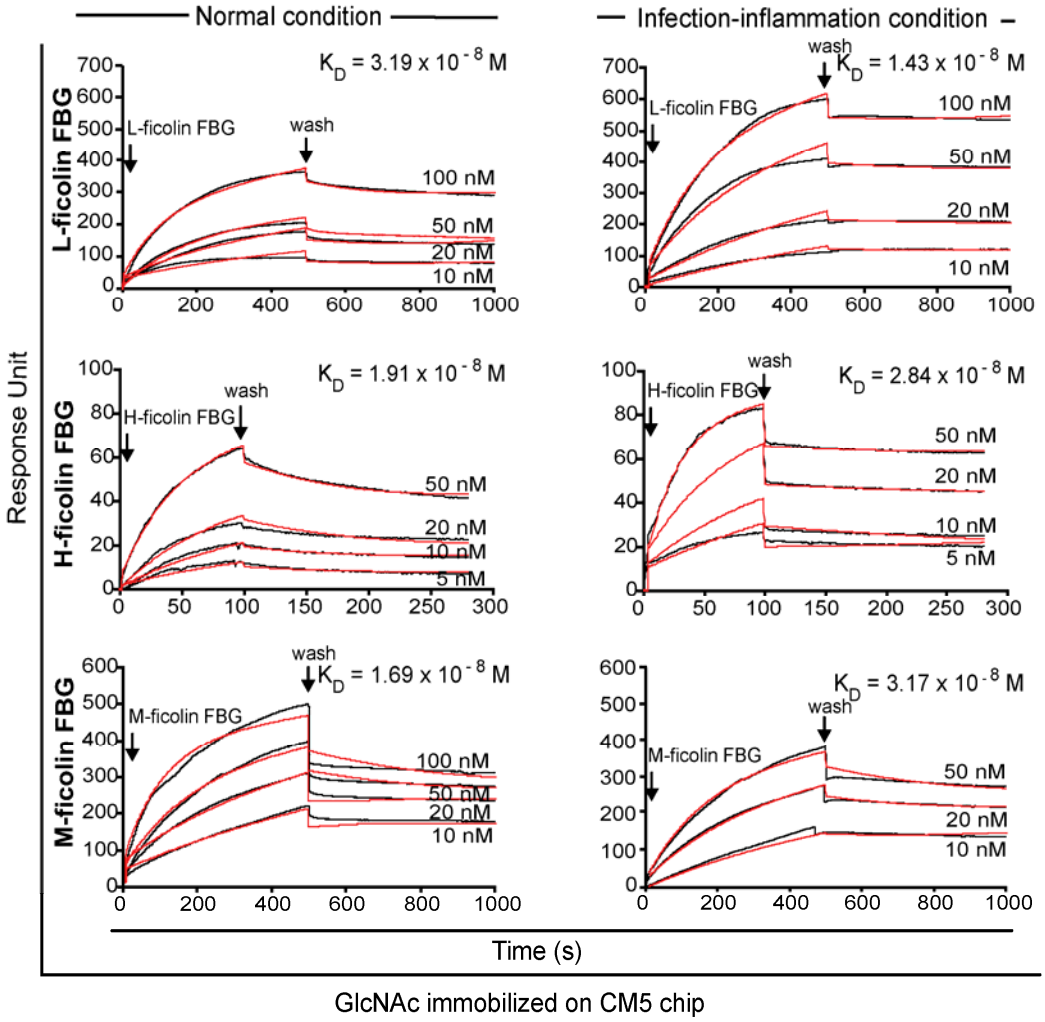

Figure 3.14: All three ficolin FBG bind to GlcNAc with similar affinity under both normal and infection-inflammation conditions. Surface Plasmon Resonance (response unit) studies were performed to show interaction between ficolin FBGs and GlcNAc under normal and infection-inflammation conditions. GlcNAc-BSA was immobilized on the CM5 chip to expose GlcNAc as a ligand for ficolin FBG. Increasing concentrations of L-, H- or M- ficolin FBG were injected to study association followed by buffer flow (wash) to study dissociation. Data were analyzed using BIAevaluation 3.2 software. The binding curves (black) are overlaid with the fit of 1:1 interaction model (red).

As ficolins bind to GlcNAc with similar affinity under both normal and infection-inflammation conditions (Figure 3.14), this provided us with a uniform platform to study IgG**:**ficolin interaction. Next, we studied the binding affinity of IgG to ficolin bound to the immobilized GlcNAc (bacterial mimic), under both normal and infection-inflammation conditions. When IgG was injected over H-ficolin FBG (pre-bound to the GlcNAc-immobilized chip), we observed a 100-fold increase in the binding affinity (K_D) between ficolin FBG and IgG, corresponding to a 10-fold increase in association rate constant (k_{on}) and a 10-fold decrease in dissociation rate constant (k_{off}), under infection-inflammation condition compared to normal condition (**Figure 3.15**). Human serum albumin (HSA, blue line) used as a negative control, showed no binding to H-ficolin FBG, indicating the specificity of interaction between ficolin FBG and IgG. Such a significant increase in affinity might be attributable to conformational changes in the proteins under mild acidosis and hypocalcaemia induced by the infection-inflammation condition. Alternatively, local acidosis could have changed the protonation state of certain amino acid residues, and exposed new interaction sites, leading to increased affinity between ficolin and IgG.

3.5. Ficolin FBG binds IgG Fc at distinct sites remote from the FcγR1 binding site

Since we have delineated the infection-mediated IgG**:**ficolin interaction to the FBG domain of ficolin, it was imperative to locate their precise binding interfaces in view of rationalizing how this complex might spatially interact with FcγR1 on the monocytes, leading to the IgG**:**ficolin mediated

phagocytosis (Figure 3.6).

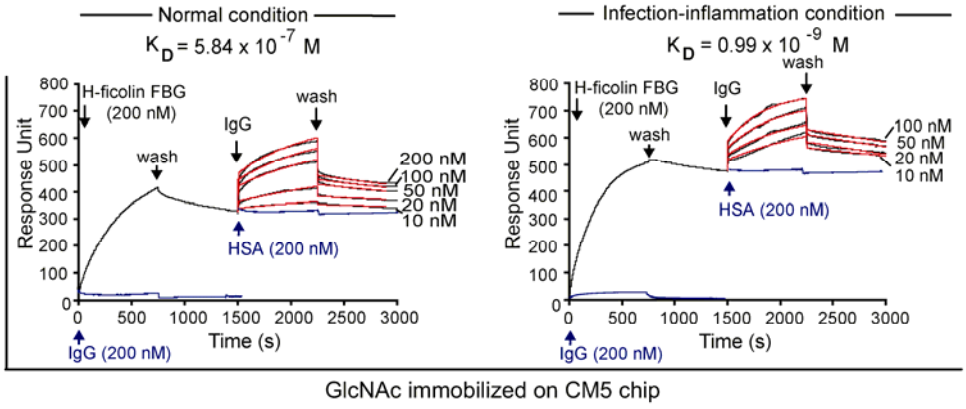

Figure 3.15: IgG binds to PAMP-associated ficolin with 100-fold higher affinity under infection-inflammation condition. SPR analysis of the binding affinity (K_D) between purified human IgG and H-ficolin FBG on GlcNAc under normal and infection-inflammation condition. GlcNAc was immobilized on CM5 chip followed by injection of H-ficolin FBG for 750 s (association time) and buffer for 750 s (dissociation time). Increasing concentrations of IgG were injected over the bound FBG under similar run conditions. $K_D = k_{off}/k_{on}$. Normal condition: $k_{off} \sim 10^{-4}$ s^{-1}; $k_{on} \sim 10^3$ $M^{-1}s^{-1}$. Infection-inflammation condition: $k_{off} \sim 10^{-5}$ s^{-1}; $k_{on} \sim 10^4$ $M^{-1}s^{-1}$. Negative controls: HSA injected after ficolin FBG; IgG injected over GlcNAc-immobilized chip (blue), both showed no binding. Data were analyzed using BIAevaluation 3.2 software. The binding curves (black) are overlaid with the fit of 1:1 interaction model (red). Data represent data from 3 independent experiments.

3.5.1. HDMS identifies binding interfaces between IgG:H-ficolin

We experimentally mapped the interaction sites using amide hydrogen-deuterium exchange coupled with mass spectrometry (HDMS). A reduction in deuterium incorporation in the presence of a protein partner indicates corresponding specific peptide sequence(s) involved in the interaction surface (Hoofnagle et al., 2003, Mandell et al., 1998). The differential incorporation of deuterium for each peptide was calculated across all time points of interaction. Considering the effects of both pH and calcium on IgG**:**ficolin interaction, the same typical infection-inflammation condition of pH 6.5, 2.0 mM calcium was chosen as comparison to normal condition of pH 7.4 and 2.5 mM calcium.

Comparing the extent of deuterium incorporation in H-ficolin alone and H-ficolin incubated with IgG at physiological condition (pH 7.4 and 2.5 mM Ca^{2+}), we found three peptides located in the FBG: YRAGFGNQESEFWLGNENLHQ (150-170), AHYATFRLLGEVDHYQL (193-209) and NGRYAVSEAAAHKYGID (264-280), which show marked differences in deuterium incorporation when in complex with IgG (**Figure 3.16**). The presence of IgG decreased the deuterium incorporation in these ficolin FBG peptides, suggesting that they are the binding sites for IgG. These observations are consistent with the ELISA (Figure 3.11) and SPR (Figure 3.15) results, which indicated that ficolin FBG harbors the binding sites for natural IgG (**Figure 3.17**).

Under the infection-inflammation condition (pH 6.5 and 2.0 mM Ca^{2+}), an additional peptide, YDADHDSSNSNC (234-245) (Figures 3.16 and 3.17), also in the P subdomain of FBG, showed decreased deuterium uptake. This supports our postulate of an infection-induced change in the ficolin that may expose additional sites for the IgG to bind, and also agrees with the 100-fold increase in affinity between ficolin FBG and IgG under the infection-inflammation condition (Figure 3.15).

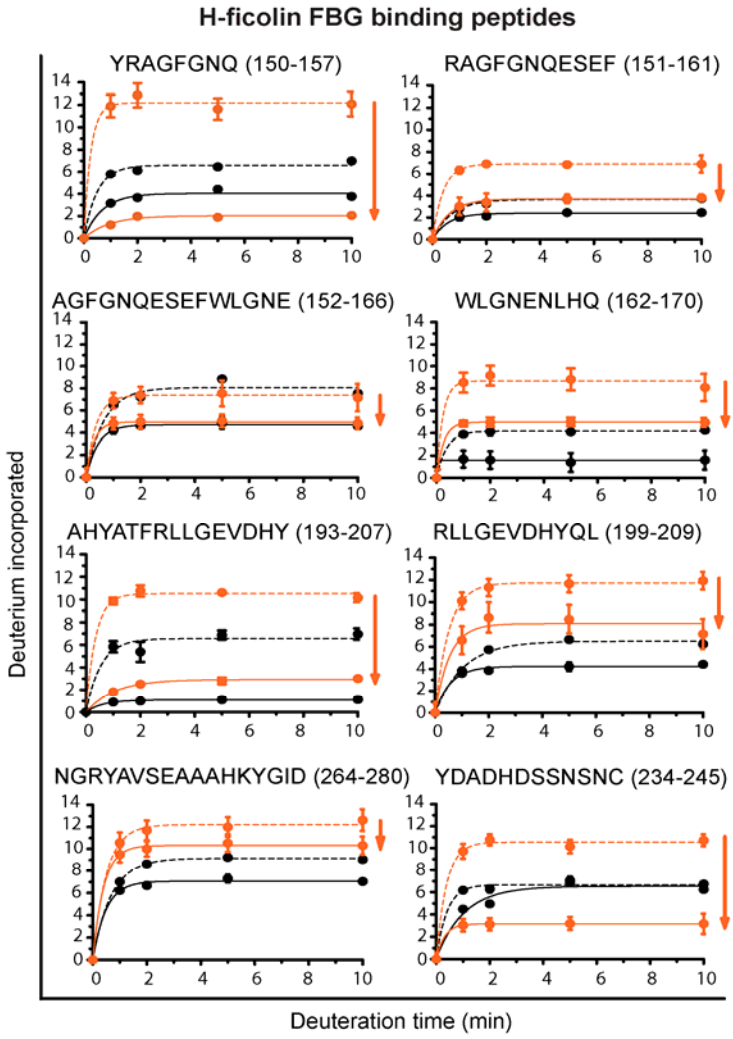

Figure 3.16: Hydrogen-deuterium exchange mass spectrometry (HDMS) identified IgG interaction sites on H-ficolin. Deuterium incorporation in proteins over time is annotated as follows: solid lines, presence of both IgG and H-ficolin; dashed lines (control), presence of only H-ficolin; black lines, normal condition (pH 7.4, 2.5 mM Ca^{2+}); and orange lines, infection-inflammation condition (pH 6.5, 2.0 mM Ca^{2+}). The amino acid sequence of the peptides is indicated in each panel. 16 peptides of H-ficolin (85% coverage) were selected for plotting the graphs based on the mass spectrometric peak quality. Binding peptides of H-ficolin showing decreased deuterium incorporation in the presence of both the proteins as compared to individual protein under both conditions, in particular under infection-inflammation condition are indicated by downward orange arrow. Results are mean ± S.D. from 3 independent experiments.

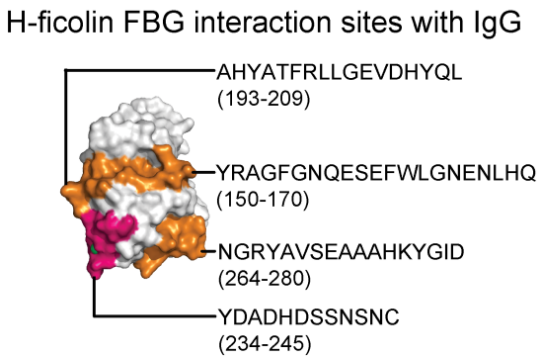

Figure 3.17: HDMS identified H-ficolin peptides interacting with IgG. H-ficolin FBG structure shows interactive peptides (orange), which exhibit decreased deuterium uptake when both H-ficolin and IgG were present. The additional H-ficolin FBG peptide (^{234}YDADHDSSNSNC^{245}) interacting with IgG only under infection-inflammation condition is highlighted in pink.

In addition, the IgG**:**H-ficolin complex exhibited four ficolin FBG peptides spanning residues 90-98 (PRNCRELLS), 107-115 (YHLCLPEGR), 134-145 (QRRQDGSVDFFR) and 286-297 (GVGHPYRRVRMM), each showing increased deuterium uptake (**Figure 3.18**, blue box), indicating greater solvent accessibility. This also suggests infection-inflammation induced changes to the FBG domain, which may expose sites, which do not bind IgG, but are available to interact with other serum proteins as well. The H-ficolin peptides showing no difference in deuterium incorporation in the presence or absence of IgG are shown as non-binding control peptides (Figure 3.18).

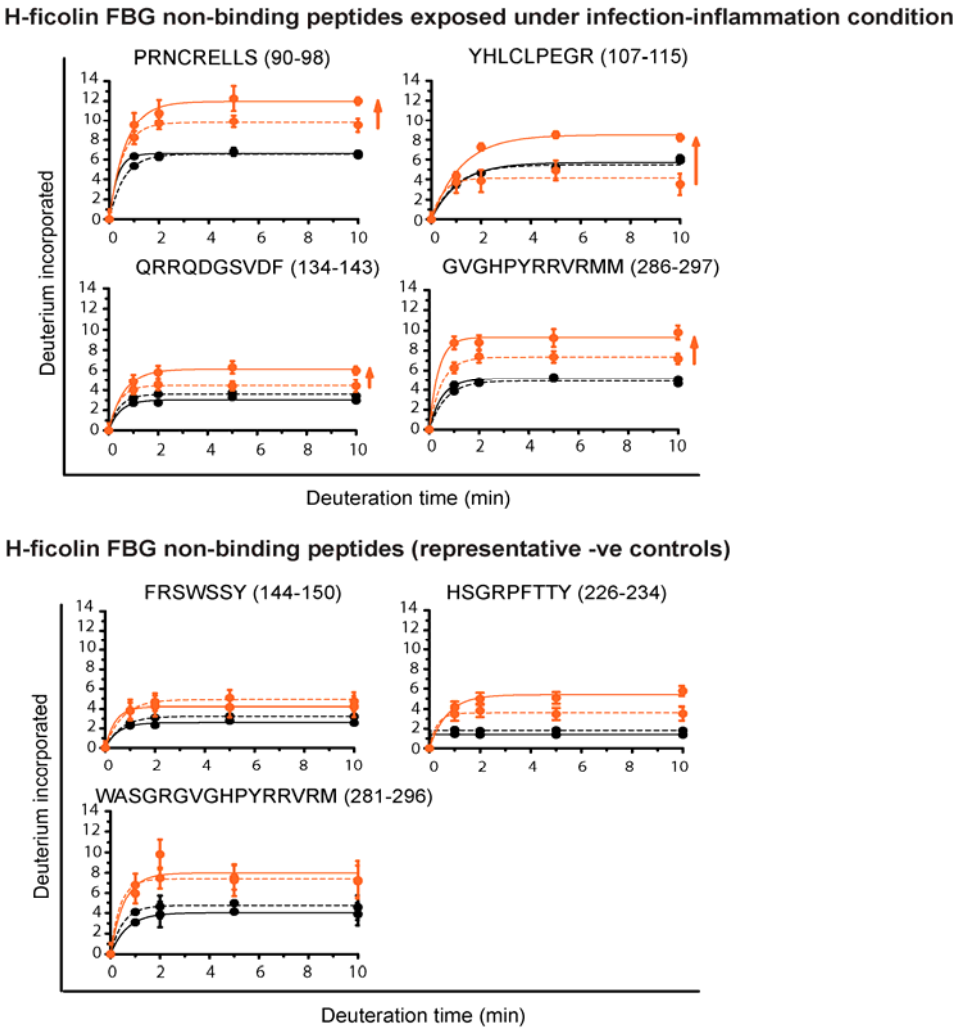

Figure 3.18: HDMS showed the non-interactive peptides of H-ficolin. Deuterium incorporation in proteins over time is annotated as follows: solid lines, presence of both IgG and H-ficolin; dashed lines (control), presence of only H-ficolin; black lines, normal condition (pH 7.4, 2.5 mM Ca^{2+}); and orange lines, infection-inflammation condition (pH 6.5, 2.0 mM Ca^{2+}). The amino acid sequence of the peptides is indicated in each panel. 16 peptides of H-ficolin (85% coverage) were selected for plotting the graphs based on the mass spectrometric peak quality. H-ficolin non-binding peptides showing increased deuterium incorporation in the presence of both proteins as compared to H-ficolin alone (under infection-inflammation condition) are indicated by upward orange arrow. Representative non-binding peptides showing no difference in deuterium incorporation in the presence of individual proteins or both proteins serve as negative controls. Results are mean ± S.D. from 3 independent experiments.

We also used HDMS to experimentally determine the contact surfaces on the IgG molecule when complexed with H-ficolin. The IgG peptides: DTLMISRTPEVTCVV (278-292), 337-347 (VLHQDWLNGKE) and 394-406 (LTCLVKGFYPSDI), corresponding to the CH2-CH3 interface in the Fc region showed decreased deuterium incorporation in presence of H-ficolin (**Figure 3.19**), suggesting that the CH2-CH3 interface contains interaction sites for the ficolin (**Figure 3.20**). The IgG peptides with no difference in deuterium incorporation in the presence or absence of H-ficolin are shown as non-binding control peptides (**Figure 3.21**). The peptides involved in binding to H-ficolin remained unchanged at both normal and infection-inflammation conditions, implying that the IgG structure is more constrained compared to the H-ficolin structure in terms of binding interface. This suggests that the flexibility in H-ficolin probably plays an important role in IgG**:**ficolin interaction, in terms of regulating their affinity under normal and infection-inflammation conditions so as to avoid non-specific interaction and subsequent downstream immune activation.

3.5.2. Sequence alignment of IgG and IgA heavy chains and ficolin FBG domains show conserved amino acids in binding peptides

Sequence alignment of the ficolin FBG domains and the heavy chains of IgG and IgA further suggested that the HDMS-defined interacting peptides in both the ficolin and immunoglobulin harbor conserved amino acids (**Figure 3.22**; red boxes) where changes in the charge of some key residue side-chains might expose them for interaction with the cognate protein (IgG/ficolin).

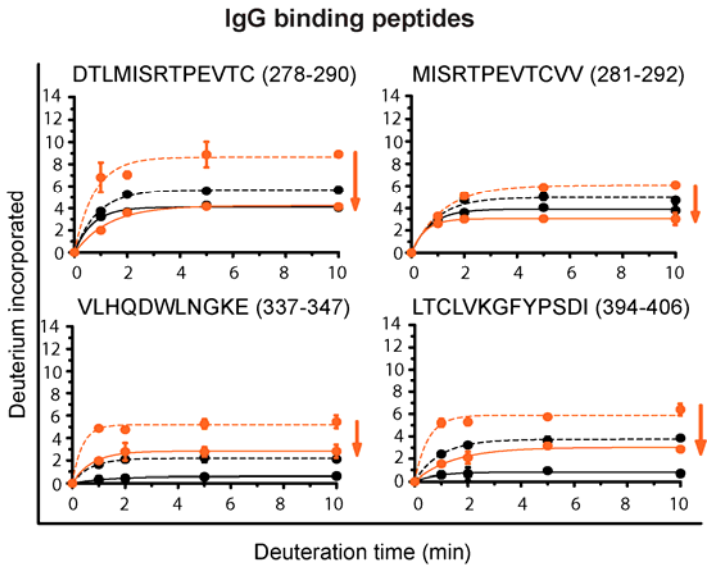

Figure 3.19: HDMS identified H-ficolin interaction sites on IgG. Deuterium incorporation in proteins over time is annotated as follows: solid lines, presence of both IgG and H-ficolin; dashed lines (control), presence of only IgG; black lines, normal condition (pH 7.4, 2.5 mM Ca^{2+}); and orange lines, infection-inflammation condition (pH 6.5, 2.0 mM Ca^{2+}). The amino acid sequence of the peptides is indicated in each panel. 18 peptides of IgG (70% coverage) were selected for plotting the graphs based on the mass spectrometric peak quality. Binding peptides of IgG showing decreased deuterium incorporation in the presence of both the proteins as compared to individual protein under both conditions, in particular under infection-inflammation condition are indicated by downward orange arrow. Results are mean ± S.D. from 3 independent experiments.

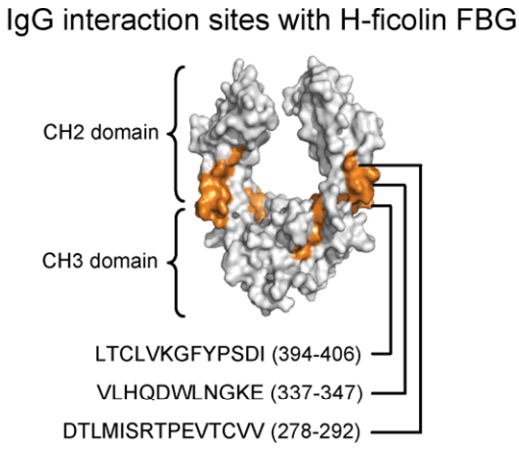

Figure 3.20: HDMS identified IgG peptides interacting with H-ficolin. IgG Fc structure shows interactive peptides (orange), which exhibit decreased deuterium uptake when both H-ficolin and IgG were present.

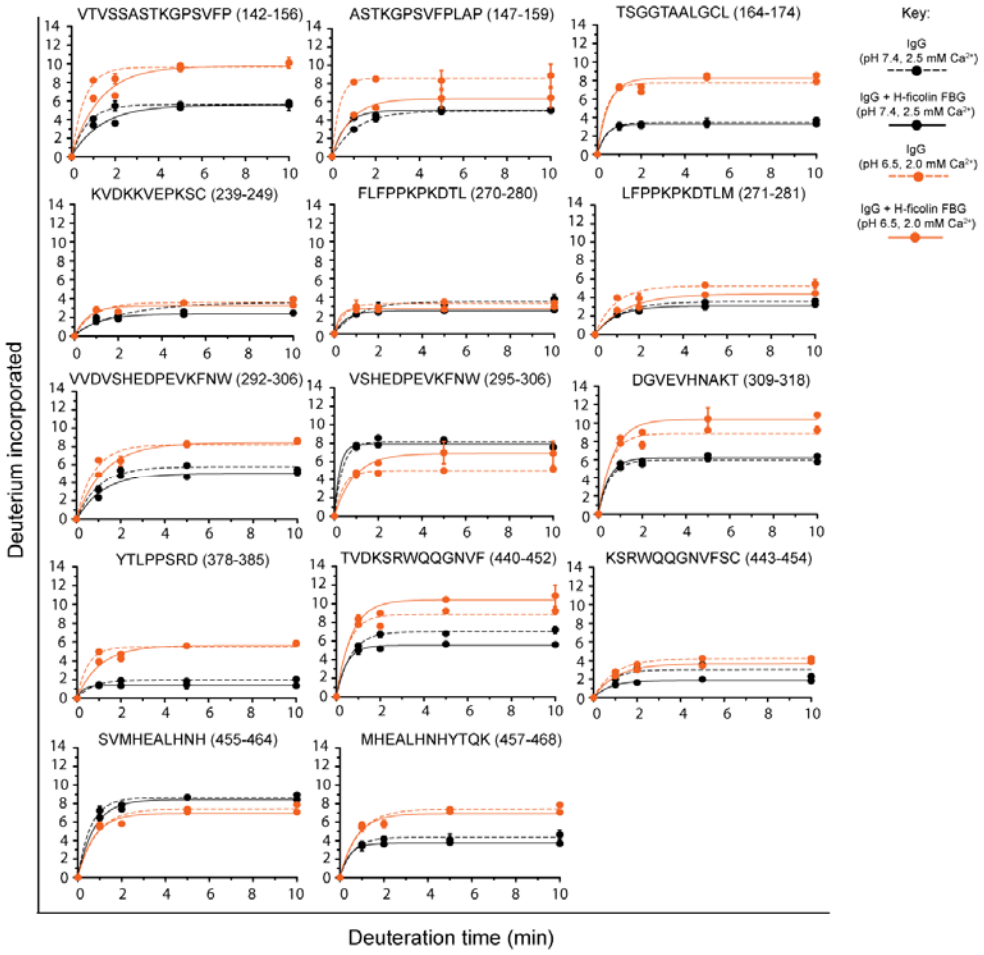

Figure 3.21: HDMS showed the non-interactive peptides of IgG. Deuterium incorporation in proteins over time is annotated as follows: solid lines, presence of both IgG and H-ficolin; dashed lines (control), presence of only IgG; black lines, normal condition (pH 7.4, 2.5 mM Ca^{2+}); and orange lines, infection-inflammation condition (pH 6.5, 2.0 mM Ca^{2+}). The amino acid sequence of the peptides is indicated in each panel. 18 peptides of IgG (70% coverage) were selected for plotting the graphs based on the mass spectrometric peak quality. IgG non-binding peptides showing no difference in deuterium incorporation in the presence of individual proteins or both proteins serve as negative controls. Results are mean ± S.D. from 3 independent experiments.

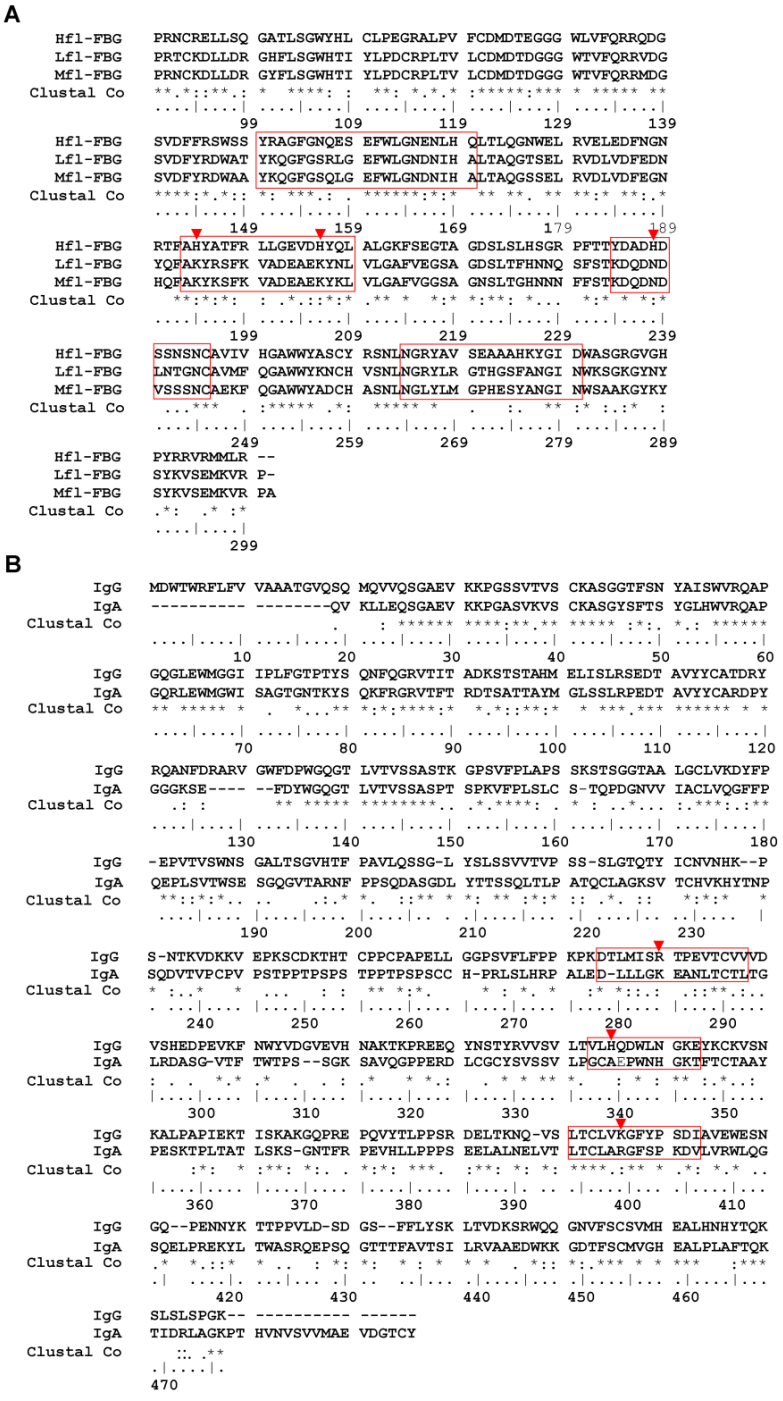

Figure 3.22: Sequence alignment of human ficolin FBGs & IgG with IgA heavy chains - highlighting interacting peptides. Sequence alignment of (**A**) the three ficolin FBGs and (**B**) IgG with IgA using ClustalW, with the interacting peptides (boxed) and residues (arrow head) highlighted.

3.5.3. SPR binding analysis of wild type (WT) and mutant peptides with cognate proteins reveals critical binding residues

It is likely that under the infection-inflammation condition where mild acidosis prevails, the protonation of the amino acid side chains could have led to stronger electrostatic interactions between proteins. Based on the HDMS results, we synthesized peptides derived from IgG and ficolin, and performed surface plasmon resonance (SPR) analysis to characterize the real-time biointeraction between these peptides and the cognate proteins (ficolin or IgG, respectively). We also synthesized single- and double- mutant peptides where arginine, lysine and histidine (which contain positively charged side chains) were substituted with alanine (which contains non-polar side chain). We used ficolin bound to GlcNAc-immobilized chips or IgG bound to FcγR1-immobilized chips for the SPR analysis.

Figure 3.23 shows that the IgG peptides**:** DTLMISRTPEVTCVV$^{278-292}$ (peptide **1**) and LTCLVKGFYPSDI$^{394-406}$ (peptide **6**) bound to ficolin on GlcNAc-chip with similar affinity ($K_D \sim 10^{-6}$ M) under normal and infection-inflammation conditions. However, the binding was abolished by a point mutation of R (peptide **2**) or K (peptide **7**) to uncharged A residue. As the side chain of H residue undergoes a change from zero charge (at pH 7.4) to +1 charge (at pH 6.5), it is likely that H contributed to the enhanced binding at lower pH. Indeed, an H-A mutation (peptide **4**, VLAQDWLNGKE) abolished the interaction between this IgG peptide and ficolin at pH 6.5. Furthermore, peptide **3** (VLHQDWLNGKE$^{337-347}$) and its K-A substitution mutant, peptide **5** (VLHQDWLNGAE), still retained enhanced interaction with ficolin under

the infection-inflammation condition, indicating that K^{346} may not be the critical residue. Taken together, our results suggest that the enhanced interaction between ficolin and IgG is due to increased electrostatic interactions between charged side chains of amino acids (R & K under normal condition and R, K & H under the infection-inflammation condition). All mutant peptides (**2,4,5,7)** were tested for binding to ficolin, but for mutant peptides which do not bind, only representative non-binding sensograms for peptides 3 and 5 (normal condition) were shown on the SPR plots.

Additionally, we tested the binding of HDMS-derived ficolin peptides to IgG. Wildtype (WT): peptide **8**, $AHYATFRLLGEVDHYQL^{193-209}$ and peptide **13**, $YDADHDSSNSNC^{234-245}$, the extra binding peptide under the infection-inflammation condition, were compared with their corresponding mutants. **Figure 3.24** shows a 100-fold increase in the binding affinity of $AHYATFRLLGEVDHYQL^{193-209}$ to IgG on FcγR1-chip under the infection-inflammation condition. The two H residues likely contribute to the interaction since H-A mutation, either singly (peptides **10** & **11**) or doubly (peptide **12**) completely abrogated the binding of the ficolin peptides to IgG. Consistently, ficolin peptide **13**, $YDADHDSSNSNC^{234-245}$ showed no binding to IgG under normal condition but high affinity under the infection-inflammation condition. Conceivable, mild acidosis (pH 6.5) changed the charge of the H residue side-chain from 0 to +1, which increased the binding interaction between the ficolin and IgG. All mutant peptides (**9, 10, 11, 12, and 14)** were tested for binding to IgG, but for mutant peptides, which do not bind, only a representative, peptide 12, was shown on the SPR plots.

Figure 3.23: Surface plasmon resonance to characterize the binding affinities between IgG peptides and H-ficolin under normal and infection-inflammation conditions. GlcNAc-BSA was immobilized on the CM5 chip to expose GlcNAc as a ligand for ficolin. H-ficolin was first injected over GlcNAc-imobilized chip for 100s (association time) followed by buffer flow (wash) for 200s (dissociation time). IgG peptides (WT or mutants) are tabulated below the graph. Peptides, injected directly over the GlcNAc-immobilized chip as controls, showed no direct binding to GlcNAc (blue). Increasing concentrations of IgG peptides (5, 10, 20 and 50 μM) were injected over the H-ficolin (bound to the chip) for 100 s (association time) followed by buffer flow for 200 s (dissociation time). Mutant peptides (with Arg, Lys or His substituted to Ala) injected under similar conditions did not bind or bound with lesser affinity to H-ficolin. Human serum albumin (HSA) injected after H-Ficolin injection served as a negative control (blue, see top panel). Data were analyzed using BIAevaluation software 3.2. The binding curves (black) are overlaid with the fit of 1:1 interaction model (red). The plots are a typical representation of 3 independent experiments.

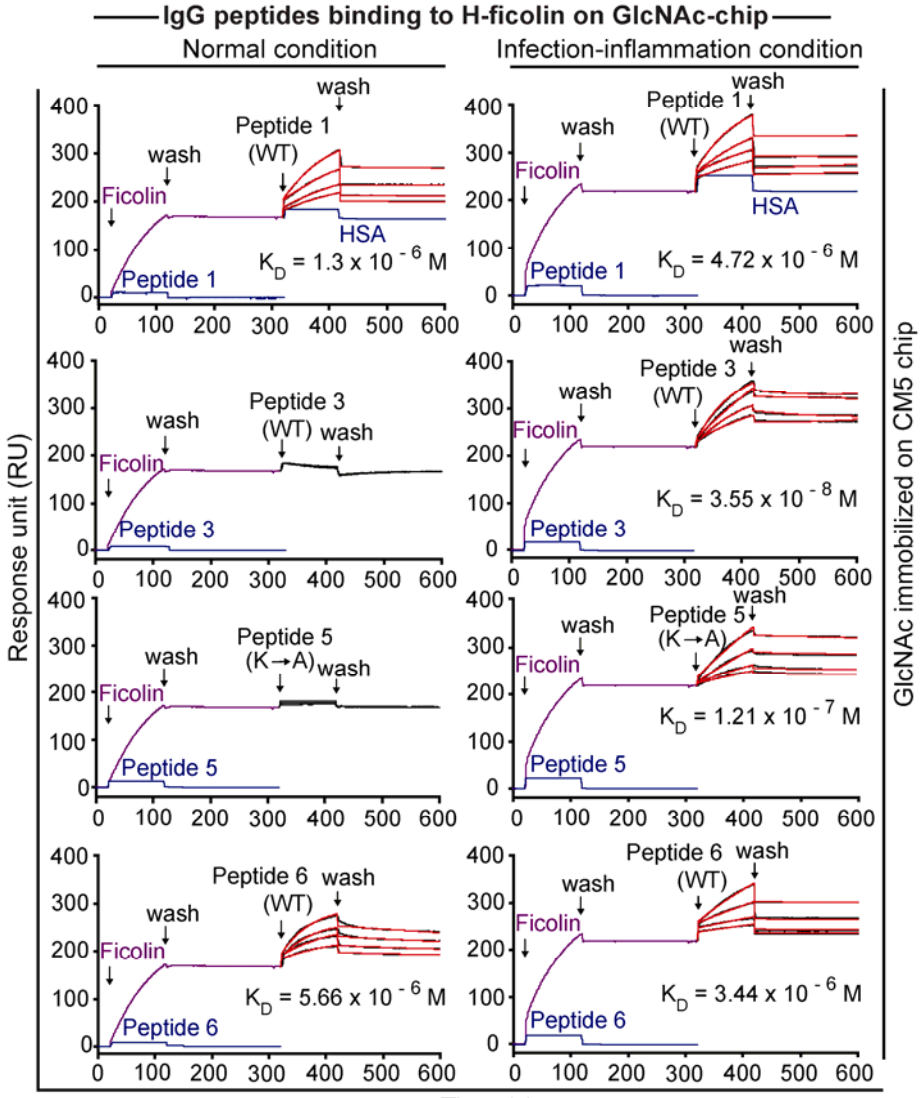

IgG Peptides	Sequence	Mutation	K_D (M) Normal	K_D (M) Infection-inflammation
1	^{278}DTLMISRTPEVTCVV^{292}	WT	1.3 x 10 - 6	4.72 x 10 - 6
2	DTLMISATPEVTCVV	R → A	n.b.	n.b.
3	^{337}VLHQDWLNGKE^{347}	WT	n.b.	3.55 x 10 - 8
4	VLAQDWLNGKE	H → A	n.b.	n.b.
5	VLHQDWLNGAE	K → A	n.b.	1.21 x 10 - 7
6	^{394}LTCLVKGFYPSDI^{406}	WT	5.66 x 10 - 6	3.44 x 10 - 6
7	LTCLVAGFYPSDI	K → A	n.b.	n.b.

n.b. refers to **non-binding** peptides where K_D value could not be determined due to lack of binding, hence no curve-fitting was performed according to 1:1 Langmuir binding model. Non-binding mutant peptide data are not shown. Representative sensogram of non-binding peptides here are peptides 3&5 under normal condition.

Figure 3.24: Surface plasmon resonance to characterize the binding affinities between H-ficolin peptides and IgG under normal and infection-inflammation conditions. FcγR1 was immobilized on the CM5 chip to expose FcγR1 as a receptor for IgG. IgG was first injected over FcγR1-imobilized chip for 100s (association time) followed by buffer flow (wash) for 200s (dissociation time). H-ficolin peptides (WT or mutants) are tabulated below the graph. Peptides, injected directly over the FcγR1-immobilized chip as controls, showed no direct binding to GlcNAc (blue). Increasing concentrations of H-ficolin peptides (5, 10, 20 and 50 μM) were injected over the bound IgG (bound to the chip) for 100 s (association time) followed by buffer flow for 200 s (dissociation time). Mutant peptides (with Arg, Lys or His substituted to Ala) injected under similar conditions did not bind or bound with lesser affinity to IgG. Human serum albumin (HSA) injected after IgG injection served as a negative control (blue, see top panel). Data were analyzed using BIAevaluation software 3.2. The binding curves (black) are overlaid with the fit of 1:1 interaction model (red). The plots are a typical representation of 3 independent experiments.

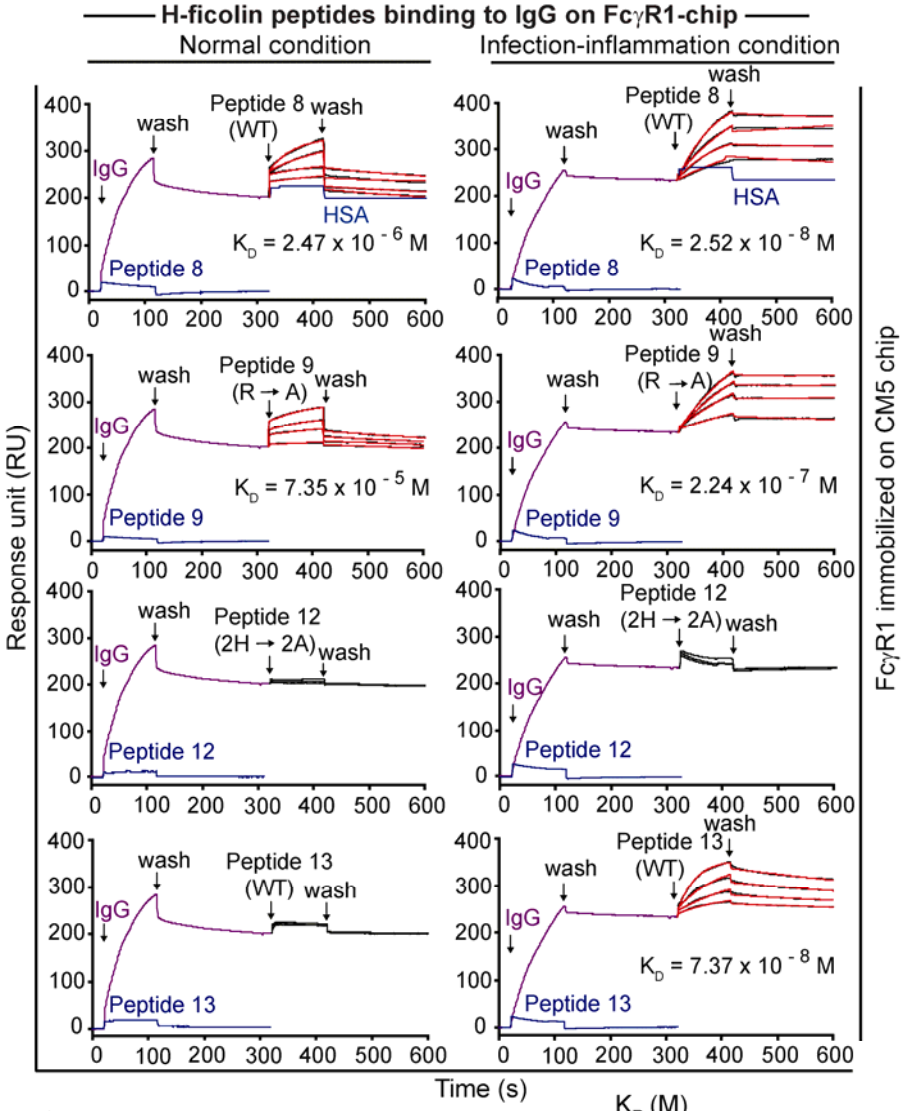

H-ficolin Peptides	Sequence	Mutation	K_D (M) Normal	K_D (M) Infection-inflammation
8	^{193}AHYATFRLLGEVDHYQL^{209}	WT	2.47 x 10 - 6	2.52 x 10 - 8
9	AHYATFALLGEVDHYQL	R → A	7.35 x 10 - 5	2.24 x 10 - 7
10	AAYATFRLLGEVDHYQL	H → A	n.b.	n.b.
11	AHYATFRLLGEVDAYQL	H → A	n.b.	n.b.
12	AAYATFRLLGEVDAYQL	2H → 2A	n.b.	n.b.
13	^{234}YDADHDSSNSNC^{245}	WT	n.b.	7.37 x 10 - 8
14	YDADADSSNSNC	H → A	n.b.	n.b.

n.b. refers to **non-binding** peptides where K_D value could not be determined due to lack of binding, hence no curve-fitting was performed according to 1:1 Langmuir binding model. Non-binding mutant peptide data are not shown. Representative sensogram of non-binding peptides here are peptides 12 under normal and infection-inflammation conditions &13 under normal condition.

Overall, we found that multiple positively charged side chains of arginine and lysine contributed to the binding affinity under normal condition while histidine contributes to higher affinity under the infection-inflammation condition.

3.5.4. Random docking and HDMS guided docking of IgG Fc:H-ficolin FBG

We used computational random docking to predict the binding interfaces based on known structures of H-ficolin FBG and IgG Fc regions. The two known crystal structures used in the study were H-ficolin FBG (ligand-free; PDB entry code: 2J64) and human IgG-Fc (PDB entry code: 1H3Y). **Figure 3.25** shows the predicted binding interface between H-ficolin and FBG. The enlarged view of H-ficolin FBG depicts the three sub-domains: A, B and P sub-domain. The P sub-domain harbors the pH-sensitive region, calcium and the ligand (GlcNAc) binding sites (Garlatti et al., 2007) as indicated.

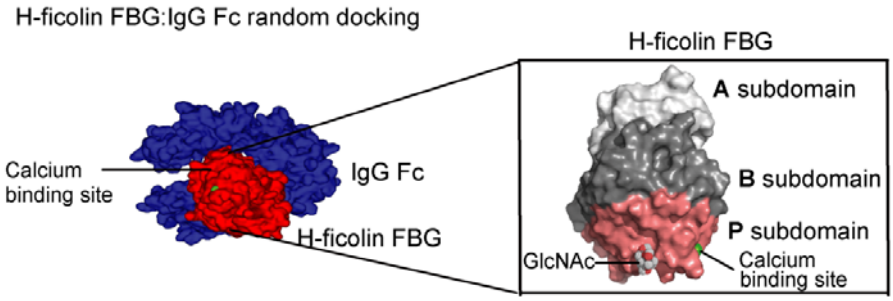

Figure 3.25: *In silico* random docking of H-ficolin FBG onto IgG Fc. Computational random docking of H-ficolin FBG**:**IgG Fc structures. The inset shows the H-ficolin FBG subdomains (A, B, P) and the calcium- and GlcNAc- binding sites.

Following from HDMS-directed mapping of the IgG**:**H-ficolin interaction interfaces, a guided *in silico* docking (**Figure 3.26**) showed a non-symmetric heterodimer model with a higher score indicating higher stability than that generated by random docking (Figure 3.25**; Table 3.1**). The molecular docking analysis further confirmed that the flexible conformational change in the P subdomain of H-ficolin FBG under the infection-inflammation condition led to enhanced interaction with IgG, whereas IgG was comparatively more rigid and its binding site with H-ficolin FBG did not depend on pH and calcium conditions. These results further corroborate the presence of specific interacting peptides in the FBG and Fc CH2-CH3 domains of the IgG**:**H-ficolin interface, respectively, thus lending credence to the model structure of the two interacting proteins and supporting a 1:1 interaction between IgG:ficolin.

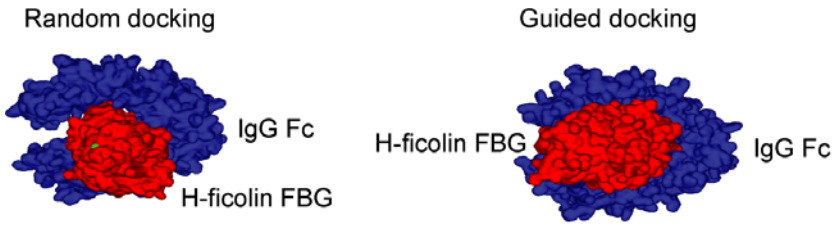

Figure 3.26: *In silico* HDMS-guided docking of H-ficolin FBG onto IgG Fc. *In silico* docking of H-ficolin FBG and IgG Fc guided by HDMS-directed identification of IgG:H-ficolin interaction interfaces shows a non-symmetric heterodimer model with a higher score (higher stability; see Table 3.1) than that generated by random docking.

3.5.5. Computational superimposition studies show ficolin and FcγR1 bind IgG at distinct sites

By computational superimposition of the HDMS-guided H-ficolin FBG**:**IgG Fc complex with the known crystal structure of IgG Fc**:**FcγR1 (PDB ID:

1T83), we found that H-ficolin and FcγR1 bind to distinct sites on IgG (**Figure 3.27A**). This indicates that ficolin does not compete with FcγR1 for binding to IgG. This leads us to propose a three protein complex model wherein the bacteria opsonized by IgG**:**H-ficolin complex are plausibly presented to FcγR1 on the monocytes leading to phagocytosis (**Figure 3.27B**).

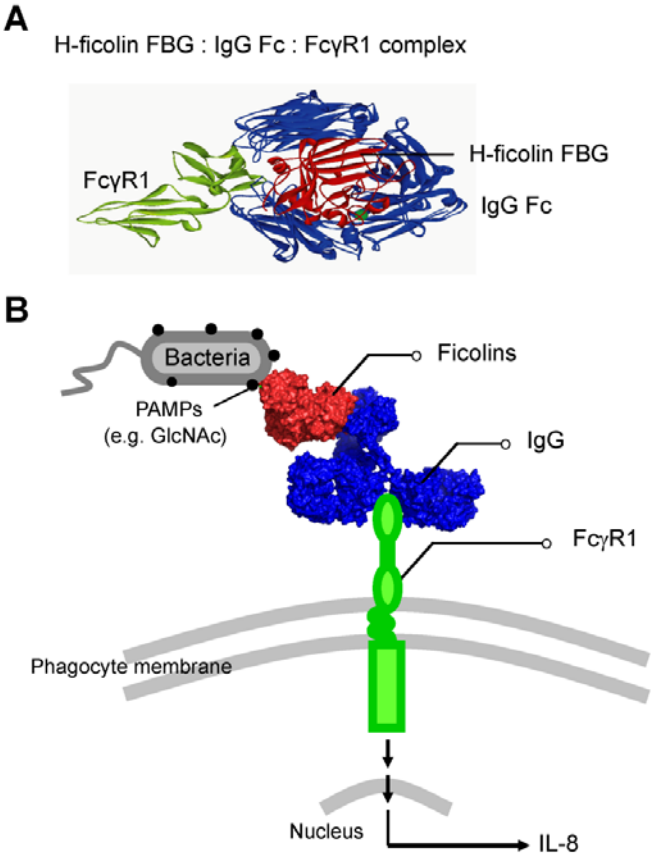

Figure 3.27: Model of bacteria-ficolin:IgG:FcγR1-monocytes. (**A**) Computational low energy superimposition of HDMS-guided H-ficolin FBG**:**IgG Fc complex to the known crystal structures of IgG Fc and FcγR1 shows that H-ficolin FBG and FcγR1 bind at independent sites on IgG Fc, and hence indicates the possible interaction amongst ficolin, IgG and FcγR1. (**B**) Proposed model to illustrate the novel mechanism of bacterial recognition and phagocytosis through the assembly of ficolin (*red*), natural IgG (*blue*) and FcγR1 (*green*) on the monocytes, forming [bacteria-ficolin**:**IgG**:**FcγR1-monocytes]. Natural IgG acts as a crucial bridge between ficolin-opsonized bacteria and FcγR1 on monocytes, leading to direct and rapid phagocytosis of the pathogen and upregulation of pro-inflammatory IL8.

Table 3.1: Parameters for computational docking analysis.

ZDOCK	pose	IgG	H-ficolin	E_elec2 kcal/mol	E_sol kcal/mol	E_RDOCK kcal/mol	SA buried $Å^2$	Δ SAS $Å^2$	ZRank Score
Blocking residues			86-145						
Random	4			-38.64	0.9	-33.88	5100.83	3623.86	-117.275
Guided	44			-38.34	8.1	-26.41	1610.63	3496.36	-76.426

E_RDOCK is the Dock Final RDOCK energy: E_RDock=E_sol+beta*E_elec2 (beta=0.9)
E_elec2 is Electrostatic energy after second minimization with ionic residues in the charged state
E_sol is the Desolvation energy based on the Atomic Contact Energy (ACE)
ZRank Score is the energy of the docked pose calculated by the ZRank re-scoring method (lower score energy indicates higher affinity).
SA buried is the area of molecular surface buried during the complex formation.
Δ SAS is the changed area of solvent accessible surface during the complex formation.

* This result was obtained in collaboration with Dr. Yang Lifeng.

3.6. Molecular interactions on monocytes link humoral to cellular immunity

Having ascertained the interaction interfaces and contact points between the natural IgG and ficolin, and based on the premise that IgG interacts with the monocyte FcγR1, we investigated the biological significance of the interactions amongst the three proteins - ficolin, IgG and FcγR1. We tracked the humoral-to-cellular pathway of the IgG**:**ficolin opsonized bacterial mimic (GlcNAc bead) in the presence of monocytes.

3.6.1. IgG bridges ficolin opsonized bacterial mimic to FcγR1 on the monocyte surface

By immunofluorescence microscopy, we systematically demonstrated the uptake of the GlcNAc-beads (bacterial mimic) in presence of ficolin, IgG or IgG**:**ficolin complexes, by human primary monocytes or U937 cell line. The bacterial mimic opsonized with only ficolin or IgG alone, were not recognized by the monocytes. This recapitulates the importance of natural IgG in the recognition and phagocytosis of ficolin opsonized bacteria. When the GlcNAc-beads were opsonized with the complex, we observed co-localization of ficolin and IgG on the surface, showing that the bacterial mimic had been recognized by the monocytes. Moreover, only in the presence of IgG, the ficolin opsonized GlcNAc-beads co-localized with FcγR1 on the monocyte surface (**Figure 3.28**), further showing that IgG**:**ficolin opsonized bacterial mimic is recognized by FcγR1 receptor.

Figure 3.28: Co-localization analysis of Ficolin, IgG and FcγR1 on human primary monocytes and cell lines. (**A and B**) Confocal microscopy shows co-localization of ficolin (red) and IgG (green) or ficolin (red) and FcγR1 (green) on (A) human monocytes and (B) U937 cells. The cell nuclei were stained with DAPI (blue). Magnification and scale bars: (100x objective; scale bar, 10 μm) for human monocytes; (63x objective; scale bar, 5 μm) for cell lines. Ficolin co-localizes with FcγR1 only in the presence of IgG, indicating that IgG in the IgG**:**ficolin complex acts as a bridge between ficolin and FcγR1. Data are representative of three independent experiments.

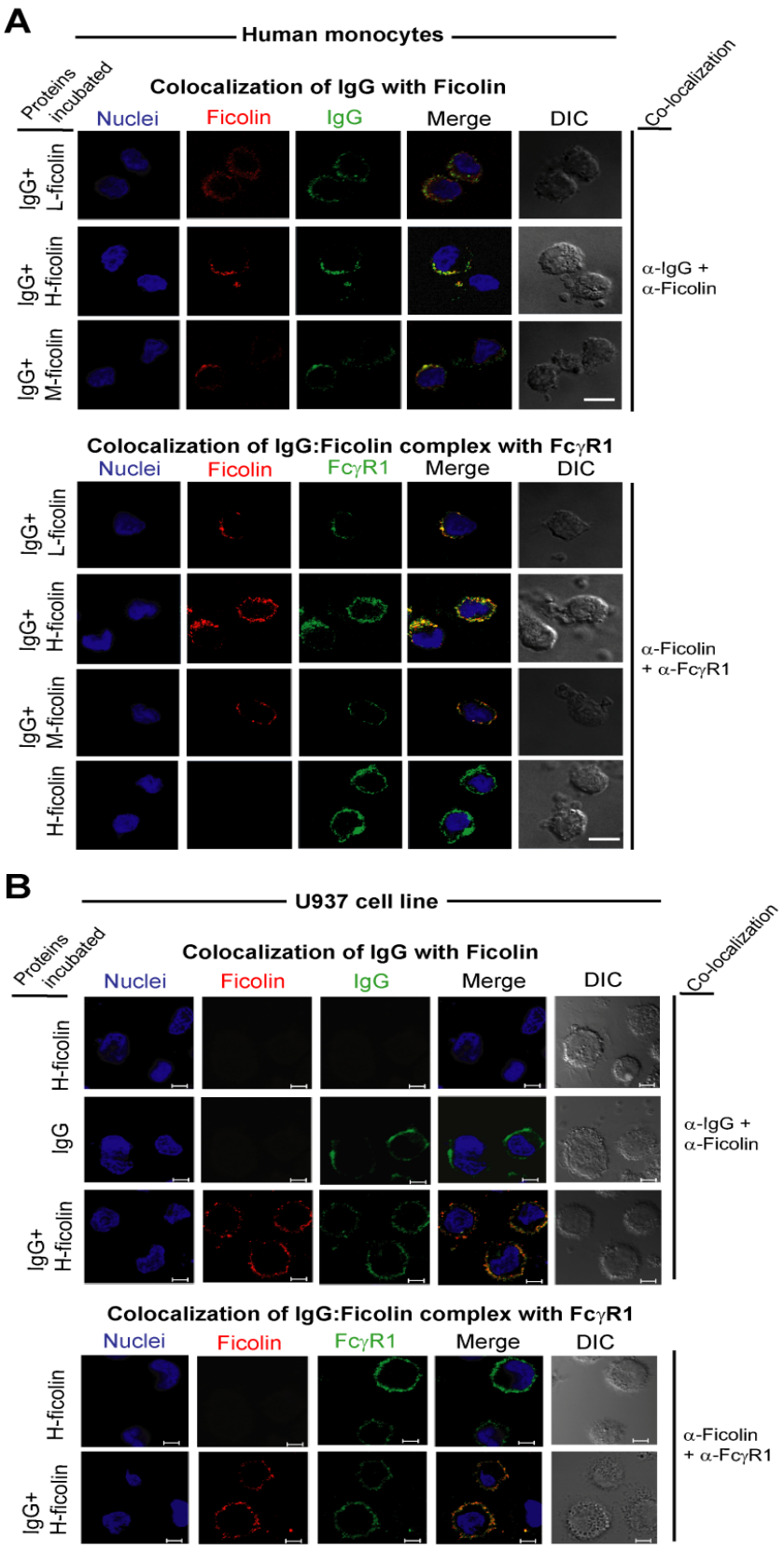
A
Human monocytes
Proteins incubated
Colocalization of IgG with Ficolin
Nuclei
Ficolin
IgG
Merge
DIC
Co-localization
IgG+ L-ficolin
IgG+ H-ficolin
IgG+ M-ficolin
α-IgG + α-Ficolin
Colocalization of IgG:Ficolin complex with FcγR1
Nuclei
Ficolin
FcγR1
Merge
DIC
IgG+ L-ficolin
IgG+ H-ficolin
IgG+ M-ficolin
H-ficolin
α-Ficolin + α-FcγR1
B
U937 cell line
Proteins incubated
Colocalization of IgG with Ficolin
Nuclei
Ficolin
IgG
Merge
DIC
Co-localization
H-ficolin
IgG
IgG+ H-ficolin
α-IgG + α-Ficolin
Colocalization of IgG:Ficolin complex with FcγR1
Nuclei
Ficolin
FcγR1
Merge
DIC
H-ficolin
IgG+ H-ficolin
α-Ficolin + α-FcγR1

3.6.2. Infection-inflammation condition increases IgG:ficolin complex formation with FcγR1 on monocytes

The *in vivo* interplay of the three proteins was further examined by preliminary yeast three-hybrid analysis. **Figure 3.29** shows a strong IgG**:**FcγR1 interaction but a weak-to-no interaction between ficolin and FcγR1 in the absence of IgG. Co-transformation of IgG and ficolin in the yeast potentiated their respective interactions, indicating that ficolin, IgG and FcγR1 form a complex in which IgG acts as a bridge.

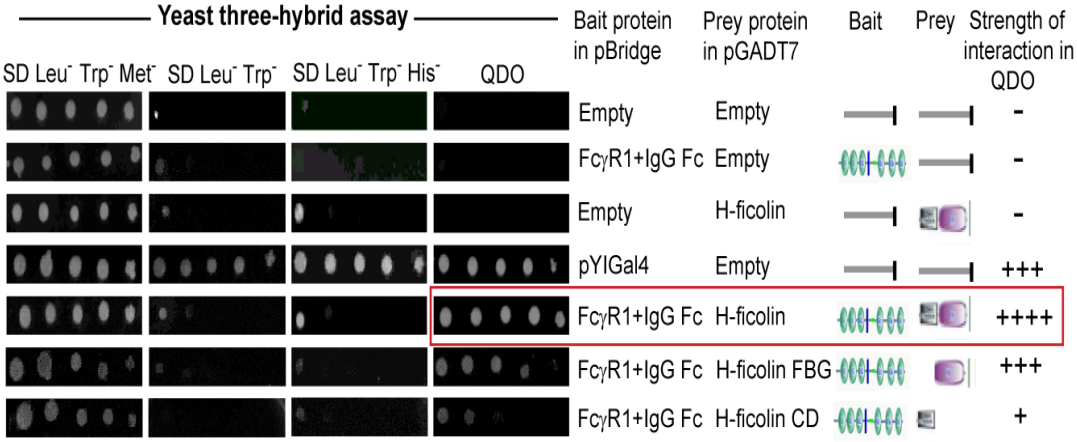

Figure 3.29: Yeast 3-hybrid assay characterizes protein:protein interactions. Amongst the three proteins: H-ficolin (full length, FBG domain or collagen-like domain), IgG Fc and FcγR1, the strength of the interaction was determined by growth on QDO plates, and is annotated by +/-. The box indicates the strongest interaction between H-ficolin and FcγR1 in presence of IgG.

To strengthen our observation, we used proximity ligation assay (PLA) to demonstrate protein-protein interactions *in situ*. Monocytes challenged with IgG**:**ficolin-opsonized GlcNAc-beads, displayed IgG**:**ficolin and ficolin**:**FcγR1 interaction only in the presence of IgG on the cell surface (**Figure 3.30A**). Quantification of PLA signals (each red dot signifies a

complex) showed greater numbers of IgG**:**ficolin complexes under the infection-inflammation condition compared to the normal condition. Only in the presence of IgG, ficolin**:**FcγR1 complexes were observed (**Figure 3.30B**). Moreover, only pre-formed GlcNAc-ficolin**:**IgG were engaged on the monocytes, recapitulating the significance of natural IgG in bridging ficolin and FcγR1, and resulting in phagocytosis.

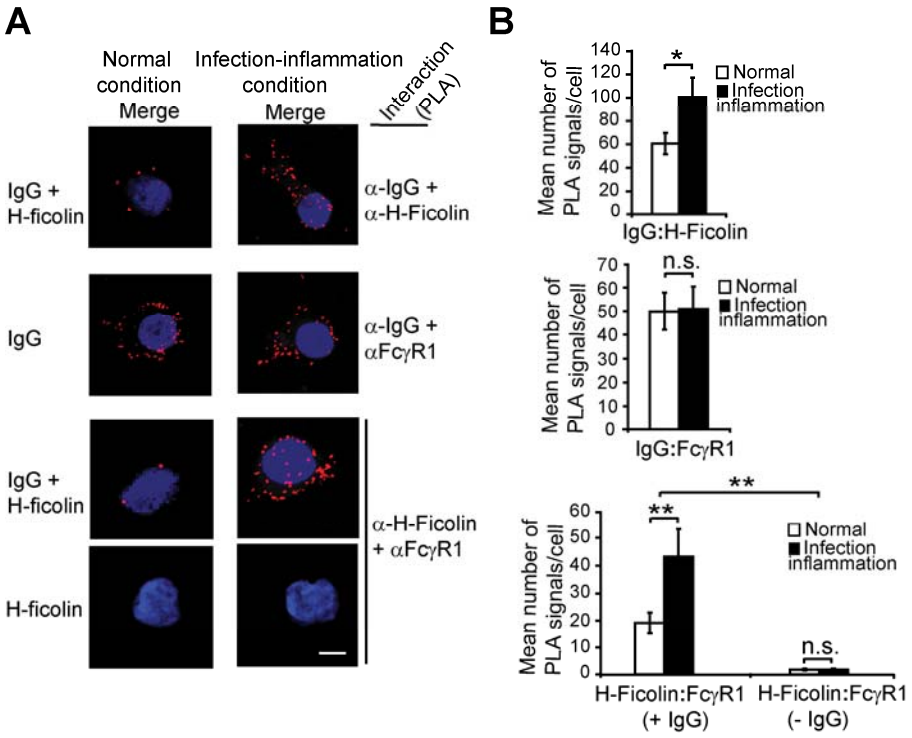

Figure 3.30: Ficolin:IgG:FcγR1 interactions - assembly on human primary monocytes. (**A**) *In situ* proximity ligation assay (PLA) shows interaction (each red dot signifying a signal) between IgG**:**H-ficolin and IgG**:**FcγR1 on the monocytes under normal and infection-inflammation conditions. The third row shows apparent /indirect interaction between H-ficolin and FcγR1 (due to the IgG in the IgG**:**H-ficolin complex interacting with FcγR1), i.e. H-ficolin is brought into proximity to FcγR1 only in the presence of IgG. 100X objective. Scale bar, 5 μm. (**B**) Quantification of the number of PLA signals of interaction between IgG**:**H-ficolin and IgG**:**FcγR1 and apparent /indirect interaction between H-ficolin**:**FcγR1 (with or without IgG). The interaction complexes per cell were scored using Image J software. Duplicates of 50 cells each were enumerated for each condition tested. *p<0.05; **p<0.01; n.s., not significant. Three independent experiments were performed.

Similar observations were made with U937 monocytes (**Figure 3.31A**). The specificity of interaction between ficolin, IgG and FcγR1 was verified by the lack of HSA-IgG interaction on the monocyte surface (**Figure 3.31B**) and further confirmed by the absence of such complexes on HEK293T cells (**Figure 3.31C**), which lack FcγR1.

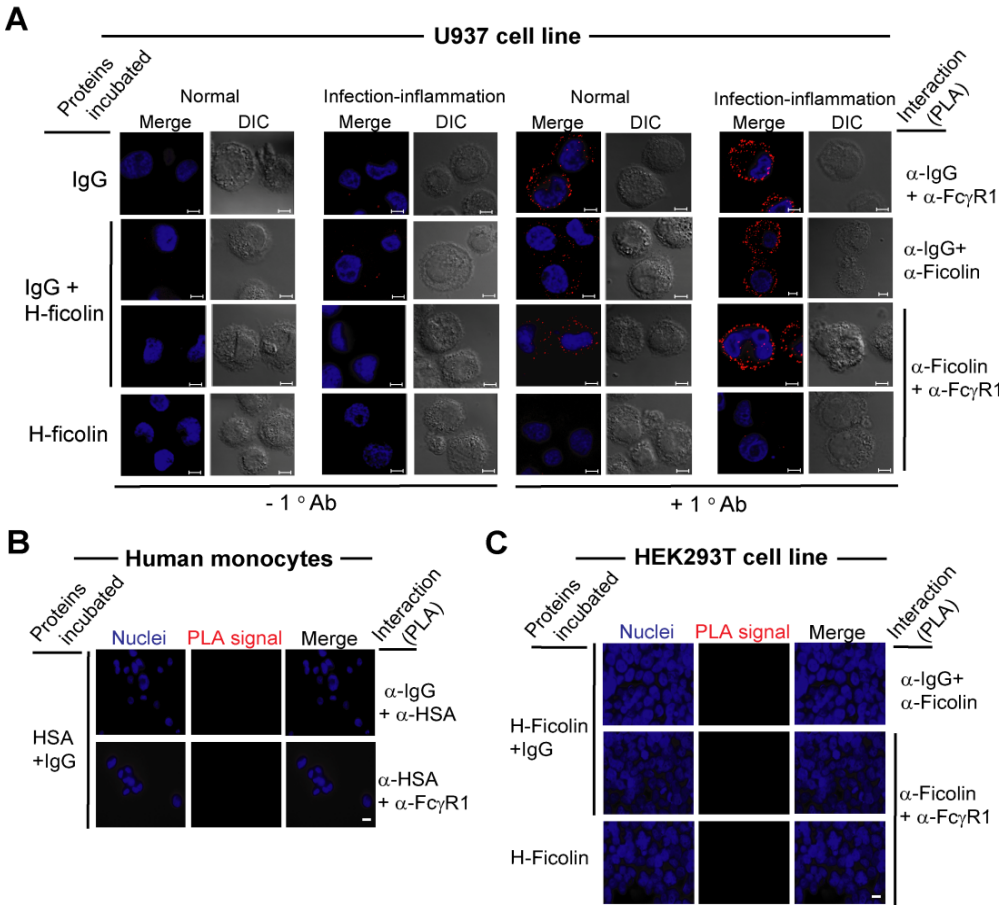

Figure 3.31: Molecular interactions between ficolin, IgG and FcγR1. (**A**) *In situ* proximity ligation assay (PLA) identifies interactions (under normal and infection-inflammation conditions) between IgG**:**ficolin, IgG**:**FcγR1 and ficolin**:**FcγR1 for U937 cells. Each red dot represents an interaction. Negative controls (-1^{o} Ab) involved similar reactions in the absence of primary antibodies. (**B**) Negative control protein (HSA) used in *in situ* proximity ligation assay (PLA) shows no interactions between HSA**:**IgG or HSA**:**FcγR1 on human monocytes. (**C**) HEK 293T cells, verified to be negative for FcγR1, were used as a negative control. *In situ* proximity ligation assay (PLA) shows no interaction between IgG**:**H-ficolin and H-ficolin**:**FcγR1. Magnification and scale bars: 63x objective; scale bar, 5 µm. Data are representative of three independent experiments.

Next, we characterized the molecular interactions between ficolin, IgG and FcγR1. We first immobilized FcγR1 on a CM5 chip (mimicking the receptor on the surface of monocytes). Then IgG was bound to FcγR1. Injection of H-ficolin FBG over IgG bound to immobilized FcγR1 showed 100-fold higher affinity (K_D) between IgG**:**H-ficolin FBG under the infection-inflammation condition as compared to normal condition (**Figure 3.32**), similar to the interaction on the bacterial mimic surface (Figure 3.15). The interactions were specific since ficolin FBG itself did not bind to the immobilized FcγR1, and the negative control, HSA, did not bind IgG (Figure 3.32, blue). Conceivably the assembly of ficolin**:**IgG**:**FcγR1 links the bacteria to the monocytes where IgG bridges ficolin-bound bacteria to the FcγR1.

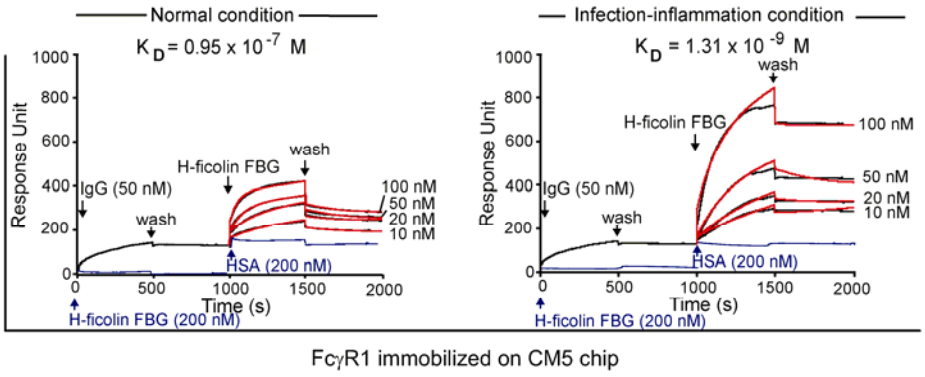

Figure 3.32: Ficolin binds to IgG bound to FcγR1 with higher affinity under infection-inflammation condition. SPR analysis of the binding affinity (K_D) between H-ficolin FBG and IgG under normal and infection-inflammation condition conditions. IgG was first injected for 750 s (association time) over FcγR1-immobilized CM5 chip followed by buffer flow for 750 s (dissociation time). Then, increasing concentrations of H-ficolin FBG were injected over the bound IgG for 750 s (association time) followed by buffer flow for 750 s (dissociation time). $K_D = k_{off}/k_{on}$. Normal condition: $k_{off} \sim 10^{-4}$ s^{-1}; $k_{on} \sim 10^{3}$ $M^{-1}s^{-1}$. Infection-inflammation condition: $k_{off} \sim 10^{-5}$ s^{-1}; $k_{on} \sim 10^{4}$ $M^{-1}s^{-1}$. Negative controls: HSA injected after H-ficolin FBG injection showed no binding to IgG or H-ficolin FBG, serving as a negative control (blue) for binding specificity between ficolin FBG**:**IgG. H-ficolin injected over the FcγR1-immobilized chip showed no binding (blue), serving as specificity control for interaction between IgG**:**FcγR1. Data were analyzed using BIAevaluation 3.2 software. The binding curves (black) are overlaid with the fit of 1:1 interaction model (red). Data are representative from 3 independent experiments.

3.7. IgG:ficolin complex mediated recognition is independent of C3

It is reported that C3 alpha chain covalently interacts with IgG heavy chain when in the presence of immune complexes (Sahu et al., 1994). Thus, we sought to determine whether C3 might be involved in IgG**:**ficolin interaction or in fine-tuning the mechanism. We performed various *in vitro*, *ex-vivo* and *in vivo* experiments (e.g. bacteria binding, pulldown and immunohistochemistry) under normal and infection-inflammation conditions, using **(i)** normal human serum containing C3 and human serum depleted of C3 ($C3^-$ serum), and **(ii)** wildtype (WT) and $C3^{-/-}$ mice to verify the potential involvement of C3 in IgG**:**ficolin interaction in the immune complex. **(iii)** We further verified our results by infecting WT and $C3^{-/-}$ mice with *P. aeruginosa*, and compared their sera for potential involvement of C3 in the formation of IgG**:**ficolin immune complexes, which might occur in *in vivo* experimental infection.

3.7.1. C3 is absent in purified native proteins and IgG:ficolin complex

We first checked for the presence of C3 in the purified native proteins: (i) ficolin, (ii) IgG, both purified from uninfected human serum and (iii) IgG**:**ficolin complexes purified from uninfected human serum which had been pretreated under simulated infection-inflammation condition; this induces the formation of IgG**:**ficolin complexes. Recombinant ficolin (rFicolin) was used as an internal control for the anti-H-ficolin antibody probe, showing a single band corresponding to 37 kDa. **Figure 3.33** shows that C3 was present in the undepleted "Uninfected serum" (lane 5), but was undetectable in the purified

native ficolin (lane 2), purified native IgG (lane 3) or purified IgG**:**ficolin complexes (lane 4) isolated from simulated infection-inflammation treated serum. Furthermore, we observed that IgG and ficolin were not co-purified but were isolated separately from uninfected human serum. Only when the serum was simulated to infection-inflammation condition, were IgG and ficolin co-purified as IgG**:**ficolin complex on GlcNAc-beads.

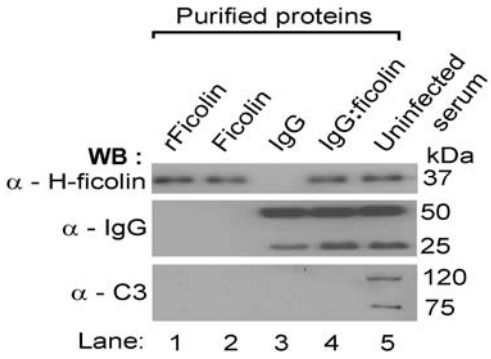

Figure 3.33: Purified ficolin, purified IgG and purified IgG:ficolin complex from C3-containing uninfected human serum. Purified proteins were probed with anti-H-ficolin, anti-IgG and anti- C3. A single band corresponding to 37 kDa of H-ficolin was detected. Two bands corresponding to 50 kDa (H-chain) and 25 kDa (L-chain) of IgG were detected. Uninfected serum (lane 5) showed two bands of C3 corresponding to 120 kDa (alpha chain) and 75 kDa (beta chain). No C3 was detected in the purified proteins and soluble immune complex (IgG**:**ficolin). The samples were resolved in SDS-PAGE (12%) under reducing conditions.

3.7.2. IgG:ficolin complex on the bacterial mimic is formed independently of C3

To study the potential contribution of C3 in enabling IgG interaction with ficolin bound on GlcNAc-beads, we compared normal human serum depleted of C3 alone ($C3^-$ serum) with serum depleted of both C3 and ficolin ($C3^-$ $Ficolin^-$ serum). We depleted C3 by incubating the serum overnight with anti-C3 immobilized on Protein G-Sepharose beads at 4˚C. The resulting serum was analyzed by Western blot, which showed effective depletion of C3, albeit

with some inevitable loss of serum IgG during the depletion process, due to its binding to available sites on the Protein G-Sepharose (**Figure 3.34**). The ficolin level remained unaffected by depletion.

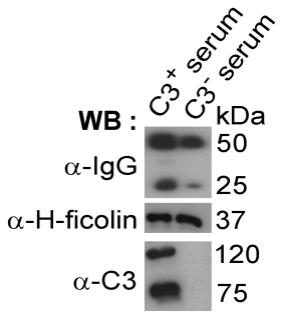

Figure 3.34: Detection of IgG, ficolin and C3 in human serum before ($C3^+$) and after ($C3^-$) depletion of C3. Effective depletion of C3 (120 kDa, alpha chain and 75 kDa, beta chain) was observed in C3- serum. Some loss of IgG (50 kDa, heavy chain and 25 kDa, light chain) occurred in C3- serum due to the depletion process. Ficolin (37 kDa) level remained unchanged. The samples were resolved in SDS-PAGE (12%) under reducing conditions.

This depletion allowed us to check for the potential influence of C3 on IgG deposition on GlcNAc-beads under normal (pH 7.2, 2.5 mM Ca^{2+}) and simulated infection-inflammation condition (pH 6.5, 2.0 mM Ca^{2+}). Using the C3-depleted human serum ($C3^-$ serum), we showed that IgG was still recruited onto GlcNAc beads only in the presence of ficolin **(Figure 3.35)**. In C3-containing serum ($C3^+$ serum), C3 was recruited onto IgG bound to ficolin-beads, causing a shift in the band size of IgG (see arrowheads). Under the infection-inflammation condition, the deposition of IgG increased by 3.5- fold. The apparent lesser deposition of IgG to GlcNAc beads (in $C3^-$ serum, right panel) is due to the depletion-related loss of IgG (Figure 3.35 and explanation above). This result suggests that natural IgG**:**ficolin interaction occurs regardless of C3, and the complex formation is enhanced under the infection-

inflammation condition.

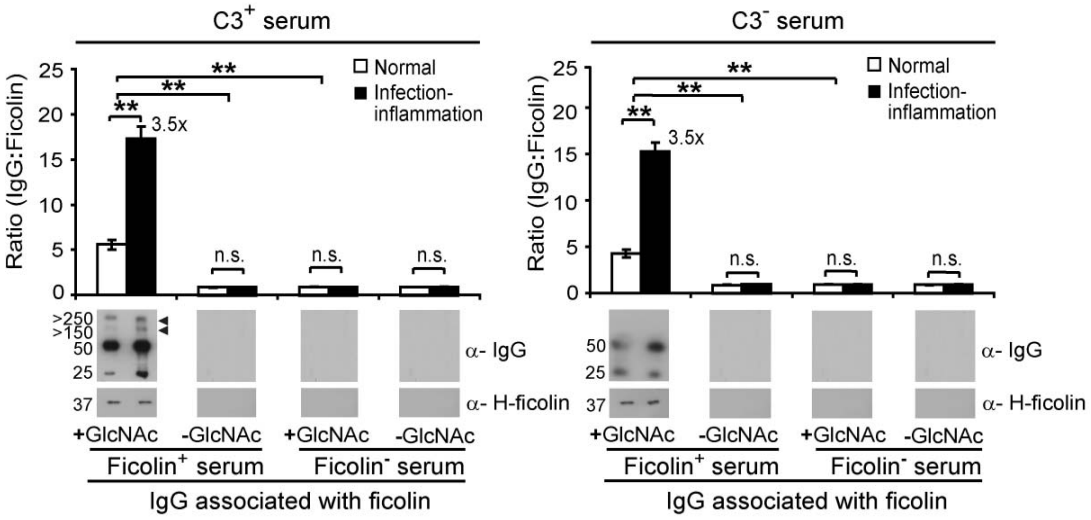

Figure 3.35: Co-IP to determine the potential effect of C3 on the specific interaction between IgG and ficolin in human serum. GlcNAc beads used as bacterial mimic were incubated with human serum under "normal" (pH 7.2, 2.5 mM Ca^{2+}; white bar) and "infection-inflammation" (pH 6.5, 2.0 mM Ca^{2+}; black bar) conditions, in the presence and absence of ficolin or C3 or both. Under the infection-inflammation condition, IgG was more intensely recruited onto the beads in the presence of ficolin. The presence or absence of C3 did not affect the binding. C3 was recruited to IgG on the ficolin-bound GlcNAc beads. Data are presented as ratio of density of IgG to ficolin deposited on beads, showing mean +/- s.e.m. from 3 independent experiments. Representative Western blots are shown. The samples were resolved in SDS-PAGE (12%) under reducing conditions. $^{**}p<0.01$. n.s., not significant.

In case C3 is found only on immune complexes *in vivo*, but not co-purified with free /uncomplexed IgG and ficolin, we further checked for the potential deposition of C3 onto GlcNAc-beads in ficolin-depleted human serum (Ficolin$^-$ serum) or IgG-depleted human serum (IgG$^-$ serum) under normal and infection-inflammation conditions, *ex vivo* (**Figure 3.36**). The results below show that:

(a) After both ficolin and IgG (from the human serum) were bound to

the GlcNAc beads, there was a shift in the band sizes of IgG and C3 (>250 and >150 kDa, see arrowheads). We also observed discrete bands of 65 and 43 kDa, which are C3 alpha chain fragments (lanes 5 & 6, "Undepleted serum"; boxed) as was similarly reported in literature (Lutz et al., 1996).

(b) Under the infection-inflammation condition, more of IgG and C3 alpha chain are pulled down, with concomitant increase in intensity of the higher molecular weight bands (>250 and >150 kDa) and C3 alpha chain fragments of 65 & 43 kDa (lane 6). Under normal condition (lane 5), we observe some C3 recruited to the beads, which could be due to low level of IgG bound to the GlcNAc-ficolin (as shown in our earlier biochemical studies).

(c) We did not observe a shift in the size of ficolin (37 kDa). This is likely due to the electrostatic interaction between IgG**:**ficolin as was found in our study (Figures 3.23 and 3.24). Hence, ficolin and IgG will dissociate from each other during sample processing and resolving under reducing SDS PAGE.

Lane 13 (positive control) shows the presence of ficolin, IgG and C3 in uninfected human serum. Altogether, the results confirm that**:** (i) the presence of C3, IgG and ficolin in the GlcNAc-bead pulldown; (ii) that C3 is recruited only to immobilized IgG**:**ficolin complex (supported by the lack of C3 deposition when the serum was depleted of either ficolin or IgG (lanes 1-4); and (iii) that in the absence of GlcNAc (lanes 7-12), no IgG**:**ficolin complex was observed, indicating specificity of the IgG**:**ficolin interaction with a bacterial mimic.

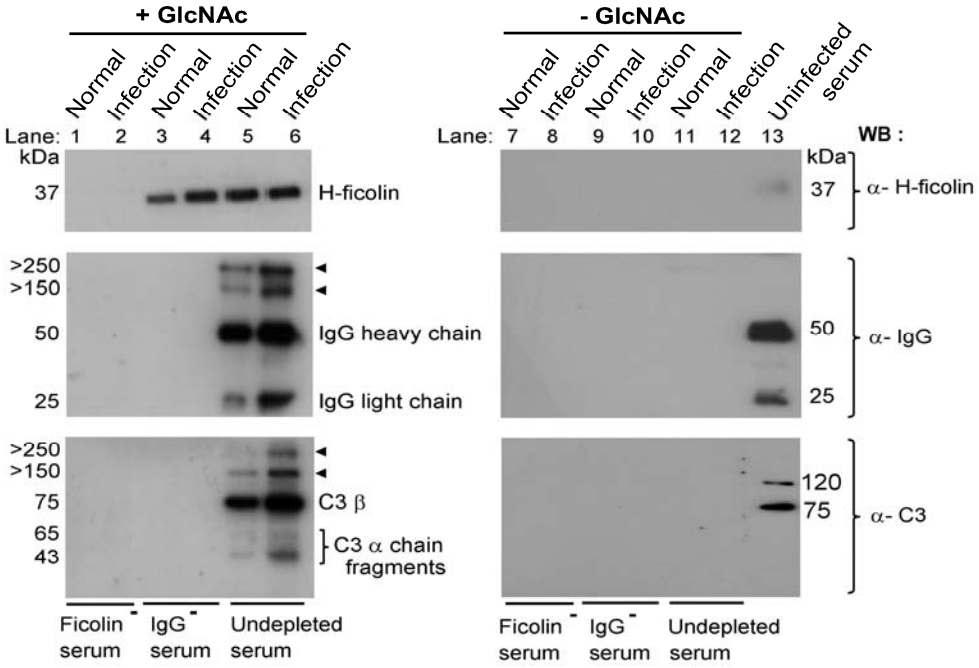

Figure 3.36: Detection of human H-ficolin, IgG and C3 pulled down on GlcNAc beads under normal and infection:inflammation conditions. C3 in the undepleted serum is recruited via its alpha chain onto the IgG heavy chain (IgG HC) bound to ficolin-GlcNAc beads, giving rise to a shift in band sizes of C3 and IgG (see arrowheads). Depletion of either ficolin (lanes 1,2) or IgG (lanes 3,4) from the serum showed no binding of C3 to the GlcNAc beads. Under the infection-inflammation condition (annotated as "Infection" on the top of the lane), more of the IgG and C3 alpha chain are pulled down, with concomitant increase in intensity of the higher molecular weight bands (>250 and >150 kDa) and C3 alpha chain fragments of 65 & 43 kDa (lane 6). The samples were resolved in SDS-PAGE (12%) under reducing conditions. Ficolin, IgG and C3 associated with the beads were detected using respective polyclonal antibodies. "-GlcNAc" (lanes 7-12) was the negative control. Lane 13 shows the presence of ficolin, IgG and C3 of the expected band sizes, present in the uninfected human serum.

To further rule out the potential involvement of C3 *in vivo*, we infected WT mice with *P. aeruginosa* and monitored the levels of ficolin and C3 associated with IgG in the serum during the early phase of infection for up to 24 h. Our samples included: (i) "WT serum" (containing C3) as a positive control; (ii) C3-deficient mouse serum, "*C3*$^{-/-}$ serum" and (iii) IgG purified from uninfected *C3*$^{-/-}$ serum as negative control. **Figure 3.37** shows that C3 is

present in the WT serum (positive control) and absent in *C3*$^{-/-}$ serum (negative control). C3 is not detectable in any of the: (a) purified IgG from WT serum (from uninfected control mice, lane 1) or from *C3*$^{-/-}$ serum (from uninfected *C3*$^{-/-}$ control mice, lane 6) and (b) IgG**:**ficolin immune complex (IgG^{WT}) purified from infected mice sera. Although C3 is known to interact non-covalently with free IgG, we did not find C3 associated with either the purified free IgG (uninfected control) or free IgG**:**ficolin complexes (3-24 hpi).

We observed increasing amounts of serum ficolin complexed with IgG (pulled down by Protein G beads) in infected serum over time post-infection (from infected WT mice, lanes 2-5), independent of C3 association in the complexes. Our results strongly indicate that C3 is not involved in the binding of natural IgG to ficolin during an infection.

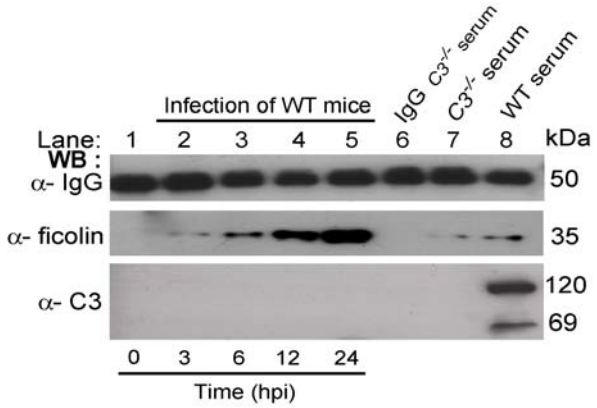

Figure 3.37: IgG:ficolin complex purified from infected mice serum does not contain C3. Co-IP shows increasing amounts of ficolin (35 kDa) associated with IgG (pulled down by Protein G beads) in the serum over time course of infection of WT mice (n=3) (lanes 2-5). No C3 was detected in the IgG purified from the sera of both uninfected (n=3) and infected mice (n=3) (lanes 1-5). No C3 was present in the IgG purified from pooled sera of uninfected *C3*$^{-/-}$ mice (n=6) (lane 6). C3 was detected (120 kDa alpha chain and 69 kDa beta chain; bottom panel) in pooled serum of WT mice (n=6) (lane 8).

3.7.3. Natural IgG recognizes ficolin bound bacteria in *C3*$^{-/-}$ mice

To prove beyond doubt that IgG**:**ficolin complex formation triggered by an infection occurs independently of C3, we tested this novel phenomenon *ex vivo* and *in vivo* in *C3*$^{-/-}$ mice. We first checked the levels of ficolin, IgG and C3 in WT and *C3*$^{-/-}$ mice prior to further *ex vivo* and *in vivo* experiments. Sera from *C3*$^{-/-}$ mice, which lack C3, contain similar levels of ficolin and IgG as that of WT mice (**Figure 3.38**).

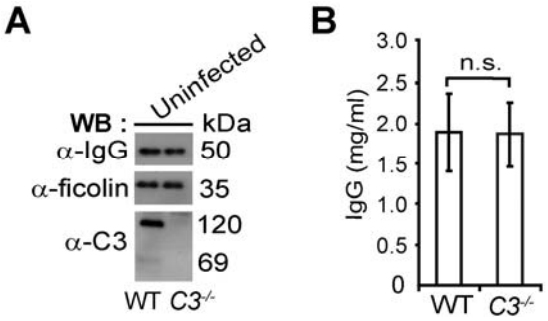

Figure 3.38: Ficolin, IgG and C3 levels in WT and *C3*$^{-/-}$ mice. (A) Immunoblot analysis of the pooled sera shows that both WT and *C3*$^{-/-}$ mice (n=6 each) express IgG and ficolin. C3 is present in WT mice but absent in *C3*$^{-/-}$ mice. (B) ELISA of pooled sera shows that both WT and *C3*$^{-/-}$ mice (n=6) harbor similar levels of IgG. Three replicates per sample were tested.

Since our study delineated the heavy chain of IgG to interact with ficolin, we focused specifically on detecting IgG heavy chain and its interactions in our mice studies. Using sera from *C3*$^{-/-}$ mice, we performed flow cytometry to check whether C3 enhances the formation of IgG**:**ficolin complexes on the *P. aeruginosa*. **Figure 3.39** shows: (a) Compared to the secondary antibody (2˚ Ab) as control (black), natural IgG (red) purified from *C3*$^{-/-}$ mice sera showed no binding to the bacteria. (b) However, IgG binding to bacteria increased dose-dependently of IgG^{-} serum (serum depleted of IgG) –

see thin blue (1:20 diluted IgG^- serum) and thick blue (1:10 diluted IgG^- serum), indicating that serum factors other than IgG might enable its binding onto the bacteria. (c) Serum depleted of both IgG and ficolin (IgG^- $Ficolin^-$ serum), showed significant reduction in the binding of IgG to the bacteria (dashed blue). These results indicate that ficolin is the crucial serum factor that recruits IgG to the bacteria. Thus ficolin aids IgG in recognizing bacteria, independent of C3.

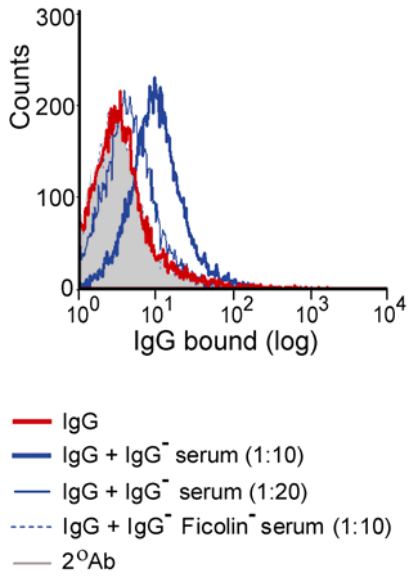

Figure 3.39: Natural IgG binds to *P. aeruginosa* independently of C3 but with the aid of ficolin. FACS to detect binding of IgG purified from pooled sera of uninfected *C3*$^{-/-}$ mice (n=6) to 10^6 cfu *P. aeruginosa*. Bacteria opsonized with proteins (annotated below figure) were incubated with anti-mouse IgG and Alexa488-conjugated secondary antibody. IgG alone does not bind to the bacteria (red). IgG^- serum dose-dependently (1:10 and 1:20 diluted) deposited IgG on the bacteria. Further depletion of ficolin from IgG^- serum (IgG^- $ficolin^-$ serum; 1:10 diluted) significantly reduced IgG binding. Data are representative of three independent experiments.

To further confirm the lack of a role for C3 in the recognition of bacteria by natural IgG, we endeavored to test the IgG**:**ficolin interaction in *C3*$^{-/-}$ mice *in vivo* during infection by *P. aeruginosa*. **Figure 3.40** shows that

the level of free IgG:ficolin complex formed in the serum increased in a time-dependent manner in both WT and *C3*$^{-/-}$ mice. Despite the absence of C3, IgG**:**ficolin complexes were formed at increasing levels over time of infection *C3*$^{-/-}$ mice, indicating no specific involvement of C3 in the formation of IgG**:**ficolin complexes during infection. Therefore, mouse natural IgG recognizes bacteria *in vivo*, in complex with ficolin, and this is independent of C3.

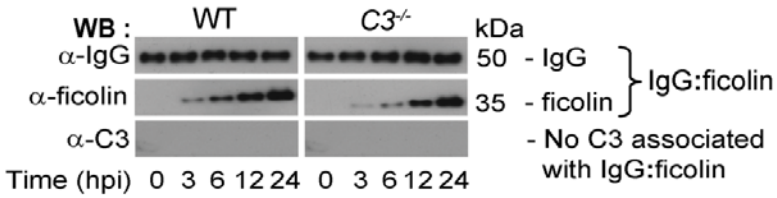

Figure 3.40: *In vivo* infection induces IgG:ficolin complex formation which increases over time, independent of C3. Co-IP to detect ficolin (35 kDa) associated with IgG (pulled down by Protein G beads) in the pooled serum of WT or *C3*$^{-/-}$ mice (n=3 each) infected with 10^6 cfu *P. aeruginosa* over time course. Ficolin associated with IgG increased over time of infection. No C3 was found to be associated with IgG**:**ficolin complex in the serum. Data are representative of three independent experiments.

Here, we detected free IgG**:**ficolin complexes in the infected mice serum using Protein G beads, which pulled down IgG and the ficolin associated with it. We did not detect any C3 associated with the free complexes. It is possible that C3 is present on the bacteria opsonized with IgG**:**ficolin complex (Figure 3.35) but not with free IgG**:**ficolin complexes, which we pulled down using Protein G beads.

As natural antibodies are known to target the opsonized pathogen complexes to the spleen to prevent the spread of infection to other vital organs,

we explored IgG**:**ficolin co-localization in the spleen by immunohistochemical (IHC) staining in WT and *C3*$^{-/-}$ mice. **Figure 3.41** shows similar increases in the IgG**:**ficolin complexes over time, indicating that the absence of C3 does not affect the co-localization of the IgG**:**ficolin complexes in the spleen, and that IgG recognizes bacteria with the aid of ficolin, independently of C3.

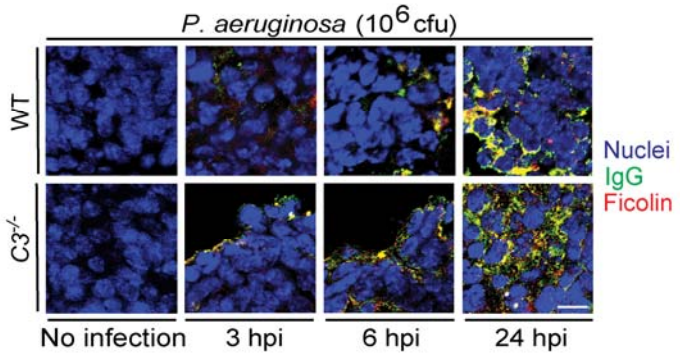

Figure 3.41: *In vivo* infection induces IgG:ficolin colocalization in mice spleen which increases over time, independent of C3. Immunofluorescence staining to detect IgG**:**ficolin co-localization in spleen sections of WT or *C3*$^{-/-}$ **mice** (n=3 each) after infection with 10^6 cfu *P. aeruginosa* over time course. Frozen sections were cut at 5 μm thickness, fixed and stained with anti-ficolin (red) and anti-mouse IgG (green). Imaging was performed using LSM meta 510 confocal microscope (100x objective. Scale bar, 10 μm). Data are representative of three independent experiments.

We also probed for C3 in the uninfected and infected spleen sections over time of infection, and observed that C3 was present in WT mice but absent in *C3*$^{-/-}$ mice (**Figure 3.42**).

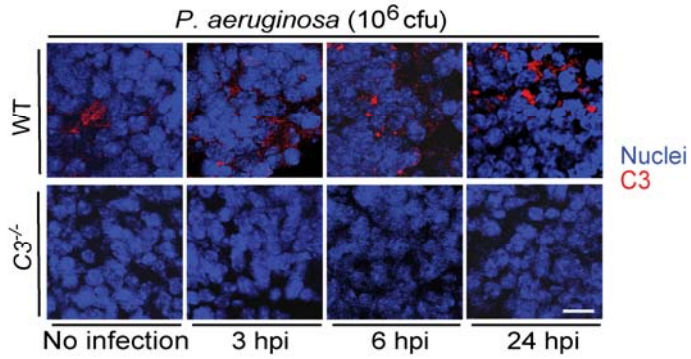

Figure 3.42: C3 is absent in spleen sections of *C3*$^{-/-}$ mice but present in WT mice over time course of infection. Immunofluorescence staining to detect C3 in spleen sections of WT or *C3*$^{-/-}$ **mice** (n=3 each) after infection with 10^6 cfu *P. aeruginosa* over time course. Frozen sections were cut at 5 μm thickness, fixed and stained with anti-C3, followed by staining with corresponding Alexa-594 conjugated secondary antibody. Imaging was performed using LSM meta 510 confocal microscope (100x objective. Scale bar, 10 μm). Data are representative of three independent experiments.

Infection-inflammation conditioned serum may result in alternative pathway activation, which might attach C3 to the IgG Fc region (as a parallel event). However, based on our results, we conclude that C3 is not involved in bringing together ficolin and natural IgG. Our data showed that IgG**:**ficolin immune complex is formed independently of C3.

3.7.4. IgG:ficolin mediated anti-microbial defense protects *C3*$^{-/-}$ mice from bacterial infection

We next checked whether IgG:ficolin mediated bacterial recognition and clearance could protect the *C3*$^{-/-}$ mice from infection. We first checked the bacterial load in WT and *C3*$^{-/-}$ mice post-infection with 10^6 cfu *P. aeruginosa*. Similar bacterial load in all tissues at 6 hpi indicates equal administration of the inocula at the start of infection. The bacterial burden in the tissues of *C3*$^{-/-}$

mice was higher than that in WT mice at 24 and 72 hpi, indicating that absence of C3 leading to failure of possible alternative pathway activation, could result in ineffective bacterial clearance and higher bacterial load in the tissues. Indeed we observed a delayed rate of clearance of *P. aeruginosa* in *C3*$^{-/-}$ mice as compared to the WT mice. However, by day 6, the pathogen clearance by the *C3*$^{-/-}$ mice became closely comparable to that of the WT mice (**Figure 3.43**).

With the above observations on bacterial clearance by *C3*$^{-/-}$ mice, we proceeded to check the status of the cytokine expression, spleen size and survival of the *C3*$^{-/-}$ mice in infection to assess the extent of damage caused by the bacterial invasion. The serum cytokines (IL6, TNFα and IL10) were measured to assess the ensuing inflammatory response of *C3*$^{-/-}$ mice to *P. aeruginosa* infection. Over the time of infection, we observed a significant increase in the levels of IL6 and TNFα and a decrease in IL10 in *C3*$^{-/-}$ mice as compared to the WT mice (**Figure 3.44**), indicating that initial impairment in the ability to clear the bacteria in the C3-deficient mice led to higher inflammation.

We next examined the extent of tissue damage resulting from infection and inflammation in the *C3*$^{-/-}$ mice. We stained the liver sections with hematoxylin and eosin, and observed that infection of both the WT and *C3*$^{-/-}$ mice was resolved over time, with no infiltration of inflammatory cells observed in either WT or *C3*$^{-/-}$ mice livers (**Figure 3.45**). This indicates that absence of C3 does not significantly affect the overall process of resolving infection and inflammation with time.

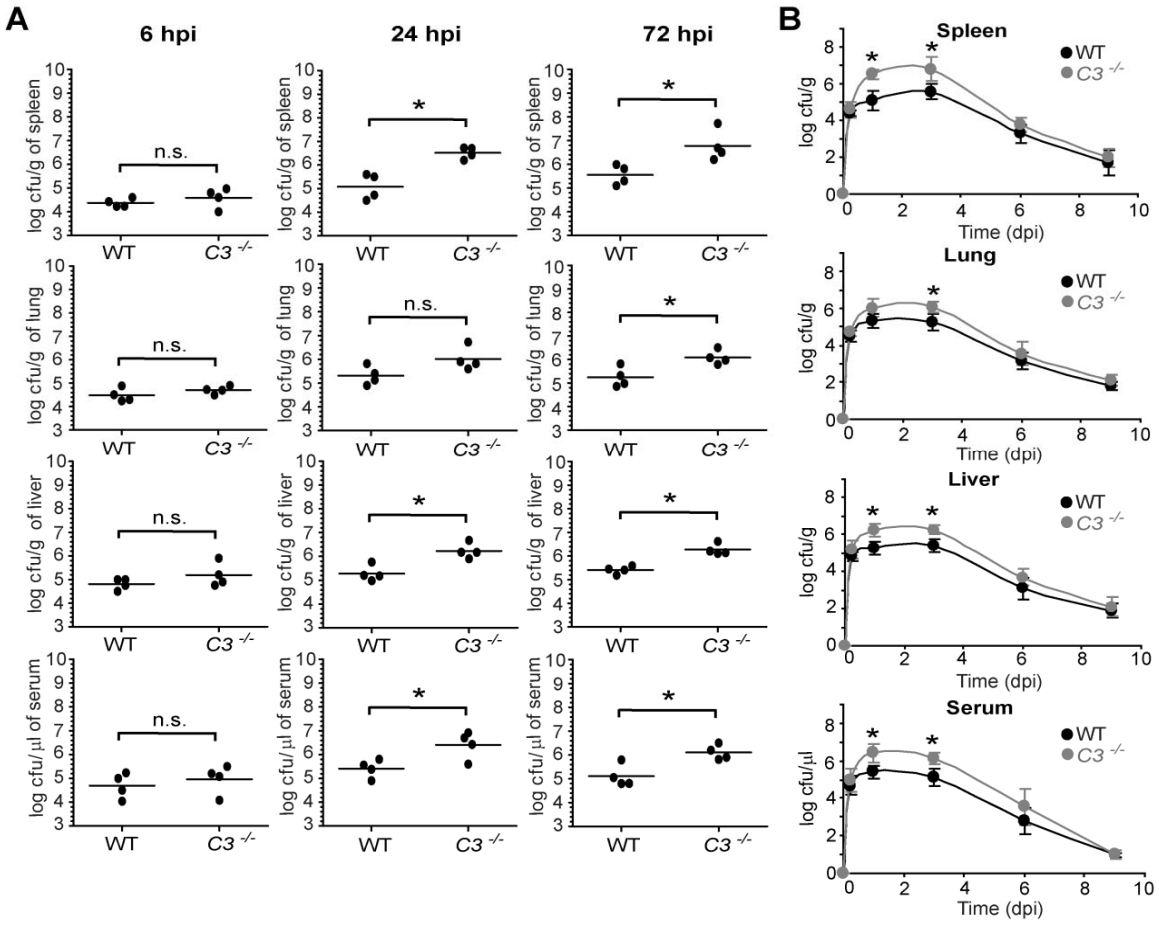

Figure 3.43: Bacterial load and clearance rate in tissues and serum of infected WT and *C3*$^{-/-}$ mice over time. (**A**) Colony forming unit (cfu) of *P. aeruginosa* per g of spleen, lung, liver and per µl of serum assessed at 6, 24 and 72 hpi in WT or *C3*$^{-/-}$ mice (n=4 each) infected intravenously with 10^6 cfu *P. aeruginosa*. Each data point represents an individual mouse. Horizontal lines represent the mean log cfu/g of organ or cfu/µl of serum. (**B**) Colony forming unit (cfu) of *P. aeruginosa* (indicating rate of bacterial clearance) per g of spleen, lung, liver and per µl of serum assessed over 9 dpi in WT or *C3*$^{-/-}$ mice (n=4 each) infected intravenously with 10^6 cfu *P. aeruginosa*. **p*<0.05, ***p*<0.01.

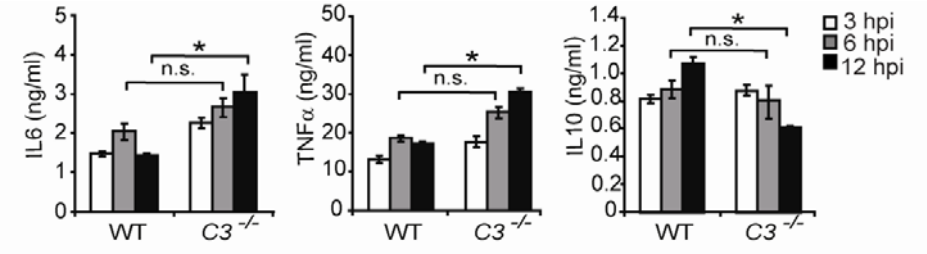

Figure 3.44: Pro- and anti-inflammatory cytokine levels in pooled mice serum from infected WT and *C3*$^{-/-}$ mice over time. ELISA to detect IL6, TNFα and IL10 levels in pooled sera of WT or *C3*$^{-/-}$ mice (n=4 each) infected with 10^6 cfu *P. aeruginosa* assessed at 3, 6 and 12 hpi. Three replicates per sample were tested. Data are representative of three independent experiments.

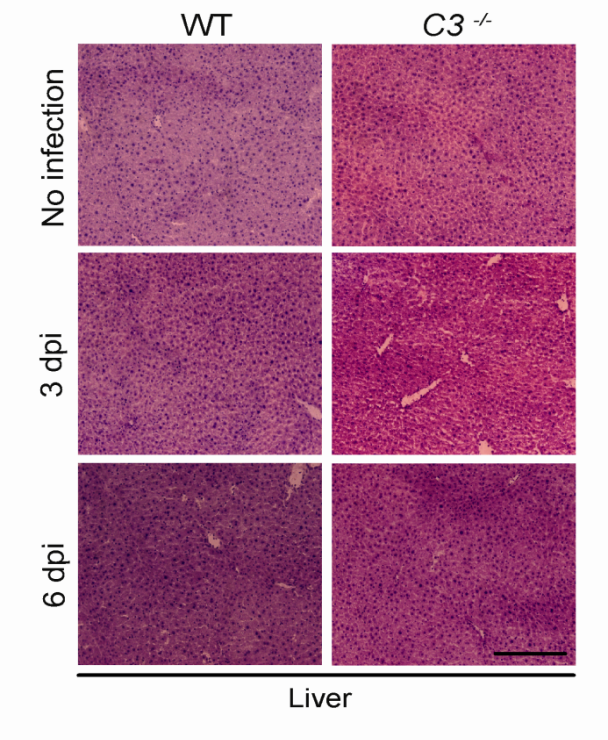

Figure 3.45: Hematoxylin and eosin staining of livers of infected WT and *C3*$^{-/-}$ mice. Hematoxylin and eosin staining of livers of WT and *C3*$^{-/-}$ mice (n=4 each) infected with 10^6 cfu *P. aeruginosa* over time course (original magnification, 100x. Scale bar, 500 μm).

Finally, we observed the survival of *C3*$^{-/-}$ mice over time post-infection. The extent of survival was slightly compromised in *C3*$^{-/-}$ mice (**Figure 3.46**). This is not surprising since the absence of C3 abrogates the alternative complement pathway. Despite the C3 deficiency, the high survival rate in the *C3*$^{-/-}$ mice also recapitulates the significance of the IgG and ficolin (present in *C3*$^{-/-}$ mice) in conferring protection against the bacterial infection. Thus, we have ruled out any potential involvement of C3 in the IgG**:**ficolin mediated immune recognition.

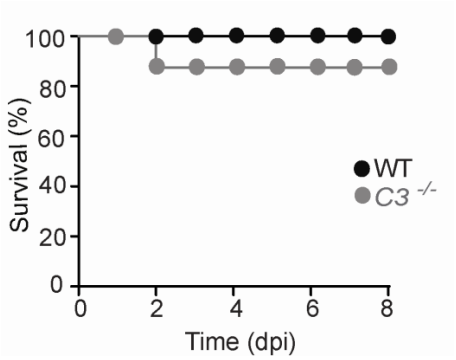

Figure 3.46: Survival curve of infected WT and *C3*$^{-/-}$ mice over time. Survival of WT and *C3*$^{-/-}$ mice infected with 10^6 cfu *P. aeruginosa* over time course (n=8 per group). Differences in survival were analyzed by the log-rank test (p>0.05).

3.8. *IgG* siRNA knockdown with partial IgG are susceptible to infection

Turning our attention to the biological significance of the perceived 'dormant' natural IgG, we performed *IgG* siRNA knockdown in mice to study possible loss of function of natural IgG during infection.

3.8.1. Natural IgG recognizes bacteria with the help of ficolins and directs the opsonized pathogen to the spleen

IgG purified from the sera of previously uninfected mice exhibited minimal binding to *P. aeruginosa* (**Figure 3.47A**), supporting that the IgG from uninfected mice are not specific to bacterial antigens, hence they are appropriately termed natural IgG. *In vitro*, IgG^- serum facilitated the binding of purified IgG to the bacteria, and ficolin was found to be the crucial serum factor enabling this process of deposition (Figure 3.47A). *Ex vivo*, the level of IgG**:**ficolin complex formed in the infected mouse serum increased in a time (0-24 hours post-infection, hpi)- and dose (10^6-10^7 cfu)- dependent manner of *P. aeruginosa* infection (**Figure 3.47B**). Since mouse ficolin A and B isoforms are orthologs of human L- and M-ficolins, respectively, and share similarity with all human ficolins at amino acid positions that interact with IgG, it is likely that mouse ficolins also interact with IgG to carry out effector functions in a similar manner. Consistent with a report that natural antibodies target the opsonized pathogen complexes to the spleen to prevent the spread of infection to other vital organs (Ochsenbein et al., 1999), we observed increased colocalization of IgG**:**ficolin complex in the spleens of infected mice over time (**Figure 3.47C**).

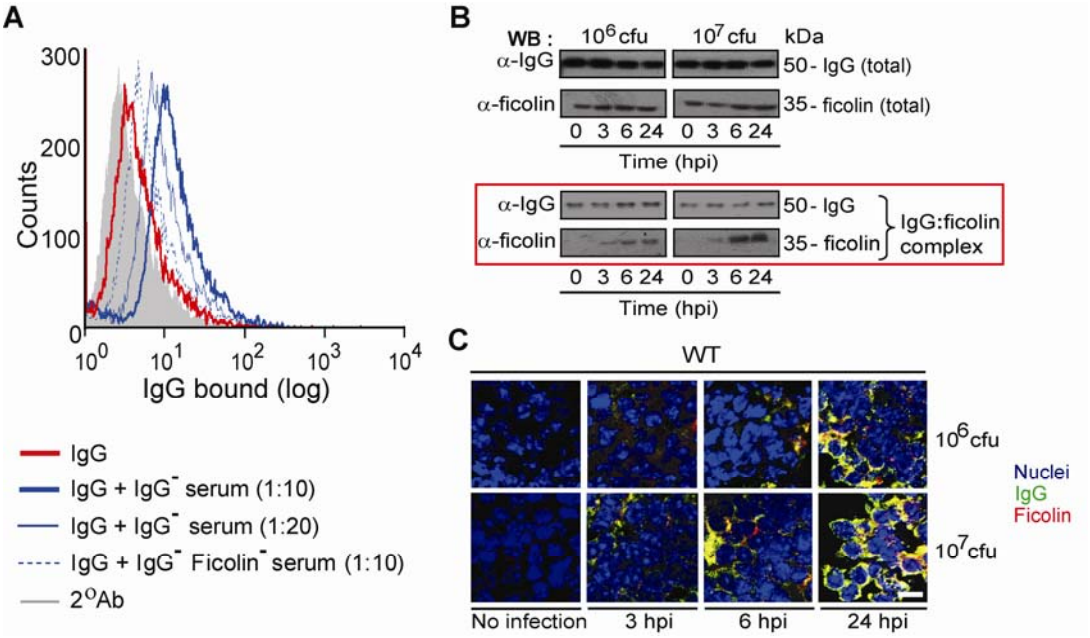

Figure 3.47: Natural IgG recognizes bacteria with the help of ficolin in mice. (**A**) FACS analysis to detect binding of IgG purified from pooled sera of uninfected WT mice (n=8) to 10^6 cfu *P. aeruginosa*. Bacteria opsonized with proteins (annotated below figure) were incubated with anti-mouse IgG and Alexa488-conjugated secondary antibody. IgG alone does not bind bacteria (red). IgG^- serum (1:10 and 1:20 diluted) facilitated dose-dependent deposition of IgG on the bacteria. Further depletion of ficolin from IgG^- serum (IgG^- $ficolin^-$ serum; 1:10 diluted) significantly reduced IgG binding. (**B**) Immunoblot analysis of IgG (50 kDa heavy chain) and ficolin levels in the pooled sera of mice (n=8) and detection of IgG**:**ficolin complex (pulled down by Protein G beads) in serum (red box), post-infection with 10^6 or 10^7 cfu *P. aeruginosa* over time course. The samples were derived from the same experiment, resolved under 12% reducing SDS-PAGE and the gels and blots were processed in parallel. (**C**) Immunofluorescence staining for co-localization of IgG**:**ficolin in spleen sections of WT mice (n=3), uninfected and infected with 10^6 or 10^7 cfu *P. aeruginosa* over time course. 100x objective. Scale bars, 10 µm. Data are representative of three independent experiments.

3.8.2. *In vivo* siRNA treatment specifically knocked down *IgG* in mice

Next, we sought to determine the action of the natural IgG in defense against bacterial infection using a siRNA knockdown mouse model by subcutaneously

implanting osmotic pumps to continuously infuse *IgG*-specific siRNA to deplete the natural IgG in the serum. Mice treated with 30 mg/kg/day of IgG-specific siRNA showed significant reduction in serum IgG within 4 days as compared to controls (PBS or control siRNA treatments). The levels of serum IgM, IgA and ficolin remained unchanged in the *IgG*-knockdown mice, thus confirming the specificity of the *IgG*-knockdown (**Figures 3.48 A and B)**.

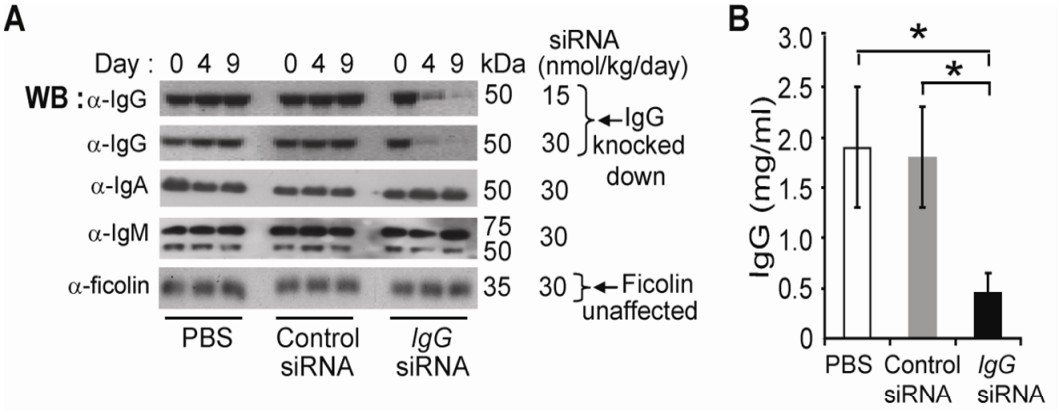

Figure 3.48: Specific knockdown of IgG by siRNA treatment in mice. (**A**) Immunoblot analysis of the heavy chains of IgG, IgA, IgM, and ficolin in pooled serum of mice (n=4) showed specific knockdown of IgG at days post-treatment with *IgG* siRNA. Mice treated with PBS or control siRNA do not show knockdown of IgG. (**B**) ELISA to detect IgG levels in pooled sera of mice (n=4) at day 4 post-treatment with PBS, control siRNA or *IgG* siRNA (30 nmol/kg/day). Three replicates per sample were tested. Data are representative of three independent experiments.

3.8.3. *IgG*-knockdown mice are more susceptible to infection

Upon intravenous infection with 10^6 cfu *P. aeruginosa*, *IgG* knockdown mice showed reduced IgG**:**ficolin complex formation in the sera (**Figure 3.49A**) and spleen (**Figure 3.49B**). These data suggest that natural IgG, through its collaboration with ficolin, plays an essential role in controlling infection.

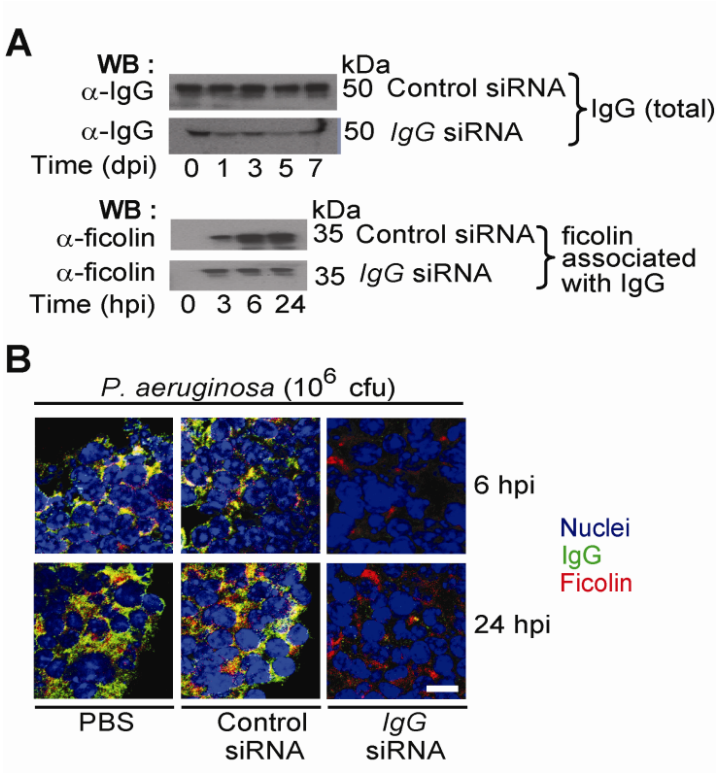

Figure 3.49: IgG:ficolin complex formation in serum and spleen of PBS, control and *IgG* siRNA knockdown mice. Mice were continuously infused with control siRNA or *IgG* siRNA (30 nmol/kg/day) via osmotic pump delivery for 14 days. After 4 days of infusion, mice were infected with 10^6 cfu *P. aeruginosa*. (**A**) Mice (n=3) treated with control siRNA and *IgG* siRNA were infected with 10^6 cfu *P. aeruginosa.* Immunoblot analysis of serum IgG levels showed reduced IgG in *IgG* siRNA knockdown mice as compared to control siRNA treated mice over the course of infection (top). More and increasing levels of "ficolin associated with IgG" are observed in control siRNA than in *IgG* siRNA knockdown mice over the course of infection (bottom). The samples were derived from the same experiment, resolved under 12% reducing SDS-PAGE and the gels and blots were processed in parallel. (**B**) Immunofluorescence staining for co-localization of IgG**:**ficolin in spleen sections of PBS, control siRNA or *IgG* siRNA knockdown mice (n=3) at indicated time points post-infection. 100x objective. Scale bar, 10 μm. Data are representative of three independent experiments.

The *IgG*-knockdown mice showed higher bacterial burdens in the spleen, lung, liver and serum, and the cfu progressively increased post-infection (**Figure 3.50**). Similar bacterial load in all tissues at 6 hpi indicated equal administration of the inoculum.

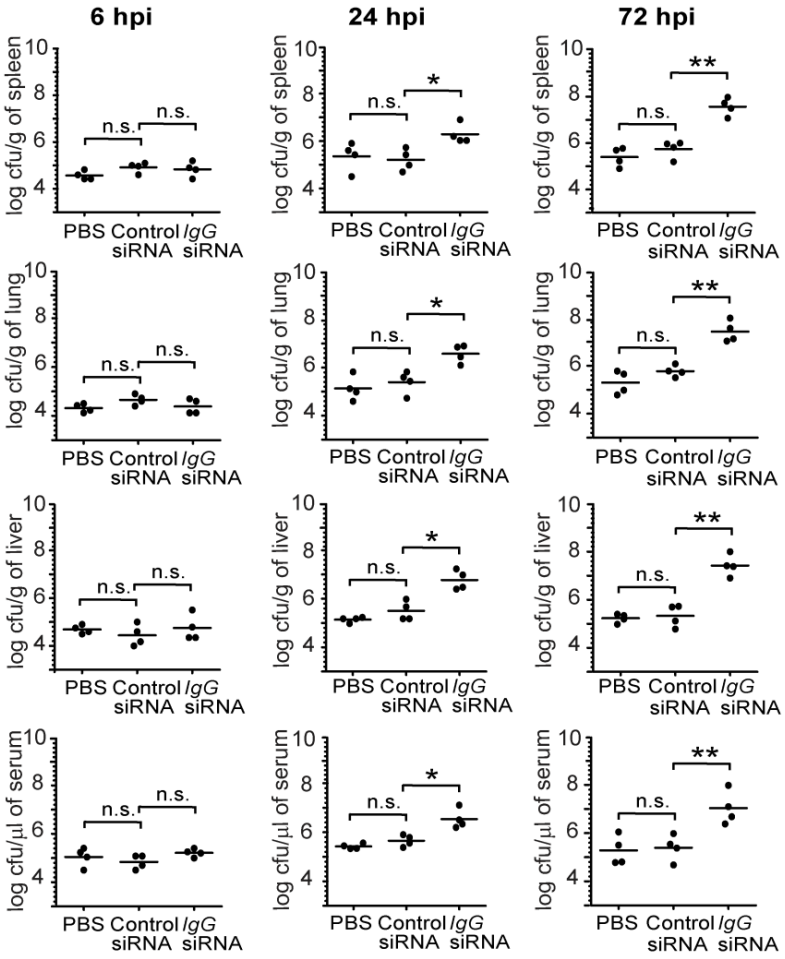

Figure 3.50: Tissue bacterial load in PBS, control and *IgG* siRNA knockdown mice. Mice were continuously infused with control siRNA or *IgG* siRNA (30 nmol/kg/day) via osmotic pump delivery for 14 days. After 4 days of infusion, mice were infected with 10^6 cfu *P. aeruginosa*. Log cfu *P. aeruginosa* per g of spleen, lung, liver and per µl of serum, assessed at 6, 24 and 72 hours post-infection (hpi) in PBS, control siRNA or *IgG* siRNA knockdown mice (n=4). Freshly dead and alive mice were examined. Each point represents an individual mouse. Horizontal lines represent the mean log cfu/g of organ or cfu/µl of serum. *p<0.05; **p<0.01; n.s., not significant.

Delayed bacterial clearance (**Figure 3.51**) correlates with the lack of IgG, which increased the susceptibility to infection. Thus, lack of IgG impairs the efficient removal of bacteria, leading to uncontrolled proliferation of the pathogen in the tissues.

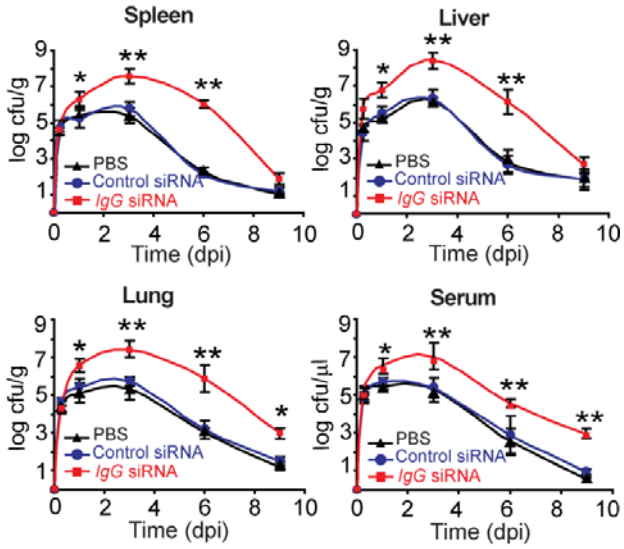

Figure 3.51: Bacterial clearance rate in PBS, control and *IgG* siRNA knockdown mice. Mice were continuously infused with control siRNA or *IgG* siRNA (30 nmol/kg/day) via osmotic pump delivery for 14 days. After 4 days of infusion, mice were infected with 10^6 cfu *P. aeruginosa*. Log cfu *P. aeruginosa* per g of spleen, liver and lung and per µl of serum of PBS, control siRNA or *IgG* siRNA knockdown mice (n=4), over 9 days post-infection (dpi). Freshly dead and alive mice were examined. **p*<0.05; ***p*<0.01; n.s., not significant.

To assess the ensuing inflammatory response, we measured IL6 and TNFα, which are functional pro-inflammatory cytokine homologs of human IL8. The *IgG* knockdown mice showed significantly higher IL6 and TNFα and lower anti-inflammatory IL10 levels (**Figure 3.52**), indicating uncontrolled inflammation, consistent with the inability to clear the bacteria.

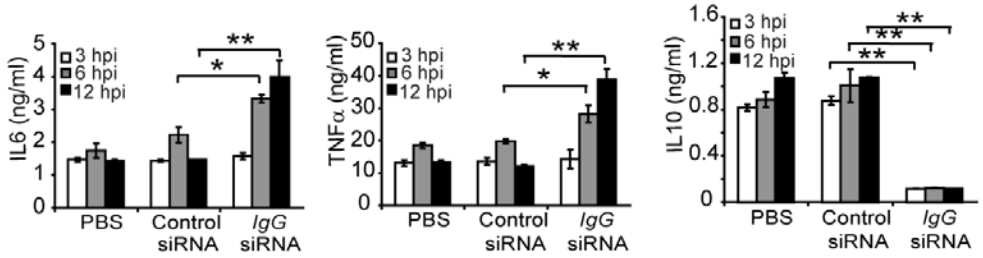

Figure 3.52: Pro- and anti-inflammatory cytokine levels in infected sera from PBS, control and *IgG* siRNA knockdown mice. ELISA to detect IL6, TNFα and IL10 levels in pooled sera from *IgG* siRNA knockdown mice (n=4 each) infected with 10^6 cfu *P. aeruginosa*, assessed at 3, 6 and 12 hpi. Infected PBS or control siRNA treated mice served as controls. **p*<0.05, ***p*<0.01. Data are representative of three independent experiments.

To study the tissue morphological damage, we did hematoxylin and eosin staining of liver sections from infected mice. We showed that the infection in control siRNA controls resolved over time with no infiltration of inflammatory cells. However, we observed inflammatory cell infiltration in the liver of *IgG* knockdown mice, characteristic of unresolved inflammation (**Figure 3.53**).

We also immunostained the spleen sections of the *IgG* siRNA knockdown mice and compared with the control mice. We did not observe germinal centers (GCs) in both control and *IgG* siRNA knockdown mice at 3 and 6 dpi (**Figure 3.54A**). GCs are sites of B cell activation during an immune response (MacLennan 1994). Since this is a primary immune response, it is likely that GCs would only appear at later time points of infection. Upon quantification, we did not observe any GCs in the white pulp areas in both the control siRNA and *IgG* siRNA knockdown mice before and after infection at 3 and 6 dpi (**Figure 3.54B**). The percentage of total white pulp area to spleen area remained unchanged over days of infection in both groups (**Figure**

3.54C), with no significant difference.

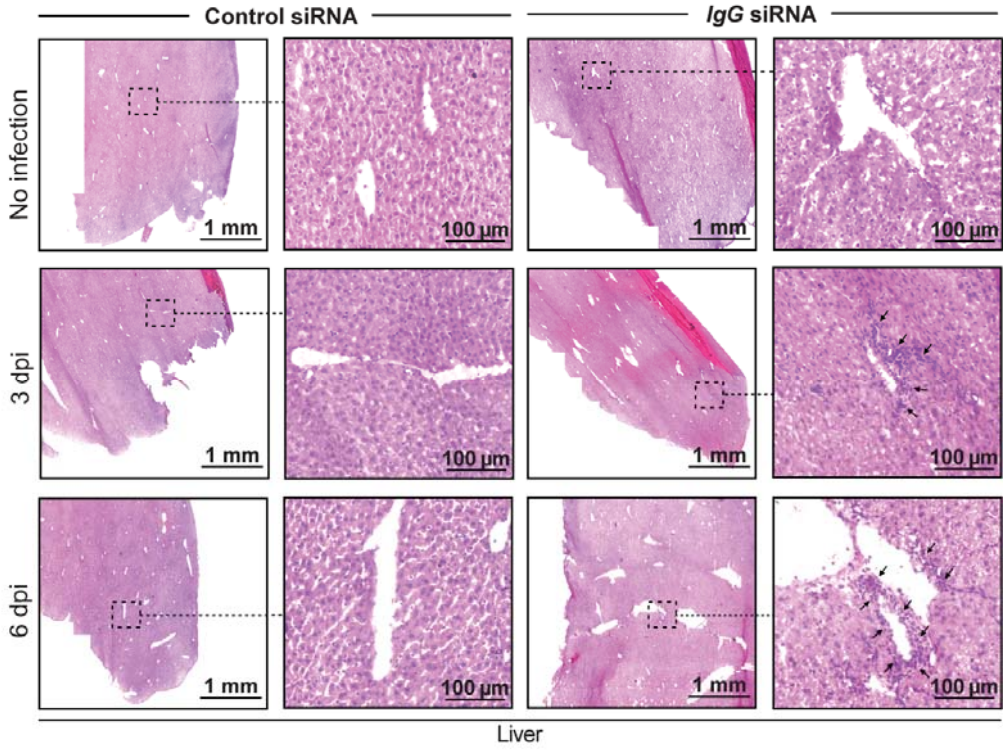

Figure 3.53: Hematoxylin and eosin staining of livers of infected control and *IgG* siRNA knockdown mice. Hematoxylin and eosin staining of livers from control siRNA and *IgG* siRNA knockdown mice (n=4) infected with 10^6 cfu *P. aeruginosa* over time course. Whole tissue section images (magnification; 2x, scale bar; 1 mm) are provided. Higher magnification to highlight areas of inflammatory cell infiltration (arrows) in liver of infected *IgG* siRNA knockdown mice. No infiltration is observed in livers of control siRNA treated mice (magnification; 20x, scale bar; 100 µm). Images were taken using Mirax Midi microscope (Carl Zeiss) and offline analysis was done using Mirax viewer software.

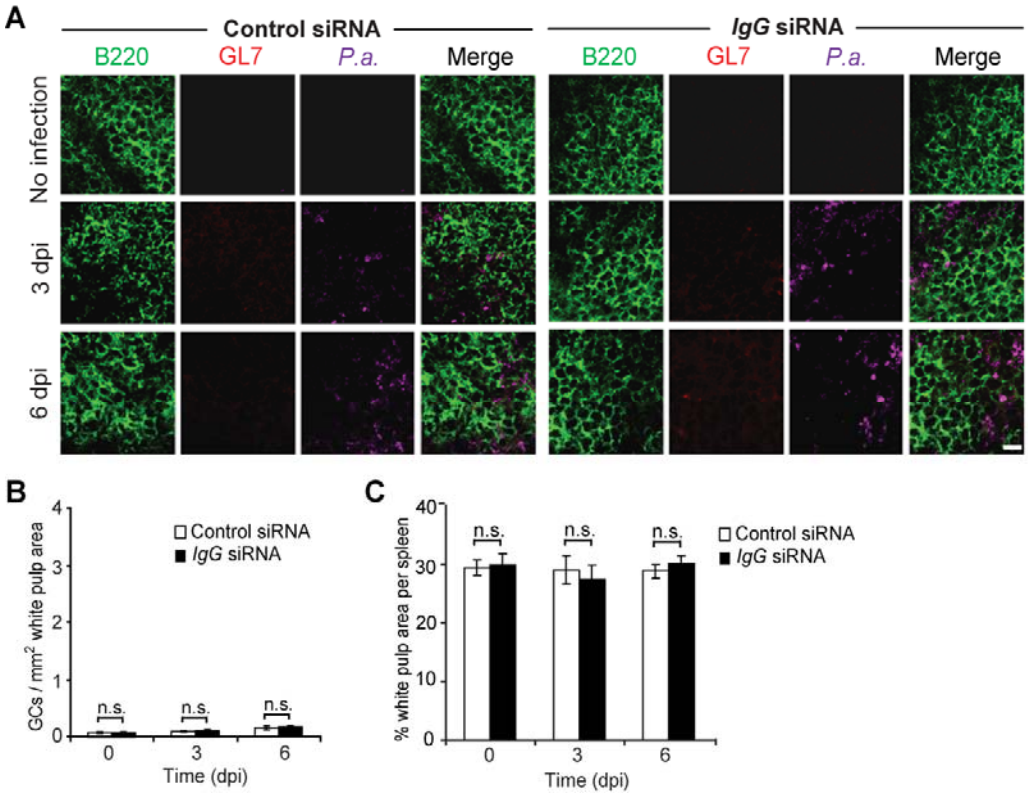

Figure 3.54: Assessment of inflammation in spleens of infected control and *IgG* siRNA knockdown mice. (**A**) Detection of GC B cells in spleen sections of control and *IgG* siRNA knockdown mice at various days post-infection (dpi). Frozen sections were cut at 5 μm thickness and stained with anti-B220 (B cell), anti-GL7 (germinal center) and anti-P.a. (bacteria). *P.a.* refers to *Pseudomonas aeruginosa*. Imaging was done using LSM meta 510 confocal microscope (63x objective. Scale bar, 10 μm). (**B and C**) Quantification of GCs per mm^2 white pulp area in spleen sections of mice at various dpi. Frozen sections were cut at 5 μm thickness and stained with hematoxylin and eosin. Total number of GCs was manually counted using bright field microscopy in three consecutive sections per spleen. Total white pulp area and spleen area per section was calculated using Image J software. The number of GCs per mm^2 white pulp area was calculated by taking an average value from the three sections. GCs per mm^2 of white pulp area and percentage of white pulp area per total spleen area in spleens of control and *IgG* siRNA knockdown mice at 0, 3 and 6 dpi. Six mice per group were studied. n.s., not significant.

The failure of *IgG* knockdown mice to clear the infection compromised survival (**Figure 3.55**). The *IgG* knockdown mice did not completely succumb to the Pseudomonas infection possibly due to sustained levels of natural IgM

and IgA (Figure 3.48A), which partially compensated for the lack of IgG. Additionally, although the *IgG* siRNA knockdown significantly reduced serum IgG level, it did not completely block *IgG* expression (Figures 3.48 A and B).

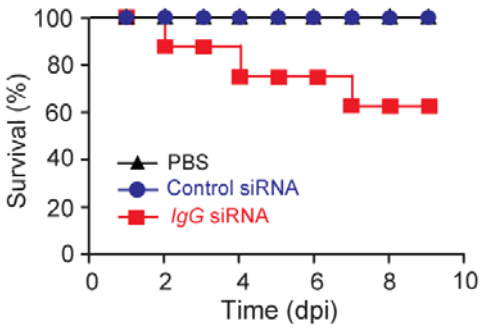

Figure 3.55: Survival curve of infected PBS, control and *IgG* siRNA knockdown mice over time. Survival of PBS, control siRNA or *IgG* siRNA knockdown mice infected with 10^6 cfu *P. aeruginosa* over time course (n=8 per group). Differences in survival were analyzed by the log-rank test (**p*<0.05).

3.9. *AID*$^{-/-}$ mice completely lacking IgG succumb to infection

To be more definitive, we used *AID*$^{-/-}$ mice to further confirm the role of natural IgG in infection. *AID*$^{-/-}$ mice lack the enzyme, activation-induced deaminase (AID) that is responsible for class switching from IgM to other immunoglobulin isotypes. Hence, these mice lack other isotypes such as IgG and IgA. Therefore, the potential loss-of-function of natural IgG mediated by ficolin was studied in these mice.

3.9.1. *AID*$^{-/-}$ mice have IgM but lack both IgG and IgA

We first checked for the presence of IgG, IgA, IgM, ficolin and C3 in WT and *AID*$^{-/-}$ mice. **Figure 3.56A** shows a Western blot indicating the presence of all

proteins in WT mice serum, whereas *AID*$^{-/-}$ mice lack IgG and IgA due to the absence of Ig-class switching. ELISA shows that the level of IgG is undetectable in *AID*$^{-/-}$ mice serum as compared to WT mice (**Figure 3.56B**).

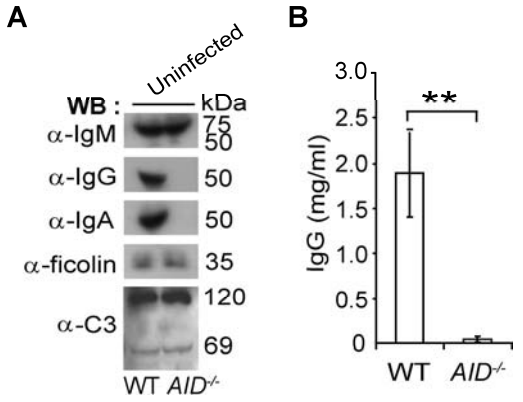

Figure 3.56: IgG and IgA are absent in *AID*$^{-/-}$ mice. (**A**) Immunoblot analysis of the heavy chains of IgG, IgA, IgM, ficolin and C3 in pooled sera of mice (n=6) show that *AID*$^{-/-}$ mice lack both IgG and IgA. (**B**) ELISA shows that pooled sera of *AID*$^{-/-}$ mice (n=6) does not contain IgG, as compared to WT mice (n=6). Three replicates per sample were tested. Data are representative of three independent experiments.

3.9.2. Impaired bacterial clearance leads to unresolved inflammation, tissue damage and higher mortality in *AID*$^{-/-}$ mice

We performed *in vivo* infection of the *AID*$^{-/-}$ mice with *P. aeruginosa*. The bacterial load in both WT and *AID*$^{-/-}$ mice post-infection was similar in all tissues at 6 hpi, indicating equal administration of the inoculum at the start of infection. However, there was significant progressive increase in the bacterial burden in all tissues of *AID*$^{-/-}$ mice as compared to WT mice at 24 and 72 hpi (**Figure 3.57A**). The bacterial load was even higher than that of *IgG* siRNA knockdown mice post- infection (Figure 3.50A), that still retained ~25% of the IgG levels as compared to the WT mice (Figure 3.48B). This indicates that complete absence of natural IgG leads to much higher susceptibility to

infection. Indeed we observed a greater delay in the rate of clearance and increased persistence of *P. aeruginosa* in tissues of *AID*$^{-/-}$ mice (**Figure 3.57B**).

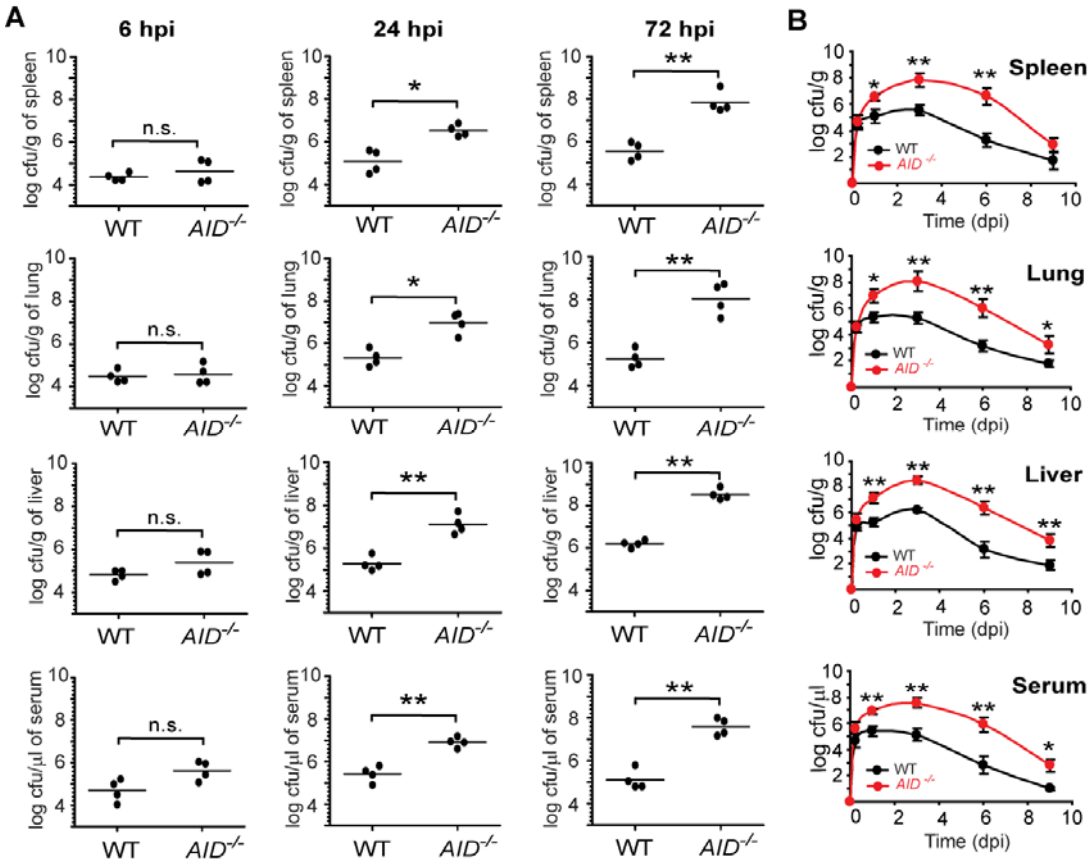

Figure 3.57: Bacterial load and clearance rate in tissues and serum of infected WT and *AID*$^{-/-}$ mice over time. (**A**) Log cfu *P. aeruginosa* per g of spleen, lung, liver and per µl of serum assessed at 6, 24 and 72 hours post-infection (hpi) in WT or *AID*$^{-/-}$ mice (n=4). Freshly dead and alive mice were examined. Each point represents an individual mouse. Horizontal lines represent the mean log cfu/g of organ or cfu/µl of serum. (**B**) Log cfu *P. aeruginosa* per g of spleen, liver and lung and per µl of serum of WT or *AID*$^{-/-}$ mice (n=4). Freshly dead and alive mice were examined over 9 days post-infection (dpi). **p*<0.05; ***p*<0.01; n.s., not significant.

Next, we measured the serum cytokines (IL6, TNFα and IL10) to assess the ensuing inflammatory response of *AID*$^{-/-}$ mice to *P. aeruginosa*

infection. Over the time of infection, we observed a significantly higher increase in the levels of IL6 and TNFα and a decrease in IL10 in *AID*$^{-/-}$ mice (without IgG) as compared to the (a) WT (with complete IgG) or (b) *IgG* siRNA knockdown mice (with near complete depletion of IgG i.e. ~25% of WT mice IgG levels) (**Figure 3.58**), indicating that impairment in the clearance of the bacteria in the *AID*$^{-/-}$ mice led to higher inflammation.

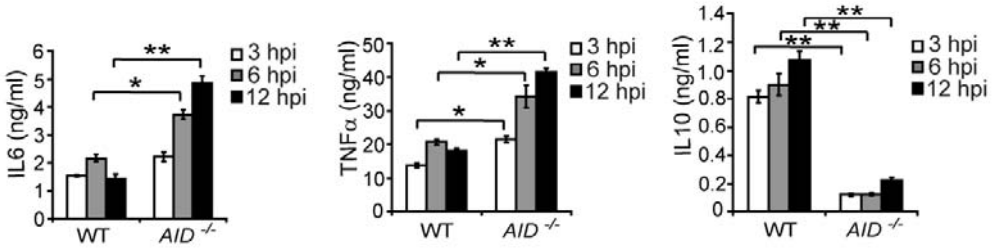

Figure 3.58: Pro- and anti-inflammatory cytokine levels in infected sera from WT and *AID*$^{-/-}$ mice. ELISA to detect IL6, TNFα and IL10 levels in pooled sera of *AID*$^{-/-}$ mice (compared to WT control mice) (n=4 each) infected with 10^6 cfu *P. aeruginosa*. Three replicates per sample were tested.

Infiltration of inflammatory cells in the liver was observed in infected *AID*$^{-/-}$ mice (**Figure 3.59**), indicating impairment in the ability to clear the bacteria and the ensuing inflammation.

In the spleen of *AID*$^{-/-}$ mice, germinal centers (GCs, stained by GL7 antibody), were present throughout (with or without infection), while the WT mice only began to show GCs by 14 dpi (**Figure 3.60A**). The existence of GCs in the uninfected *AID*$^{-/-}$ mice may be explained by the continuous antigenic stimulation by gut microbiota owing to the absence of IgA in the gut (Fagarasan et al., 2002). Quantification of the GCs per mm^2 of white pulp area in *AID*$^{-/-}$ mice showed an increase in their numbers at 9 and 14 dpi compared

to no infection (**Figure 3.60B**). This is consistent with the report of Zaheen et al., 2009. However for WT mice, we only detected marked increase in GCs per mm^2 of white pulp area by 14 dpi. The percentage of total white pulp area to spleen area remained unchanged over days of infection in both groups (**Figure 3.60C**), with no significant difference.

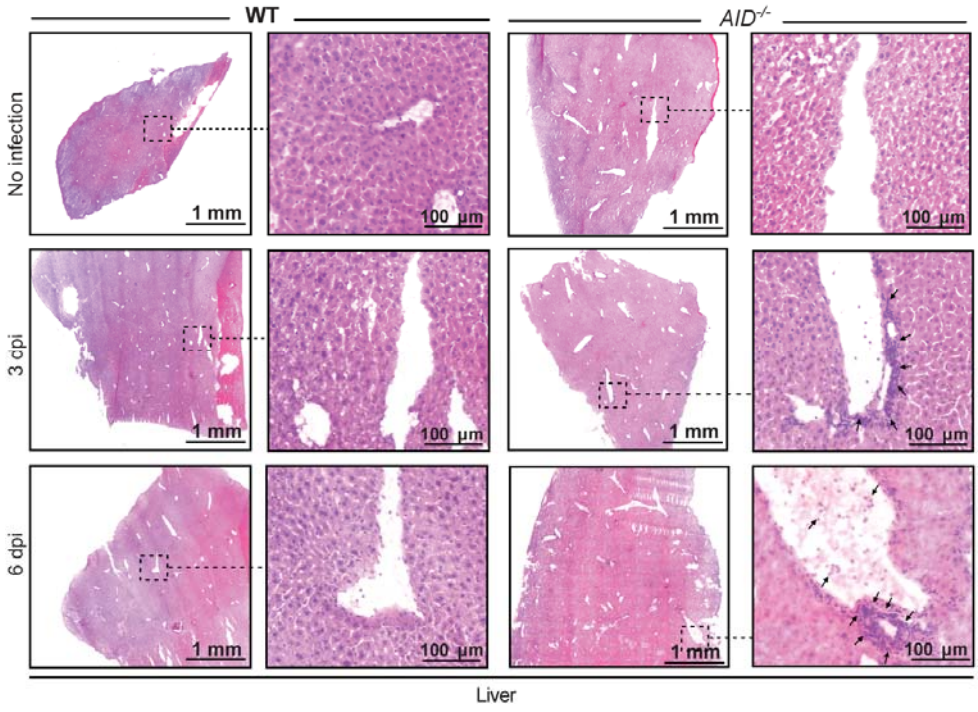

Figure 3.59: Hematoxylin and eosin staining of livers of infected WT and *AID*$^{-/-}$ mice. Hematoxylin and eosin staining of livers from WT and *AID*$^{-/-}$ mice (n=4) infected with 10^6 cfu *P. aeruginosa* over time course. Whole tissue section images (magnification; 2x, scale bar; 1 mm) are provided. Higher magnification to highlight areas of infiltration of inflammatory cell (arrows) in livers of infected *AID*$^{-/-}$ mice. No infiltration is observed in livers of WT mice (magnification; 20x, scale bar; 100 µm). Images were taken using Mirax Midi microscope (Carl Zeiss) and offline analysis was done using Mirax viewer software.

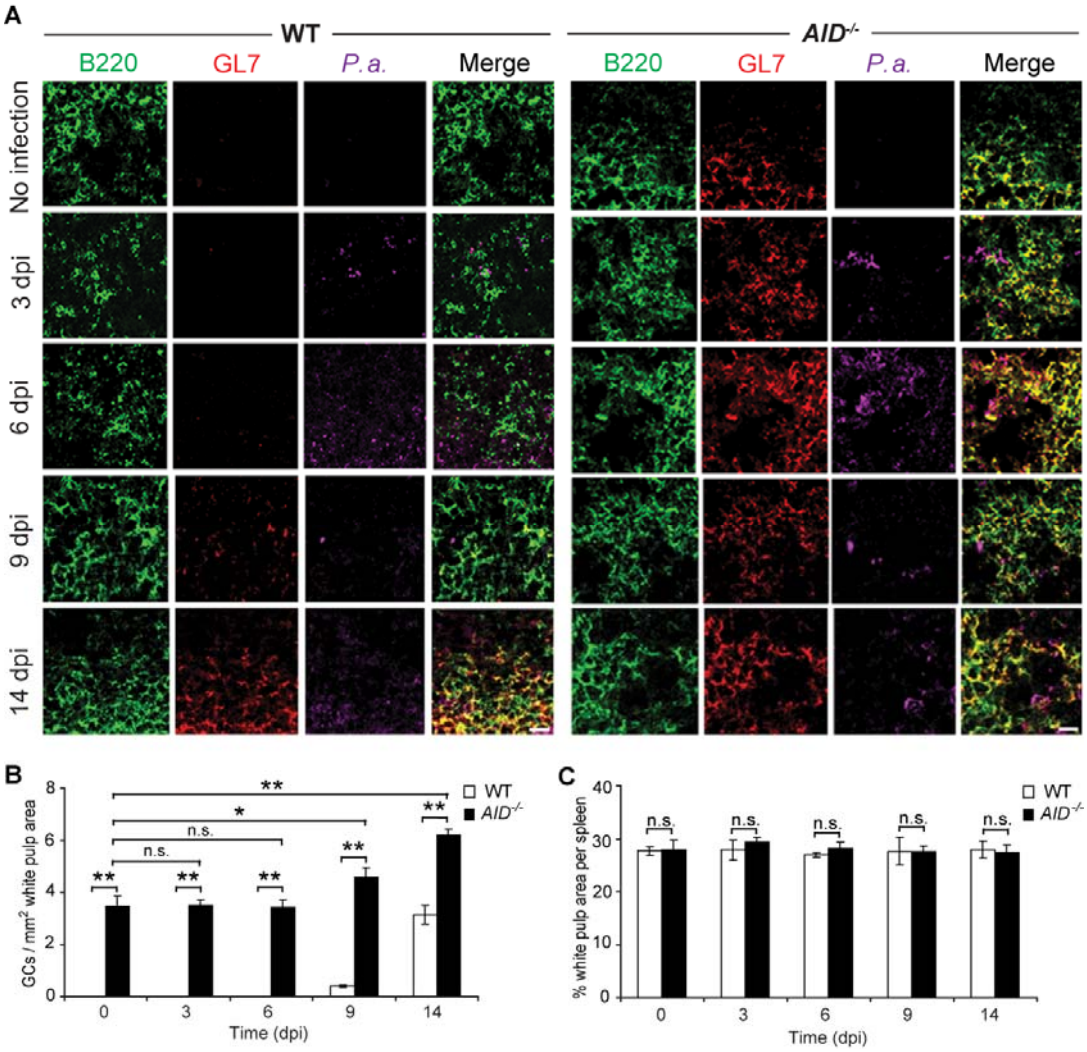

Figure 3.60: Assessment of inflammation in spleens of infected WT and *AID*$^{-/-}$ mice. (**A**) Detection of GC B cells in spleen sections of WT and *AID*$^{-/-}$ mice at various days post-infection (dpi). Frozen sections were cut at 5 µm thickness and stained with anti-B220 (B cell), anti-GL7 (germinal center) and anti-P.a. (bacteria). *P.a.* refers to *Pseudomonas aeruginosa*. Imaging was done using LSM meta 510 confocal microscope (63x objective. Scale bar, 10 µm). (**B and C**) Quantification of GCs per mm^2 white pulp area in spleen sections of WT and *AID*$^{-/-}$ mice at various dpi. Frozen sections were cut at 5 µm thickness and stained with hematoxylin and eosin. Total number of GCs was manually counted using bright field microscopy in three consecutive sections per spleen. Total white pulp area and spleen area per section was calculated using Image J software. The number of GCs per mm^2 white pulp area was calculated by taking an average value from the three sections. GCs per mm^2 of white pulp area and percentage of white pulp area per total spleen area were calculated in spleens of WT and *AID*$^{-/-}$ mice at various dpi. Six mice per group were studied. *p<0.05; **p<0.01; n.s., not significant.

Next, we observed the survival of *AID*$^{-/-}$ mice post-infection with *P. aeruginosa*. The extent of survival was significantly compromised in *AID*$^{-/-}$ mice, confirming that natural IgG confers important innate immune protection from Pseudomonas infection (**Figure 3.61**). Furthermore, the extent of survival was lower compared to *IgG* siRNA knockdown mice which had incomplete depletion of IgG. These results show that natural IgG plays an important innate immune role in limiting the infection and promoting survival.

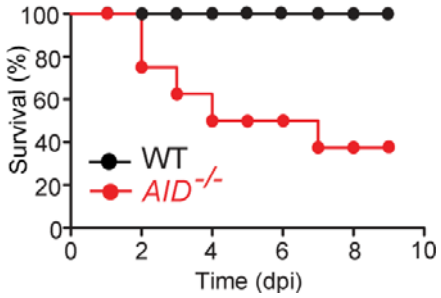

Figure 3.61: Survival of infected WT and *AID*$^{-/-}$ mice over time. Survival of WT or *AID*$^{-/-}$ mice (n=8) infected with 10^6 cfu *P. aeruginosa*. Mice were monitored continuously for up to 9 dpi. Differences in survival were analyzed by the log-rank test (**p<0.01).

3.10. Reconstitution with natural IgG confers innate immune protection to *AID*$^{-/-}$ mice

Finally, to ascertain the importance of natural IgG in clearing infection and promoting survival, we performed reconstitution experiments with the *AID*$^{-/-}$ mice using purified natural IgG (confirmed to be non-binding /non-antigen specific to *P. aeruginosa*). Six hours prior to infection with 10^6 cfu of *P. aeruginosa*, we administered a single dose of purified IgG by tail vein i.v. injection to a level equivalent to the normal serum levels of a WT mouse (2 mg/ml serum).

3.10.1. IgG:ficolin complexes effectively recognize bacteria in IgG-reconstituted *AID*$^{-/-}$ mice

Upon reconstitution with IgG, we detected increasing amounts of ficolin associated with IgG in the serum of the infected *AID*$^{-/-}$ mice in the early phase of infection (**Figure 3.62**, red box). This indicates that natural IgG would be collaborating with ficolin to recognize bacteria in these reconstituted mice in a similar manner as compared to the WT mice. We observed that (a) the serum ficolin level in PBS-reconstituted and (b) the ficolin and IgG levels in IgG-reconstituted mice remained unchanged (Figure 3.62, top 2 panels).

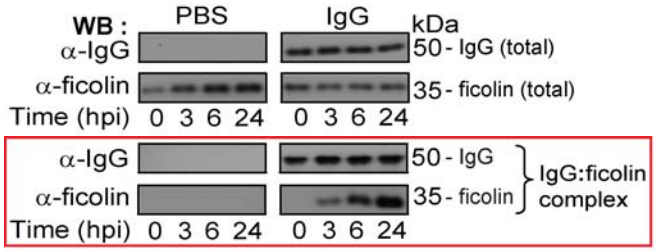

Figure 3.62: IgG:ficolin complex formation in serum of *AID*$^{-/-}$ mice reconstituted with IgG, post infection. *AID*$^{-/-}$ mice (n=8) were administered intravenously through tail vein, with 2 mg natural IgG purified from uninfected serum (to reconstitute to normal level of serum IgG of 2 mg/ml serum) or PBS (control), 6 h prior to infection with 10^6 cfu *P. aeruginosa*. Immunoblot analysis of IgG (50 kDa heavy chain) and ficolin levels in pooled sera of mice (n=8) and detection of IgG**:**ficolin complex (pulled down by Protein G beads, red box) in the serum post-infection in PBS- or IgG-reconstituted mice. The samples were derived from the same experiment, resolved under 12% reducing SDS-PAGE and the gels and blots were processed in parallel. Data are representative of three independent experiments.

3.10.2. IgG-reconstituted *AID*$^{-/-}$ are protected from infection

We checked the bacterial load in PBS and IgG-reconstituted *AID*$^{-/-}$ mice post-infection with *P. aeruginosa*. Similar bacterial load in all tissues at 6 hpi indicates equal administration of the inocula at the start of infection. The bacterial load in the tissues of IgG-reconstituted mice was significantly lower

at 24 and 72 hpi, than in PBS-reconstituted mice, indicating that natural IgG was effective in controlling bacterial proliferation in the tissues (**Figure 3.63**).

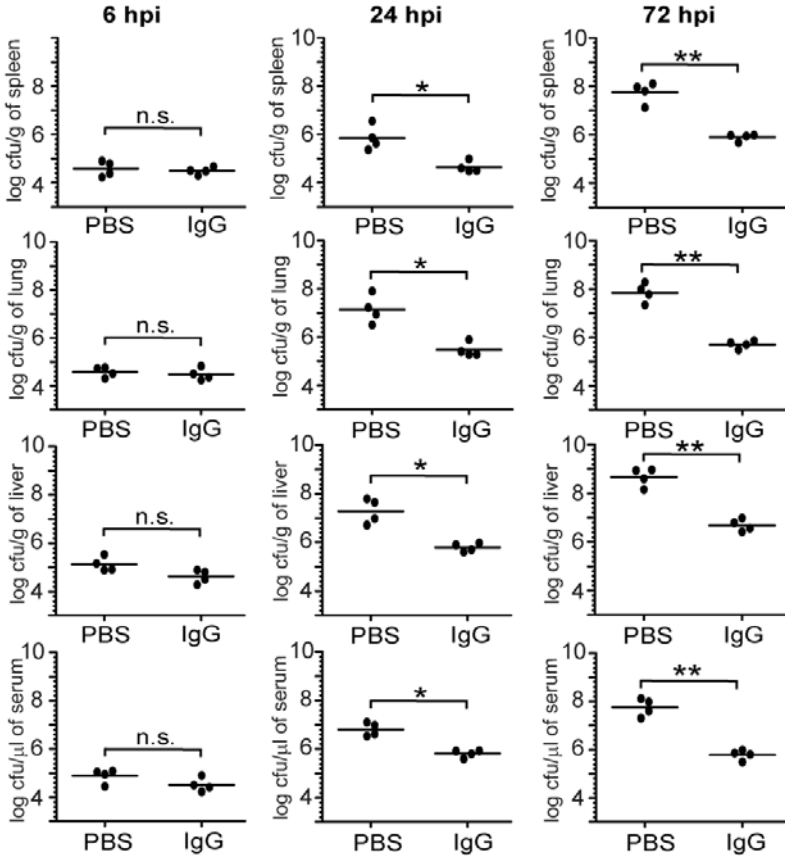

Figure 3.63: Bacterial load in tissues of PBS- and IgG-reconstituted *AID*$^{-/-}$ mice over time post infection. Log cfu *P. aeruginosa* per g of spleen, lung, liver and per µl of serum assessed at 6, 24 and 72 hpi in PBS- or IgG-reconstituted *AID*$^{-/-}$ mice (n=4). Freshly dead and alive mice were examined. Each point represents an individual mouse. Horizontal lines represent the mean log cfu/g of organ or cfu/µl of serum. *p<0.05, **p<0.01.

Additionally, the pro-inflammatory cytokines, IL6 and TNFα levels were lower, while the anti-inflammatory IL10 level was higher in the IgG-reconstituted mice, indicating that IgG**:**ficolin immune complex aided bacterial clearance and limited the extent of inflammation (**Figure 3.64**).

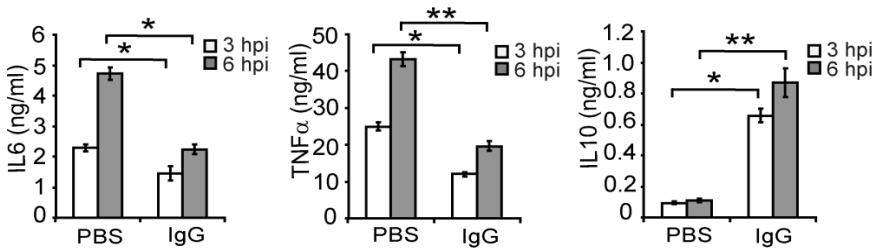

Figure 3.64: Pro- and anti-inflammatory cytokine levels in infected sera of PBS- or IgG-reconstituted *AID*$^{-/-}$ mice. ELISA to detect IL6, TNFα and IL10 levels in pooled sera of infected PBS- or IgG- reconstituted *AID*$^{-/-}$ mice. *AID*$^{-/-}$ mice (n=4) were reconstituted with purified IgG (tested to be non-binding to *P. aeruginosa*) 6 h prior to infection and infected with 10^6 cfu *P. aeruginosa*. Cytokine levels were tested at 3 and 6 hpi. Infected PBS-reconstituted *AID*$^{-/-}$ mice served as controls. Three replicates per sample were tested. *p<0.05; **p<0.01. Data are representative of three independent experiments.

Owing to the efficient removal of the bacteria and lower inflammation levels, we observed no infiltration in livers of IgG-reconstituted *AID*$^{-/-}$ mice as compared to inflammatory cell infiltration in livers of PBS-reconstituted *AID*$^{-/-}$ mice (**Figure 3.65**).

We also observed reduced GC area (stained by GL7 antibody, **Figure 3.66A**) and lower GCs per mm^2 of white pulp area in IgG-reconstituted *AID*$^{-/-}$ mice compared to PBS-reconstituted control *AID*$^{-/-}$ mice at 3 dpi, with no significant difference observed in the percentage of total white pulp area to spleen area in both PBS- and IgG-reconstituted *AID*$^{-/-}$ mice (**Figure 3.66B**). The percentage of total white pulp area to spleen area remained unchanged over days of infection in both groups (**Figure 3.66C**), with no significant difference. This suggests that natural IgG confers protection and lowers the number of GCs. IgG is reported to interact with the B-cell inhibitory Fc receptor, γRIIB1 (Zaheen et al., 2009, D'Ambrosio et al., 1995). Thus, the reconstituted IgG probably downregulates the GC B-cell survival, explaining

the drop in the number of GCs per white pulp area.

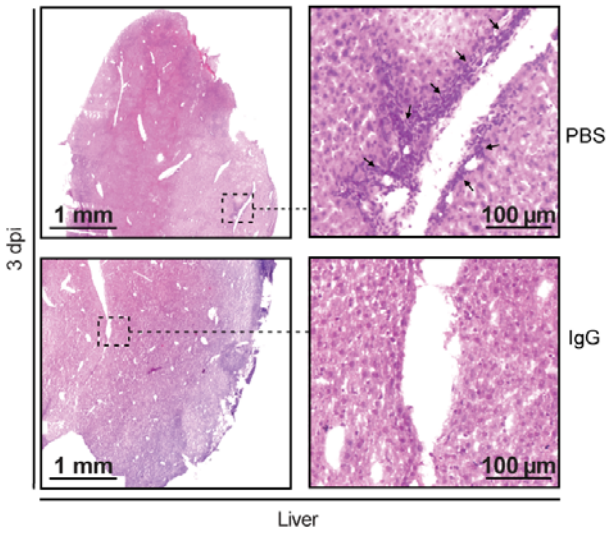

Figure 3.65: Hematoxylin and eosin staining of livers of infected PBS- or IgG-reconstituted *AID*$^{-/-}$ mice. Hematoxylin and eosin staining of livers from PBS-reconstituted (control) and IgG-reconstituted *AID*$^{-/-}$ mice (n=4) infected with 10^6 cfu *P. aeruginosa* at 3 dpi. Whole tissue section images (magnification; 2x, scale bar; 1 mm) are provided. Higher magnification to highlight areas of inflammatory cell infiltration (arrows) in liver of infected PBS-reconstituted control mice. No infiltration is observed in the liver of IgG-reconstituted *AID*$^{-/-}$ mice (magnification; 20x, scale bar; 100 µm). Images were taken using Mirax Midi microscope (Carl Zeiss) and offline analysis was done using Mirax viewer software.

Finally, we observed a significant increase in the survival of the *AID*$^{-/-}$ mice reconstituted with IgG as compared to PBS-reconstituted control mice (**Figure 3.67**). Thus, we conclude that "natural IgG**:**ficolin complex" aided anti-microbial response to limit the infection, to reduce inflammation, to diminish tissue damage which ultimately promotes survival.

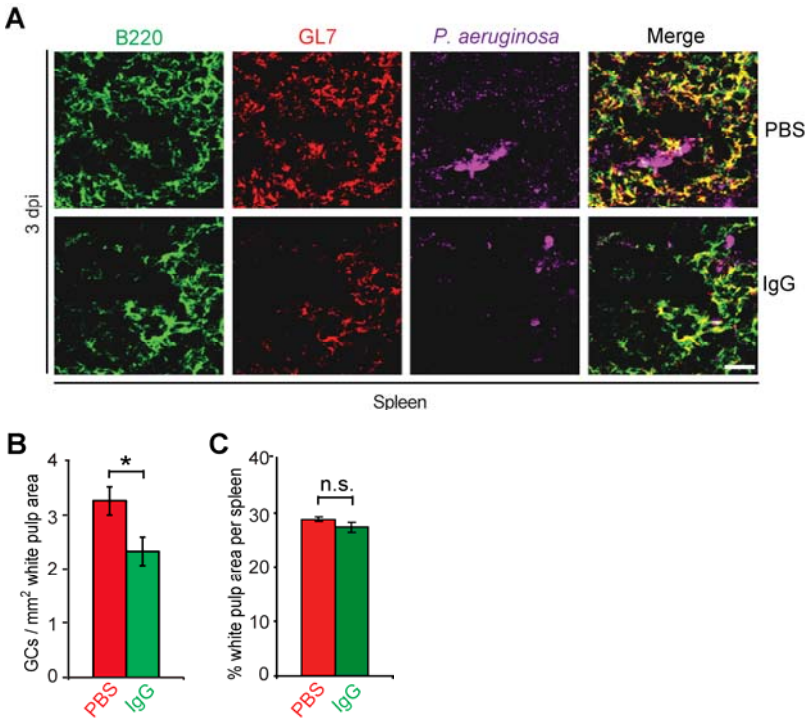

Figure 3.66: Assessment of inflammation in spleens of infected PBS- and IgG-reconstituted *AID*$^{-/-}$ mice. (**A**) Detection of GC B cells in spleens of *P. aeruginosa*-infected PBS- and IgG-reconstituted *AID*$^{-/-}$ mice (n=6). Frozen sections were cut at 5 µm thickness and stained with anti-B220 (B cell, green), anti-GL7 (germinal center, red) and anti-*P. aeruginosa* (bacteria, purple). Imaging was done using LSM meta 510 confocal microscope (63x objective. Scale bar, 10 µm). (**B and C**) Quantification of GCs per mm^2 white pulp area in spleens of mice at various dpi. Frozen sections were cut at 5 µm thickness and stained with hematoxylin and eosin. Total number of GCs was manually counted using bright field microscopy in three consecutive sections per spleen. Total white pulp area and spleen area per section was calculated using Image J software. The number of GCs per mm^2 white pulp area was calculated by taking an average value from the three sections. GCs per mm^2 of white pulp area and percentage of white pulp area per total spleen area were calculated in spleens of PBS-reconstituted and IgG-reconstituted *AID*$^{-/-}$ mice at 3 dpi. Six mice per group were studied. *p<0.05; n.s., not significant.

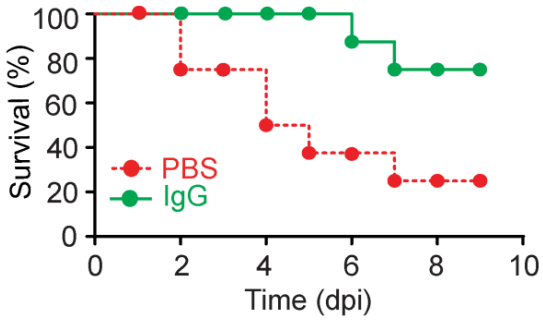

Figure 3.67: Survival of infected PBS or IgG-reconstituted *AID*$^{-/-}$ mice over time. Survival of PBS- or IgG-reconstituted *AID*$^{-/-}$ mice (n=8) infected with 10^6 cfu *P. aeruginosa*. Mice were monitored continuously for up to 9 dpi. Differences in survival were analyzed by the log-rank test (*p<0.05).

Chapter 4

DISCUSSION

CHAPTER 4: DISCUSSION

Infection is caused by a wide range of virulent microbes including pathogenic viruses (Liu and Kimura, 2007), bacteria (Monack et al., 2004), fungi (Marina et al., 2008), protozoa and multi-cellular parasites (Osnas and Lively, 2004). These pathogens pose a grave challenge to health care diagnosis and treatment. Failure to curb the infection in a timely manner may result in life-threatening septic shock, multiple organ failure and possibly death. Therefore, the immune system has come up with a range of sentinels to provide protection to the host in a timely manner.

To initiate an immediate protection against an infection, the host elicits innate immune response, where the PRRs recognize PAMPs and induce several activation cascades such as the complement pathway and signaling pathways, leading to phagocytosis and inflammatory responses for effective clearance of the pathogen. However, over production of pro-inflammatory cytokines could be dangerous to the host as exemplified by sepsis and auto-immune diseases (Poltorak et al., 1998). Therefore, the responses have to be tightly controlled by associated negative feedback mechanisms and/or by anti-inflammatory cytokines such as TGFβ, IL-10, and steroid hormones.

In addition, the innate immune response is known to play an important role in initiating and shaping the subsequent adaptive immune response (Pulendran and Ahmed, 2006). On the other hand, adaptive immunity is also reported to influence the innate immune response (Hoebe et al., 2004). Thus, the two arms of the immune response mediate each other leading to synergistic interplay for effective pathogen clearance.

4.1. Natural IgG is crucial in frontline immune defense

Despite vast amount of literature available on the functions of natural IgM, little is known about why natural antibodies of IgG and IgA isotypes, which constitute the majority of serum natural antibodies, exist in the serum and whether they are redundant or serve any function during a foreign challenge to the immune system.

In this study, we demonstrate for the first time, that natural IgG, the predominant natural antibody isotype in the serum, is not non-reactive but plays a fundamental pro-active role in systemic innate immune response. We first showed by *in vitro* studies that IgG purified from uninfected human serum is indeed able to recognize a wide variety of Gram negative and gram positive bacteria with the aid of ficolin and efficiently drives the phagocytosis of these bacteria via FcγR1 on monocytes. Natural IgG also detects pathogenic bacteria in mice in a similar manner. Our *in vivo* studies highlighted the importance of natural IgG during infection. *IgG* knockdown and $AID^{-/-}$ mice with partial and complete absence of IgG respectively, were more susceptible to infection. In fact, reconstitution of with natural IgG promoted survival in $AID^{-/-}$ mice. Thus, our *in vitro* and *in vivo* studies conclusively prove that natural IgG is not passive but plays a pivotal protective role during infection.

4.2. Natural IgG collaborates with pathogen-associated ficolins to form an interactome

Over the past decade, extensive efforts and progress have been made in our understanding of how the immune system senses and responds to microbial

pathogens. The mechanisms underlying the ligand specificity, signaling pathways, and cellular trafficking of PRRs have been extensively characterized. However, microbial pathogens consist of multiple PAMPs, which simultaneously activate numerous PRRs, and it is now clear that crosstalk between them is a prerequisite for the induction of effective immune responses. Recent studies have highlighted the potential involvement of PRR**:**PRR collaborations acting in concert during the recognition of a pathogen. For example, CRP and ficolins, which are initiators of the classical and lectin complement pathways, respectively, have been shown to interact with each other to boost the immune response against the pathogen (Ng et al., 2007; Zhang et al., 2009; Zhang et al., 2010). TLRs, in concert with other PRRs, have also been shown to orchestrate both pathogen-specific and cell type-specific host immune responses to fight infections (Gross et al., 2006). This crosstalk helps in inducing innate immune responses and in shaping the adaptive immune responses to various pathogens, including bacteria, viruses, fungi, and protozoan parasites. Thus, crosstalk between PRRs is important in mounting an effective immune response. In this thesis, we observed interaction amongst natural IgG and pathogen associated ficolin, which strongly illustrates and confirms the phenomenon of crosstalk amongst plasma proteins as an instantaneous event of pathogen recognition, which boosts immune defense.

Our findings are supported by known literature wherein IgG is known to interact with other PRRs like CRP and MBL through its heavy chain constant region (Malhotra et al., 1995). Also, ficolins have been shown to

interact with CRP through their FBG domain (Zhang et al., 2009; Zhang et al., 2010). Future *in vivo* studies using well-characterized *ficolin*$^{-/-}$ mice, double knockout mice of IgG and ficolin and *FcγR1*$^{-/-}$ mice are required to support our *in vitro* and *ex vivo* findings on the mechanism of action of natural IgG**:**ficolin mediated immune defense.

4.3. Infection-inflammation condition regulates the IgG:ficolin interaction and boots the immune response

Infection leads to influx of inflammatory cells at the site leading to inflammation. This results in a drop in the pH and calcium levels in the body fluids as compared to the normal physiological scenario. By defining typical normal condition (pH 7.4 and 2.5 mM calcium) and infection-inflammation condition (pH 6.5 and 2 mM calcium) based on previous literature (Miyazawa et al., 1990; Aubert et al., 2006), we studied the interaction between IgG and ficolin to gain insight into how changes in pH and calcium influence the interaction and the subsequent immune response leading to clearance of bacteria. We observed that the infection-inflammation condition increased the affinity between IgG and ficolin and strengthened the degree of IgG**:**ficolin mediated phagocytosis. Site-directed mutagenesis studies provided further insight into how infection induced pH change influences the electrostatic interaction between IgG and ficolin by affecting the side-chain charge on amino acids of the proteins. These results suggest that the host system takes advantage of the prevailing changes occurring in serum pH and calcium levels under infection, for better pathogen recognition and effective immune

response. In addition, these findings have given us important clues into the immuno-modulatory activities taking place during an infection so as to avoid random over-activation of the immune system.

4.4. Model to illustrate natural IgG mediated immune defense

We have shown through various *in vitro*, *ex vivo* and *in vivo* studies that natural IgG is a crucial player in frontline immune defense. We showed that it specifically collaborates with pathogen associated ficolins to stage an effective antimicrobial action against the *P. aeruginosa,* an opportunistic pathogen which causes mortality in critically ill and immuno-compromised patients (Goldman et al., 2008). The immunoevasive nature (Kharazmi 1991) and multi-drug resistance (Zaborina et al., 2008) of *P. aeruginosa* makes it very difficult to clear off this microorganism during an infection. There is a lack of effective therapies available against *P. aeruginosa* infection. However, insights gained into the mechanisms of action of natural IgG mediated pathogen recognition and clearance shown in the present work are crucial in our understanding of the host defense to counter the immune evasiveness of this pathogen. This will contribute to the development of more potent immune therapies.

Altogether, we have demonstrated a novel, fundamentally conserved role of natural IgG aided by ficolin, independent of the complement C3. The recruitment of natural IgG to the ficolin-bound pathogen effectively clears the invading bacteria through FcγR1-mediated phagocytosis (**Figure 4.1**). The results obtained from the work in this thesis have been formulated into a

manuscript, which is currently under submission (Panda et al., unpublished data).

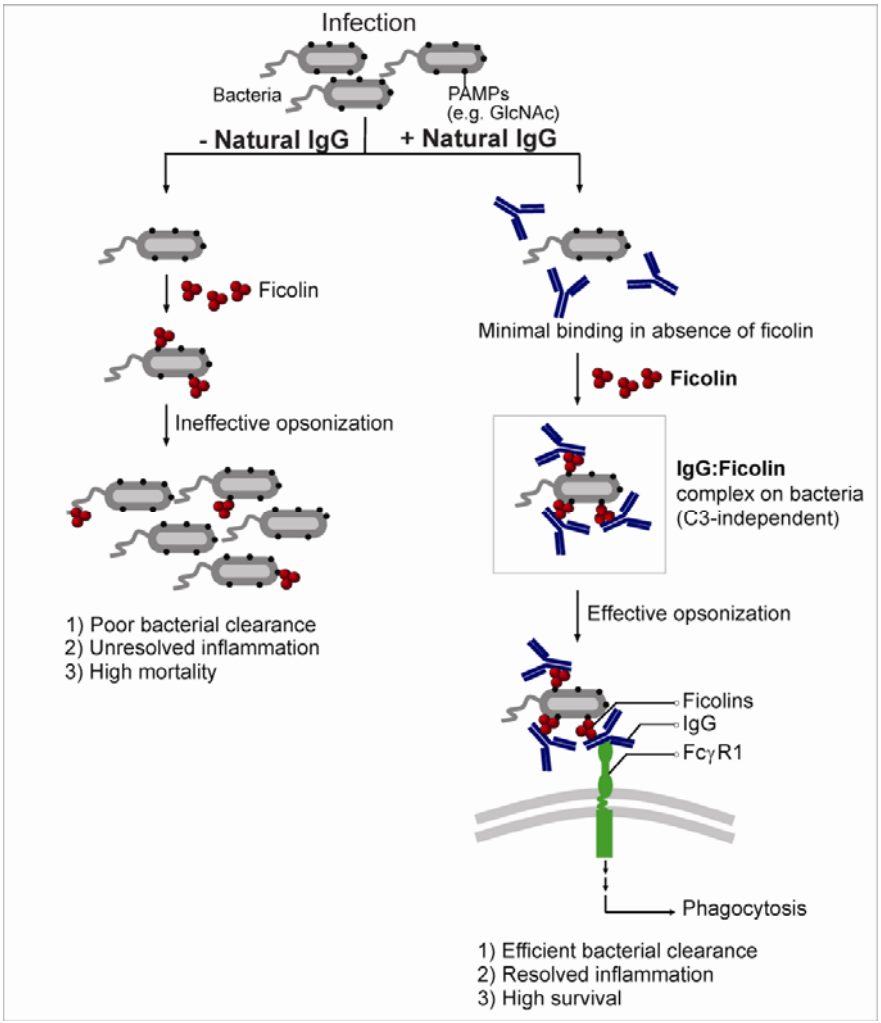

Figure 4.1: Proposed model to illustrate the novel mechanism of bacterial recognition and phagocytosis by natural IgG. Assembly of ficolin (*red*), natural IgG (*blue*) and FcγR1 (*green*) is found on monocytes, [bacteria- ficolin**:**IgG**:**FcγR1-monocytes]. Natural IgG acts as a crucial bridge between ficolin opsonized bacteria and FcγR1, leading to direct and rapid phagocytosis of the pathogen. The right side of the model illustrates that in *AID*$^{-/-}$ mice (-natural IgG), the bacterial load remained high (supported by Figure 3.57), with higher pro-inflammatory cytokine levels in the early phase of infection (supported by Figure 3.58), which compromised survival of the mice (supported by Figure 3.61). The left side of the model illustrates that reconstitution of *AID*$^{-/-}$ mice with natural IgG (+ natural IgG) conferred early innate immune protection against infection compared to PBS-reconstituted controls (supported by Figures 3.62-3.67).

Chapter 5

CONCLUSION

CHAPTER 5: CONCLUSION

The natural antibodies comprise of IgM, IgG and IgA isotypes, of which elaborate studies have been done to elucidate the mechanisms of action and function of natural IgM. However, for over five decades since its discovery, natural IgG which is the most abundant natural antibody found in the serum of newborns and previously uninfected individuals, has been considered non-reactive due to the general perception of its lack of antigen-specificity and affinity for pathogens, when studied in isolation. Thus, why natural IgG exists in the serum and what function it may play during a pathogen attack remain a very interesting biological question to explore. Hence, this thesis was focused on exploring the function of natural IgG. The results obtained in this study define for the first time, the functional and mechanistic role of natural IgG. In this study, we demonstrated that natural IgG is not non-reactive; rather it actively recognizes a broad range of pathogens with the aid of ficolin. Our findings will fundamentally alter the axiom on the inactive nature of natural IgG and provide an impetus for immunologists to reassess the attributes of natural antibodies. Additionally, our findings directly imply new therapeutic strategies to broadly enhance natural resistance to infection. The elucidation of the binding interfaces between the natural IgG and ficolin has the potential to lead to development of immuno-modulators to regulate the frontline immune defense. As a whole, new insights gained from this thesis work will drive forward research on host-microbe interaction in immunity.

Chapter 6

FUTURE PERSPECTIVES

CHAPTER 6: FUTURE PERSPECTIVES

Based on the findings in this thesis, there are several interesting questions that can be addressed in future. To further characterize the interaction of natural IgG with PRRs and explore various avenues where natural antibodies may play a critical functional role, following future studies are proposed as follows.

6.1. *In vivo* studies with *ficolin*$^{-/-}$ and *FcγR1*$^{-/-}$ mice

Our studies involving *in vitro* and *ex vivo* work show that natural IgG collaborates with pathogen associated ficolins in the serum during an infection. We could gain more insight into the mechanism of pathogen detection and antimicrobial defense by studying the complex formation and mode of bacterial clearance in *ficolin*$^{-/-}$ mice. However, the recently available *ficolin*$^{-/-}$ mice have not been phenotypically well-characterized (Kilpatrick and Chalmers, 2011). A couple of recent reports showed that *ficolin*$^{-/-}$ mice were susceptible to localized intranasal infections caused by *Streptococcus* and influenza virus (Endo et al., 2012; Pan et al., 2012). It is likely that reduction in survival was observed as ficolins are abundant in the mucosa (Akaiwa et al., 1999) and their absence will adversely affect the mice in a localized intranasal infection. However, it was found that other PRR induced immune pathways like the MBL mediated complement activation were fully functional in *ficolin*$^{-/-}$ mice during infection (Endo et al., 2012). Moreover, other serum lectins like MBL are also known to interact with IgG (Malhotra et al., 1995). Hence, it is likely that *ficolin*$^{-/-}$ mice will be protected by natural IgG mediated interaction with MBL during a systemic infection. On the other hand, we propose that

future study using *FcγR1*$^{-/-}$ mice will help to provide additional *in vivo* support for the mechanism of action of the natural IgG**:**ficolin opsonized bacterial clearance through FcgR1 receptor mediated phagocytosis.

6.2. Collaboration of natural IgG with other pathogen-associated lectins

Antigen-specific IgG has been shown to interact with other serum lectins such as CRP and MBL (Malhotra et al., 1995). It will be exciting to study the potential collaboration of natural IgG with other pathogen associated lectins and characterize their interaction under infection conditions. A variety of *in vitro* experimental techniques including ELISA, SPR, HDMS, cellular immuno-fluorescence and PLA studies could provide important advance into the biochemical characterization of the interactions. Subsequent *ex vivo* and *in vivo* studies using appropriate knockout mice models available like *mbl*$^{-/-}$ mice will additionally provide more details into the mechanism of action. These studies are crucial in extending our understanding of that natural IgG in general recognizes a wide range of pathogen associated lectins and thereby expand the range of antimicrobial functions it can perform.

6.3. Exploring role of natural IgG:ficolin in mucosal immune defense

Natural antibodies and ficolins are also abundant in the intestinal mucosa (Kroese et al., 1993;Akaiwa et al., 1999). Recent studies have highlighted the role of ficolin in preventing necrotising enterocolitis in newborns (Schlapbach et al., 2011). These reports pose interesting questions on the possible interaction between natural IgG and lectins and their protective action. We

postulate that natural IgG may interact with pathogen associated lectins to elicit frontline defense in mucosal immunity. Insights gained from the findings in this thesis provide a strong foundation for testing this hypothesis. Ultimately, a better understanding of the PRR**:**PRR interactions in the gut will provide new opportunities for the prevention and treatment of a number of inflammatory disorders.

6.4. Does natural IgA also interact with lectins during an infection?

Recent study in our lab showed that IgA interacts with ficolins (Zhang et al., 2010). In addition to ficolins, MBL is also known to interact with IgA (Roos et al., 2001) and activate the complement system in the serum. Also, MBL is seen to co-exist with IgA in immune disorders like IgA nephropathy (Endo et al., 1998; Matsuda et al., 1998; Hisano et al., 2001). Since *AID*$^{-/-}$ mice lack IgA, it will be a very good *in vivo* model to study the natural IgA**:**lectin mediated response and get a better idea of the immune strategies the host applies against infection in the gut.

BIBLIOGRAPHY

BIBLIOGRAPHY

Ackerman, A.L., and Cresswell, P. (2004). Cellular mechanisms governing cross-presentation of exogenous antigens. Nature immunology *5*, 678-684.

Adachi, O., Kawai, T., Takeda, K., Matsumoto, M., Tsutsui, H., Sakagami, M., Nakanishi, K., and Akira, S. (1998). Targeted disruption of the MyD88 gene results in loss of IL-1- and IL-18-mediated function. Immunity *9*, 143-150.

Aderem, A. and D. M., Underhill. (1999). Mechanisms of phagocytosis in macrophages. Annu Rev Immunol *17*, 593-623.

Aderka, D., Schwartz, D., Dan, M., and Levo, Y. (1987). Bacteremic hypocalcemia. A comparison between the calcium levels of bacteremic and nonbacteremic patients with infection. Arch Intern Med *147*, 232-236.

Akaiwa, M., Yae, Y., Sugimoto, R., Suzuki, S.O., Iwaki, T., Izuhara, K., and Hamasaki, N. (1999). Hakata antigen, a new member of the ficolin/opsonin p35 family, is a novel human lectin secreted into bronchus/alveolus and bile. J Histochem Cytochem *47*, 777-786.

Alberts, B., Johnson, A., Lewis, J., Raff, M., Roberts, K., and Walter, P. (2002). Molecular Biology of the Cell. 4th edition.

Alexopoulou, L., Holt, A.C., Medzhitov, R., and Flavell, R.A. (2001). Recognition of double-stranded RNA and activation of NF-kappaB by Toll-like receptor 3. Nature *413*, 732-738.

Alexopoulou, L., Thomas, V., Schnare, M., Lobet, Y., Anguita, J., Schoen, R.T., Medzhitov, R., Fikrig, E., and Flavell, R.A. (2002). Hyporesponsiveness to vaccination with Borrelia burgdorferi OspA in humans and in TLR1- and TLR2-deficient mice. Nature medicine *8*, 878-884.

Andersen, T., Munthe-Fog, L., Garred, P., and Jacobsen, S. (2009). Serum levels of ficolin-3 (Hakata antigen) in patients with systemic lupus erythematosus. The Journal of rheumatology *36*, 757-759.

Aoyagi, Y., Adderson, E.E., Min, J.G., Matsushita, M., Fujita, T., Takahashi, S., Okuwaki, Y., and Bohnsack, J.F. (2005). Role of L-ficolin/mannose-binding lectin-associated serine protease complexes in the opsonophagocytosis of type III group B streptococci. Journal of immunology *174*, 418-425.

Aubert, B., Bona, M., Boutigny, D., Couderc, F., Karyotakis, Y., Lees, J.P., Poireau, V., Tisserand, V., Zghiche, A., Grauges, E., et al., (2006). Measurements of branching fraction, polarization, and charge asymmetry of B(+/-)-->rho(+/-)rho(0) and a search for B(+/-)-->rho(+/-)f(0)(980). Physical review letters *97*, 261801.

Avrameas, S. (1991). Natural autoantibodies: from 'horror autotoxicus' to 'gnothi seauton'. Immunology today *12*, 154-159.

Banchereau, J., and Steinman, R.M. (1998). Dendritic cells and the control of immunity. Nature *392*, 245-252.

Baranov, D., and Neligan, P. (2007). Trauma and aggressive homeostasis management. Anesthesiology clinics *25*, 49-63, viii.

Barton, G. M. (2008). A calculated response: control of inflammation by the innate immune system. J Clin Invest *118*, 413–420.

Basset, C., Holton, J., O'Mahony, R., and Roitt, I. (2003). Innate immunity and pathogen-host interaction. Vaccine *21 Suppl 2*, S12-23.

Baumgarth, N., Tung, J.W., and Herzenberg, L.A. (2005). Inherent specificities in natural antibodies: a key to immune defense against pathogen invasion. Springer seminars in immunopathology *26*, 347-362.

Beers, M. (2000). The Merck Manual of Geriatrics.

Benenson, A.S. (1990). Control of Communicable Diseases in Man. 15th edition.

Bertin, J., Nir, W.J., Fischer, C.M., Tayber, O.V., Errada, P.R., Grant, J.R., Keilty, J.J., Gosselin, M.L., Robison, K.E., Wong, G.H., et al., (1999). Human CARD4 protein is a novel CED-4/Apaf-1 cell death family member that activates NF-kappaB. The Journal of biological chemistry *274*, 12955-12958.

Beutler, B. (2004). SHIP, TGF-beta, and endotoxin tolerance. Immunity *21*, 134-135.

Beutler, B., and Poltorak, A. (2000). The search for Lps: 1993-1998. Journal of endotoxin research *6*, 269-293.

Bistrian, B. (2007). Systemic response to inflammation. Nutrition reviews *65*, S170-172.

Bleves, S., Viarre, V., Salacha, R., Michel, G.P., Filloux, A., and Voulhoux, R. (2010). Protein secretion systems in Pseudomonas aeruginosa: A wealth of pathogenic weapons. International journal of medical microbiology : IJMM *300*, 534-543.

Boes, M., Esau, C., Fischer, M.B., Schmidt, T., Carroll, M., and Chen, J. (1998). Enhanced B-1 cell development, but impaired IgG antibody responses in mice deficient in secreted IgM. Journal of immunology *160*, 4776-4787.

Boyden, S.V. (1966). Natural antibodies and the immune response. Advances

in immunology *5*, 1-28.

Briles, D.E., Nahm, M., Schroer, K., Davie, J., Baker, P., Kearney, J., and Barletta, R. (1981). Antiphosphocholine antibodies found in normal mouse serum are protective against intravenous infection with type 3 streptococcus pneumoniae. The Journal of experimental medicine *153*, 694-705.

Brown, G.D., and Gordon, S. (2001). Immune recognition. A new receptor for beta-glucans. Nature *413*, 36-37.

Brown, J.S., Hussell, T., Gilliland, S.M., Holden, D.W., Paton, J.C., Ehrenstein, M.R., Walport, M.J., and Botto, M. (2002). The classical pathway is the dominant complement pathway required for innate immunity to Streptococcus pneumoniae infection in mice. Proceedings of the National Academy of Sciences of the United States of America *99*, 16969-16974.

Burton, D.R., Jefferis, R., Partridge, L.J., and Woof, J.M. (1988). Molecular recognition of antibody (IgG) by cellular Fc receptor (FcRI). Molecular immunology *25*, 1175-1181.

Burton, D.R., and Woof, J.M. (1992). Human antibody effector function. Advances in immunology *51*, 1-84.

Cairns, S.P., Westerblad, H., and Allen, D.G. (1993). Changes in myoplasmic pH and calcium concentration during exposure to lactate in isolated rat ventricular myocytes. The Journal of physiology *464*, 561-574.

Casadevall, A., Dadachova, E., and Pirofski, L.A. (2004). Passive antibody therapy for infectious diseases. Nature reviews. Microbiology *2*, 695-703.

Coutinho, A., Kazatchkine, M.D., and Avrameas, S. (1995). Natural autoantibodies. Current opinion in immunology *7*, 812-818.

Czajkowsky, D.M., and Shao, Z. (2009). The human IgM pentamer is a mushroom-shaped molecule with a flexural bias. Proceedings of the National Academy of Sciences of the United States of America *106*, 14960-14965.

Daeron, M. (1997). Fc receptor biology. Annual review of immunology *15*, 203-234.

D'Ambrosio, D., Hippen, K.L., Minskoff, S.A., Mellman, I., Pani, G., Siminovitch, K.A., and Cambier, J.C. (1995). Recruitment and activation of PTP1C in negative regulation of antigen receptor signaling by Fc gamma RIIB1. Science *268*, 293-297.

Delves, P.J., and Roitt, I.M. (2000). The immune system. Second of two parts. The New England journal of medicine *343*, 108-117.

Dempsey, P.W., Allison, M.E., Akkaraju, S., Goodnow, C.C., and Fearon, D.T. (1996). C3d of complement as a molecular adjuvant: bridging innate and acquired immunity. Science *271*, 348-350.

Dempsey, P.W., Vaidya, S.A., and Cheng, G. (2003). The art of war: Innate and adaptive immune responses. Cellular and molecular life sciences : CMLS *60*, 2604-2621.

Dinarello, C.A. (2007). Historical insights into cytokines. European journal of immunology *37 Suppl 1*, S34-45.

Dunkelberger, J.R., and Song, W.C. (2010). Complement and its role in innate and adaptive immune responses. Cell research *20*, 34-50.

Ehlers, M.R. (2000). CR3: a general purpose adhesion-recognition receptor essential for innate immunity. Microbes and infection / Institut Pasteur *2*, 289-294.

Ehrenstein, M.R., and Notley, C.A. (2010). The importance of natural IgM: scavenger, protector and regulator. Nature reviews. Immunology *10*, 778-786.

Endo, Y., Liu, Y., Kanno, K., Takahashi, M., Matsushita, M., and Fujita, T. (2004). Identification of the mouse H-ficolin gene as a pseudogene and orthology between mouse ficolins A/B and human L-/M-ficolins. Genomics *84*, 737-744.

Endo, Y., Matsushita, M. and Fujita, T. (2011). The role of ficolins in the lectin pathway of innate immunity. The International Journal of Biochemistry and Cell Biology *43*, 705-712.

Endo, M., Ohi, H., Ohsawa, I., Fujita, T., Matsushita, M., and Fujita, T. (1998). Glomerular deposition of mannose-binding lectin (MBL) indicates a novel mechanism of complement activation in IgA nephropathy. Nephrology, dialysis, transplantation : official publication of the European Dialysis and Transplant Association - European Renal Association *13*, 1984-1990.

Endo, Y., Takahashi, M., Iwaki, D., Ishida, Y., Nakazawa, N., Kodama, T., Matsuzaka, T., Kanno, K., Liu, Y., Tsuchiya, K., et al., (2012). Mice Deficient in Ficolin, a Lectin Complement Pathway Recognition Molecule, Are Susceptible to Streptococcus pneumoniae Infection. Journal of immunology *189*, 5860-5866.

Epstein, J., Eichbaum, Q., Sheriff, S., and Ezekowitz, R.A. (1996). The collectins in innate immunity. Curr. Opin. Immunol. *8*, 29–35.

Ezekowitz, R.A., Sastry, K., Bailly, P., and Warner, A. (1990). Molecular characterization of the human macrophage mannose receptor: demonstration of multiple carbohydrate recognition-like domains and phagocytosis of yeasts

in Cos-1 cells. The Journal of experimental medicine *172*, 1785-1794.

Fagarasan, S., Muramatsu, M., Suzuki, K., Nagaoka, H., Hiai, H., and Honjo, T. (2002). Critical roles of activation-induced cytidine deaminase in the homeostasis of gut flora. Science *298*, 1424-1427.

Feeney, A.J. (1990). Lack of N regions in fetal and neonatal mouse immunoglobulin V-D-J junctional sequences. The Journal of experimental medicine *172*, 1377-1390.

Felson, D.T., and McAlindon, T.E. (2000). Glucosamine and chondroitin for osteoarthritis: to recommend or not to recommend? Arthritis care and research : the official journal of the Arthritis Health Professions Association *13*, 179-182.

Feske, S. (2007). Calcium signalling in lymphocyte activation and disease. Nature reviews. Immunology *7*, 690-702.

Filiatrault, M.J., Picardo, K.F., Ngai, H., Passador, L., and Iglewski, B.H. (2006). Identification of Pseudomonas aeruginosa genes involved in virulence and anaerobic growth. Infection and immunity *74*, 4237-4245.

Fujita, T. (2002). Evolution of the lectin-complement pathway and its role in innate immunity. Nature reviews. Immunology *2*, 346-353.

Gallin J, S. R. e. (1999). Inflammation: Basic Principles and Clinical Correlates.

Garlanda, C., Hirsch, E., Bozza, S., Salustri, A., De Acetis, M., Nota, R., Maccagno, A., Riva, F., Bottazzi, B., Peri, G., et al., (2002). Non-redundant role of the long pentraxin PTX3 in anti-fungal innate immune response. Nature *420*, 182-186.

Garlatti, V., Belloy, N., Martin, L., Lacroix, M., Matsushita, M., Endo, Y., Fujita, T., Fontecilla-Camps, J.C., Arlaud, G.J., Thielens, N.M., and Gaboriaud, C. (2007). Structural insights into the innate immune recognition specificities of L- and H-ficolins. The EMBO journal *26*, 623-633.

Girardin, S.E., Boneca, I.G., Viala, J., Chamaillard, M., Labigne, A., Thomas, G., Philpott, D.J., and Sansonetti, P.J. (2003). Nod2 is a general sensor of peptidoglycan through muramyl dipeptide (MDP) detection. The Journal of biological chemistry *278*, 8869-8872.

Goldman, M., Rosenfeld-Yehoshua, N., Lerner-Geva, L., Lazarovitch, T., Schwartz, D., and Grisaru-Soen, G. (2008). Clinical features of community-acquired Pseudomonas aeruginosa urinary tract infections in children. Pediatric nephrology *23*, 765-768.

Goldsby, R. Kindt, T.J., Osborne, B.A., and Kuby, J. (2003). Antigens (Chapter 3). Immunology. 5th edition.

Good, N.E., Winget, G.D., Winter, W., Connolly, T.N., Izawa, S., and Singh, R.M. (1966). Hydrogen ion buffers for biological research. Biochemistry *5*, 467-477.

Graille, M., Stura, E.A., Corper, A.L., Sutton, B.J., Taussig, M.J., Charbonnier, J.B., and Silverman, G.J. (2000). Crystal structure of a Staphylococcus aureus protein A domain complexed with the Fab fragment of a human IgM antibody: structural basis for recognition of B-cell receptors and superantigen activity. Proc Natl Acad Sci U S A *97*, 5399-5404.

Greenberg, S. (1999). Modular components of phagocytosis. J. Leuk. Biol. 66, 712–17.

Gross, O., Gewies, A., Finger, K., Schafer, M., Sparwasser, T., Peschel, C., Forster, I., and Ruland, J. (2006). Card9 controls a non-TLR signalling pathway for innate anti-fungal immunity. Nature *442*, 651-656.

Hajjar, A.M., O'Mahony, D.S., Ozinsky, A., Underhill, D.M., Aderem, A., Klebanoff, S.J., and Wilson, C.B. (2001). Cutting edge: functional interactions between toll-like receptor (TLR) 2 and TLR1 or TLR6 in response to phenol-soluble modulin. Journal of immunology *166*, 15-19.

Hangartner, L., Zinkernagel, R.M., and Hengartner, H. (2006). Antiviral antibody responses: the two extremes of a wide spectrum. Nature reviews. Immunology *6*, 231.243.

Hansen, S., Thiel, S., Willis, A., Holmskov, U., and Jensenius, J.C. (2000). Purification and characterization of two mannan-binding lectins from mouse serum. Journal of immunology *164*, 2610-2618.

Hardy, R.R., and Hayakawa, K. (1994). CD5 B cells, a fetal B cell lineage. Adv Immunol *55*, 297-339.

Harlow, E., and Lane, D. (1988). Antibodies: A laboratory manual. Cold Spring Harbor Laboratory.

Harmsen, M., Yang, L., Pamp, S.J., and Tolker-Nielsen, T. (2010). An update on Pseudomonas aeruginosa biofilm formation, tolerance, and dispersal. FEMS immunology and medical microbiology *59*, 253-268.

Haury, M., Sundblad, A., Grandien, A., Barreau, C., Coutinho, A., and Nobrega, A. (1997). The repertoire of serum IgM in normal mice is largely independent of external antigenic contact. European journal of immunology *27*, 1557-1563.

Hayashi, F., Smith, K.D., Ozinsky, A., Hawn, T.R., Yi, E.C., Goodlett, D.R., Eng, J.K., Akira, S., Underhill, D.M., and Aderem, A. (2001). The innate immune response to bacterial flagellin is mediated by Toll-like receptor 5. Nature *410*, 1099-1103.

Haziot, A., Ferrero, E., Kontgen, F., Hijiya, N., Yamamoto, S., Silver, J., Stewart, C.L., and Goyert, S.M. (1996). Resistance to endotoxin shock and reduced dissemination of gram-negative bacteria in CD14-deficient mice. Immunity *4*, 407-414.

Hemmi, H., Kaisho, T., Takeuchi, O., Sato, S., Sanjo, H., Hoshino, K., Horiuchi, T., Tomizawa, H., Takeda, K., and Akira, S. (2002). Small anti-viral compounds activate immune cells via the TLR7 MyD88-dependent signaling pathway. Nature immunology *3*, 196-200.

Hemmi, H., Takeuchi, O., Kawai, T., Kaisho, T., Sato, S., Sanjo, H., Matsumoto, M., Hoshino, K., Wagner, H., Takeda, K., and Akira, S. (2000). A Toll-like receptor recognizes bacterial DNA. Nature *408*, 740-745.

Hershberger, C., and Binkley, S.B. (1968). Chemistry and metabolism of 3-deoxy-D-mannooctulosonic acid. I. Stereochemical determination. The Journal of biological chemistry *243*, 1578-1584.

Hisano, S., Matsushita, M., Fujita, T., Endo, Y., and Takebayashi, S. (2001). Mesangial IgA2 deposits and lectin pathway-mediated complement activation in IgA glomerulonephritis. American journal of kidney diseases : the official journal of the National Kidney Foundation *38*, 1082-1088.

Hoffmann, J.A., Kafatos, F.C., Janeway, C.A., and Ezekowitz, R.A. (1999). Phylogenetic perspectives in innate immunity. Science *284*, 1313-1318.

Holmskov, U. (2000). Collectins and collectin receptors in innate immunity. APMIS Suppl. *100*, 1–59.

Holmskov, U., Thiel, S., and Jensenius, J.C. (2003). Collections and ficolins: humoral lectins of the innate immune defense. Annual review of immunology *21*, 547-578.

Honoré, C., Hummelshoj, T., Hansen, B.E., Madsen, H.O., Eggleton, P., and Garred, P. (2007). The innate immune component ficolin 3 (Hakata antigen) mediates the clearance of late apoptotic cells. Arthritis and rheumatism *56*, 1598-1607.

Ichijo, H., Hellman, U., Wernstedt, C., Gonez, L.J., Claesson-Welsh, L., Heldin, C.H., and Miyazono, K. (1993). Molecular cloning and characterization of ficolin, a multimeric protein with fibrinogen- and collagen-like domains. The Journal of biological chemistry *268*, 14505-14513.

Ichijo, H., Ronnstrand, L., Miyagawa, K., Ohashi, H., Heldin, C.H., and Miyazono, K. (1991). Purification of transforming growth factor-beta 1 binding proteins from porcine uterus membranes. The Journal of biological chemistry *266*, 22459-22464.

Indik, Z.K., Park, J.G., Hunter, S., and Schreiber, A.D. (1995). The molecular dissection of Fc gamma receptor mediated phagocytosis. Blood *86*, 4389-4399.

Inohara, N., Koseki, T., del Peso, L., Hu, Y., Yee, C., Chen, S., Carrio, R., Merino, J., Liu, D., Ni, J., and Nunez, G. (1999). Nod1, an Apaf-1-like activator of caspase-9 and nuclear factor-kappaB. The Journal of biological chemistry *274*, 14560-14567.

Inohara, N., Ogura, Y., Fontalba, A., Gutierrez, O., Pons, F., Crespo, J., Fukase, K., Inamura, S., Kusumoto, S., Hashimoto, M., et al., (2003). Host recognition of bacterial muramyl dipeptide mediated through NOD2. Implications for Crohn's disease. The Journal of biological chemistry *278*, 5509-5512.

Isada, C.M., Kasten, B.L., Goldman, M.P. (2003). Infectious Diseases Handbook. 5th Edition. American Pharmaceutical Association.

Issekutz, A.C., and Bhimji, S. (1982). Role for endotoxin in the leukocyte infiltration accompanying Escherichia coli inflammation. Infection and immunity *36*, 558-566.

Iwasaki, A., and Medzhitov, R. (2004). Toll-like receptor control of the adaptive immune responses. Nature immunology *5*, 987-995.

Jack, D.L., Klein, N.J., and Turner, M.W. (2001). Mannose-binding lectin: targeting the microbial world for complement attack and opsonophagocytosis. Immunological reviews *180*, 86-99.

Janeway, C.A., Jr., and Medzhitov, R. (2002). Innate immune recognition. Annual review of immunology *20*, 197-216.

Janeway, C.A., Travers, P., Walport, M., and Shlomchik, M.J. (2005). Immunobiology: the immune system in health and disease. 6th edition.

Jensen, M.L., Honoré, C., Hummelshoj, T., Hansen, B.E., Madsen, H.O., and Garred, P. (2007). Ficolin-2 recognizes DNA and participates in the clearance of dying host cells. Molecular immunology *44*, 856-865.

Jung, D., and Alt, F.W. (2004). Unraveling V(D)J recombination; insights into gene regulation. Cell *116*, 299-311.

Kantor, A.B., and Herzenberg, L.A. (1993). Origin of murine B cell lineages. Annu Rev Immunol *11*, 501-538.

Keirstead, N.D., Lee, C., Yoo, D., Brooks, A.S., and Hayes, M.A. (2008). Porcine plasma ficolin binds and reduces infectivity of porcine reproductive and respiratory syndrome virus (PRRSV) *in vitro*. Antiviral research *77*, 28-38.

Kelsoe, G. (1996). Life and death in germinal centers (redux). Immunity *4*, 107-111.

Kharazmi, A. (1991). Mechanisms involved in the evasion of the host defence by Pseudomonas aeruginosa. Immunology letters *30*, 201-205.

Kilpatrick, D.G., and Chalmers, J.D. (2011). Human L-Ficolin (Ficolin-2) and its clinical significance. Journal of Biomedicine and Biotechnology. doi:10.1155/2012/138797.

Klein, U., and Dalla-Favera, R. (2008). Germinal centres: role in B-cell physiology and malignancy. Nature reviews. Immunology *8*, 22-33.

Kopp, E.B., and Medzhitov, R. (1999). The Toll-receptor family and control of innate immunity. Current opinion in immunology *11*, 13-18.

Kraal, G., van der Laan, L.J., Elomaa, O., and Tryggvason, K. (2000). The macrophage receptor MARCO. Microbes and infection / Institut Pasteur *2*, 313-316.

Krarup, A., Thiel, S., Hansen, A., Fujita, T., and Jensenius, J.C. (2004). L-ficolin is a pattern recognition molecule specific for acetyl groups. The Journal of biological chemistry *279*, 47513-47519.

Kroese, F.G., Ammerlaan, W.A., and Kantor, A.B. (1993). Evidence that intestinal IgA plasma cells in mu, kappa transgenic mice are derived from B-1 (Ly-1 B) cells. Int Immunol *5*, 1317-1327.

Kube, D., Sontich, U., Fletcher, D., and Davis, P.B. (2001). Proinflammatory cytokine responses to P. aeruginosa infection in human airway epithelial cell lines. Am J Physiol Lung Cell Mol Physiol *280*, L493-502.

Kuraya, M., Ming, Z., Liu, X., Matsushita, M., and Fujita, T. (2005). Specific binding of L-ficolin and H-ficolin to apoptotic cells leads to complement activation. Immunobiology *209*, 689-697.

Kurt-Jones, E.A., Popova, L., Kwinn, L., Haynes, L.M., Jones, L.P., Tripp, R.A., Walsh, E.E., Freeman, M.W., Golenbock, D.T., Anderson, L.J., and Finberg, R.W. (2000). Pattern recognition receptors TLR4 and CD14 mediate response to respiratory syncytial virus. Nature immunology *1*, 398-401.

Kwon, D.H., and Lu, C.D. (2006). Polyamines induce resistance to cationic peptide, aminoglycoside, and quinolone antibiotics in Pseudomonas aeruginosa PAO1. Antimicrobial agents and chemotherapy *50*, 1615-1622.

Laterveer, L., Lindley, I.J., Hamilton, M.S., Willemze, R., and Fibbe, W.E. (1995). Interleukin-8 induces rapid mobilization of hematopoietic stem cells with radioprotective capacity and long-term myelolymphoid repopulating ability. Blood *85*, 2269-2275.

Liu, B., and Kimura, Y. (2007). Local immune response to respiratory syncytial virus infection is diminished in senescence-accelerated mice.J Gen Virol *88(Pt 9)*, 2552-2558.

Liu, Y., Endo, Y., Homma, S., Kanno, K., Yaginuma, H., and Fujita, T. (2005). Ficolin A and ficolin B are expressed in distinct ontogenic patterns and cell types in the mouse. Molecular immunology *42*, 1265-1273.

Look, M., Bandyopadhyay, A., Blum, J.S., and Fahmy, T.M. (2010). Application of nanotechnologies for improved immune response against infectious diseases in the developing world. Advanced drug delivery reviews *62*, 378-393.

Lyczak, J.B., Cannon, C.L., and Pier, G.B. (2000). Establishment of Pseudomonas aeruginosa infection: lessons from a versatile opportunist. Microbes and infection / Institut Pasteur *2*, 1051-1060.

Lynch, N.J., Roscher, S., Hartung, T., Morath, S., Matsushita, M., Maennel, D.N., Kuraya, M., Fujita, T., and Schwaeble, W.J. (2004). L-ficolin specifically binds to lipoteichoic acid, a cell wall constituent of Gram-positive bacteria, and activates the lectin pathway of complement. Journal of immunology *172*, 1198-1202.

Ma, Y.G., Cho, M.Y., Zhao, M., Park, J.W., Matsushita, M., Fujita, T., and Lee, B.L. (2004). Human mannose-binding lectin and L-ficolin function as specific pattern recognition proteins in the lectin activation pathway of complement. The Journal of biological chemistry *279*, 25307-25312.

Ma, Y., Uemura, K., Oka, S., Kozutsumi, Y., Kawasaki, N., and Kawasaki, T. (1999). Antitumor activity of mannan-binding protein *in vivo* as revealed by a virus expression system: mannan-binding proteindependent cell-mediated cytotoxicity. Proceedings of the National Academy of Sciences of the United States of America *96*, 371-375.

MacLennan, I.C. (1994). Germinal centers. Annual review of immunology *12*, 117-139.

Malhotra, R., Wormald, M.R., Rudd, P.M., Fischer, P.B., Dwek, R.A., and Sim, R.B. (1995). Glycosylation changes of IgG associated with rheumatoid arthritis can activate complement via the mannose-binding protein. Nature medicine *1*, 237-243.

Manz, R.A., Hauser, A.E., Hiepe, F., and Radbruch, A. (2005). Maintenance

of serum antibody levels. Annual review of immunology *23*, 367-386.

Marina, M., Maiale, S.J., Rossi, F.R., Romero, M.F., Rivas, E.I., Garriz, A., Ruiz, O.A., and Pieckenstain, F.L. (2008). Apoplastic polyamine oxidation plays different roles in local responses of tobacco to infection by the necrotrophic fungus Sclerotinia sclerotiorum and the biotrophic bacterium Pseudomonas viridiflava. Plant physiology *147*, 2164-2178.

Marnell, L., Mold, C., and Du Clos, T.W. (2005). C-reactive protein: ligands, receptors and role in inflammation. Clinical immunology *117*, 104-111.

Marsh, C.B., Anderson, C.L., Lowe, M.P., and Wewers, M.D. (1996). Monocyte IL-8 release is induced by two independent Fc gamma R- mediated pathways. J Immunol *157*, 2632-2637.

Marshak-Rothstein, A., and Rifkin, I.R. (2007). Immunologically active autoantigens: the role of toll-like receptors in the development of chronic inflammatory disease. Annual review of immunology *25*, 419-441.

Martinez, D., Vermeulen, M., Trevani, A., Ceballos, A., Sabatte, J., Gamberale, R., Alvarez, M.E., Salamone, G., Tanos, T., Coso, O.A., and Geffner, J. (2006). Extracellular acidosis induces neutrophil activation by a mechanism dependent on activation of phosphatidylinositol 3-kinase/Akt and ERK pathways. Journal of immunology *176*, 1163-1171.

Matsuda, M., Shikata, K., Wada, J., Sugimoto, H., Shikata, Y., Kawasaki, T., and Makino, H. (1998). Deposition of mannan binding protein and mannan binding protein-mediated complement activation in the glomeruli of patients with IgA nephropathy. Nephron *80*, 408-413.

Matsushita, M., Endo, Y., Hamasaki, N., and Fujita, T. (2001). Activation of the lectin complement pathway by ficolins. International immunopharmacology *1*, 359-363.

Matsushita, M., Endo, Y., Taira, S., Sato, Y., Fujita, T., Ichikawa, N., Nakata, M., and Mizuochi, T. (1996). A novel human serum lectin with collagen- and fibrinogen-like domains that functions as an opsonin. The Journal of biological chemistry *271*, 2448-2454.

Medzhitov, R., and Janeway, C.A., Jr. (1997). Innate immunity: the virtues of a nonclonal system of recognition. Cell *91*, 295-298.

Medzhitov, R., Preston-Hurlburt, P., and Janeway, C.A., Jr. (1997). A human homologue of the Drosophila Toll protein signals activation of adaptive immunity. Nature *388*, 394-397.

Meurs, E., Chong, K., Galabru, J., Thomas, N.S., Kerr, I.M., Williams, B.R., and Hovanessian, A.G. (1990). Molecular cloning and characterization of the

human double-stranded RNA-activated protein kinase induced by interferon. Cell *62*, 379-390.

Michael, J.G. (1969). Natural antibodies. Current topics in microbiology and immunology *48*, 43-62.

Miyazawa, K., and Inoue, K. (1990). Complement activation induced by human C-reactive protein in mildly acidic conditions. Journal of immunology *145*, 650-654.

Molina, H., Holers, V.M., Li, B., Fung, Y., Mariathasan, S., Goellner, J., Strauss-Schoenberger, J., Karr, R.W., and Chaplin, D.D. (1996). Markedly impaired humoral immune response in mice deficient in complement receptors 1 and 2. Proceedings of the National Academy of Sciences of the United States of America *93*, 3357-3361.

Monack, D.M., Mueller, A., and Falkow, S. (2004). Persistent bacterial infections: the interface of the pathogen and the host immune system. Nature Reviews Microbiology *2*, 747-765.

Morris, C.G., and Low, J. (2008). Metabolic acidosis in the critically ill: part 1. Classification and pathophysiology. Anaesthesia *63*, 294-301.

Morse, S.S. (1995). Factors in the emergence of infectious diseases. Emerging infectious diseases *1*, 7-15.

Muramatsu, M., Kinoshita, K., Fagarasan, S., Yamada, S., Shinkai, Y., and Honjo, T. (2000). Class switch recombination and hypermutation require activation-induced cytidine deaminase (AID), a potential RNA editing enzyme. Cell *102*, 553-563.

Muto, S., Sakuma, K., Taniguchi, A., and Matsumoto, K. (1999). Human mannose binding lectin preferentially binds to human colon adenocarcinoma cell lines expressing high amount of Lewis A and Lewis B antigens. Biol. Pharm. Bull. *22*, 347–52.

Nathan, C. (2006). Neutrophils and immunity: challenges and opportunities. Nature reviews. Immunology *6*, 173-182.

Nauta, A.J., Raaschou-Jensen, N., Roos, A., Daha, M.R., Madsen, H.O., Borrias-Essers, M.C., Ryder, L.P., Koch, C., and Garred, P. (2003). Mannose-binding lectin engagement with late apoptotic and necrotic cells. European journal of immunology *33*, 2853-2863.

Ng, P.M., Le Saux, A., Lee, C.M., Tan, N.S., Lu, J., Thiel, S., Ho, B., and Ding, J.L. (2007). C-reactive protein collaborates with plasma lectins to boost immune response against bacteria. The EMBO journal *26*, 3431-3440.

Ochsenbein, A.F., Fehr, T., Lutz, C., Suter, M., Brombacher, F., Hengartner, H., and Zinkernagel, R.M. (1999). Control of early viral and bacterial distribution and disease by natural antibodies. Science *286*, 2156-2159.

Oettinger, M.A., Schatz, D.G., Gorka, C., and Baltimore, D. (1990). RAG-1 and RAG-2, adjacent genes that synergistically activate V(D)J recombination. Science *248*, 1517-1523.

Ogden, C.A., deCathelineau, A., Hoffmann, P.R., Bratton, D., Ghebrehiwet, B., Fadok, V.A., and Henson, P.M. (2001). C1q and mannose binding lectin engagement of cell surface calreticulin and CD91 initiates macropinocytosis and uptake of apoptotic cells. The Journal of experimental medicine *194*, 781-795.

Ogden, C.A., Kowalewski, R., Peng, Y., Montenegro, V., and Elkon, K.B. (2005). IGM is required for efficient complement mediated phagocytosis of apoptotic cells *in vivo*. Autoimmunity *38*, 259-264.

Ohno, N., and Morrison, D.C. (1989). Lipopolysaccharide interaction with lysozyme. Binding of lipopolysaccharide to lysozyme and inhibition of lysozyme enzymatic activity. The Journal of biological chemistry *264*, 4434-4441.

Osnas, E.E., and Lively, C.M. (2004). Parasite dose, prevalence of infection and local adaptation in a host-parasite system. Parasitology *128*, 223-228.

Palm, N.W., and Medzhitov, R. (2009). Pattern recognition receptors and control of adaptive immunity. Immunological reviews *227*, 221-233.

Pancer, Z., and Cooper, M.D. (2006). The evolution of adaptive immunity. Annual review of immunology *24*, 497-518.

Panda, S., Zhang, J., Anand, G.S., Tan, N.S., Ho, B. and Ding, J.L. Manuscript in submission.

Pasare, C., and Medzhitov, R. (2005). Toll-like receptors: linking innate and adaptive immunity. Advances in experimental medicine and biology *560*, 11-18.

Pikaar, J.C., Voorhout, W.F., van Golde, L.M., Verhoef, J., Van Strijp, J.A., and van Iwaarden, J.F. (1995). Opsonic activities of surfactant proteins A and D in phagocytosis of gram-negative bacteria by alveolar macrophages. The Journal of infectious diseases *172*, 481-489.

Pober, J.S., and Sessa, W.C. (2007). Evolving functions of endothelial cells in inflammation. Nature reviews. Immunology *7*, 803-815.

Poltorak, A., He, X., Smirnova, I., Liu, M.Y., Van Huffel, C., Du, X., Birdwell,

D., Alejos, E., Silva, M., Galanos, C., et al., (1998). Defective LPS signaling in C3H/HeJ and C57BL/10ScCr mice: mutations in Tlr4 gene. Science *282*, 2085-2088.

Prince, A.A., Steiger, J.D., Khalid, A.N., Dogrhamji, L., Reger, C., Eau Claire, S., Chiu, A.G., Kennedy, D.W., Palmer, J.N., and Cohen, N.A. (2008). Prevalence of biofilm-forming bacteria in chronic rhinosinusitis. American journal of rhinology *22*, 239-245.

Pulendran, B., and Ahmed, R. (2006). Translating innate immunity into immunological memory: implications for vaccine development. Cell *124*, 849-863.

Quartier, P., Potter, P.K., Ehrenstein, M.R., Walport, M.J., and Botto, M. (2005). Predominant role of IgM-dependent activation of the classical pathway in the clearance of dying cells by murine bone marrow-derived macrophages *in vitro*. European journal of immunology *35*, 252-260.

Raetz, C.R., Guan, Z., Ingram, B.O., Six, D.A., Song, F., Wang, X., and Zhao, J. (2009). Discovery of new biosynthetic pathways: the lipid A story. Journal of lipid research *50 Suppl*, S103-108.

Raetz, C.R., Ulevitch, R.J., Wright, S.D., Sibley, C.H., Ding, A., and Nathan, C.F. (1991). Gram-negative endotoxin: an extraordinary lipid with profound effects on eukaryotic signal transduction. FASEB journal : official publication of the Federation of American Societies for Experimental Biology *5*, 2652-2660.

Raetz, C.R., and Whitfield, C. (2002). Lipopolysaccharide endotoxins. Annual review of biochemistry *71*, 635-700.

Ravetch, J.V., and Bolland, S. (2001). IgG Fc receptors. Annual review of immunology *19*, 275-290.

Ravetch, J.V., and Clynes, R.A. (1998). Divergent roles for Fc receptors and complement *in vivo*. Annual review of immunology *16*, 421-432.

Rebouillat, D., Hovnanian, A., David, G., Hovanessian, A.G., and Williams, B.R. (2000). Characterization of the gene encoding the 100-kDa form of human 2',5' oligoadenylate synthetase. Genomics *70*, 232-240.

Reginster, J.Y., Deroisy, R., Rovati, L.C., Lee, R.L., Lejeune, E., Bruyere, O., Giacovelli, G., Henrotin, Y., Dacre, J.E., and Gossett, C. (2001). Long-term effects of glucosamine sulphate on osteoarthritis progression: a randomised, placebo-controlled clinical trial. Lancet *357*, 251-256.

Revy, P., Muto, T., Levy, Y., Geissmann, F., Plebani, A., Sanal, O., Catalan, N., Forveille, M., Dufourcq-Labelouse, R., Gennery, A., et al., (2000).

Activation-induced cytidine deaminase (AID) deficiency causes the autosomal recessive form of the Hyper-IgM syndrome (HIGM2). Cell *102*, 565-575.

Richards, J.J., Ballard, T.E., Huigens, R.W., 3rd, and Melander, C. (2008). Synthesis and screening of an oroidin library against Pseudomonas aeruginosa biofilms. Chembiochem : a European journal of chemical biology *9*, 1267-1279.

Rojas, R., and Apodaca, G. (2002). Immunoglobulin transport across polarized epithelial cells. Nature reviews. Molecular cell biology *3*, 944-955.

Rorvig, S., Honoré, C., Larsson, L.I., Ohlsson, S., Pedersen, C.C., Jacobsen, L.C., Cowland, J.B., Garred, P., and Borregaard, N. (2009). Ficolin-1 is present in a highly mobilizable subset of human neutrophil granules and associates with the cell surface after stimulation with fMLP. Journal of leukocyte biology *86*, 1439-1449.

Roos, A., Bouwman, L.H., van Gijlswijk-Janssen, D.J., Faber-Krol, M.C., Stahl, G.L., and Daha, M.R. (2001). Human IgA activates the complement system via the mannan-binding lectin pathway. Journal of immunology *167*, 2861-2868.

Ross, G.D., Reed, W., Dalzell, J.G., Becker, S.E., and Hogg, N. (1992). Macrophage cytoskeleton association with CR3 and CR4 regulates receptor mobility and phagocytosis of iC3b-opsonized erythrocytes. Journal of leukocyte biology *51*, 109-117.

Russell, J.A. (2011). Bench-to-bedside review: Vasopressin in the management of septic shock. Critical care *15*, 226.

Ryan, K.J., and Ray, C.G. (2004). Sherris Medical Microbiology. 4th edition. McGraw Hill.

Salvatore, S., Heuschkel, R., Tomlin, S., Davies, S.E., Edwards, S., Walker-Smith, J.A., French, I., and Murch, S.H. (2000). A pilot study of N-acetyl glucosamine, a nutritional substrate for glycosaminoglycan synthesis, in paediatric chronic inflammatory bowel disease. Alimentary pharmacology & therapeutics *14*, 1567-1579.

Sant, A.J. (1994). Endogenous antigen presentation by MHC class II molecules. Immunologic research *13*, 253-267.

Schlapbach, L.J., Mattmann, M., Thiel, S., Boillat, C., Otth, M., Nelle, M., Wagner, B., Jensenius, J.C., and Aebi, C. (2010). Differential role of the lectin pathway of complement activation in susceptibility to neonatal sepsis. Clinical infectious diseases : an official publication of the Infectious Diseases Society of America *51*, 153-162.

Schlapbach, L.J., Thiel, S., Kessler, U., Ammann, R.A., Aebi, C., and Jensenius, J.C. (2011). Congenital H-ficolin deficiency in premature infants with severe necrotising enterocolitis. Gut *60*, 1438-1439.

Schumann, R.R., Leong, S.R., Flaggs, G.W., Gray, P.W., Wright, S.D., Mathison, J.C., Tobias, P.S., and Ulevitch, R.J. (1990). Structure and function of lipopolysaccharide binding protein. Science *249*, 1429-1431.

Serhan, C.N., and Savill, J. (2005). Resolution of inflammation: the beginning programs the end. Nature immunology *6*, 1191-1197.

Shibuya, A., Sakamoto, N., Shimizu, Y., Shibuya, K., Osawa, M., Hiroyama, T., Eyre, H.J., Sutherland, G.R., Endo, Y., Fujita, T., et al., (2000). Fc alpha/mu receptor mediates endocytosis of IgM-coated microbes. Nature immunology *1*, 441-446.

Sidman, C.L., Shultz, L.D., Hardy, R.R., Hayakawa, K., and Herzenberg, L.A. (1986). Production of immunoglobulin isotypes by Ly-1+ B cells in viable motheaten and normal mice. Science *232*, 1423-1425.

Simmen, H.P., and Blaser, J. (1993). Analysis of pH and pO2 in abscesses, peritoneal fluid, and drainage fluid in the presence or absence of bacterial infection during and after abdominal surgery. American journal of surgery *166*, 24-27.

Stavnezer, J., and Amemiya, C.T. (2004). Evolution of isotype switching. Seminars in immunology *16*, 257-275.

Stavnezer, J., Guikema, J.E., and Schrader, C.E. (2008). Mechanism and regulation of class switch recombination. Annual review of immunology *26*, 261-292.

Subramaniam, K.S., Datta, K., Quintero, E., Manix, C., Marks, M.S., and Pirofski, L.A. (2010). The absence of serum IgM enhances the susceptibility of mice to pulmonary challenge with Cryptococcus neoformans. Journal of immunology *184*, 5755-5767.

Takahashi, K., Ip, W.E., Michelow, I.C., and Ezekowitz, R.A. (2006). The mannose-binding lectin: a prototypic pattern recognition molecule. Current opinion in immunology *18*, 16-23.

Takeuchi, O., Hoshino, K., Kawai, T., Sanjo, H., Takada, H., Ogawa, T., Takeda, K., and Akira, S. (1999). Differential roles of TLR2 and TLR4 in recognition of gram-negative and gram-positive bacterial cell wall components. Immunity *11*, 443-451.

Takeuchi, O., Sato, S., Horiuchi, T., Hoshino, K., Takeda, K., Dong, Z., Modlin, R.L., and Akira, S. (2002). Cutting edge: role of Toll-like receptor 1

in mediating immune response to microbial lipoproteins. Journal of immunology *169*, 10-14.

Tarlinton, D. (1998). Germinal centers: form and function. Current opinion in immunology *10*, 245-251.

Tarlinton, D.M., and Smith, K.G. (2000). Dissecting affinity maturation: a model explaining selection of antibody-forming cells and memory B cells in the germinal centre. Immunology today *21*, 436-441.

Taylor, K., McCullough, B., Clarke, D.J., Langley, R.J., Pechenick, T., Hill, A., Campopiano, D.J., Barran, P.E., Dorin, J.R., and Govan, J.R. (2007). Covalent dimer species of beta-defensin Defr1 display potent antimicrobial activity against multidrug-resistant bacterial pathogens. Antimicrobial agents and chemotherapy *51*, 1719-1724.

Teh, C., Le, Y., Lee, S.H., and Lu, J. (2000). M-ficolin is expressed on monocytes and is a lectin binding to N-acetyl-D-glucosamine and mediates monocyte adhesion and phagocytosis of Escherichia coli. Immunology *101*, 225-232.

Thomas, C.A., Li, Y., Kodama, T., Suzuki, H., Silverstein, S.C., and El Khoury, J. (2000). Protection from lethal gram-positive infection by macrophage scavenger receptor-dependent phagocytosis. The Journal of experimental medicine *191*, 147-156.

Trevani, A.S., Andonegui, G., Giordano, M., Lopez, D.H., Gamberale, R., Minucci, F., and Geffner, J.R. (1999). Extracellular acidification induces human neutrophil activation. Journal of immunology *162*, 4849-4857.

The World Health Report (1996).

The World Health Report (2004).

Underhill, D.M., and Ozinsky, A. (2002). Phagocytosis of microbes: complexity in action. Annual review of immunology *20*, 825-852.

Underhill, D.M., Ozinsky, A., Smith, K.D., and Aderem, A. (1999). Toll-like receptor-2 mediates mycobacteria-induced proinflammatory signaling in macrophages. Proceedings of the National Academy of Sciences of the United States of America *96*, 14459-14463.

van Zwieten, R., R. Wever, et al., (1981). Extracellular proton release by stimulated neutrophils. J Clin Invest *68(1)*, 310-313.

Vermeulen, M., Giordano, M., Trevani, A.S., Sedlik, C., Gamberale, R., Fernandez-Calotti, P., Salamone, G., Raiden, S., Sanjurjo, J., and Geffner, J.R. (2004). Acidosis improves uptake of antigens and MHC class I-restricted

presentation by dendritic cells. Journal of immunology *172*, 3196-3204.

Victora, G.D., and Nussenzweig, M.C. (2012). Germinal centers. Annual review of immunology *30*, 429-457.

Watts, C. (1997). Capture and processing of exogenous antigens for presentation on MHC molecules. Annual review of immunology *15*, 821-850.

Wong, W.W., Klickstein, L.B., Smith, J.A., Weis, J.H., and Fearon, D.T. (1985). Identification of a partial cDNA clone for the human receptor for complement fragments C3b/C4b. Proceedings of the National Academy of Sciences of the United States of America *82*, 7711-7715.

Wright, J., J. H. Schwartz, et al., (1986). Proton secretion by the sodium/hydrogen ion antiporter in the human neutrophil. J Clin Invest *77(3)*, 782-788.

Wu, C.M., Cao, J.L., Zheng, M.H., Ou, Y., Zhang, L., Zhu, X.Q., and Song, J.X. (2008). Effect and mechanism of andrographolide on the recovery of Pseudomonas aeruginosa susceptibility to several antibiotics. The Journal of international medical research *36*, 178-186.

Yancopoulos, G.D., Desiderio, S.V., Paskind, M., Kearney, J.F., Baltimore, D., and Alt, F.W. (1984). Preferential utilization of the most JH-proximal VH gene segments in pre-B-cell lines. Nature *311*, 727-733.

Yoshizawa, S., Nagasawa, K., Yae, Y., Niho, Y., and Okochi, K. (1997). A thermolabile beta 2-macroglycoprotein (TMG) and the antibody against TMG in patients with systemic lupus erythematosus. Clinica chimica acta; international journal of clinical chemistry *264*, 219-225.

Yother, J., Volanakis, J.E., and Briles, D.E. (1982). Human C-reactive protein is protective against fatal Streptococcus pneumoniae infection in mice. Journal of immunology *128*, 2374-2376.

Zaheen, A., Boulianne, B., Parsa, J.Y., Ramachandran, S., Gommerman, J.L., and Martin, A. (2009). AID constrains germinal center size by rendering B cells susceptible to apoptosis. Blood *114*, 547-554.

Zaborina, O., Holbrook, C., Chen, Y., Long, J., Zaborin, A., Morozova, I., Fernandez, H., Wang, Y., Turner, J.R., and Alverdy, J.C. (2008). Structure-function aspects of PstS in multi-drug-resistant Pseudomonas aeruginosa. PLoS pathogens *4*, e43.

Zar, T., Yusufzai, I., Sullivan, A., and Graeber, C. (2007). Acute kidney injury, hyperosmolality and metabolic acidosis associated with lorazepam. Nature clinical practice. Nephrology *3*, 515-520.

Zhang, J., Koh, J., Lu, J., Thiel, S., Leong, B.S., Sethi, S., He, C.Y., Ho, B., and Ding, J.L. (2009). Local inflammation induces complement crosstalk which amplifies the antimicrobial response. PLoS Pathog *5*, e1000282.

Zhang, J., Yang, L., Ang, Z., Yoong, S.L., Tran, T.T., Anand, G.S., Tan, N.S., Ho, B., and Ding, J.L. (2010). Secreted M-ficolin anchors onto monocyte transmembrane G protein-coupled receptor 43 and cross talks with plasma C-reactive protein to mediate immune signaling and regulate host defense. J Immunol *185*, 6899-6910.

Zhou, Z.H., Zhang, Y., Hu, Y.F., Wahl, L.M., Cisar, J.O., and Notkins, A.L. (2007). The broad antibacterial activity of the natural antibody repertoire is due to polyreactive antibodies. Cell Host Microbe *1*, 51-61.